INTERNATIONAL CENTER FOR NUMERICAL METHODS IN ENGINEERING

Constitutive Modeling and Numerical Analysis of Thermo-Mechanical Phase-Change Systems

M. Chiumenti
C. Agelet de Saracibar
M. Cervera

Monograph CIMNE Nº-48, March 1999

Constitutive Modeling and Numerical Analysis of Thermo-Mechanical Phase-Change Systems

M. Chiumenti
C. Agelet de Saracibar
M. Cervera

Monograph CIMNE Nº 48, March 1999

International Center for Numerical Methods in Engineering
Gran Capitán s/n, 08034 Barcelona, Spain

The cover designed by: Jordi Pallí

First published, March 1999

Edited by:
International Center for Numerical Methods in Engineering
C/ Gran Capitán, s/n
08034 Barcelona, Spain

ISBN: 84-89925-39-9
Deposito Legal: B-17971-99

Contents

1 Introduction **11**

1.1 Motivations and Goals 11

1.1.1 Numerical solution of coupled problems 12

1.1.2 Numerical solution of frictional contact problems . . . 13

1.2 Overview 14

2 Formulation of the Coupled Problem **17**

2.1 Local governing equations 17

2.1.1 General form of the local balance laws 18

2.1.2 Additive decomposition 20

2.1.3 A-priori stability estimate 22

2.2 Constitutive equations 24

2.2.1 Coleman's method 24

2.2.2 Definition of the free energy function 27

2.2.3 Phase Change Contributions 30

2.3 Evolution laws 33

2.3.1 Introduction 34

2.3.2 Principle of maximum dissipation 35

2.3.3 Definition of the purely viscous model 39

2.3.4 A J2-flow thermo-viscoplastic model 40

2.3.5 Mechanical dissipation 41

2.3.6 Thermal dissipation 42

2.4 Equivalent forms of the energy equation 43

2.4.1 Entropy form 43

2.4.2 Temperature form 44

2.5 Weak Form of the Governing Equations 45

2.5.1 Weak form of the balance of momentum equation . . . 45

2.5.2 Mixed Variational Formulation 45

2.5.3 Weak form of the energy equation 48

3 Formulation of the Contact Problem **51**
3.1 Notation and Problem Definition 51
3.1.1 Notation 52
3.1.2 Parametrization of the contact surfaces 53
3.1.3 Closest-point projection and contact pressure 54
3.1.4 Convected basis, metric and curvature tensors 55
3.1.5 Slip velocity and frictional traction 56
3.2 Governing Equations 57
3.3 Additive Decomposition 59
3.4 Constitutive Equations 59
3.4.1 Free energy function definition 59
3.4.2 Thermal contact model 62
3.5 Evolution Laws 64
3.6 Thermo-frictional Dissipation 65
3.7 Wear Phenomena 66
3.8 Equivalent forms of the energy equation 67
3.8.1 Entropy form 67
3.8.2 Temperature form 67
3.9 A-priori stability estimate 68
3.10 Contact Contribution to the Weak form 69

4 Time Integration of the Coupled Problem **71**
4.1 Time stepping schemes 71
4.1.1 Simultaneous algorithm 73
4.1.2 Block-iterative algorithm 73
4.2 Fractional step methods 75
4.2.1 Time-stepping algorithms 75
4.2.2 Local evolution problem 76
4.2.3 Product formula algorithm 77
4.2.4 Operator splits: a-priory stability estimate 80
4.3 Time-discrete variational formulation 83
4.3.1 Isentropic split 84
4.3.2 Isothermal split 87
4.4 Time-integration of the constitutive equations 90
4.4.1 Elasto-plastic operator split 91
4.4.2 Linear multi-step methods 92

4.4.3 Isentropic algorithm 93
4.4.4 Isothermal algorithm 102
4.5 Phase-change integration 107

5 Time Integration of the Contact Problem 109
5.1 Local evolution problem 109
5.2 Operator splits 110
5.2.1 Isentropic operator split 110
5.2.2 Isothermal operator split 111
5.3 Time-discrete Contribution to the Weak form 113
5.4 Isentropic Algorithm 113
5.4.1 Mechanical phase (isentropic split) 113
5.4.2 Thermal phase (isentropic split) 117
5.5 Isothermal Algorithm 121
5.5.1 Mechanical phase (isothermal split) 121
5.5.2 Thermal phase (isothermal split) 124

6 Space Discretization 125
6.1 The Galerkin projection 125
6.2 Mixed approximation: *B-bar* projection method 127
6.3 Integration Rules 132
6.3.1 Integration of the thermal problem 133
6.3.2 Phase change integration 135

7 Numerical Simulations 137
7.1 Cooling of a Pressurized Thick-walled Cylinder 138
7.2 Flat Sheet Sliding Test 140
7.3 Cylindrical Aluminium Solidification Test 153
7.4 Solidification of a RENAULT Clio Crankshaft 162

List of Figures

2.1 Thermo-mechanical rheological model 21
2.2 Latent heat function 31
2.3 Thermal deformation including straining contribution 33

3.1 Schematic description of two interacting bodies at reference and current placements. Reference and current placement of contact surfaces. 52
3.2 Contact surface parametrization. Parametrization map of reference and current placement of a contact surface. 54

6.1 Cooling of an indefinite cylinder. (a) Open integration rule (b) Close integration rule. 134
6.2 Space integration of the latent heat function. 135

7.1 Cooling of a pressurized thick-walled cylinder. Initial geometry and boundary conditios. 138
7.2 Quasi-static cooling of a thermo-elastic pressurized cylinder. Radial displacement (a) and temperature evolution (b) at the inner and outer surfaces, using both the isothermal and the isentropic operator splits, for the weakly coupled case. 141
7.3 Quasi-static cooling of a thermo-elastic pressurized cylinder. Radial displacement (a) and temperature evolution (b) at the inner and outer surfaces, using both the isothermal and the isentropic operator splits, for the strongly coupled case. 142
7.4 Quasi-static cooling of a thermo-plastic pressurized cylinder. Radial displacement (a) and temperature evolution (b) at the inner and outer surfaces, using both the isothermal and the isentropic operator splits, for the weakly coupled case. 143

7.5 Quasi-static cooling of a thermo-plastic pressurized cylinder. Radial displacement (a) and temperature evolution (b) at the inner and outer surfaces, using both the isothermal and the isentropic operator splits, for the strongly coupled case. 144
7.6 Dynamicic cooling of a thermo-elastic pressurized cylinder. Radial displacement (a) and temperature evolution (b) at the inner and outer surfaces, using both the isothermal and the isentropic operator splits, for the weakly coupled case. 145
7.7 Dynamic cooling of a thermo-elastic pressurized cylinder. Radial displacement (a) and temperature evolution (b) at the inner and outer surfaces, using both the isothermal and the isentropic operator splits, for the strongly coupled case. 146
7.8 Dynamic cooling of a thermo-plastic pressurized cylinder. Radial displacement (a) and temperature evolution (b) at the inner and outer surfaces, using both the isothermal and the isentropic operator splits, for the weakly coupled case. 147
7.9 Dynamic cooling of a thermo-plastic pressurized cylinder. Radial displacement (a) and temperature evolution (b) at the inner and outer surfaces, using both the isothermal and the isentropic operator splits, for the strongly coupled case. 148
7.10 Flat sheet sliding test. Finite element mesh and sliding cycle. (a) Initial configuration and application of the normal force; (b) Sliding process; (c) Release of the normal force and (d) return to the initial position. 149
7.11 Flat sheet sliding test. (a) Hardening plasticity and (b) frictional hardening laws for the GA and EG steel materials. . . 151
7.12 Flat sheet sliding test. Tangential force versus number of passes during the sliding tests using a GA steel sheet at different constant normal forces. 154
7.13 Flat sheet sliding test. Tangential force versus number of passes during the sliding tests using a GA steel sheet at different constant normal forces. 155
7.14 Flat sheet sliding test. Tangential force versus number of passes during the sliding tests using a GA steel sheet at different constant normal forces. 156
7.15 Flat sheet sliding test. Tangential force versus number of passes during the sliding tests using a GA steel sheet at different constant normal forces. 157

7.16 Flat sheet sliding test. Wear profile. 158
7.17 Cylindrical aluminiun solidification test. Thermocouple locations in the mould and casting. 159
7.18 Cylindrical aluminium solidification test. Geometry. 160
7.19 Cylindrical aluminiun solidification test. (a) Original and (b) deformed mesh. 163
7.20 Cylindrical aluminiun solidification test. Comparison between computed and experimental results. (a) Temperature evolution at the casting center, casting surface and mould surface. (b) Radial displacement at the casting and mould surfaces. . 164
7.21 Cylindrical aluminiun solidification test. Comparison between isothermal and isentropic operator splits. (a) Temperature evolution at the casting center, casting surface and mould surface. (b) Radial displacement at the casting and mould surfaces. 165
7.22 Cylindrical aluminiun solidification test. Temperature evolution: (a) 10 secs., (b) 20 secs., (c) 40 secs. and (d) 90 secs. . . 166
7.23 Solidification of a RENAULT Clio Crankshaft. (a) Geometry and (b) finite element mesh of the part. 168
7.24 Solidification of a RENAULT Clio Crankshaft. Thermocouples positions. 169
7.25 Solidification of a RENAULT Clio Crankshaft. Material upsetting. 169
7.26 Solidification of a RENAULT Clio Crankshaft. Temperature evolution at different points. 170
7.27 Solidification of a RENAULT Clio Crankshaft. Temperature evolution at different points. 171
7.28 Solidification of a RENAULT Clio Crankshaft. Temperature distribution in the part at different stages of the solidification process. 172
7.29 Solidification of a RENAULT Clio Crankshaft. Temperature distribution on the part surface at different stages of the solidification process. 173
7.30 Solidification of a RENAULT Clio Crankshaft. Temperature evolution at different stages of the solidification process. Section x.-y. 174

7.31 Solidification of a RENAULT Clio Crankshaft. Temperature evolution at different stages of the solidification process. Section x.-z. 175
7.32 Solidification of a RENAULT Clio Crankshaft. Evolution of the mushy zone in sez. x.-y and x-z. 176

Chapter 1

Introduction

The main objective of the research presented in this work is the formulation, analysis and implementation of efficient numerical algorithms for dissipative dynamical systems in solid mechanics. The dissipative structure exhibited by the systems considered is described in detail for the coupled thermoviscoplastic problem including phase change phenomena and extended to the frictional thermomechanical contact problem.

The goal of this initial chapter is to motivate the methodology used in this investigation. A short review of the literature for the problem under consideration is also included, along with a number of issues that were open in the initial stage of this research. This chapter concludes with an overview of the topics treated in this dissertation.

1.1 Motivations and Goals

The numerical simulation of coupled thermo-mechanical solidification processes has been one of the research topics of great interest over the last years. Also, during the last decade, growing interest on this and related topics has been shown by many industrial companies, such as automotive and aeronautical, motivated by the need to get high quality final products and to reduce manufacturing costs. However, and despite the enormous progress achieved lately in the computational mechanics, the large scale numerical simulation of these problems continues to be nowadays a very complex task. This is mainly due to the highly nonlinear nature of the problem, usually involving nonlinear constitutive behavior, liquid-solid, solid-solid phase changes, nonlinear

thermal and mechanical boundary conditions, frictional contact interaction and complex coupled thermo-mechanical phenomena. Hence, an important motivation behind the research presented in this dissertation is to present a possible formulation of the coupled problem consistently derived within a thermodynamic framework followed by a detailed description of its time integration and space discretization. The result is an efficient solution via large-scale numerical simulations of industrial solidification processes arising in the context of solid mechanics.

This work focuses on *dissipative dynamical systems* such as coupled thermoplastic and frictional thermomechanical contact problems. The numerical solution of these systems requires integration strategies in time, referred to as *time-stepping algorithms*. The notion of dissipativity is due to a decay in time of the energy of the system. This notion is closely related to that of *numerical stability* appropriate for this class of problems [Armero & Simo-93]. A large number of different concepts of stability can be found in the numerical analysis literature. The intuitive idea underlying all these concepts can be briefly described as a sort of control in the possible growth of the computed solution due to the numerical errors that inevitably appear in the approximate numerical solution of the problem [Armero & Simo-93]. Given the practical importance of this property, efficiency of an implicit numerical scheme necessarily involves *unconditional stability*, that is the possibility of achieving stability with independence of the time step. The formulation of unconditionally stable algorithms to solve thermomechanical frictional contact problems including phase change phenomena is so the main goal of this work.

1.1.1 Numerical solution of coupled problems

The solution of coupled problems considered consists of an up-to-date finite element numerical model for fully coupled thermomechanical systems, focusing in the simulation of solidification processes of industrial metal parts. The formulation of the governing equations is consistently derived within a thermodynamic context. The proposed constitutive model is defined by a *thermo-viscoelastic-viscoplastic* free energy function which includes a contribution for *multiphase changes*. The continuous transition between the initial fluid-like and the final solid-like behavior of the part is modelled by considering separate deviatoric viscous and elastoplastic responses as a function of the solid fraction. Viscous behavior is based on the Norton law characteristic

of viscous fluids. A particular J2-thermo-viscoplastic algorithm with temperature dependent mechanical and thermal properties has been developed. Nonlinear kinematic and isotropic hardening due to plastic deformation and thermal softening of the yield stress due to the temperature evolution is assumed. Multiphase change contribution is taken into account assuming both the latent heat release and the straining effects during phase changes.

Fractional step methods arising from an operator split of the governing differential equations are considered. Isentropic and isothermal splits are introduced and their nonlinear stability issues is discussed. A key point of the formulation of either the *isentropic* or the *isothermal splits* is the set up of the additional design constraints defining the numerical solution strategy. These additional constraints motivate the definition of a set of variables and nonlinear operators introduced in the present formulation. Within the time discrete setting, the additive operator splits lead to a *product formula algorithms* and to a *staggered solution scheme* of the coupled problem. Finally, the time discrete variational formulations of the coupled problem, using either the isentropic or the isothermal splits are introduced.

1.1.2 Numerical solution of frictional contact problems

The treatment of contact problems using finite elements is currently a research topic of substantial interest. Application of the developing technology include the areas of metal forming, crashworthiness, bulking response of structures, study and prevention of wear, among others. In many (if not all) of these fields, friction plays a noticeable role at the contact interface.

The formulation for the finite element treatment of multibody, large deformation frictional contact problems is presented. The general approach used consists in developing the governing equations in the continuum setting first, before deriving the corresponding finite element equations. In particular, this procedure yields a characterization of the frictional constraint (assuming a generalized Coulomb law) suitable for arbitrary discretization. Of particular interest will be the use of *a-priori stability estimates* to guide the development of integrators for the frictional evolution equations so that *unconditionally stable staggered algorithms* for thermomechanical frictional problem can be defined.

A phenomenological model for frictional contact accounting for *wear effects* is also proposed. The goal is the *generalization of the Coulomb law* to account for a *non linear friction coefficient* assumed to be a function of the

frictional dissipation, in a theory analogous to classical hardening plasticity. Finally, within the computational scheme, a robust algorithm based on the operator split method (elastic predictor - frictional sliding corrector) is used for the numerical integration of the frictional constitutive equations.

1.2 Overview

The work concentrates on the formulation and integration of the coupled thermomechanical problem including the phase change contribution and the frictional contact interaction at the contact interface. This first part is followed by a number of numerical simulation assessing the theoretical results previously obtained.

Chapter-2 defines the coupled thermomechanical problem in solid mechanics. The local governing equations are introduced first (section-2.1). The dissipative structure behind these equations is identified, leading to the formulation of an a-priori stability estimates that play a key role in the time integration schemes presented in chapter-4. The constitutive equations follows by applying Coleman's method to the dissipation inequality defined by the rate of the free energy function introduced to describe the thermo-viscoelastic-viscoplastic behavior (section-2.2). In section 2.3 the evolution laws for the internal variables are obtained by applying the principle of maximum internal dissipation. The equivalent forms of the energy equation are presented in section 2.4 and finally, the weak form of the governing equations is presented in section 2.5.

Chapter-3 deals with the formulation of the contact problem. Section 3.1 introduces the notation and the problem definition. Follow the governing equations defined taking into account the energy and momentum balance at the contact interface (section 3.2) . The constitutive equations and the evolution law are obtained by the definition of a frictional contact free energy function and by the principle of maximum frictional dissipation, in section 3.4 and 3.5, respectively. The wear phenomena is explained in section 3.7. Extension of the a-priori stability estimate to the contact interface is presented in section 3.9 and finally, in section 3.10 the contact contribution to the weak form is given.

Chapter-4 introduces the time integration of the coupled problem. A brief review of the possible time-stepping schemes is presented in section 4.1. The fractional step method and the resulting product formula of the

governing equations of the coupled problem is described in section 4.2. In section 4.3 the time discrete variational formulation is presented for both the isentropic and the isothermal splits. The time-integration of the constitutive equations in case of both the isentropic and isothermal algorithms is shown in section 4.4. Section 4.5 deals with the time integration of the phase change contribution.

Chapter-5 defines the time integration of the contact problem. Section 5.1 describes the local evolution problem while in section 5.2 both the isentropic and the isothermal operator splits are defined. The time-discrete contribution to the weak form of the contact problem is presented in section 5.3. Finally, the isentropic and the isothermal algorithms are given in section 5.4 and 5.5, respectively.

Chapter-6 deals with the space discretization of the coupled thermomechanical problem including the contribution at the contact interface. The Galerkin projection of the variational equations is presented in section 6.1. Section 6.2. describes the mixed approximation known as b-bar projection method used in the discretization of the momentum balance equation. Finally, this chapter concludes with some integration rules specifications.

Chapter-7 shows a number of numerical simulation assessing the theoretical results obtained in the previous chapters.

Chapter-8 includes some concluding remarks summarizing the major results obtained in this work. Suggestion for future research are also presented.

Chapter 2

Formulation of the Coupled Problem

This chapter deals with the formulation of the coupled thermo-mechanical problem. Coupled problems arise frequently in engineering applications. As defined by Zienkiewicz & Taylor [Zienkiewicz-91]: "*coupled systems and formulations are those applicable to multiple domains and dependent variables which describe different physical phenomena and in which neither domain can be solved while separated form the other, and neither set of dependent variables can be eliminated at the differential equations level*".

The formulation of the model has been consistently derived within a thermodynamic framework.

The constitutive behavior has been defined by a thermoplastic free energy function, including a thermal multi-phase change contribution. Plastic response has been modeled considering a J2 thermo-viscoplastic temperature dependent constitutive model, including plastic hardening and thermal softening. Liquid-like behavior has been modeled by a purely viscous model and a smooth transition to the solid-like model has been assumed.

The weak form of the balance equations that governs the coupled problem is presented.

2.1 Local governing equations

The local system of partial differential equations governing the coupled thermo-mechanical problem is defined by the momentum and energy balance equa-

tions, restricted by the inequalities arising from the second law of thermodynamics. This system will be supplemented by suitable constitutive equations. Additionally one must supply prescribed boundary and initial conditions.

2.1.1 General form of the local balance laws

Let $\Omega \in \Re^{dim}$ be the set with smooth boundary $\partial\Omega$ of a continuum body β in the space dimension $\Re^{dim}$. Let $[0, T]$ be the time interval of interest.

The local form of the *balance of momentum equation* also known as *Cauchy's equation of motion* [Malvern-69] ,[Truesdell-65] is given by

$$\nabla \cdot \boldsymbol{\sigma} + \mathbf{b} = \rho_o \frac{d\mathbf{v}}{dt} \tag{2.1}$$

where $\boldsymbol{\sigma}$ is the Cauchy stress tensor, $\nabla \cdot (\circ)$ is the reference divergence operator, $\mathbf{b}$ is the vector of forces per unit of volume, ρ_o is the density in the reference configuration and $\mathbf{v}$ is the velocity field.

The *balance of energy* equation can be written as

$$\dot{E} = \boldsymbol{\sigma} : \dot{\boldsymbol{\varepsilon}} - \nabla \cdot \mathbf{Q} + R \tag{2.2}$$

so that the increase of the internal energy $\dot{E}$ per unit of volume consists of three parts: the stress power $\boldsymbol{\sigma} : \dot{\boldsymbol{\varepsilon}}$ which represents the mechanical work done by the external forces not converted into kinetic energy, the heat supplied by the internal sources per unit of volume R, and the term $-\nabla \cdot \mathbf{Q}$ which is the heat provided by the flow of thermal energy through the boundary into the system. The balance of energy equation is the local form for the *First law of Thermodynamics* [Truesdell-65].

The *Second law of Thermodynamics* limits the direction of the energy transformations and it postulates that there exists a state function called entropy S so that

$$\Delta S = S_2 - S_1 \geq \int_1^2 \frac{dQ}{\Theta} \tag{2.3}$$

where dQ is the heat input during the process, $\Theta > 0$ the absolute temperature and indices 1 and 2 denote the starting and ending points of a thermodynamic process. From equation (2.3) it is seen that the change in entropy of the system for any process can never be negative. It is zero for a *reversible process* if there is no heat inflow to the system and positive for an

irreversible process [Truesdell-65], [Malvern-69], [Khan & Huang-95]. Taking into account that the heat input into the system is given by

$$dQ = R\,dV - \mathbf{Q}\cdot\mathbf{n}\,dS \tag{2.4}$$

then we can define the rate of entropy as

$$\frac{d}{dt}\int_\Omega S\,dV \geq \int_\Omega \frac{R}{\Theta}\,dV - \int_{\partial\Omega}\frac{\mathbf{Q}\cdot\mathbf{n}}{\Theta}\,dS \tag{2.5}$$

where S is now the entropy per unit of volume. This relation is the so called *Clausius-Duhem inequality* [Truesdell-65], [Khan & Huang-95]. Using the divergence theorem

$$\frac{d}{dt}\int_\Omega S\,dV \geq \int_\Omega \frac{R}{\Theta}\,dV - \int_\Omega \nabla\cdot\left(\frac{\mathbf{Q}}{\Theta}\right)\,dV \tag{2.6}$$

Since the choice of volume Ω is arbitrary, the following local form of the Clausius-Duhem inequality is derived as

$$\dot{S} \geq \frac{R}{\Theta} - \nabla\cdot\left(\frac{\mathbf{Q}}{\Theta}\right) \tag{2.7}$$

To covert this inequality into an equation, it is possible to introduce a thermomechanical variable $D \geq 0$ usually referred as *thermomechanical dissipation*, so that

$$D = \Theta\dot{S} - R + \Theta\ \nabla\cdot\left(\frac{\mathbf{Q}}{\Theta}\right) \geq 0 \tag{2.8}$$

Observe that the positiveness of the dissipation term resumes the second law of thermodynamics, in fact, the relation $D \geq 0$ defines the direction allowed in a thermomechanical transformation, so that in case of reversible process $D = 0$, while in case of an irreversible process the dissipation will be strictly positive $D > 0$.

A stronger format for the previous equation (2.8) is given by the following relations

$$D_{int} = \Theta\dot{S} - R + \nabla\cdot\mathbf{Q} \geq 0 \tag{2.9a}$$

$$D_{cond} = -\frac{\mathbf{Q}\nabla\Theta}{\Theta} \geq 0 \tag{2.9b}$$

where D_{int} and D_{cond} are the internal dissipation and the dissipation by conduction, respectively. Equation (2.9*a*) is known in the literature [Truesdell-65] as the *Clausius-Plank equation.* Taking into account the balance of energy equation (2.2) the following format for the Clausius-Plank equation is also available

$$D_{int} = \Theta\dot{S} - \dot{E} + \boldsymbol{\sigma} : \dot{\boldsymbol{\varepsilon}} \geq 0 \tag{2.10}$$

Thus, the first order system of local equations that govern the coupled thermo-mechanical problem is the following

$$\dot{\mathbf{u}} = \mathbf{v} \tag{2.11a}$$
$$\rho_o\dot{\mathbf{v}} = \nabla\cdot\boldsymbol{\sigma} + \mathbf{b} \tag{2.11b}$$
$$\Theta\dot{S} = R - \nabla\cdot\mathbf{Q} + D_{int} \tag{2.11c}$$

restricted by the inequalities arising from the second law of thermodynamics

$$D = D_{int} + D_{cond} \geq 0 \tag{2.12a}$$

$$D_{int} = \Theta\dot{S} - \dot{E} + \boldsymbol{\sigma} : \dot{\boldsymbol{\varepsilon}} \geq 0 \tag{2.12b}$$
$$D_{cond} = -\frac{\mathbf{Q}\nabla\Theta}{\Theta} \geq 0 \tag{2.12c}$$

2.1.2 Additive decomposition

Figure (2.1) shows the rheological model considered for the mechanical behavior. Let's assume an *additive decomposition* of the total strain tensor $\boldsymbol{\varepsilon}$ into its *elastic* and *inelastic* parts $\boldsymbol{\varepsilon}^E$ and $\boldsymbol{\varepsilon}^I$, respectively, that is

$$\boldsymbol{\varepsilon} = \boldsymbol{\varepsilon}^E + \boldsymbol{\varepsilon}^I \tag{2.13}$$

where the elastic strain tensor $\boldsymbol{\varepsilon}^E$ is given by the sum of the effective elastic deformation plus the thermal deformation, $\boldsymbol{\varepsilon}^e$ and $\boldsymbol{\varepsilon}^\theta$, respectively, so that

$$\boldsymbol{\varepsilon}^E = \boldsymbol{\varepsilon}^e + \boldsymbol{\varepsilon}^\theta \tag{2.14}$$

while the inelastic strain tensor involves the viscoelastic and viscoplastic effects

$$\boldsymbol{\varepsilon}^I = \boldsymbol{\varepsilon}^v + \boldsymbol{\varepsilon}^{vp} \tag{2.15}$$

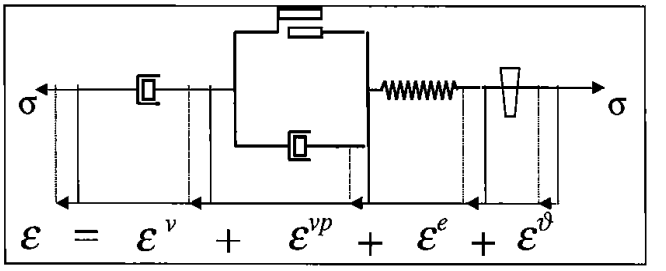

Figure 2.1: Thermo-mechanical rheological model

Another hypothesis is the split of total entropy S into its *elastic* and *inelastic* part, S^E and S^I, respectively, as

$$S = S^E + S^I \tag{2.16}$$

It is now possible to write in a new format the energy equation (2.9*a*) using the elastic entropy S^E as the state variable

$$\Theta \dot{S}^E = R - \nabla \cdot \mathbf{Q} + D_{mech} \tag{2.17a}$$

where the decomposition of the internal dissipation D_{int} into *mechanical* and *thermal* part, D_{mech} and D_{ther}, respectively, is assumed

$$D_{int} = D_{mech} + D_{ther} \geq 0 \tag{2.18}$$

so that the thermal dissipation results in

$$D_{ther} = \Theta \dot{S}^I \tag{2.19}$$

Taking care of previous assumptions, the first order system of local equations that governs the coupled thermo-mechanical problem is the following [Armero-Thesis-93], [Complas-97], [Alaska-97]

$$\dot{\mathbf{u}} = \mathbf{v} \tag{2.20a}$$
$$\rho_o \dot{\mathbf{v}} = \nabla \cdot \boldsymbol{\sigma} + \mathbf{b} \tag{2.20b}$$
$$\Theta \dot{S}^E = R - \nabla \cdot \mathbf{Q} + D_{mech} \tag{2.20c}$$

restricted by the following inequalities

$$D = D_{mech} + D_{ther} + D_{cond} \geq 0 \tag{2.21a}$$

$$D_{mech} = \Theta \dot{S}^E - \dot{E} + \boldsymbol{\sigma} : \dot{\boldsymbol{\varepsilon}} \geq 0 \tag{2.21b}$$

$$D_{ther} = \Theta \dot{S}^I \tag{2.21c}$$

$$D_{cond} = -\frac{\mathbf{Q} \nabla \Theta}{\Theta} \geq 0 \tag{2.21d}$$

together with the boundary conditions

$$\begin{array}{rcl} \mathbf{u} = \bar{\mathbf{u}} & \text{on} & \partial\Omega_u \times [0,T] \\ \boldsymbol{\sigma} \cdot \mathbf{n} = \bar{\mathbf{t}} & \text{on} & \partial\Omega_t \times [0,T] \\ \Theta = \bar{\Theta} & \text{on} & \partial\Omega\theta \times [0,T] \\ \mathbf{Q} \cdot \mathbf{n} = \mathbf{q}_n & \text{on} & \partial\Omega_q \times [0,T] \end{array} \tag{2.22}$$

and the initial conditions

$$\begin{array}{rcl} \mathbf{u} = \mathbf{u}_o & \text{in} & \Omega \times [0] \\ \mathbf{v} = \mathbf{v}_o & \text{in} & \Omega \times [0] \\ \Theta = \Theta_o & \text{in} & \Omega \times [0] \end{array} \tag{2.23}$$

2.1.3 A-priori stability estimate

The central issue in the analysis of algorithms for coupled problems concerns the appropriate notion of nonlinear stability. The goal of this section is to describe the dissipative structure behind the thermo-mechanical problem [Armero & Simo-93].

Let $L(\mathbf{u}, \mathbf{v}, \Theta)$ be a functional given by

$$L(\mathbf{u}, \mathbf{v}, \Theta) = \int_\Omega \left(E - \Theta_o S^E + \frac{1}{2} \rho_o \mathbf{v}^2 \right) dV + V_{ext}(\mathbf{u}) \tag{2.24}$$

where $V_{ext}(\mathbf{u})$ is the potential energy function associated to the external mechanical loads

$$\frac{d}{dt} V_{ext}(\mathbf{u}) = -\int_\Omega \mathbf{v} \cdot \mathbf{b} \, dV - \int_{\partial\Omega} \mathbf{v} \cdot \bar{\mathbf{t}} \, dS \tag{2.25}$$

If we assume that no external heat sources are present, i.e., $R = 0$, and that the thermal boundary conditions (2.22) are such that

$$(\Theta_o - \Theta) \, \mathbf{Q} \cdot \mathbf{n} = 0 \quad \text{on} \quad \partial\Omega \times [0,T] \tag{2.26}$$

then the a-priori stability estimate provides that [Armero-Thesis-93]

$$\frac{d}{dt}L(\mathbf{u},\mathbf{v},\Theta) \leq 0 \quad \text{in} \quad \Omega \times [0,T] \tag{2.27}$$

so that the nonlinear stability is ensured if $L(\mathbf{u},\mathbf{v},\Theta)$ is a non-increasing Lyapunov-like function along the flow generated by the thermo-plastic problem [Coleman & Dill-73], [Armero-Thesis-93].

The rate of change of $L(\mathbf{u},\mathbf{v},\Theta)$ along the dynamics generated by the coupled problem is computed as

$$\frac{d}{dt}L(\mathbf{u},\mathbf{v},\Theta) = \int_\Omega \left(\dot{E} - \Theta_o \dot{S}^E + \rho_o \mathbf{v}\cdot\dot{\mathbf{v}}\right) dV - \int_\Omega \mathbf{v}\cdot\mathbf{b}\, dV - \int_{\partial\Omega} \mathbf{v}\cdot\bar{\mathbf{t}}\, dS \tag{2.28}$$

If we remember the relation existing between the traction vector $\mathbf{t}$ and the Cauchy stress tensor $\boldsymbol{\sigma}$, that is $\bar{\mathbf{t}} = \boldsymbol{\sigma}\cdot\mathbf{n}$ then the last term in equation (2.28) can be developed as

$$\begin{aligned}\int_{\partial\Omega} \mathbf{v}\cdot\mathbf{t}\, dS &= \int_{\partial\Omega} \mathbf{v}\cdot(\boldsymbol{\sigma}\cdot\mathbf{n})\, dS = \int_\Omega \nabla\cdot(\mathbf{v}\cdot\boldsymbol{\sigma})\, dV \\ &= \int_\Omega \mathbf{v}\cdot(\nabla\cdot\boldsymbol{\sigma})\, dV + \int_\Omega \nabla\mathbf{v} : \boldsymbol{\sigma}\, dV = \cdots\end{aligned} \tag{2.29}$$

and taking into account that the gradient of the velocity field is equal to the rate of strain tensor $\dot{\boldsymbol{\varepsilon}}$, that is $\nabla\mathbf{v} = \dot{\boldsymbol{\varepsilon}}$, then it is possible to follow developing the above equation as

$$\cdots = \int_\Omega \mathbf{v}\cdot(\nabla\cdot\boldsymbol{\sigma})\, dV + \int_\Omega (\boldsymbol{\sigma} : \dot{\boldsymbol{\varepsilon}})\, dV \tag{2.30}$$

Substituting (2.30) within equation (2.28) then

$$\begin{aligned}\frac{d}{dt}L(\mathbf{u},\mathbf{v},\Theta) &= \int_\Omega \mathbf{v}\cdot(\rho_o\dot{\mathbf{v}} - \nabla\cdot\boldsymbol{\sigma} - \mathbf{b})\, dV \\ &\quad + \int_\Omega \left(\dot{E} - \Theta_o \dot{S}^E - \boldsymbol{\sigma} : \dot{\boldsymbol{\varepsilon}}\right) dV\end{aligned} \tag{2.31}$$

If we take into account equations (2.20b) and (2.21b) then it results

$$\frac{d}{dt}L(\mathbf{u},\mathbf{v},\Theta) = \int_\Omega \left[(\Theta - \Theta_o)\, \dot{S}^E - D_{mech}\right] dV \tag{2.32}$$

Making use of equation (2.20c) and using Green's formula along with the thermal boundary conditions then

$$\frac{d}{dt}L(\mathbf{u},\mathbf{v},\Theta) = -\int_\Omega \left[D_{mech} + \left(\frac{\Theta-\Theta_o}{\Theta}\right)(\nabla\cdot\mathbf{Q} - D_{mech})\right] dV \quad (2.33)$$

$$= -\int_\Omega \left[\left(\frac{\Theta_o}{\Theta}\right) D_{mech} - \nabla\left(\frac{\Theta-\Theta_o}{\Theta}\right)\cdot\mathbf{Q}\right] dV$$

$$-\int_{\partial\Omega}\left(\frac{\Theta-\Theta_o}{\Theta}\right)\mathbf{Q}\cdot\mathbf{n}\,dS \quad (2.34)$$

$$= -\int_\Omega \left(\frac{\Theta_o}{\Theta}\right)\left[D_{mech} - \frac{\nabla\Theta\cdot\mathbf{Q}}{\Theta}\right] dV \quad (2.35)$$

Taking into account the expression of the dissipation by conduction (2.21d), we finally obtain

$$\frac{d}{dt}L(\mathbf{u},\mathbf{v},\Theta) = -\int_\Omega \frac{\Theta_o}{\Theta}(D_{mech} + D_{cond})\,dV \leq 0 \quad (2.36)$$

This condition is regarded as a fundamental a-priori estimate for the thermo-viscoplastic evolution problem which must be preserved by the time-stepping algorithm [Armero & Simo-92], [Armero-Thesis-93], [Armero & Simo-92].

2.2 Constitutive equations

In thermodynamics the internal energy E, entropy S and the Cauchy stress tensor $\boldsymbol{\sigma}$ are all considered state functions that can be determined by the state variables. The formulas that relate the state functions to the state variables are called *state equations* or *constitutive equations*.

2.2.1 Coleman's method

In case of thermo-elasticity one can expect that the state variables would be the stain tensor $\boldsymbol{\varepsilon}$ and the temperature field Θ since the state function S and $\boldsymbol{\sigma}$ are determined completely by the their current values. Thus, for an ideal thermo-elastic behavior

$$S = S(\boldsymbol{\varepsilon},\Theta) \quad (2.37a)$$

$$\boldsymbol{\sigma} = \boldsymbol{\sigma}(\boldsymbol{\varepsilon},\Theta) \quad (2.37b)$$

The situation becomes much more complex if inelastic deformations can occur. For example, stresses of a plastically deformed body cannot be determined by the current value of the deformation $\boldsymbol{\varepsilon}$ only. The history of the deformation is also necessary so that simple constitutive equation, such as (2.37*b*), cannot describe correctly the plastic deformation of solids. If S and $\boldsymbol{\sigma}$ are assumed to be state functions, we face two fundamental problems. First, we have to find or specify the set of the state variables that uniquely define the current state. Second, the mathematical forms of the constitutive equations should be determined after the state variables are chosen. This involves the experimental evaluation and the mathematical formalization.

To solve the problem of specifying state variables, two different methods are usually adopted. The first method ignores the problem of state variables and assume that S and $\boldsymbol{\sigma}$ are determined by the histories of $\boldsymbol{\varepsilon}$ and Θ, and not by their current values only [Coleman-64]. Therefore these quantities should be expressed as the functionals, not functions, of $\boldsymbol{\varepsilon}$ and Θ. The second method introduces the concept of internal variables [Coleman-67]. In this method it is postulated that the current state of an inelastically deformed solid can be determined by the current values of $\boldsymbol{\varepsilon}$ and Θ as well as a set of internal variables. The history of the deformation is indirectly included in the evolution of these internal variables. Since the state functions can be expressed by

$$S = S\left(\boldsymbol{\varepsilon}, \boldsymbol{\varepsilon}^I, \boldsymbol{\alpha}^I, \Theta\right) \tag{2.38a}$$

$$\boldsymbol{\sigma} = \boldsymbol{\sigma}\left(\boldsymbol{\varepsilon}, \boldsymbol{\varepsilon}^I, \boldsymbol{\alpha}^I, \Theta\right) \tag{2.38b}$$

where $\boldsymbol{\varepsilon}^I$ is the inelastic strain tensor and $\boldsymbol{\alpha}^I$ is a set of generic internal variable that defines the material behavior. The specific meaning for each internal variable and the actual number need to be chosen and identified for different materials and different conditions. Different choices result in different constitutive models.

Taking into account the additive decomposition of the strain tensor (2.13), usually the state functions are defined in term of the elastic deformation $\boldsymbol{\varepsilon}^E = \boldsymbol{\varepsilon} - \boldsymbol{\varepsilon}^I$, and considering equation (2.21*b*) it is possible to replace the total entropy with the elastic entropy as the primary variable to define the energy equation, so that the choice of the state functions and state variable that define the coupled problem when inelastic deformation can occur results in

$$S^E = S^E\left(\boldsymbol{\varepsilon} - \boldsymbol{\varepsilon}^I, \boldsymbol{\alpha}^I, \Theta\right) = S^E\left(\boldsymbol{\varepsilon}^E, \boldsymbol{\alpha}^I, \Theta\right) \tag{2.39a}$$

$$\boldsymbol{\sigma} = \boldsymbol{\sigma}\left(\boldsymbol{\varepsilon} - \boldsymbol{\varepsilon}^I, \boldsymbol{\alpha}^I, \Theta\right) = \boldsymbol{\sigma}\left(\boldsymbol{\varepsilon}^E, \boldsymbol{\alpha}^I, \Theta\right) \tag{2.39b}$$

In what follows *Coleman's method* is used to obtain the constitutive equations that characterize the material behavior. Let $\Psi\left(\boldsymbol{\varepsilon}^E, \boldsymbol{\alpha}^I, \Theta\right)$ be the *Helmholtz free energy function* (per unit reference volume) obtained from the internal energy $E\left(S^E, \boldsymbol{\varepsilon}^E, \boldsymbol{\alpha}^I\right)$ by the Legendre transform

$$\Psi = E - \Theta S^E \tag{2.40}$$

so that its rate is

$$\dot{\Psi} = \dot{E} - \dot{\Theta} S^E - \Theta \dot{S}^E \tag{2.41}$$

and using equation (2.21*b*) we can also write

$$\dot{\Psi} = \boldsymbol{\sigma} : \dot{\boldsymbol{\varepsilon}} - \dot{\Theta} S^E - D_{mech} \tag{2.42}$$

If we differentiate the free energy function with respect to the state variables we obtain

$$\begin{aligned} \dot{\Psi} &= \frac{\partial \Psi}{\partial \boldsymbol{\varepsilon}^E} : \dot{\boldsymbol{\varepsilon}}^E + \frac{\partial \Psi}{\partial \boldsymbol{\alpha}^I} : \dot{\boldsymbol{\alpha}}^I + \frac{\partial \Psi}{\partial \Theta}\dot{\Theta} \\ &= \frac{\partial \Psi}{\partial \boldsymbol{\varepsilon}^E} : \dot{\boldsymbol{\varepsilon}} - \frac{\partial \Psi}{\partial \boldsymbol{\varepsilon}^E} : \dot{\boldsymbol{\varepsilon}}^I + \frac{\partial \Psi}{\partial \boldsymbol{\alpha}^I} : \dot{\boldsymbol{\alpha}}^I + \frac{\partial \Psi}{\partial \Theta}\dot{\Theta} \end{aligned} \tag{2.43}$$

From equations (2.42) and (2.43) it is possible to obtain the following inequality

$$D_{mech} = \left(\boldsymbol{\sigma} - \frac{\partial \Psi}{\partial \boldsymbol{\varepsilon}^E}\right) : \dot{\boldsymbol{\varepsilon}} - \left(S^E + \frac{\partial \Psi}{\partial \Theta}\right)\dot{\Theta} + \frac{\partial \Psi}{\partial \boldsymbol{\varepsilon}^E} : \dot{\boldsymbol{\varepsilon}}^I - \frac{\partial \Psi}{\partial \boldsymbol{\alpha}^I} : \dot{\boldsymbol{\alpha}}^I \geq 0 \tag{2.44}$$

Applying Coleman's method [Coleman-64], we obtain the definition of the constitutive equations as

$$\boldsymbol{\sigma} = \frac{\partial \Psi\left(\boldsymbol{\varepsilon}^E, \boldsymbol{\alpha}^I, \Theta\right)}{\partial \boldsymbol{\varepsilon}^E} \tag{2.45a}$$

$$S^E = -\frac{\partial \Psi\left(\boldsymbol{\varepsilon}^E, \boldsymbol{\alpha}^I, \Theta\right)}{\partial \Theta} \tag{2.45b}$$

where the internal dissipation is given by

$$D_{mech} = \boldsymbol{\sigma} : \dot{\boldsymbol{\varepsilon}}^I + \boldsymbol{\beta}^I : \dot{\boldsymbol{\alpha}}^I \geq 0 \tag{2.46}$$

being for definition

$$\boldsymbol{\beta}^I = -\frac{\partial \Psi\left(\boldsymbol{\varepsilon}^E, \boldsymbol{\alpha}^I, \Theta\right)}{\partial \boldsymbol{\alpha}^I} \tag{2.47}$$

Equation (2.46) is known in the literature as *the reduced equation of dissipation.*

2.2.2 Definition of the free energy function

We have seen how it is possible to formulate and obtain the constitutive equation that govern the thermo-mechanical problem starting from the definition of the potential $\Psi\left(\boldsymbol{\varepsilon}^E, \Theta, \boldsymbol{\alpha}^I\right)$. A possible choice of the set of internal variables to particularize the free energy function to the case of thermo-viscoplastic behavior is given by $\boldsymbol{\alpha}^I = [\xi, \boldsymbol{\zeta}]$, that is the isotropic and kinematic hardening variables, respectively. Thus, a possible format of the free energy function $\Psi = \Psi\left(\boldsymbol{\varepsilon}^E, \Theta, \boldsymbol{\zeta}, \xi\right)$ is given as the sum of following contributions

$$\Psi = \Psi\left(\boldsymbol{\varepsilon}^E, \Theta, \boldsymbol{\zeta}, \xi\right) = W\left(\boldsymbol{\varepsilon}^E\right) + M\left(\boldsymbol{\varepsilon}^E, \Theta\right) + T\left(\Theta\right) + K\left(\boldsymbol{\zeta}, \xi, \Theta\right) \tag{2.48}$$

where $W\left(\boldsymbol{\varepsilon}^E, \Theta\right)$, $M\left(\boldsymbol{\varepsilon}^E, \Theta\right)$, $T\left(\Theta\right)$ and $K\left(\boldsymbol{\zeta}, \xi, \Theta\right)$ are the elastic stored energy, the coupling potential, the thermal potential and the plastic hardening potential, respectively [Agelet-97], [Alaska-97], [Buenos-Aires-98], [SanDiego-98], [Cancun-99]. The expressions chosen here for these terms are the following

$$W\left(\boldsymbol{\varepsilon}^E, \Theta\right) = \frac{1}{2} k\left(\Theta\right) tr^2\left(\boldsymbol{\varepsilon}^E\right) + \bar{G}\left(\Theta\right) dev^2\left(\boldsymbol{\varepsilon}^E\right) \tag{2.49a}$$

$$M\left(\boldsymbol{\varepsilon}^E, \Theta\right) = -k\left(\Theta\right) e^{\theta}\left(\Theta\right) \boldsymbol{\varepsilon}^E : \mathbf{1} \tag{2.49b}$$

$$T\left(\Theta\right) = -\int_{\Theta_o}^{\Theta} d\bar{\Theta} \int_{\Theta_o}^{\bar{\Theta}} \frac{C_v\left(\hat{\Theta}\right)}{\hat{\Theta}} d\hat{\Theta} \tag{2.49c}$$

$$K\left(\boldsymbol{\zeta}, \xi, \Theta\right) = \left[\sigma_\infty\left(\Theta\right) - \sigma_o\left(\Theta\right)\right]\left[\xi - \frac{1 - exp\left(-\delta\xi\right)}{\delta}\right] + \frac{1}{2} H\left(\Theta\right) \xi^2 + \frac{1}{3} K\left(\Theta\right) \left\|\boldsymbol{\zeta}\right\|^2 \tag{2.49d}$$

where $k\left(\Theta\right)$ is the bulk modulus, $\alpha\left(\Theta\right)$ the thermal volumetric-change coefficient, Θ_o the initial temperature field, $C_v\left(\Theta\right)$ the heat capacity at constant volume (without including the phase change contribution), $\sigma_o\left(\Theta\right)$ the initial flow stress, $\sigma_\infty\left(\Theta\right)$ the saturation hardening limit, $H\left(\Theta\right)$ the linear isotropic hardening coefficient, $K\left(\Theta\right)$ the linear kinematic hardening coefficient and finally $\mathbf{1} = \delta_{ij} \mathbf{e}_i \otimes \mathbf{e}_j$ the rank-two symmetric unit tensor.

A modified shear modulus $\bar{G}\left(\Theta\right)$ is considered to remove the deviatoric elastic potential in the liquid-like phase. This modified shear modulus takes the form

$$\bar{G}\left(\Theta\right) = \frac{G\left(\Theta\right)}{f_S\left(\Theta\right)} \tag{2.50}$$

where $G(\Theta)$ is the standard temperature dependent shear modulus and $f_S(\Theta)$ represents the solid-fraction function.

Term $e^{\theta}(\Theta)$ is the volumetric thermal deformation and it is defined as

$$e^{\theta}(\Theta) = 3\left[\alpha(\Theta)(\Theta - \Theta_{ref}) - \alpha(\Theta_o)(\Theta_o - \Theta_{ref})\right] \tag{2.51}$$

where the reference temperature Θ_{ref} is the environment temperature during the experimental evaluation of the dilatation coefficient $\alpha(\Theta)$.

This given, the constitutive equations that govern the coupled problem result in

$$\boldsymbol{\sigma} = \frac{\partial \Psi}{\partial \boldsymbol{\varepsilon}^E} = k(\Theta)\left[tr\left(\boldsymbol{\varepsilon}^E\right) - e^{\theta}(\Theta)\right]\mathbf{1} + 2\bar{G}(\Theta)\, dev\left(\boldsymbol{\varepsilon}^E\right) \tag{2.52a}$$

$$S^E = -\frac{\partial \Psi}{\partial \Theta} = \int_{\Theta_o}^{\Theta} \frac{C_v\left(\hat{\Theta}\right)}{\hat{\Theta}} d\hat{\Theta} - W_{\Theta} - M_{\Theta} - K_{\Theta} \tag{2.52b}$$

being

$$W_{\Theta} = \frac{1}{2} k_{\Theta}\, tr^2\left(\boldsymbol{\varepsilon}^E\right) + \bar{G}_{\Theta}\, dev^2\left(\boldsymbol{\varepsilon}^E\right) \tag{2.53}$$

$$\begin{aligned} M_{\Theta} = {} & -3\{\alpha(\Theta)\, k(\Theta) + [\alpha_{\Theta}\, k(\Theta) + \alpha(\Theta)\, k_{\Theta}](\Theta - \Theta_{ref}) \\ & -\alpha(\Theta_o)\, k_{\Theta}(\Theta_o - \Theta_{ref})\}\, tr\left(\boldsymbol{\varepsilon}^E\right) \end{aligned} \tag{2.54}$$

$$\begin{aligned} K_{\Theta} = {} & (\sigma_{\infty,\Theta} - \sigma_{o,\Theta})\left[\xi - \frac{1 - exp(-\delta\xi)}{\delta}\right] \\ & + \frac{1}{2} H_{\Theta}\xi^2 + \frac{1}{3} K_{\Theta} \|\boldsymbol{\zeta}\|^2 \end{aligned} \tag{2.55}$$

where $(\circ)_{\Theta}$ represents the derivative of the argument with respect to the temperature field.

If we define the volumetric elastic strain as

$$e^e = tr\left(\boldsymbol{\varepsilon}^E\right) - e^{\theta}(\Theta) \tag{2.56}$$

then the definition of the stress tensor results in

$$\boldsymbol{\sigma} = p\mathbf{1} + \mathbf{s} \tag{2.57a}$$

$$p = k(\Theta)\, e^e \tag{2.57b}$$

$$\mathbf{s} = 2\bar{G}(\Theta)\, dev\left(\boldsymbol{\varepsilon}^e\right) \tag{2.57c}$$

where $p = \frac{1}{3} tr(\boldsymbol{\sigma})$ and $\mathbf{s} = dev(\boldsymbol{\sigma})$ are the pressure and the deviator of the stress tensor, respectively.

The mechanical dissipation is obtained as

$$D_{mech} = \boldsymbol{\sigma} : \dot{\boldsymbol{\varepsilon}}^{v} + \boldsymbol{\sigma} : \dot{\boldsymbol{\varepsilon}}^{vp} + q\dot{\xi} + \mathbf{q} : \dot{\boldsymbol{\zeta}} \geq 0 \tag{2.58}$$

where the state variables q and $\mathbf{q}$ are defined as the derivatives of the free energy function with respect to ξ and $\boldsymbol{\zeta}$, respectively, so that

$$q = -\frac{\partial \Psi}{\partial \xi} = -K_{\xi} \tag{2.59a}$$

$$\mathbf{q} = -\frac{\partial \Psi}{\partial \boldsymbol{\zeta}} = -\frac{2}{3} K \boldsymbol{\zeta} \tag{2.59b}$$

where

$$K_{\xi} = [\sigma_{\infty}(\Theta) - \sigma_{o}(\Theta)][1 - exp(-\delta\xi)] + H(\Theta)\xi \tag{2.60}$$

Finally, let's introduce in this section the *Fourier's law* as the constitutive law that governs the heat flux, so that

$$\mathbf{Q} = -\mathbf{k}(\Theta) \nabla\Theta \tag{2.61}$$

where $\mathbf{k}(\Theta) = k(\Theta)\ \mathbf{1}$ is the conductivity tensor. Note that due to the restriction on the dissipation by conduction (2.21*d*) it results

$$D_{cond} = -\frac{\mathbf{Q}\nabla\Theta}{\Theta} \geq 0 \quad \Rightarrow \quad k(\Theta) \geq 0 \tag{2.62}$$

Remark 1 *In case of constant heat capacity coefficient the thermal potential* $T(\Theta)$ *can be expressed by*

$$T(\Theta) = C_{v}\left[(\Theta - \Theta_{o}) - \Theta \ln\left(\frac{\Theta}{\Theta_{o}}\right)\right]$$

therefore, the definition of the elastic entropy changes in

$$S^{E} = -\frac{\partial \Psi}{\partial \Theta} = C_{v} \ln\left(\frac{\Theta}{\Theta_{o}}\right) - W_{\Theta} - M_{\Theta} - K_{\Theta}$$

Remark 2 *Due to the fact that usually the material properties are input as piece-wise functions then the second derivatives are assumed to be zero and only the first derivatives are taken into account.*

2.2.3 Phase Change Contributions

In this section the formulation of the coupled problem is extended to take into account the phase chance contribution. Two are the main effects that we want to consider: the *latent heat release* and the *straining* during the phase changes.

Latent heat release

The latent heat release can be defined as the product between the total amount of latent heat L and a particular function $f_S(\Theta)$ that controls the heat flow during the phase change process, so that

$$L(\Theta) = L\, f_S(\Theta) \tag{2.64}$$

$L(\Theta)$ is the so called *latent heat function* [Celentano-94]. In case of a single phase change $f_S(\Theta)$ represents the *solid-fraction function* so that the latent heat will be released (or absorbed) depending on the fraction of solid existing in the considered volume. This function takes the form

$$f_S(\Theta) = \begin{cases} 0 & \text{if} \quad \Theta \geq \Theta_L \\ 0 \leq f_S(\Theta) \leq 1 & \text{if} \quad \Theta_S < \Theta < \Theta_L \\ 1 & \text{if} \quad \Theta \leq \Theta_S \end{cases} \tag{2.65}$$

where Θ_L and Θ_S are the liquid and solid temperature, respectively.

If we assume the more general case of multi-phase-changes then the latent heat function can be written as

$$L(\Theta) = \sum_{k=1}^{NPC} L^{(k)}\, f_P^{(k)}(\Theta) \tag{2.66}$$

where $L^{(k)}$ are the different amounts of latent heat to be released during the NPC phase changes and $f_P^{(k)}(\Theta)$ are the associated phase-fraction functions.

To account for this contribution, the definition of the free energy function must be modified adding a new term $\Psi^{pc}(\Theta)$ related to the rate of latent heat released during the phase change, so that

$$\hat{\Psi}\left(\boldsymbol{\varepsilon}^E, \Theta, \boldsymbol{\zeta}, \xi\right) = \Psi\left(\boldsymbol{\varepsilon}^E, \Theta, \boldsymbol{\zeta}, \xi\right) + \Psi^{pc}(\Theta) \tag{2.67}$$

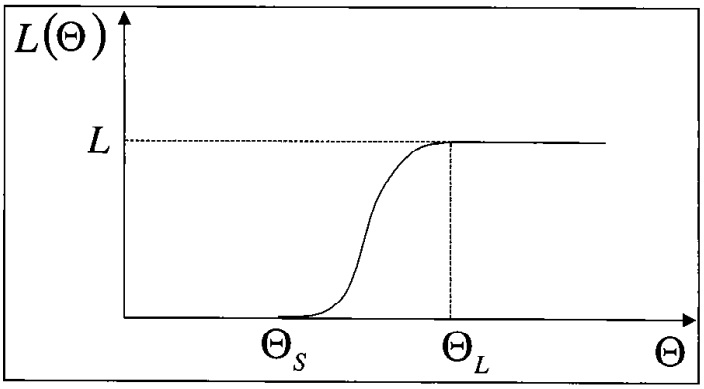

Figure 2.2: Latent heat function

where $\Psi\left(\varepsilon^E, \Theta, \zeta, \xi\right)$ corresponds to the previous definition of the free energy function without including the phase change contribution while $\Psi^{pc}(\Theta)$ can be assumed in the integral form as

$$\Psi^{pc}(\Theta) = -\int_{\Theta_o}^{\Theta} d\bar{\Theta} \int_{\Theta_o}^{\bar{\Theta}} \frac{L_\Theta}{\hat{\Theta}} d\hat{\Theta} \tag{2.68}$$

where $L_\Theta = dL/d\Theta$.

As a consequence of this assumption the definition of the elastic entropy must be modified, so that

$$\hat{S}^E = -\frac{\partial \hat{\Psi}}{\partial \Theta} = -\left(\frac{\partial \Psi}{\partial \Theta} + \frac{\partial \Psi^{pc}}{\partial \Theta}\right) \tag{2.69}$$

so that it is possible to identify two different contributions to the elastic entropy function, respectively given by

$$S^E = -\frac{\partial \Psi}{\partial \Theta} = \int_{\Theta_o}^{\Theta} \frac{C_v\left(\hat{\Theta}\right)}{\hat{\Theta}} d\hat{\Theta} - W_\Theta - M_\Theta - K_\Theta \tag{2.70a}$$

$$S^{pc} = -\frac{\partial \Psi^{pc}}{\partial \Theta} = \int_{\Theta_o}^{\Theta} \frac{L_\Theta}{\hat{\Theta}} d\hat{\Theta} \tag{2.70b}$$

Thus, the total entropy function is now given by the sum of following contributions

$$S = S^E + S^I + S^{pc} \tag{2.71a}$$

or

$$S = \hat{S}^E + S^I \tag{2.71b}$$

Observing that it is verified the following equation

$$\Theta \dot{S}^{pc} = \dot{L} \tag{2.72}$$

that relates the rate of latent heat released to the rate of entropy associated to the phase change contribution, then the balance of energy law accounting for the phase change contribution can be enforced in the equivalent form by the following system of equations

$$\Theta \dot{S}^E = R - \nabla \cdot \mathbf{Q} + D_{mech} - \dot{L} \tag{2.73a}$$

$$\Theta \dot{S}^I = D_{ther} \tag{2.73b}$$

$$\Theta \dot{S}^{pc} = \dot{L} \tag{2.73c}$$

or alternatively by

$$\Theta \dot{\hat{S}}^E = R - \nabla \cdot \mathbf{Q} + D_{mech} \tag{2.74a}$$

$$\Theta \dot{S}^I = D_{ther} \tag{2.74b}$$

Straining during phase change

The straining during phase change is a particular volumetric contraction or dilatation that occurs when the material is changing its internal structure (see figure (2.3)). Its direct consequence is the modification of the volumetric thermal deformation e^{θ} (Θ) to accounts for this effect. Using the same notation presented in the above section, the evolution law of the straining term can be defined as [Celentano-94],

$$\dot{e}^{pc}(\Theta) = \sum_{k=1}^{NPC} \frac{\Delta V^{(k)}}{V_o} \dot{f}_P^{(k)}(\Theta) \tag{2.75}$$

where V_o is the volume at the initial temperature and $\Delta V^{(k)}$ the total volume change observed for the k^{th} phase change.

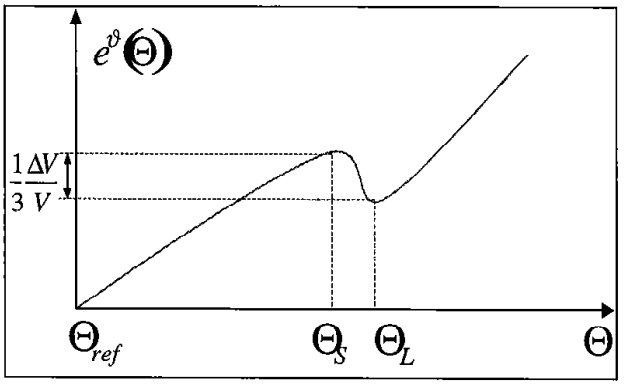

Figure 2.3: Thermal deformation including straining contribution

This given, the volumetric thermal deformation results in the following expression

$$\begin{aligned} e^{\theta}(\Theta) &= 3\left[\alpha(\Theta)(\Theta-\Theta_{ref})-\alpha(\Theta_o)(\Theta_o-\Theta_{ref})\right] \\ &\quad +\left[e^{pc}(\Theta)-e^{pc}(\Theta_o)\right] \end{aligned} \tag{2.76a}$$

where it is possible to observe that the evolution law (2.75) has been integrated between the initial and the current temperature field, Θ_o and Θ, respectively [Buenos-Aires-98].

Note that, due to the new definition of the volumetric thermal deformation, the evaluation of elastic entropy S^E must change according to the new value of term M_Θ that depends on the derivative of e^{θ} with respect to Θ.

2.3 Evolution laws

The formulation of the coupled thermo-mechanical model is completed by specifying the evolution equations of the inelastic quantities previously introduced.

2.3.1 Introduction

The basic idea is to try to formulate a model the closest as possible to the experimental observation. The main difficulty is the very different behavior of the liquid phase compared with the solid phase. The liquid phase is characterized by a purely viscous behavior so that both the elastic and the plastic deformation must be neglected. On the other hand, when the material is solid a standard elastic-viscoplastic behavior should be taken into account.

In the literature there are different models to simulate the liquid-like behavior [Bellet-93], [Fortin-85], [Celentano-94]. In the following section two classical models are introduced.

Modified shear modulus model [Celentano-94]. Let Θ_L and Θ_S be the liquid and the solid phase change temperature, respectively. The idea consists of reducing to zero the deviatoric part of the stress tensor $\mathbf{s} = dev(\boldsymbol{\sigma})$ in the liquid phase. This is obtained assuming a modified shear modulus $\bar{G}(\Theta)$ depending on the fraction of solid $f_S(\Theta)$, in the following form

$$\bar{G}(\Theta) = \begin{cases} 0 & \text{if} \quad \Theta \geq \Theta_L \\ 0 \leq f_S(\Theta)\, G(\Theta_S) \leq G(\Theta_S) & \text{if} \quad \Theta_S < \Theta < \Theta_L \\ G(\Theta) & \text{if} \quad \Theta \leq \Theta_S \end{cases} \tag{2.77}$$

In the hypothesis of an elasto-plastic constitutive model the stress tensor is so computed as

$$\begin{aligned} \boldsymbol{\sigma} &= p\mathbf{1} + \bar{\mathbf{s}} \\ p &= k(\Theta)\, e^e \\ \bar{\mathbf{s}} &= 2\bar{G}(\Theta)\, dev(\boldsymbol{\varepsilon} - \boldsymbol{\varepsilon}^p) = f_S(\Theta)\, \mathbf{s} \end{aligned} \tag{2.78}$$

This model is very easy to implement, in fact it requires only the evaluation of the solid-fraction function $f_S(\Theta)$ to modify the value of the shear modulus in the liquid-like phase. On the other hand it must be noted that the deformation occurred during the liquid phase or in the mushy zone is elastic and not inelastic (irreversible). In fact, when the temperature drops to the solid limit Θ_S the shear modulus recovers its value and in the hypothesis of an hyperelastic constitutive model, the stresses due to the deviatoric deformation are recovered and not dissipated through a viscous process.

Degenerated visco-plastic model. In this case the main idea is to use a standard viscoplastic model reducing the radius of the von Mises cylinder

$R(q,\Theta)$ according to the solid-fraction function $f_S(\Theta)$, that is

$$\bar{R}(q,\Theta) = \begin{cases} 0 & \text{if} \quad \Theta \geq \Theta_L \\ 0 \leq f_S(\Theta)\, R(q,\Theta_S) \leq R(q,\Theta) & \text{if} \quad \Theta_S < \Theta < \Theta_L \\ R(q,\Theta) & \text{if} \quad \Theta \leq \Theta_S \end{cases} \tag{2.79}$$

Note that if $\Theta \geq \Theta_L$ the viscoplastic potential $\Phi(\mathbf{s},q,\Theta)$ associated to the viscoplastic model degenerate in a purely-viscous potential

$$\Phi(\mathbf{s},q) = \|\mathbf{s}\| - R(q,\Theta) \rightarrow \|\mathbf{s}\| \tag{2.80}$$

The evolution of the plastic multiplier transforms into

$$\gamma = \frac{1}{\eta}\ \langle \Phi(\mathbf{s},q) \rangle \rightarrow \gamma = \frac{1}{\eta}\ \|\mathbf{s}\| \tag{2.81}$$

so that

$$\dot{\boldsymbol{\varepsilon}}^{vp} = \gamma \mathbf{n} = \frac{1}{\eta}\, \mathbf{s} \tag{2.82}$$

Therefore, it is possible to obtain a purely viscous relation between the deviator of the stress tensor $\mathbf{s}$ and the rate of visco-plastic strain $\dot{\boldsymbol{\varepsilon}}^{vp}$, governed by the viscous parameter η

$$\mathbf{s} = \eta \dot{\boldsymbol{\varepsilon}}^{vp} \tag{2.83}$$

In this case if the value of the viscous parameter η is enough small compared with the shear modulus G, then the total deformation will be essentially visco-plastic, to say irreversible. The result is a model much more close to the experimental observation. The only disadvantage is that at the end of the analysis it is impossible to distinguish between the viscoplastic and the viscous deformations produced in the liquid phase because the model use always the same variable $\boldsymbol{\varepsilon}^{vp}$ during all the solidification process.

In this work the constitutive model is formulated assuming both viscous and viscoplastic deformations. The associated evolution laws are obtained accommodating the principle of maximum dissipation to the case of a thermo-viscoelastic-viscoplastic potential.

2.3.2 Principle of maximum dissipation

In the fundamental work of Mandel [Mandel-72] the yield criterion for *associative plasticity* is postulated using the classical isothermal version of

the *principle of maximum plastic dissipation* of von Mises. Simo & Miehe [Simo & Miehe-92] observe that temperature effects are ignored in Mandel's work and remove this restriction by appealing to a thermomechanical extension of this classical principle. In this work the principle of maximum dissipation has been extended to the thermo-viscoelastic-viscoplastic case.

Let us consider the generalized stress tensor $\boldsymbol{\Sigma} = [\mathbf{s}, \mathbf{q}, q]$ and the generalized inelastic strain tensor $\mathbf{E}^I = [\boldsymbol{\varepsilon}^I, \boldsymbol{\zeta}, \xi]$ where $\mathbf{s} = dev(\boldsymbol{\sigma})$ is the deviator of the stress tensor, $\mathbf{q}$ and q are the conjugate variables of $\boldsymbol{\zeta}$ and ξ dealing with the kinematic and isotropic hardening, respectively.

Let us assume a generic thermo-visco-elastic and thermo-visco-plastic potentials, $\Lambda(\mathbf{T}, \vartheta)$ and $\Phi(\boldsymbol{\Sigma}, \Theta)$, respectively, and let us consider the thermomechanical dissipation D_{int} given by

$$D_{int} = D_{mech} + D_{ther} = \boldsymbol{\Sigma} \cdot \dot{\mathbf{E}}^I + \Theta \dot{S}^I \geq 0 \tag{2.84}$$

Let $\mathbf{T}$ and ϑ be the generic stress and temperature fields and consider the following dissipation functional

$$L(\mathbf{T}, \vartheta, \eta) = -D_{int}(\mathbf{T}, \vartheta) + \frac{1}{\eta} \Xi(\mathbf{T}, \vartheta) \tag{2.85}$$

where $1/\eta > 0$ is a penalty parameter associated to the functional L.

Function $\Xi(\mathbf{T}, \vartheta)$ must be monotone and must satisfy the conditions

$$\Xi(\mathbf{T}, \vartheta) = \begin{cases} \Xi(\mathbf{T}, \vartheta) & \Longleftrightarrow \quad \Xi(\mathbf{T}, \vartheta) > 0 \\ 0 & \Longleftrightarrow \quad \Xi(\mathbf{T}, \vartheta) \leq 0 \end{cases} \tag{2.86}$$

A possible assumption proposed in this work is to consider

$$\Xi(\mathbf{T}, \vartheta) = \lambda(\vartheta) \frac{1}{2} \langle \Lambda(\mathbf{T}, \vartheta) \rangle^2 + \mu(\mathbf{T}, \vartheta) \frac{1}{n+1} \langle \Phi(\mathbf{T}, \vartheta) \rangle^{n+1} \tag{2.87}$$

where coefficients $\lambda(\vartheta)$ and $\mu(\mathbf{T}, \vartheta)$ are given by

$$\lambda(\vartheta) = 1 - f_S(\vartheta) = f_L(\vartheta) \tag{2.88a}$$

$$\mu(\mathbf{T}, \vartheta) = f_S(\vartheta) \frac{\langle \Phi(\mathbf{T}, \vartheta) \rangle}{\Phi(\mathbf{T}, \vartheta)} \tag{2.88b}$$

being $f_S(\vartheta)$ and $f_L(\vartheta)$ the solid and the liquid fraction function.

Thus, the optimally conditions for this unconstrained minimization problem are

$$\left.\frac{\partial\, L\left(\mathbf{T},\vartheta,\eta\right)}{\partial\,\mathbf{T}}\right|_{\mathbf{T}=\boldsymbol{\Sigma}} = \mathbf{0} \tag{2.89a}$$

$$\left.\frac{\partial\, L\left(\mathbf{T},\vartheta,\eta\right)}{\partial\,\vartheta}\right|_{\vartheta=\Theta} = 0 \tag{2.89b}$$

so that the visco-elasto-plastic flow rule results in the following relations

$$\dot{\mathbf{E}}^I = \frac{1}{\eta}\frac{\partial\Xi\left(\boldsymbol{\Sigma},\Theta\right)}{\partial\boldsymbol{\Sigma}} \tag{2.90a}$$

$$\dot{S}^I = \frac{1}{\eta}\frac{\partial\,\Xi\left(\boldsymbol{\Sigma},\Theta\right)}{\partial\,\Theta} \tag{2.90b}$$

that is

$$\dot{\boldsymbol{\varepsilon}}^I = \frac{1}{\eta}\frac{\partial\Xi\left(\mathbf{s},\mathbf{q},q,\Theta\right)}{\partial\mathbf{s}} \tag{2.91a}$$

$$\dot{\boldsymbol{\zeta}} = \frac{1}{\eta}\frac{\partial\Xi\left(\mathbf{s},\mathbf{q},q,\Theta\right)}{\partial\mathbf{q}} \tag{2.91b}$$

$$\dot{\xi} = \frac{1}{\eta}\frac{\partial\Xi\left(\mathbf{s},\mathbf{q},q,\Theta\right)}{\partial q} \tag{2.91c}$$

$$\dot{S}^I = \frac{1}{\eta}\frac{\partial\,\Xi\left(\mathbf{s},\mathbf{q},q,\Theta\right)}{\partial\,\Theta} \tag{2.91d}$$

Due to the definition of potential $\Xi\left(\boldsymbol{\Sigma},\Theta\right)$, it is possible to develop the above expressions to separate the contributions coming from the visco-elastic and visco-plastic potentials, $\Lambda\left(\mathbf{s}\right)$ and $\Phi\left(\boldsymbol{\Sigma},\Theta\right)$, respectively, in the following additive form

$$\dot{\boldsymbol{\varepsilon}}^I = \gamma^{v}\frac{\partial\Lambda}{\partial\mathbf{s}} + \gamma^{vp}\frac{\partial\Phi}{\partial\mathbf{s}} \tag{2.92a}$$

$$\dot{\boldsymbol{\zeta}} = \gamma^{vp}\frac{\partial\Phi}{\partial\mathbf{q}} \tag{2.92b}$$

$$\dot{\xi} = \gamma^{vp}\frac{\partial\Phi}{\partial q} \tag{2.92c}$$

$$\dot{S}^I = \gamma^{v}\frac{\partial\Lambda}{\partial\Theta} + \gamma^{vp}\frac{\partial\Phi}{\partial\Theta} \tag{2.92d}$$

where the visco-elastic and the visco-plastic multipliers, γ^v and γ^{vp}, are respectively defined as

$$\gamma^v = \frac{\lambda(\Theta)}{\eta} \langle \Lambda(\boldsymbol{\Sigma},\Theta) \rangle = \frac{1}{\eta^v} \langle \Lambda(\boldsymbol{\Sigma},\Theta) \rangle \tag{2.93a}$$

$$\gamma^{vp} = \frac{\mu(\boldsymbol{\Sigma},\Theta)}{\eta} \langle \Phi(\boldsymbol{\Sigma},\Theta) \rangle^n = \frac{1}{\eta^{vp}} \langle \Phi(\boldsymbol{\Sigma},\Theta) \rangle^n \tag{2.93b}$$

being η^v and η^{vp} the viscous parameters associated to the visco-elastic and visco-plastic processes, respectively.

It is so possible to identify the first and the second term of equation (2.92*a*) with the evolution laws of the visco-elastic and visco-plastic strain tensors $\boldsymbol{\varepsilon}^v$ and $\boldsymbol{\varepsilon}^{vp}$, respectively

$$\dot{\boldsymbol{\varepsilon}}^v = \gamma^v \frac{\partial \Lambda}{\partial \mathbf{s}} = \gamma^v \mathbf{m} \tag{2.94a}$$

$$\dot{\boldsymbol{\varepsilon}}^{vp} = \gamma^{vp} \frac{\partial \Phi}{\partial \mathbf{s}} = \gamma^{vp} \mathbf{n} \tag{2.94b}$$

where vectors $\mathbf{n}$ and $\mathbf{m}$ are given by

$$\mathbf{m} = \frac{\partial \Lambda}{\partial \mathbf{s}} \tag{2.95a}$$

$$\mathbf{n} = \frac{\partial \Phi}{\partial \mathbf{s}} \tag{2.95b}$$

Observe that the evolution law of the visco-elastic strain tensor $\boldsymbol{\varepsilon}^v$ only depends on the definition of the visco-elastic potential $\Lambda(\mathbf{s})$ while the evolution law of the visco-plastic tensor $\boldsymbol{\varepsilon}^{vp}$ depends the specified visco-plastic potential $\Phi(\boldsymbol{\Sigma},\Theta)$.

In analogous way, the inelastic entropy can be splitted in two terms, respectively given by

$$\dot{S}^v = \gamma^v \frac{\partial \Lambda(\boldsymbol{\Sigma},\Theta)}{\partial \Theta} \tag{2.96a}$$

$$\dot{S}^{vp} = \gamma^{vp} \frac{\partial \Phi(\boldsymbol{\Sigma},\Theta)}{\partial \Theta} \tag{2.96b}$$

so that

$$S^I = S^v + S^{vp}$$

where S^v is associated to the visco-elastic potential, and S^{vp} to the visco-plastic one.

Thus, when the material is liquid, its behavior is described by a visco-elastic potential while when it is solid it is defined by a standard visco-plastic potential. These limit cases are resumed in the following table

$$\begin{array}{llll} \text{If} \quad \Theta \geq \Theta_L \quad \text{then} & \Xi(\boldsymbol{\Sigma},\Theta) = \frac{1}{2}\langle \Lambda(\boldsymbol{\Sigma},\Theta)\rangle^2 & \rightarrow & \dot{\boldsymbol{\varepsilon}}^I = \dot{\boldsymbol{\varepsilon}}^v \\ \text{If} \quad \Theta \leq \Theta_S \quad \text{then} & \Xi(\boldsymbol{\Sigma},\Theta) = \frac{1}{n+1}\langle \Phi(\boldsymbol{\Sigma},\Theta)\rangle^{n+1} & \rightarrow & \dot{\boldsymbol{\varepsilon}}^I = \dot{\boldsymbol{\varepsilon}}^{vp} \end{array} \tag{2.97}$$

It is also very interesting to observe that, due to the previous definition of coefficients $\lambda(\Theta)$ and $\mu(\boldsymbol{\Sigma},\Theta)$, during both the liquid-like and the solid phases as well as in the mushy-phase, the equivalent viscosity of the model η^{eq} is given by the parameter η, input as a material property of the model. In fact, in the mushy zone if $\Phi(\boldsymbol{\Sigma},\Theta) > 0$ it results

$$\begin{aligned} \frac{1}{\eta^{eq}} &= \frac{1}{\eta^v} + \frac{1}{\eta^{vp}} \\ &= \frac{\lambda(\Theta)}{\eta} + \frac{\mu(\boldsymbol{\Sigma},\Theta)}{\eta} = \frac{1}{\eta} \end{aligned} \tag{2.98}$$

as well as in the limit cases

$$\left.\begin{array}{c} f_S(\Theta) = 0 \\ \text{or} \\ \Phi(\boldsymbol{\Sigma},\Theta) \leq 0 \end{array}\right\} \rightarrow \begin{array}{c} \lambda(\Theta) = 1 \\ \mu(\boldsymbol{\Sigma},\Theta) = 0 \end{array} \rightarrow \eta^{eq} = \eta \tag{2.99}$$

$$\left.\begin{array}{c} f_S(\Theta) = 1 \\ \text{and} \\ \Phi(\boldsymbol{\Sigma},\Theta) > 0 \end{array}\right\} \rightarrow \begin{array}{c} \lambda(\Theta) = 0 \\ \mu(\boldsymbol{\Sigma},\Theta) = 1 \end{array} \rightarrow \eta^{eq} = \eta \tag{2.100}$$

2.3.3 Definition of the purely viscous model

The specialization of the viscous potential $\Lambda(\mathbf{s})$ to account for a purely viscous behavior to simulate the liquid-like phase can be given by the following simple assumption

$$\Lambda(\mathbf{s}) = \|\mathbf{s}\| \tag{2.101}$$

The resulting evolution law for the viscous strain tensor is obtained applying equation (2.94a), so that

$$\dot{\boldsymbol{\varepsilon}}^v = \gamma^v \frac{\partial \Lambda(\mathbf{s})}{\partial \mathbf{s}} = \gamma^v \mathbf{m} \tag{2.102}$$

being

$$\mathbf{m} = \frac{\mathbf{s}}{\|\mathbf{s}\|} \tag{2.103a}$$

$$\gamma^v = \frac{\lambda(\Sigma,\Theta)}{\eta} \|\mathbf{s}\| \tag{2.103b}$$

Recovering the definition of η^v the evolution law can be rewritten as

$$\dot{\boldsymbol{\varepsilon}}^v = \frac{1}{\eta^v}\mathbf{s} \tag{2.104}$$

that is the *Norton's law* of a purely viscous material.

Finally, in the next table the range of values assumed by the viscous parameter η^v is presented

$$\begin{array}{ccc} \Theta \geq \Theta_L & \rightarrow & \eta^v = \eta \\ \Theta_S < \Theta < \Theta_L & \rightarrow & \eta^v = \dfrac{\eta}{\lambda(\Sigma,\Theta)} \\ \Theta \leq \Theta_S & \rightarrow & \eta^v = \infty \end{array} \tag{2.105}$$

2.3.4 A J2-flow thermo-viscoplastic model

In this section the specialization of function $\Phi(\mathbf{s},\mathbf{q},q,\Theta)$ to deal with von Mises yield criterion with an isotropic and kinematic hardening combined with a thermal softening effect is presented.

Von Mises yield surface is assumed in the form

$$\Phi(\mathbf{s},\mathbf{q},q,\Theta) = \|\mathbf{s}-\mathbf{q}\| - R(q,\Theta) \leq 0 \tag{2.106}$$

where $R(q,\Theta)$ is the radius of the yield surface given by

$$R(q,\Theta) = \sqrt{\frac{2}{3}}\left[\sigma_0(\Theta) - q\right] \tag{2.107}$$

and $\sigma_0(\Theta)$ is the flow stress.

According to equation (??) the evolution laws for the plastic variables are given by

$$\dot{\boldsymbol{\varepsilon}}^p = \gamma^{vp}\frac{\partial\Phi(\mathbf{s},\mathbf{q},q,\Theta)}{\partial\mathbf{s}} = \gamma^{vp}\mathbf{n} \tag{2.108a}$$

$$\dot{\boldsymbol{\zeta}} = \gamma^{vp}\frac{\partial\Phi(\mathbf{s},\mathbf{q},q,\Theta)}{\partial\mathbf{q}} = -\gamma^{vp}\mathbf{n} \tag{2.108b}$$

$$\dot{\xi} = \gamma^{vp}\frac{\partial\Phi(\mathbf{s},\mathbf{q},q,\Theta)}{\partial q} = \gamma^{vp}\sqrt{\frac{2}{3}} \tag{2.108c}$$

where $\mathbf{n}$ is the unit normal to the yield surface and γ^{vp} is the viscoplastic parameter, respectively given by

$$\mathbf{n} = \frac{\mathbf{s}-\mathbf{q}}{\|\mathbf{s}-\mathbf{q}\|} = \frac{\boldsymbol{\beta}}{\|\boldsymbol{\beta}\|} \tag{2.109a}$$

$$\gamma^{vp} = \frac{1}{\eta^{vp}} \langle \Phi(\boldsymbol{\Sigma},\Theta) \rangle^n \tag{2.109b}$$

being the viscoplastic parameter η^{vp} given by

$$\eta^{vp} = \frac{\eta}{\mu(\boldsymbol{\Sigma},\Theta)} \tag{2.110}$$

In the next table the range of values assumed by the viscoplastic parameter η^{vp} is presented

$$\begin{array}{ccc} \Theta \geq \Theta_L & \rightarrow & \eta^{vp} = \infty \\ \Theta_S < \Theta < \Theta_L & \rightarrow & \eta^{vp} = \dfrac{\eta}{\mu(\boldsymbol{\Sigma},\Theta)} \\ \left.\begin{array}{c} \Theta \leq \Theta_S \\ \text{and} \\ \Phi(\boldsymbol{\Sigma},\Theta) > 0 \end{array}\right\} & \rightarrow & \eta^{vp} = \eta \end{array} \tag{2.111}$$

Observe that in case of decreasing values of the viscous parameter η, in the limit $\eta \rightarrow 0$ one recovers the rate independent plastic formulation, that is the Kuhn-Tuker conditions and the consistency requirement must be satisfied

$$\gamma^{vp} \geq 0 \tag{2.112a}$$

$$\Phi(\mathbf{s},\mathbf{q},q) \leq 0 \tag{2.112b}$$

$$\gamma^{vp}\Phi(\mathbf{s},\mathbf{q},q) = 0 \tag{2.112c}$$

$$\gamma^{vp}\,\dot{\Phi}(\mathbf{s},\mathbf{q},q) = 0 \tag{2.112d}$$

2.3.5 Mechanical dissipation

Taking into account that the mechanical dissipation $D_{mech} = \boldsymbol{\Sigma} \cdot \dot{\mathbf{E}}^I \geq 0$ plays an important rule in the reduced equation of dissipation (2.17a) then it can be interesting to introduce in this section an useful expression to compute this term. For this reason let us split the mechanical dissipation

into viscous and plastic dissipation named D_{visc} and D_{plas}, respectively, so that

$$D_{mech} = D_{visc} + D_{plas} \geq 0 \tag{2.113}$$

where

$$D_{visc} = \mathbf{s} : \dot{\boldsymbol{\varepsilon}}^{v} \geq 0 \tag{2.114}$$

$$D_{plas} = \boldsymbol{\Sigma} \cdot \dot{\mathbf{E}}^{vp} \geq 0 \tag{2.115}$$

Taking into account the expressions given for the evolution law (2.108a, 2.108b, 2.108c) and (2.102) it is possible to write

$$D_{visc} = \gamma^{v}\, \mathbf{s} : \mathbf{m} = \gamma^{v} \left\| \mathbf{s} \right\| = \gamma^{v} \Lambda \left(\mathbf{s} \right) = \eta^{v} \left(\gamma^{v} \right)^{2} \tag{2.116}$$

and

$$\begin{aligned} D_{plas} &= \gamma^{vp} \left(\mathbf{s} - \mathbf{q} \right) : \mathbf{n} + \gamma^{vp} \sqrt{\frac{2}{3}} q = \gamma^{vp} \left(\left\| \mathbf{s} - \mathbf{q} \right\| + \sqrt{\frac{2}{3}} q \right) \\ &= \gamma^{vp} \left[\Phi \left(\boldsymbol{\Sigma}, \Theta \right) + \sqrt{\frac{2}{3}} \sigma_{0} \left(\Theta \right) \right] \\ &= \gamma^{vp} \left(\eta^{vp} \gamma^{vp} \right)^{\frac{1}{n}} + \gamma^{vp} \sqrt{\frac{2}{3}} \sigma_{0} \left(\Theta \right) \end{aligned} \tag{2.117a}$$

so that

$$\begin{aligned} D_{mech} &= \left[\gamma^{v} \Lambda \left(\mathbf{s} \right) + \gamma^{vp} \Phi \left(\boldsymbol{\Sigma}, \Theta \right) \right] + \gamma^{vp} \sqrt{\frac{2}{3}} \sigma_{0} \left(\Theta \right) \\ &= \eta^{v} \left(\gamma^{v} \right)^{2} + \gamma^{vp} \left(\eta^{vp} \gamma^{vp} \right)^{\frac{1}{n}} + \gamma^{vp} \sqrt{\frac{2}{3}} \sigma_{0} \left(\Theta \right) \geq 0 \end{aligned} \tag{2.118a}$$

2.3.6 Thermal dissipation

Thermal dissipation $D_{ther} = \Theta \dot{S}^{I} \geq 0$ can be computed using equations $(2.96a, 2.96b)$ particularized for the models previously introduced, as

$$\dot{S}^{v} = \gamma^{v} \frac{\partial \Lambda \left(\boldsymbol{\Sigma}, \Theta \right)}{\partial \Theta} = 0 \tag{2.119a}$$

$$\dot{S}^{vp} = \gamma^{vp} \frac{\partial \Phi \left(\boldsymbol{\Sigma}, \Theta \right)}{\partial \Theta} = -\gamma^{vp} \sqrt{\frac{2}{3}} \frac{d\, \sigma_{0} \left(\Theta \right)}{d \Theta} \tag{2.119b}$$

so that

$$D_{ther} = -\gamma^{vp}\sqrt{\frac{2}{3}}\frac{d\,\sigma_0\,(\Theta)}{d\Theta}\Theta \geq 0 \tag{2.120}$$

This result and the inequality $D_{ther} \geq 0$ lead to the restriction

$$\frac{d\,\sigma_0\,(\Theta)}{d\Theta} \leq 0 \tag{2.121}$$

that is, only *thermal softening* is allowed.

2.4 Equivalent forms of the energy equation

In this section two alternative forms of the energy equation (2.9*a*) are introduced. This equivalent equations are obtained as follows.

2.4.1 Entropy form

The entropy form of the balance of energy equation is given by

$$\Theta\dot{S} = R - \nabla\cdot\mathbf{Q} + D_{int} \tag{2.122}$$

Taking into account the additive decomposition of the entropy function (2.71*a*) and the phase change contribution (2.72) it is also possible to consider the following equivalent system of equations

$$\Theta\dot{S}^E = R - \nabla\cdot\mathbf{Q} + D_{mech} - \dot{L} \tag{2.123a}$$
$$\Theta\dot{S}^I = D_{ther} \tag{2.123b}$$
$$\Theta\dot{S}^{pc} = \dot{L} \tag{2.123c}$$

showing the local evolution of the different contributions of the entropy function.

Another possible format can be the following (see [Agelet-97], [Alaska-97])

$$\Theta\,\dot{\hat{S}}^E = R - \nabla\cdot\mathbf{Q} + D_{mech} \tag{2.124a}$$
$$\Theta\dot{S}^I = D_{ther} \tag{2.124b}$$

where in this case the phase change contribution is included into the definition of $\hat{S}^E$.

2.4.2 Temperature form

Applying the chain rule to the elastic entropy function then it results

$$\Theta \dot{S}^E = C_S \dot{\Theta} + H^{ep} \tag{2.125}$$

thus, equation (2.123a) can be written as

$$C\dot{\Theta} = R - \nabla \cdot \mathbf{Q} + D_{mech} - \dot{L} - H^{ep} \tag{2.126}$$

where the following notation has been introduced

$$C = \Theta \frac{\partial S^E}{\partial \Theta} = C_v - \Theta \left(W_{\Theta\Theta} + M_{\Theta\Theta} + K_{\Theta\Theta} \right) \tag{2.127a}$$

$$H^{ep} = \Theta \left[\frac{\partial S^E}{\partial \boldsymbol{\varepsilon}^E} : \dot{\boldsymbol{\varepsilon}}^E + \frac{\partial S^E}{\partial \xi} \dot{\xi} \right] = -\Theta \left[\frac{\partial \boldsymbol{\sigma}}{\partial \Theta} : \dot{\boldsymbol{\varepsilon}}^E - \frac{\partial q}{\partial \Theta} \dot{\xi} \right] \tag{2.127b}$$

being C the *heat capacity* (not including the phase change contribution) and H^{ep} the *structural elasto-plastic heating* [Armero-Thesis-93].

Due to the fact that the latent heat function L only depends on the temperature field, it is also possible to write the balance of energy equation (2.126) as

$$\hat{C}\dot{\Theta} = R - \nabla \cdot \mathbf{Q} + D_{mech} - H^{ep} \tag{2.128}$$

where $\hat{C}$ is given by

$$\hat{C} = \Theta \frac{\partial \hat{S}^E}{\partial \Theta} = C + \frac{dL}{d\Theta} \tag{2.129}$$

that is the heat capacity including the phase change contribution [Agelet-97], [Alaska-97].

Given the practical physical significance of the temperature in front of the entropy, an efficient numerical analysis of the coupled problem considers the temperature as an independent variable together with the displacement field [Armero & Simo- 91], [Armero & Simo-92], [Armero-Thesis-93]. For this reason, most of the algorithms found in the literature for the thermo-mechanical coupled problem are based on the temperature form of the energy equation. The analysis presented in this work will show the important role played by the entropy form, even with the temperature as independent variable.

2.5 Weak Form of the Governing Equations

In this section the weak form of both the balance of momentum and balance of energy equations are presented. A mixed variational formulation to deal with either the volume-preserving plastic flow or the viscous behavior is also formulated.

2.5.1 Weak form of the balance of momentum equation

Let Ω be integration domain with smooth boundaries $\partial\Omega$. Let $\delta\boldsymbol{\eta}$ be the test function associated to the displacement field $\mathbf{u}$. The weak form of the balance of momentum equation (2.1) in the hypothesis of a quasi-static process results in

$$\langle \delta\boldsymbol{\eta}, \nabla \cdot \boldsymbol{\sigma} \rangle + \langle \delta\boldsymbol{\eta}, \mathbf{b} \rangle = \mathbf{0} \tag{2.130}$$

where $\mathbf{b}$ is the vector of forces per unit of volume.

Applying the divergence theorem to the first term in the above equation yields

$$\langle \delta\boldsymbol{\eta}, \nabla \cdot \boldsymbol{\sigma} \rangle = -\langle \nabla (\delta\boldsymbol{\eta}), \boldsymbol{\sigma} \rangle + \langle \delta\boldsymbol{\eta}, \bar{\mathbf{t}} \rangle_{\partial\Omega} \tag{2.131}$$

where $\bar{\mathbf{t}} = \boldsymbol{\sigma} \cdot \mathbf{n}$ is the prescribed surface traction. Substituting into (2.130) the result is

$$\langle \nabla^s (\delta\boldsymbol{\eta}), \boldsymbol{\sigma} \rangle = \langle \delta\boldsymbol{\eta}, \mathbf{b} \rangle + \langle \delta\boldsymbol{\eta}, \bar{\mathbf{t}} \rangle_{\partial\Omega} \tag{2.132}$$

that is the standard format of the weak form of the balance of momentum equation.

2.5.2 Mixed Variational Formulation

This section is concerned with the treatment of volume constraints arising either from the assumption of incompressible or nearly incompressible elastic response, or from the hypothesis of assuming volume-preserving plastic flow. The mixed formulation [Simo-85] that will be presented it is also very interesting to deal with the numerical locking problems generated by the different stiffness that the material assumes during the solidification process, i.e. when the part is in a liquid-like phase while the mould is solid. In the context of elasticity, problems arising from the numerical treatment of the incompressibility constraint are well known and have received considerable attention in the computational literature [Carey & Oden-83]. The method of Lagrangian multipliers, the penalty function method [Hughes-79], or iterative

updating schemes based upon the use of augmented Lagrangian [Fortin-82] are approaches currently followed. In the next section a mixed procedure is proposed, based on perturbed Lagrangian formulation in which pressure and associated volume-preserving deformation are regarded as independent field variables.

Additive split of the strain tensor

In the context of linearized theory, the point of departure is the introduction of the additive decomposition of the strain tensor $\boldsymbol{\varepsilon}$ into its deviatoric and spherical parts

$$\boldsymbol{\varepsilon} = \nabla^s \mathbf{u} = \frac{1}{3} e^{vol} \mathbf{1} + \mathbf{e} \tag{2.133}$$

where

$$e^{vol} = tr(\boldsymbol{\varepsilon}) = tr(\nabla^s \mathbf{u}) = \nabla \cdot \mathbf{u} \tag{2.134a}$$

$$\mathbf{e} = dev(\boldsymbol{\varepsilon}) = dev(\nabla^s \mathbf{u}) \tag{2.134b}$$

being $\mathbf{u}$ the displacement field, and $\mathbf{1} = \delta_{ij} \mathbf{e}_i \otimes \mathbf{e}_j$ the rank-two symmetric unit tensor (that is the metric tensor in the Cartesian coordinate system).

Now, suppose to consider the spherical part of the strain tensor as an *additional independent variable field* θ so that

$$\bar{\boldsymbol{\varepsilon}} = \overline{\nabla}^s \mathbf{u} = \mathbf{e} + \frac{1}{3} \theta \mathbf{1} \tag{2.135}$$

If we introduce the projection operators as

$$\mathbf{I}^{vol} = \frac{1}{3} \mathbf{1} \otimes \mathbf{1} \tag{2.136a}$$

$$\mathbf{I}^{dev} = \mathbf{I} - \mathbf{I}^{vol} \tag{2.136b}$$

where $\mathbf{I} = \frac{1}{2} \left[\delta_{ik} \delta_{jl} + \delta_{il} \delta_{jk} \right] \mathbf{e}_i \otimes \mathbf{e}_j \otimes \mathbf{e}_k \otimes \mathbf{e}_l$ is the rank-four symmetric unit tensor, and taking into account that the following relations are also verified

$$\mathbf{I} = \mathbf{I}^{vol} + \mathbf{I}^{dev} \tag{2.137}$$

and

$$\mathbf{I}^{vol} : \mathbf{I}^{dev} = \mathbf{I}^{dev} : \mathbf{I}^{vol} = 0 \tag{2.138a}$$

$$\left(\mathbf{I}^{vol} \right)^2 = \mathbf{I}^{vol} \tag{2.138b}$$

$$\left(\mathbf{I}^{dev} \right)^2 = \mathbf{I}^{dev} \tag{2.138c}$$

then it is possible to write

$$\mathbf{I}^{vol} \ : \ \boldsymbol{\varepsilon} = \frac{1}{3} tr\left(\nabla^s \mathbf{u}\right) \mathbf{1} \tag{2.139a}$$

$$\mathbf{I}^{dev} \ : \ \boldsymbol{\varepsilon} = dev\left(\nabla^s \mathbf{u}\right) \tag{2.139b}$$

Finally, let the elastic response be characterized by a stored energy function of the form

$$\overline{W}\left(\bar{\boldsymbol{\varepsilon}}\right) = \overline{W}\left(\mathbf{e}, \theta\right) \tag{2.140}$$

then the stress tensor is given by

$$\overline{\boldsymbol{\sigma}} = \frac{\partial \overline{W}\left(\bar{\boldsymbol{\varepsilon}}\right)}{\partial \bar{\boldsymbol{\varepsilon}}} \tag{2.141}$$

and the tangent elasticities result in

$$\overline{\mathbf{C}} = \frac{\partial^2 \overline{W}\left(\bar{\boldsymbol{\varepsilon}}\right)}{\partial \bar{\boldsymbol{\varepsilon}} \, \partial \bar{\boldsymbol{\varepsilon}}} \tag{2.142}$$

Variational principle

Let $\Omega \subset \Re^n$ denote the reference configuration of the body with smooth boundary $\partial\Omega$. Let $\mathbf{u}\left(\mathbf{x}\right)$ be the displacement field, which is prescribed as $\overline{\mathbf{u}}\left(\mathbf{x}\right)$ on $\partial\Omega_{\mathbf{u}}$ and $\bar{\mathbf{t}}\left(\mathbf{x}\right) = \boldsymbol{\sigma} \cdot \mathbf{n}$ the traction vector specified on $\partial\Omega_{\boldsymbol{\sigma}}$ so that $\partial\Omega = \partial\Omega_{\mathbf{u}} \cup \partial\Omega_{\boldsymbol{\sigma}}$ and $\partial\Omega_{\mathbf{u}} \cap \partial\Omega_{\boldsymbol{\sigma}} = \emptyset$.

Consider the following *perturbed Lagrangian functional*

$$L\left(\mathbf{u}, p, \theta\right) = \int_{\Omega} \overline{W}\left(\boldsymbol{\varepsilon}\right) \, dV + \int_{\Omega} p \, \left[tr\left(\boldsymbol{\varepsilon}\right) - \theta\right] \, dV + \Pi\left(\mathbf{u}\right) \tag{2.143}$$

where p is the pressure and $\Pi\left(\mathbf{u}\right)$ is the total potential energy associated with the loading, that is

$$\Pi\left(\mathbf{u}\right) = -\int_{\Omega} \mathbf{b} \cdot \mathbf{u} \, dV - \int_{\partial\Omega} \bar{\mathbf{t}} \cdot \mathbf{u} \, dS \tag{2.144}$$

The functional (2.143)may be viewed as a form of the *Hu-Washizu variational principle* [Nagtegaal-74]. Let $\boldsymbol{\eta} \in \left\{H^1\left(\Omega\right) : \boldsymbol{\eta}|_{\partial\Omega_{\mathbf{u}}} = 0\right\}$ be the test function (virtual displacements) associated with the functional (2.143) for a solution $\left(\mathbf{u} - \overline{\mathbf{u}}\right) \in H^1\left(\Omega\right)$, $p \in L^2\left(\Omega\right)$ and $\theta \in L^2\left(\Omega\right)$. Similarly, for the test

function q and γ associated to the variables p and θ, respectively. Consider the following directional derivatives (variations)

$$D_{\mathbf{u}}L(\mathbf{u},p,\theta)\cdot\boldsymbol{\eta} = \left.\frac{d}{d\alpha}\right|_{\alpha=0} L(\mathbf{u}+\alpha\boldsymbol{\eta},p,\theta)=0 \quad \forall\boldsymbol{\eta}\in H^1 \tag{2.145a}$$

$$D_pL(\mathbf{u},p,\theta)\cdot q = \left.\frac{d}{d\alpha}\right|_{\alpha=0} L(\mathbf{u},p+\alpha q,\theta)=0 \quad \forall q\in L^2 \tag{2.145b}$$

$$D\theta L(\mathbf{u},p,\theta)\cdot\gamma = \left.\frac{d}{d\alpha}\right|_{\alpha=0} L(\mathbf{u},p,\theta+\alpha\gamma)=0 \quad \forall\gamma\in L^2 \tag{2.145c}$$

that is

$$\langle dev(\nabla^s\boldsymbol{\eta}), dev(\overline{\boldsymbol{\sigma}})\rangle + \langle div(\boldsymbol{\eta}), p\rangle - G = 0 \tag{2.146a}$$

$$\langle q, [div(\mathbf{u})-\theta]\rangle = 0 \tag{2.146b}$$

$$\left\langle \gamma, \left[-p+\frac{1}{3}tr(\overline{\boldsymbol{\sigma}})\right]\right\rangle = 0 \tag{2.146c}$$

where $G=-D_{\mathbf{u}}\Pi(\mathbf{u})\cdot\boldsymbol{\eta}$ is the virtual work due to the external forces.

Note that taking into account equation (2.146*a*) equilibrium between the virtual work of the internal and external forces is recovered, while equations (2.146*b*), (2.146c) are the *weak forms* of the following relations

$$\theta = div(\mathbf{u}) \tag{2.147a}$$

$$p = \frac{1}{3}tr(\overline{\boldsymbol{\sigma}}) \tag{2.147b}$$

2.5.3 Weak form of the energy equation

Let Ω be integration domain with smooth boundaries $\partial\Omega$. Let $\delta\vartheta$ be the test function associated to the temperature field Θ. Let choose the balance of energy equation in entropy form given by equation (2.123*a*) then the weak form associated results in

$$\left\langle \delta\vartheta, \Theta\dot{S}^E+\dot{L}\right\rangle = \langle\delta\vartheta,R\rangle - \langle\delta\vartheta,\nabla\cdot\mathbf{Q}\rangle + \langle\delta\vartheta,D_{mech}\rangle \tag{2.148}$$

Integrating by part the conductivity term in the previous equation

$$\langle \delta\vartheta, \nabla \cdot \mathbf{Q} \rangle = \langle \nabla (\delta\vartheta), k \nabla\Theta \rangle + \langle \delta\vartheta, \bar{q} \rangle_{\partial\Omega} \tag{2.149}$$

where $\bar{q} = \mathbf{Q} \cdot \mathbf{n}$ is the flux normal to the boundaries. Substituting the result in (2.148) then the weak form of the energy equation is the following

$$\left\langle \delta\vartheta, \Theta \dot{S}^E + \dot{L} \right\rangle + \langle \nabla (\delta\vartheta), k \nabla\Theta \rangle = G^\vartheta \tag{2.150}$$

where G^ϑ is the thermal work due to the internal sources, the mechanical dissipation and the prescribed heat flux, given by

$$G^\vartheta = \langle \delta\vartheta, R \rangle - \langle \delta\vartheta, \bar{q} \rangle_{\partial\Omega} + \langle \delta\vartheta, D_{mech} \rangle \tag{2.151}$$

Chapter 3

Formulation of the Contact Problem

This chapter has its main focus in the thermo-mechanical coupled contact problem, and describes a new theoretical framework within a *stable* time integration scheme can be developed and understood. The overall approach is similar to that utilized in the study of thermoplasticity in bulk materials presented in the preceding chapter, but requires developments of the appropriate interface kinematics and thermomechanical restrictions to enable new stability estimates to be constructed and numerically approximated. The ideas of the thermodynamically based stability estimates have been extended for the thermomechanical contact problem by developing a new a priori stability estimate for the fully coupled formulation.

Finally a numerical model for the simulation of frictional *wear* behavior is developed replacing the constant frictional coefficient in the classical Coulomb law by a nonlinear function of an internal variable related to the slip distance.

3.1 Notation and Problem Definition

In this section the notation used to define the contact problem is introduced [Laursen & Simo-91]-[Laursen & Simo-93b] and [Agelet-97b]. Moreover the parametrization of the contact surfaces and the definition of closest-point-projection will allow the description of the contact constrains.

3.1.1 Notation

Let $2 \leq n_{\text{dim}} \leq 3$ be the space dimension and $I = [0, T] \subset \Re_+$ the time interval of interest. Let the open sets $\Omega^{(1)} \subset \Re^{n_{\text{dim}}}$ and $\Omega^{(2)} \subset \Re^{n_{\text{dim}}}$ with smooth boundaries $\partial\Omega^{(1)}$ and $\partial\Omega^{(2)}$ and closures $\bar{\Omega}^{(1)} = \Omega^{(1)} \cup \partial\Omega^{(1)}$ and $\bar{\Omega}^{(2)} = \Omega^{(2)} \cup \partial\Omega^{(2)}$, be the reference placement of two continuum bodies $\beta^{(1)}$ and $\beta^{(2)}$, with material particles labeled $\mathbf{X} \in \bar{\Omega}^{(1)}$ and $\mathbf{Y} \in \bar{\Omega}^{(2)}$, respectively.

Denote by $\varphi^{(i)} : \bar{\Omega}^{(1)} \times I \rightarrow \Re^{n_{\text{dim}}}$ the orientation preserving deformation map of the body $\beta^{(i)}$, with material velocities $\mathbf{V}^{(i)} = \partial_t \varphi^{(i)}$ and deformation gradients $\mathbf{F}^{(i)} = D\varphi^{(i)}$. For each time $t \in I$, the mapping $\varphi_t^{(i)}$ represents a one-parameter family of configuration indexed by t, which maps the reference placement of body $\beta^{(i)}$ onto its current placement $S_t^{(i)} : \varphi_t^{(i)}\left(\beta^{(i)}\right) \subset \Re^{n_{\text{dim}}}$.

We will denote as the *contact surface* $\Gamma^{(i)} \subset \partial\Omega^{(i)}$ the part of the boundary of the body $\beta^{(i)}$ such that all material points where contact will occur at any time $t \in I$ are included. The current placement of the contact surface $\Gamma^{(i)}$ is given by $\gamma^{(i)} = \varphi_t^{(i)}\left(\Gamma^{(i)}\right)$.

Attention will be focussed to material points on these surfaces denoted as $\mathbf{X} \in \Gamma^{(1)}$ and $\mathbf{Y} \in \Gamma^{(2)}$. Current placement of these particles is given by $\mathbf{x} = \varphi_t^{(1)}(\mathbf{X}) \in \gamma^{(1)}$ and $\mathbf{y} = \varphi_t^{(2)}(\mathbf{Y}) \in \gamma^{(2)}$. See figure (3.1) for an illustration of the notation to be used.

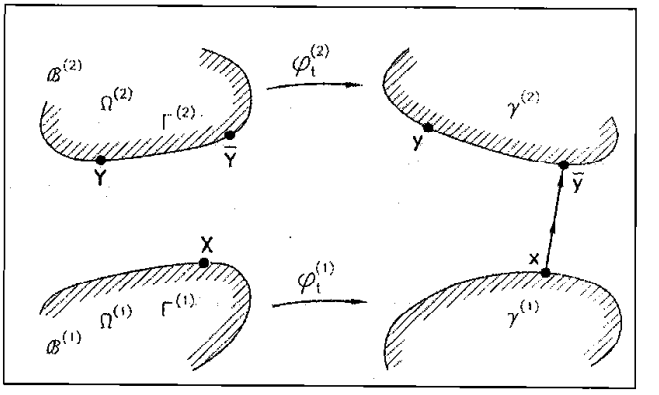

Figure 3.1: Schematic description of two interacting bodies at reference and current placements. Reference and current placement of contact surfaces.

Using a standard notation in contact mechanics ([Laursen & Simo-91]-

[Laursen & Simo-93b] and [Agelet-97b]) we will assign to each pair of contact surfaces involved in the problem, the roles of *slave* and *master* surface. In particular, let $\Gamma^{(1)}$ be the *slave surface* and Γ be the *master surface*. Additionally, we will denote slave particles and master particles to the material points of the slave and master surfaces, respectively. With this notation in hand, we will require that any slave particle may not penetrate the master surface, at any time $t \in I$. Although in the continuum setting the slave-master notation plays no role, in the discrete setting this choice becomes important.

3.1.2 Parametrization of the contact surfaces

Let $\mathbf{A}^{(i)} \subset \Re^{n_{\dim}-1}$ be a parent domain for the contact surface of body $\beta^{(i)}$. A parametrization of the contact surface for each body $\beta^{(i)}$ is introduced by a family of (orientation preserving) one-parameter mappings indexed by time, $\psi_t^{(i)} : \mathbf{A}^{(i)} \subset \Re^{n_{\dim}-1} \rightarrow \Re^{n_{\dim}}$ such that $\Gamma^{(i)} = \psi_o^{(i)}\left(\mathbf{A}^{(i)}\right)$ and $\gamma^{(i)} = \psi_t^{(i)}\left(\mathbf{A}^{(i)}\right)$. Using the mapping composition rule, it also follows that $\psi_t^{(i)} = \varphi_t^{(i)} \circ \psi_o^{(i)}$. In what follows, it will be assumed that this parametrization has the required smoothness conditions.

Within the slave-master surface role, focus will be placed on the parametrization of the master surface. Using the parametrization of the contact surfaces introduced above we consider a point $\boldsymbol{\xi} = (\xi^1, \xi^2) \in \mathbf{A}^{(2)}$ of the parent domain, such that

$$\mathbf{Y} = \psi_o^{(2)}(\boldsymbol{\xi}) \tag{3.1a}$$

$$\mathbf{y} = \psi_t^{(2)}(\boldsymbol{\xi}) \tag{3.1b}$$

and

$$\mathbf{E}_\alpha(\boldsymbol{\xi}) = \psi_{o,\alpha}^{(2)}(\boldsymbol{\xi}) \tag{3.2a}$$

$$\mathbf{e}_\alpha(\boldsymbol{\xi}) = \psi_{t,\alpha}^{(2)}(\boldsymbol{\xi}) \tag{3.2b}$$

where $\mathbf{Y}$ and $\mathbf{y}$ are, respectively, the reference and current placement of a master particle and $\mathbf{E}_\alpha(\boldsymbol{\xi})$ and $\mathbf{e}_\alpha(\boldsymbol{\xi}), \alpha = 1, 2$ are the convected surface basis attached to the master particle $\mathbf{Y} \in \Gamma^{(2)}$, on the reference and current configuration, respectively. Here $(\cdot)_{,\alpha}$ denotes partial derivative with respect to ξ^α. Figure (3.2) shows the parametrization map of reference and current placement of a contact surface.

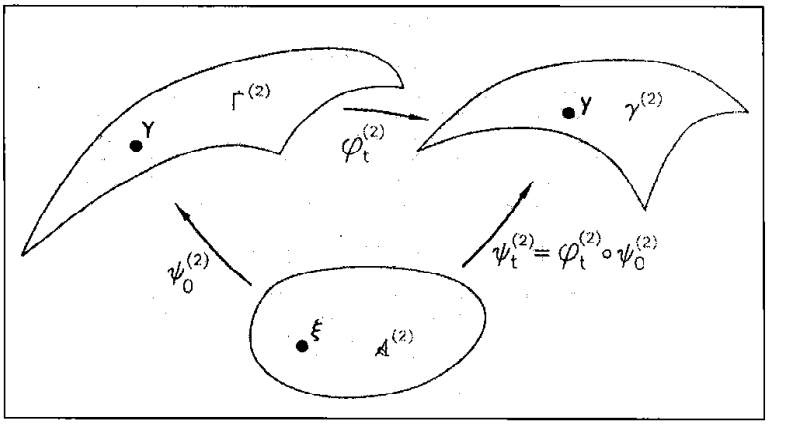

Figure 3.2: Contact surface parametrization. Parametrization map of reference and current placement of a contact surface.

3.1.3 Closest-point projection and contact pressure

Let $\bar{\mathbf{y}}(\mathbf{X},t) \in \gamma^{(2)}$ be the closest-point projection of the current position of the slave particle $\mathbf{X}$ onto the current placement of the master surface $\Gamma^{(2)}$, defined as

$$\bar{\mathbf{y}}(\mathbf{X},t) = \varphi_t^{(2)}\left(\bar{\mathbf{Y}}\right) \tag{3.3}$$

where

$$\bar{\mathbf{Y}}(\mathbf{X},t) = \arg \min_{\mathbf{Y}\in\Gamma^{(2)}} \left\| \varphi_t^{(1)}(\mathbf{X}) - \varphi_t^{(2)}(\mathbf{Y}) \right\| \tag{3.4}$$

and let $g_N(\mathbf{X},t)$ be the gap function defined for any slave particle $\mathbf{X} \in \Gamma$ and for any time $t \in I$ as

$$g_N(\mathbf{X},t) = -\left[\varphi_t^{(1)}(\mathbf{X}) - \varphi_t^{(2)}\left(\bar{\mathbf{Y}}(\mathbf{X},t)\right)\right] \cdot \boldsymbol{\nu} \tag{3.5}$$

where $\boldsymbol{\nu} \in S^{(2)}$ is the unit outward normal field to the current placement of the master surface particularized at the closest-point projection $\bar{\mathbf{y}}(\mathbf{X},t) \in \gamma^{(2)}$.

Let $\boldsymbol{\sigma}^{(1)}(\mathbf{X},t)$ be the Cauchy stress tensor and $\mathbf{N}^{(1)}(\mathbf{X})$ the unit outward normal to the slave surface $\Gamma^{(1)}$ in the reference configuration. The nominal

frictional contact traction at $\mathbf{X} \in \Gamma^{(1)}$ is given by

$$\mathbf{t}^{(1)}(\mathbf{X},t) = \boldsymbol{\sigma}^{(1)}(\mathbf{X},t) \cdot \mathbf{N}^{(1)}(\mathbf{X}) \tag{3.6}$$

and the contact nominal pressure $t_N(\mathbf{X},t)$ is defined as

$$t_N(\mathbf{X},t) = \mathbf{t}^{(1)}(\mathbf{X},t) \cdot \boldsymbol{\nu} \tag{3.7}$$

3.1.4 Convected basis, metric and curvature tensors

Associated to the closest-point projection given by (3.3), for some point $\bar{\boldsymbol{\xi}}(\mathbf{X},t) = \left(\bar{\xi}^1, \bar{\xi}^2\right) \in \mathbf{A}^{(2)}$ of the parent domain we will have

$$\bar{\mathbf{Y}}(\mathbf{X},t) = \psi_o^{(2)}\left(\bar{\boldsymbol{\xi}}\right) \tag{3.8a}$$

$$\bar{\mathbf{y}}(\mathbf{X},t) = \psi_t^{(2)}\left(\bar{\boldsymbol{\xi}}\right) \tag{3.8b}$$

Attached to the master particle $\bar{\mathbf{Y}}(\mathbf{X},t)$ we define the convected surface basis on the reference and current configurations, respectively, as

$$\boldsymbol{\tau}_\alpha^{ref}(\mathbf{X},t) = \mathbf{E}_\alpha\left(\bar{\boldsymbol{\xi}}\right) \tag{3.9a}$$

$$\boldsymbol{\tau}_\alpha(\mathbf{X},t) = \mathbf{e}_\alpha\left(\bar{\boldsymbol{\xi}}\right) \tag{3.9b}$$

Additionally, the unit outward normal $\boldsymbol{\nu}^{ref} \in S^{(2)}$ and $\boldsymbol{\nu} \in S^{(2)}$ at the master particle $\bar{\mathbf{Y}}(\mathbf{X},t)$ on the reference and current configurations, respectively, can be defined as

$$\boldsymbol{\nu}^{ref} = \frac{\boldsymbol{\tau}_1^{ref} \times \boldsymbol{\tau}_2^{ref}}{\left\|\boldsymbol{\tau}_1^{ref} \times \boldsymbol{\tau}_2^{ref}\right\|} \tag{3.10a}$$

$$\boldsymbol{\nu} = \frac{\boldsymbol{\tau}_1 \times \boldsymbol{\tau}_2}{\|\boldsymbol{\tau}_1 \times \boldsymbol{\tau}_2\|} \tag{3.10b}$$

The vectors $\boldsymbol{\tau}_\alpha^{ref}(\mathbf{X},t) \in T_{\nu^{ref}} S^{(2)}$ and $\boldsymbol{\tau}_\alpha(\mathbf{X},t) \in T_\nu S^{(2)}$ span the tangent spaces $T_{\nu^{ref}} S^{(2)}$ and $T_\nu S^{(2)}$ to the $S^{(2)}$ unit sphere at $\boldsymbol{\nu}^{ref}$ and $\boldsymbol{\nu}$, respectively. Here the tangent space to the $S^{(2)}$ unit sphere at $\boldsymbol{\nu} \in S^{(2)}$ is defined as

$$T_\nu S^{(2)} = \{\delta\boldsymbol{\nu} \in \Re^{n_{\dim}} : \delta\boldsymbol{\nu} \cdot \boldsymbol{\nu} = 0\} \tag{3.11}$$

The convected surface basis vectors $\boldsymbol{\tau}_\alpha^{ref}$ and $\boldsymbol{\tau}_\alpha$, augmented with the unit outward normal $\boldsymbol{\nu}^{ref}$ and $\boldsymbol{\nu}$, provides local spatial frames at the master

particle $\bar{\mathbf{Y}}(\mathbf{X},t)$ on the reference and current configurations, respectively. The convected surface basis vectors $\boldsymbol{\tau}\alpha^{ref}$ and $\boldsymbol{\tau}$, induces a surface metric or first fundamental form on the reference and current configurations, defined respectively as

$$M_{\alpha\beta} = \boldsymbol{\tau}_{\alpha}^{ref} \cdot \boldsymbol{\tau}_{\beta}^{ref} \tag{3.12a}$$

$$m_{\alpha\beta} = \boldsymbol{\tau}_{\alpha} \cdot \boldsymbol{\tau}_{\beta} \tag{3.12b}$$

Inverse surface metrics $M^{\alpha\beta}$ and $m^{\alpha\beta}$ are defined in the usual manner. Additionally, dual surface basis on the reference and current configurations are straightforward defined respectively as

$$\boldsymbol{\tau}_{ref}^{\alpha} = M^{\alpha\beta}\,\boldsymbol{\tau}_{\beta}^{ref} \tag{3.13a}$$

$$\boldsymbol{\tau}^{\alpha} = m^{\alpha\beta}\,\boldsymbol{\tau}_{\beta} \tag{3.13b}$$

The variation of the convected surface basis along the convected coordinates, together with the unit normal, induces the second fundamental form or surface curvature defined, on the reference and current configurations, as

$$k_{\alpha\beta}^{ref} = \mathbf{E}_{\alpha,\beta}\left(\bar{\boldsymbol{\xi}}\right) \cdot \boldsymbol{\nu}^{ref} \tag{3.14a}$$

$$k_{\alpha\beta} = \mathbf{e}_{\alpha,\beta}\left(\bar{\boldsymbol{\xi}}\right) \cdot \boldsymbol{\nu} \tag{3.14b}$$

3.1.5 Slip velocity and frictional traction

The relative slip velocities in the convected and current configuration are defined as

$$\mathbf{v}_{T}^{ref}(\mathbf{X},t) = \frac{d}{dt}\left[\bar{\mathbf{Y}}(\mathbf{X},t)\right] \tag{3.15a}$$

$$\mathbf{v}_{T}(\mathbf{X},t) = \mathbf{F}_{t}^{(2)}\left(\bar{\boldsymbol{\xi}}(\mathbf{X},t)\right) \cdot \mathbf{v}_{T}^{ref}(\mathbf{X},t) \tag{3.15b}$$

and, applying the chain rule

$$\mathbf{v}_{T}^{ref}(\mathbf{X},t) = \dot{\xi}^{\alpha}\,\boldsymbol{\tau}_{\alpha}^{ref} \tag{3.16a}$$

$$\mathbf{v}_{T}(\mathbf{X},t) = \dot{\xi}^{\alpha}\,\boldsymbol{\tau}_{\alpha} \tag{3.16b}$$

The one-forms associated to these objects are defined as

$${}^{b}\mathbf{v}_{T}^{ref}(\mathbf{X},t) = \dot{\xi}^{\alpha}\,M_{\alpha\beta}\,\boldsymbol{\tau}_{ref}^{\beta} \tag{3.17a}$$

$${}^{b}\mathbf{v}_{T}(\mathbf{X},t) = \dot{\xi}^{\alpha}\,M_{\alpha\beta}\,\boldsymbol{\tau}^{\beta} \tag{3.17b}$$

Finally, we define the nominal frictional tangent traction $\mathbf{t}_T(\mathbf{X},t)$ as (minus) the projection of the nominal frictional contact traction $\mathbf{t}^{(1)}(\mathbf{X},t)$ onto the unit normal $\boldsymbol{\nu}$, as

$$\mathbf{t}_T(\mathbf{X},t) = t_T^{\alpha}(\mathbf{X},t)\,\boldsymbol{\tau}_{\alpha} \tag{3.18}$$

3.2 Governing Equations

In this section the main focus is the formulation and treatment of the contact problem recovering the same general structure used to describe the constitutive framework for the bulk continua. In particular we will emphatize an entropy form of the energy equation defined on the contact interface, which is a key aspect of the isentropic split of the coupled problem first presented in the previous chapter for the thermoplastic continua. It is this approach that will be extended in this work to encompass thermo-frictional contact problems [Laursen-98].

Let us extend the balance equations coming from the first and second laws of thermodynamics, to account for the contributions at the contact interfaces.

First, let us consider the balance of energy equation. If we denote with $\dot{E}^*$ the time derivative of the total internal energy given by

$$\dot{E}^* = \int_{\Omega} \dot{E}\, dV + \int_{\Gamma^{(1)}} \dot{E}_c\, dS \tag{3.19}$$

being $\dot{E}$ the stored energy per unit volume in the bulk medium (see eq. 2.2) and $\dot{E}_c$ the stored energy per unit area on the contact interface $\Gamma^{(1)}$ defined as

$$\dot{E}_c = t_N\,\dot{g}_N + t_{T\alpha}\,\dot{g}_T^{\alpha} + \left[Q_c^{(1)} + Q_c^{(2)}\right] \tag{3.20}$$

where g_T^{α} is the tangential gap function given in term of slip velocity by integrating within the convected framework

$$g_T^{\alpha} = \int_{t_c}^{t} \dot{\xi}^{\alpha}\, dt \tag{3.21}$$

being t_c the initial time of contact for the point in question. $Q_c^{(1)}$ and $Q_c^{(2)}$ are the heat fluxes per unit reference surface $\Gamma^{(1)}$ supplied at the interface, assumed positive if they are flowing out of the bodies into the interface region.

Let us now consider the second law of thermodynamics. Suppose also in this case that the total entropy of the system S^* can be given by

$$\dot{S}^* = \int_{\Omega} \dot{S}\, dV + \int_{\Gamma^{(1)}} \dot{S}_c\, dS \tag{3.22}$$

being $\dot{S}$ the entropy per unit volume in the bulk media (see eq. 2.7) and $\dot{S}_c$ the entropy per unit area on the contact interface $\Gamma^{(1)}$ satisfying the following restriction

$$\dot{S}_c \geq \frac{Q_c^{(1)}}{\Theta^{(1)}} + \frac{Q_c^{(2)}}{\Theta^{(2)}} \tag{3.23}$$

where $\Theta^{(1)}$ and $\Theta^{(2)}$ are the contact interface temperatures. Also in this case it is possible to introduce a dissipation term due to the contact effects D_c so that the total dissipation D^* on the system is given by

$$D^* = D + D_c \geq 0 \tag{3.24}$$

where

$$D_c = \Theta_c\, \dot{S}_c - \left[\frac{Q_c^{(1)}}{\Theta^{(1)}} + \frac{Q_c^{(2)}}{\Theta^{(2)}}\right] \Theta_c \geq 0 \tag{3.25}$$

being Θ_c the characteristic temperature at the contact interface (not generally the same as either $\Theta^{(1)}$ or $\Theta^{(2)}$) [Laursen-98].

Following the same methodology presented for the bulk continua the dissipation due to contact can be spitted in internal dissipation and dissipation by conduction as

$$D_c = D_{c,int} + D_{c,cond} \geq 0 \tag{3.26a}$$

$$D_{c,int} = \Theta_c\, \dot{S}_c - \left[Q_c^{(1)} + Q_c^{(2)}\right] \geq 0 \tag{3.26b}$$

$$D_{c,cond} = \frac{Q_c^{(1)}}{\Theta^{(1)}} \left(\Theta^{(1)} - \Theta_c\right) + \frac{Q_c^{(2)}}{\Theta^{(2)}} \left(\Theta^{(2)} - \Theta_c\right) \geq 0 \tag{3.26c}$$

Finally, substituting equation (3.26*b*) into the balance of energy equation (3.20) it is possible to obtain the equation of dissipation as

$$D_{c,int} = \Theta_c\, \dot{S}_c - \dot{E}_c + t_N\, \dot{g}_N + t_{T\alpha}\, \dot{g}_T^{\alpha} \geq 0 \tag{3.27}$$

3.3 Additive Decomposition

In the following, we will assume that the tangential gap function can be additively decomposed into elastic (reversible) and inelastic parts [Laursen-98] via

$$g_T^{\alpha} = g_T^{e\,\alpha} + g_T^{p\,\alpha} \tag{3.28}$$

Hence, the split the total entropy generated at the contact interface can also be partitioned into elastic and inelastic parts as [Cancun-99]

$$S_c = S_c^e + S_c^p \tag{3.29}$$

so that the energy equation at the contact interface can be written as

$$D_{c,\,mech} = \Theta_c \dot{S}_c^e - \dot{E}_c + t_N \dot{g}_N + t_{T\,\alpha} \dot{g}_T^{\alpha} \geq 0 \tag{3.30}$$

Note that the internal dissipation due to contact has been decomposed into mechanical and thermal part, respectively given by

$$D_{c,\,mech} = \Theta_c \dot{S}_c^e - \left[Q_c^{(1)} + Q_c^{(2)}\right] \geq 0 \tag{3.31a}$$

$$D_{c,\,ther} = \Theta_c \dot{S}_c^p \geq 0 \tag{3.31b}$$

so that

$$D_{c,\,int} = D_{c,\,mech} + D_{c,\,ther} \geq 0 \tag{3.32}$$

3.4 Constitutive Equations

In what follows the contact free energy function is introduced. The constitutive equations of both contact pressure and tangential traction as well as the elastic entropy are obtained. Finally, the heat conduction and heat convection laws are discussed.

3.4.1 Free energy function definition

Starting from the definition of the internal energy as a function of

$$E_c = E_c\left(g_N, g_T^{e\,\alpha}, S_c^e, \zeta_c\right) \tag{3.33}$$

it is possible to define a free energy function Ψ_c via Legendre transformation as

$$\Psi_c = E_c - \Theta_c S_c^e = \Psi_c(g_N, g_T^{e\alpha}, \Theta_c, \zeta_c) \tag{3.34}$$

Internal variable ζ_c deals with a hardening-like behavior of the frictional law characteristic of the wear phenomena [Agelet & Chiumenti-95], [Chiumenti & Agelet-95].

Following a standard argument in thermodynamics (see section 2.2.2 in previous chapter), one may time differentiate equation (3.34) to obtain

$$\dot{\Psi}_c = \dot{E}_c - \Theta_c \dot{S}_c^e - \dot{\Theta}_c S_c^e \tag{3.35a}$$

$$= \frac{\partial \Psi_c}{\partial g_N}\dot{g}_N + \frac{\partial \Psi_c}{\partial g_T^{e\alpha}}\dot{g}_T^{e\alpha} + \frac{\partial \Psi_c}{\partial \Theta_c}\dot{\Theta}_c + \frac{\partial \Psi_c}{\partial \zeta_c}\dot{\zeta}_c \tag{3.35b}$$

Taking into account the energy equation at the contact interface (3.30)then

$$D_{c,mech} = \left(t_N - \frac{\partial \Psi_c}{\partial g_N}\right)\dot{g}_N + \left(t_{T\alpha} - \frac{\partial \Psi_c}{\partial g_T^{e\alpha}}\right)\dot{g}_T^{\alpha} - \left(S_c^e + \frac{\partial \Psi_c}{\partial \Theta_c}\right)\dot{\Theta}_c - \frac{\partial \Psi_c}{\partial g_T^{e\alpha}}\dot{g}_T^{p\alpha} - \frac{\partial \Psi_c}{\partial \zeta_c}\dot{\zeta}_c \geq 0 \tag{3.36}$$

which must hold for any $\dot{g}_N$, $\dot{g}_T^{\alpha}$ and $\dot{\Theta}_c$. Applying Coleman's method, it results

$$t_N = \frac{\partial \Psi_c}{\partial g_N} \tag{3.37a}$$

$$t_{T\alpha} = \frac{\partial \Psi_c}{\partial g_T^{e\alpha}} \tag{3.37b}$$

$$S_c^e = -\frac{\partial \Psi_c}{\partial \Theta_c} \tag{3.37c}$$

and the reduced equation of mechanical dissipation at the contact interface is given by

$$D_{c,mech} = t_{T\alpha}\,\dot{g}_T^{p\alpha} + q_c\dot{\zeta}_c \geq 0 \tag{3.38}$$

where q_c is the conjugate variable to the hardening-like parameter ζ_c defined as

$$q_c = -\frac{\partial \Psi_c}{\partial \zeta_c} \tag{3.39}$$

Let us now particularize the free energy function to obtain the standard restrictions at the contact interface, assuming the following terms [Cancun-99]

$$\Psi_c\left(g_N, g_T^{e\alpha}, \Theta_c, \zeta_c\right) = W_c\left(g_N, g_T^{e\alpha}\right) + T_c\left(\Theta_c\right) + K_c\left(\Theta_c, \zeta_c\right) \tag{3.40}$$

being $W_c\left(g_N, g_T^{e\alpha}\right)$, $T_c\left(\Theta_c\right)$ and $K_c\left(\Theta_c, \zeta_c\right)$ the stored energy due to the bodies interaction at the contact interface, the thermo-contact potential and the hardening-like potential, respectively given by

$$W_c\left(g_N, g_T^{e\alpha}\right) = \frac{1}{2}\,\epsilon_N\,\langle g_N\rangle^2 + \frac{1}{2}\,\epsilon_T\,g_T^{e\alpha}\,M_{\alpha\beta}\,g_T^{e\beta} \tag{3.41a}$$

$$T_c\left(\Theta_c\right) = C_{co}\left[\left(\Theta_c - \Theta_o\right) - \Theta_c \log\left(\Theta_c/\Theta_o\right)\right] \tag{3.41b}$$

$$K_c\left(\Theta_c, \zeta_c\right) = \sum_{p=1}^{m} \frac{1}{p+1}\mu_p\left(\Theta_c\right)\,\zeta_c^{p+1} \tag{3.41c}$$

where Θ_o is the initial temperature field, C_{co} is the heat capacity associated with the contact interface and ϵ_N and ϵ_T are the normal and tangential penalty parameters, respectively, that provide a *penalty regularization* of the contact constrains [Laursen & Simo-93].

From this definition the constitutive equations that completely specify the thermomechanical contact framework result in

$$t_N = \epsilon_N\,\langle g_N\rangle \tag{3.42a}$$

$$t_{T\alpha} = \epsilon_T\,M_{\alpha\beta}\,g_T^{e\beta} \tag{3.42b}$$

$$S_c^e = C_{co}\log\left(\Theta_c/\Theta_o\right) - \sum_{p=1}^{m}\frac{1}{p+1}\frac{d\mu_p\left(\Theta_c\right)}{d\,\Theta_c}\,\zeta_c^{p+1} \tag{3.42c}$$

$$q_c = -\sum_{p=1}^{m}\mu_p\left(\Theta_c\right)\,\zeta_c^{p} \tag{3.42d}$$

Equation (3.42*a*) defines the normal pressure as

$$t_N\left(\mathbf{X},t\right) = \begin{cases} 0 & \text{if} \quad g_N\left(\mathbf{X},t\right) \le 0 \\ \epsilon_N\;g_N\left(\mathbf{X},t\right) & \text{if} \quad g_N\left(\mathbf{X},t\right) > 0 \end{cases} \tag{3.43}$$

which are the regularization of the contact constraints of impenetrability and non-adhesion, respectively given in Khun-Tucker form as

$$t_N\left(\mathbf{X},t\right) \ge 0 \tag{3.44a}$$

$$g_N\left(\mathbf{X},t\right) \le 0 \tag{3.44b}$$

$$g_N\left(\mathbf{X},t\right)\,t_N\left(\mathbf{X},t\right) = 0 \tag{3.44c}$$

Remark 3 *Observe that the hardening-like potential $K_c(\Theta_c, \zeta_c)$ makes the difference between the definition of the free energy function presented in [Laursen-98] and [Cancun-99], respectively. In fact, we will see that in the analysis of stability for the staggered solution of the coupled contact problem, this term generates a contribution (the frictional heating) that makes the standard isothermal split conditionally stable. Thus, it results very interesting the formulation of an unconditionally stable algorithm using an isentropic operator split [Cancun-99].*

3.4.2 Thermal contact model

To complete the thermomechanical frictional contact model, the heat conduction and heat convection laws must be considered [Wriggers & Miehe-92], [Zavarise & Wriggers-92].

Heat conduction model

Heat conduction through the contact surface $Q^{(i)}_{c,\,cond}$ has been assumed to be a function of coefficient $h^{(i)}_{cond}$ depending on of the normal contact pressure t_N and the mean gas temperature Θ_g, multiplied by the thermal gap $g^{(i)}_{\Theta} = \left(\Theta^{(i)} - \Theta_c\right)$ of the form

$$Q^{(i)}_{c,\,cond} = h^{(i)}_{cond}\left(t_N, \Theta_g\right) g^{(i)}_{\Theta} \tag{3.45a}$$

In the literature it is possible to find different relations to define the heat conduction coefficient $h^{(i)}_{cond}$.

General contact pressure-temperature dependent heat conduction model. The resistance against heat transfer is mainly due to the low percentage of surface area which is really in contact. The presence of a reduced set of spots surrounded by microcavities characterizes the contact area. Hence, heat transfer takes place by heat conduction through the spots and the heat conduction through the gas contained in the microcavities. Other effects such radiation between microcavities surfaces can in general be omitted since both bodies are very close to each other. Making the usual assumption that both heat conduction mechanisms, through the spots and through the gas contained in the microcavities, act in parallel, the heat transfer coefficient $h_{cond}\left(t_N\right)$ can be expressed as

$$h_{cond}\left(t_N, \Theta_g\right) = h_S\left(t_N\right) + h_G\left(t_N, \Theta_g\right) \tag{3.46}$$

where $h_S(t_N)$ is heat conduction through the spots, assumed to be a function of the contact pressure t_N, and $h_G(t_N, \Theta_g)$ is the heat conduction through the gas contained in the microcavities, assumed to be a function of the contact pressure t_N and the mean gas temperature Θ_g. Based on a statistical model the heat transfer coefficient through the spots is given by

$$h_S(t_N) = \frac{1.25\,\bar{k}\,\bar{m}}{\bar{\sigma}} \left[\frac{t_N}{c_1} \left(1.62 \frac{10^6 \bar{\sigma}}{m} \right)^{-c_2} \right]^{\frac{0.95}{1+0.71\,c_2}} \tag{3.47}$$

where $\bar{\sigma}$ is the surface roughness, $\bar{k}$ is the mean thermal conductivity (depending on the conductivities of the two interacting bodies), $\bar{m}$ is the mean asperity slope and c_1 and c_2 describe the hardness variation [Song-87], [Wriggers & Miehe-92].

The heat transfer through the gas or liquid contained in the microcavities is mainly governed by conduction. This fact results from the small height of the microcavities which do not allow convective flow. The expression for this coefficient results in

$$h_G(t_N, \Theta_g) = \frac{k_g}{1.36\,\bar{\sigma}} \sqrt{-\log\left(5.59 \frac{t_N}{H_e} \right) + c_g \Theta_g} \tag{3.48}$$

where k_g is the gas conductivity, H_e the Vickers hardness and c_g the constitutive constant for the gas [Yovanovich-81].

Simplified contact pressure dependent heat conduction model. For high pressures, a simplified contact pressure dependent model can be derived as

$$h_{cond}(t_N) = h_{co} \left(\frac{t_N}{H_e} \right)^{\epsilon} \tag{3.49}$$

where h_{co} is the contact resistance coefficient and ϵ is a constant coefficient [Zavarise & Wriggers-92].

Heat convection model

Heat convection between the two bodies arises when they separate from each other. Heat convection flux $Q^{(i)}_{c,conv}$ has been assumed to be a function of coefficient $h^{(i)}_{conv}$ depending on the mechanical gap g_N multiplied by the thermal gap $\bar{g}^{(i)}_{\Theta} = \left(\Theta^{(i)} - \Theta_g\right)$ of the form

$$Q^{(i)}_{c,conv} = h^{(i)}_{conv}(g_N)\, \bar{g}^{(i)}_{\Theta} \tag{3.50a}$$

where Θ_g is the mean gas temperature.

The definition of the heat convection coefficient h_{conv} depends on the conductivities of the interacting bodies. If the conductivities of the two bodies are very different then h_{conv} can be assumed *constant*, otherwise it is possible to consider the following expression

$$h_{conv}\left(g_N\right) = \frac{k_a}{g_N + \dfrac{k_a}{h_{o,\,conv}}}$$

where k_a is the conductivity of the air (or the gas around the bodies) and $h_{o,\,conv}$ is the initial value of the interfacial heat transfer coefficient [Ransing-98].

3.5 Evolution Laws

Consider the following slip function defined as

$$\Phi_c\left(t_N, {}^b\mathbf{t}_T, \Theta_c, q_c\right) = \left\|{}^b\mathbf{t}_T\right\|_{ref} - \left[\mu_o\left(\Theta_c\right) - q_c\right] t_N \leq 0 \tag{3.51}$$

where

$$\left\|{}^b\mathbf{t}_T\right\|_{ref} = \sqrt{t_{T\,\alpha}\; M^{\alpha\beta}\, t_{T\,\beta}} \tag{3.52}$$

This function represents a modified version of the *Coulomb law* for frictional contact problem where both a mechanical hardening and a thermal softening are assumed [Cancun-99].

Let us introduce the evolution laws of the thermomechanical frictional contact problem as

$$L_{\mathbf{v}_T}\left(g_T^p\right) = \gamma_c \mathbf{n}_c \rightarrow \dot{g}_T^{p\,\alpha} = \gamma_c n_c^{\alpha} \tag{3.53a}$$

$$\dot{\zeta}_c = \gamma_c\, t_N \tag{3.53b}$$

$$\dot{S}_c^p = -\gamma_c \frac{d\mu_o\left(\Theta_c\right)}{d\,\Theta_c} \tag{3.53c}$$

where γ_c is the slip consistency parameter and $\mathbf{n}_c$ is unit normal to the frictional surface given by

$$\mathbf{n}_c = \frac{{}^b\mathbf{t}_T}{\left\|{}^b\mathbf{t}_T\right\|_{ref}} \rightarrow n_c^{\alpha} = \frac{M^{\alpha\beta}\, t_{T\,\beta}}{\sqrt{t_{T\,\alpha}\; M^{\alpha\beta}\, t_{T\,\beta}}} \tag{3.54}$$

Frictional constraints are expressed as Kuhn-Tucker complementarity conditions as

$$\gamma_c \geq 0 \tag{3.55a}$$
$$\Phi_c\left(t_N, t_{T\alpha}, \Theta_c, q_c\right) \leq 0 \tag{3.55b}$$
$$\gamma_c \Phi_c\left(t_N, t_{T\alpha}, \Theta_c, q_c\right) - 0 \tag{3.55c}$$

augmented by the consistency requirement

$$\gamma_c \dot{\Phi}_c\left(t_N, t_{T\alpha}, \Theta_c, q_c\right) = 0 \tag{3.56}$$

Taking into account this results and making use of equations (3.17*b*) and (3.42*b*), the evolution law of the frictional tangent traction results in

$$L_{\mathbf{v}_T}\left({}^b\mathbf{t}_T\left(\mathbf{X},t\right)\right) = \in_T \left[{}^b\mathbf{v}_T\left(\mathbf{X},t\right) - \gamma_c\, \mathbf{n}_c\right] \tag{3.57}$$

where $L_{\mathbf{v}_T}\left({}^b\mathbf{t}_T\left(\mathbf{X},t\right)\right) = \dot{t}_{T\alpha}\, \boldsymbol{\tau}^{\alpha}$ is the Lie derivative of the frictional tangent traction along the flow induced by the relative slip velocity $\mathbf{v}_T$.

3.6 Thermo-frictional Dissipation

Making use of the evolution laws of the internal variables it is possible to obtain a compact expression of the mechanical and thermal dissipation, respectively given by

$$\begin{aligned} D_{c,\,mech} &= t_{T\alpha}\, \dot{g}_T^{p\alpha} + q_c \dot{\zeta}_c \\ &= \gamma_c \left\| {}^b\mathbf{t}_T^{ref} \right\| + \gamma_c q_c\, t_N \\ &= \gamma_c \left[\Phi_c + \mu_o\left(\Theta_c\right) t_N\right] \\ &= \gamma_c \left[\mu_o\left(\Theta_c\right) t_N\right] \geq 0 \end{aligned} \tag{3.58}$$

and

$$\begin{aligned} D_{c,\,ther} &= \Theta_c\, \dot{S}_c^p \\ &= -\gamma_c\, t_N \frac{d\mu_o\left(\Theta_c\right)}{d\,\Theta_c} \Theta_c \geq 0 \end{aligned} \tag{3.59}$$

Observe that according to the inequality on the thermal dissipation the following constraint must be verified

$$\frac{d\mu_o\left(\Theta_c\right)}{d\,\Theta_c} \leq 0 \tag{3.60}$$

so that only *thermal softening* is permitted, in full analogy with the constraint on the initial flow stress parameter obtained in the bulk continua formulation.

3.7 Wear Phenomena

Frictional behavior at the contact surfaces, between two bodies sliding relative to one another, highly depends on the nature and topography of the surfaces in contact, such as the hardness and the geometry of the microasperities, surface coating, etc., as well as on the environmental factors, such as the lubrication, which characterize the state conditions of the contact surfaces [Laursen-98], [Lassen & Bay-93]. These state conditions at the contact surfaces may be constantly changing as a consequence of complex phenomena taking place during continuous sliding of the bodies, such as the wear due to the evolution of the surfaces topography, i.e., deformation of the microasperities, worn of surface coating, etc., internal straining, chemical reactions, etc.

Despite these facts, most of the current applications reported in the literature are restricted to a standard Coulomb law, using a constant friction coefficient μ_o such as

$$\Phi_c\left(t_N, t_{T\alpha}\right) = \left\| {}^{b}\mathbf{t}_T^{ref} \right\| - \mu_o \, t_N \leq 0 \tag{3.61}$$

Such simple models may represent only a limited range of tribological situations and it appears to be necessary to develop a class of models which incorporate the state conditions and their evolution at the contact surfaces, taking into account the influence of complex phenomena such as wear, lubrication and chemical reactions, among others.

A generalization of the Coulomb law is presented in this work, within a fully non-linear kinematic setting, including large slip and finite deformation, introducing the hardening-like variable ζ_c. It is possible to observe that this variable allows the simulation of *frictional wear behavior* at the contact interface [Agelet & Chiumenti-95], [Chiumenti & Agelet-95]. In fact, replacing the value of q_c given by equation (3.42*d*) we can obtain the expression of the frictional coefficient as

$$\mu\left(\zeta_c, \Theta_c\right) = \mu_o + \sum_{p=1}^{m} \mu_p\left(\Theta_c\right) \zeta_c^p \tag{3.62}$$

so that either a *thermal softening*, due to the temperature dependence of the frictional coefficient, or a *mechanical hardening* are available in the model.

Note that the Coulomb law can be written in the equivalent form,

$$\Phi_c\left(t_N, t_{T\alpha}, \Theta_c, \zeta_c\right) = \left\| {}^{b}\mathbf{t}_T^{ref} \right\| - \mu\left(\zeta_c, \Theta_c\right) t_N \leq 0 \tag{3.63}$$

once defined the expression of the frictional coefficient given by (3.62).

3.8 Equivalent forms of the energy equation

In this section two alternative forms of the energy equation at the contact interface are introduced. These equivalent equations are obtained as follows.

3.8.1 Entropy form

The entropy form of the balance of energy equation at the contact interface is given by

$$\Theta_c \dot{S}_c = \left[Q_c^{(1)} + Q_c^{(2)}\right] + D_{c,\,int} \tag{3.64}$$

Taking into account the additive decomposition of the entropy function (3.29) it is also possible to consider the following equivalent system of equations

$$\Theta_c \dot{S}_c^e = \left[Q_c^{(1)} + Q_c^{(2)}\right] + D_{c,\,mech} \tag{3.65a}$$

$$\Theta_c \dot{S}_c^p = D_{c,\,cond} \tag{3.65b}$$

showing the local evolution of the different contributions of the entropy function.

3.8.2 Temperature form

Applying the chain rule to the elastic entropy function

$$\Theta_c \dot{S}_c^e = C_c \dot{\Theta}_c + H^{fc} \tag{3.66}$$

where the following notation has been introduced

$$C_c = \Theta_c \frac{\partial S_c^e}{\partial \Theta_c} = C_{co} - \frac{\partial^2 K_c}{\partial \Theta_c \partial \Theta_c} \tag{3.67a}$$

$$H^{fc} = \Theta_c \frac{\partial S_c^e}{\partial \zeta_c} \dot{\zeta}_c = -\Theta_c \frac{\partial q_c}{\partial \Theta_c} \dot{\zeta}_c \tag{3.67b}$$

being C_c the *heat capacity* associated with the contact interface and H^{fc} the *frictional contact heating.*

Thus, equation (3.65a) can be transformed into [Cancun-99],

$$C_c \dot{\Theta}_c = \left[Q_c^{(1)} + Q_c^{(2)}\right] + D_{c,\,mech} - H^{fc} \tag{3.68}$$

Remark 4 *Note that the frictional contact heating appears only if q_c depends on the temperature fields. This is possible only if both the thermal softening and the mechanical hardening of the friction coefficient $\mu_p(\Theta_c)$ are taken into account in the definition of the free energy function.*

3.9 A-priori stability estimate

The goal in this section is the extension of the a-priori stability estimate criteria to the case of thermo-frictional problems.

Conserving the same notation introduced in the preceding chapter, let's increment the functional $L(\mathbf{u},\mathbf{v},\Theta)$ by the term due to the contact interaction

$$\begin{aligned} L(\mathbf{u},\mathbf{v},\Theta) &= \int_\Omega \left(E - \Theta_o S^E + \frac{1}{2}\rho_o \mathbf{v}^T \cdot \mathbf{v} \right) dV + V_{ext}(\mathbf{u}) \\ &\quad + \int_{\Gamma^{(1)}} (E_c - \Theta_o S_c^e)\, dS \end{aligned} \tag{3.69}$$

The a-priori stability estimate provides that

$$\frac{d}{dt} L(\mathbf{u},\mathbf{v},\Theta) \leq 0 \tag{3.70}$$

so that the nonlinear stability is ensured if $L(\mathbf{u},\mathbf{v},\Theta)$ is a non-increasing Lyapunov-like function along the flow generated by the thermo-plastic problem. Therefore the rate of change of $L(\mathbf{u},\mathbf{v},\Theta)$ along the dynamics generated by the coupled problem is computed as

$$\begin{aligned} \frac{d}{dt} L(\mathbf{u},\mathbf{v},\Theta) &= -\int_\Omega \frac{\Theta_o}{\Theta} (D_{mech} + D_{cond})\, dV \\ &\quad - \int_{\Gamma^{(1)}} \frac{\Theta_o}{\Theta_c} (D_{c,\,mech} + D_{c,\,cond})\, dS \leq 0 \end{aligned} \tag{3.71}$$

This condition is regarded as a fundamental a-priori estimate for the thermo-plastic evolution problem accounting for the frictional contact interaction which must be preserved by the time-stepping algorithm [Armero & Simo-93], [Laursen & Chawla-97].

3.10 Contact Contribution to the Weak form

The frictional contact contribution to the weak form of the momentum balance equation can be conveniently expressed as

$$G_c = \langle \delta g_N, t_N \rangle_{\Gamma^{(1)}} + \langle \delta \bar{\xi}^{\alpha} , t_{T\alpha} \rangle_{\Gamma^{(1)}} \tag{3.72}$$

where $\delta(\cdot)$ is an admissible variation of its argument and $\langle \cdot, \cdot \rangle_{\Gamma^{(1)}}$ denotes the $L_2\left(\Gamma^{(1)}\right)$-inner product on the boundary $\Gamma^{(1)}$.

To obtain these contributions we used of the *equilibrium condition* at the *contact interface* [Agelet-97b]. Therefore, for each point $\mathbf{X} \in \Gamma^{(1)}$, we require that both the frictional contact force induced on body $\beta^{(2)}$ at the material point $\bar{\mathbf{Y}}(\mathbf{X}, t)$ must be *equal* and *opposite* to that produced on body $\beta^{(1)}$ at point $\mathbf{X}$. Mathematically, this equilibrium condition take the form

$$\mathbf{t}^{(1)}(\mathbf{X}, t)\, d\Gamma^{(1)} + \mathbf{t}^{(2)}(\mathbf{X}, t)\, d\Gamma^{(2)} = 0 \tag{3.73}$$

The expressions for δg_N and $\delta \bar{\xi}^{\alpha}$ can be found in [Laursen & Simo-91] and therefore will not be given here.

The contact contribution to the weak form of the energy balance equation can be obtained taking into account the heat flux interchanged at the contact interface. Applying the divergence theorem, the result previously obtained with equation (2.149) changes in

$$\langle \delta\vartheta, \nabla \cdot \mathbf{Q} \rangle = \langle \nabla(\delta\vartheta), k\nabla\Theta \rangle + \langle \delta\vartheta, \bar{q} \rangle_{\partial\Omega} + \left\langle \delta\vartheta^{(1)}, Q_c^{(1)} \right\rangle_{\Gamma^{(1)}} + \left\langle \delta\vartheta^{(2)}, \bar{Q}_c^{(2)} \right\rangle_{\Gamma^{(2)}} \tag{3.74}$$

so that assuming the following hypothesis

$$\left\langle \delta\vartheta^{(2)}, \bar{Q}_c^{(2)} \right\rangle_{\Gamma^{(2)}} = \left\langle \delta\vartheta^{(2)}, Q_c^{(2)} \right\rangle_{\Gamma^{(1)}} \tag{3.75}$$

the contact contribution to the weak form of the energy balance equation can be written as

$$G_c^{\vartheta} = -\left\langle \delta\vartheta^{(1)}, Q_c^{(1)} \right\rangle_{\Gamma^{(1)}} - \left\langle \delta\vartheta^{(2)}, Q_c^{(2)} \right\rangle_{\Gamma^{(1)}} \tag{3.76}$$

Chapter 4

Time Integration of the Coupled Problem

This chapter deals with the numerical solution of the coupled thermo-mechanical problem involving the transformation of an infinite dimensional transient system, governed by a system of quasi-linear partial differential equations into a sequence of discrete non-linear algebraic problems by means of a Galerkin finite element projection and a time marching scheme for the advancement of the primary nodal variables, displacements and temperatures, together with a return mapping algorithm for the advancement of the internal variables.

A fractional step method arising from an operator split of the governing differential equations has been used to solve the non-linear coupled system of equations, leading to a staggered product formula solution algorithm [Armero & Simo-92], [Armero & Simo-93], [Armero-Thesis-93]. An isentropic and isothermal operator splits are formulated and their non-linear stability issues are discussed. The final goal is to get an accurate, efficient and robust numerical model, allowing the numerical simulation of solidification processes in the metal casting industry.

4.1 Time stepping schemes

The numerical solution of the coupled thermo-mechanical problem involves the time marching scheme for the advancement of the primary nodal variables: displacements and temperatures.

With regard to the time stepping scheme different strategies are possi-

ble, but they can be grouped in two categories: *simultaneous* time-stepping algorithms and *staggered* time-stepping algorithms.

Simultaneous time-stepping algorithms solve both the mechanical and the thermal equilibrium equations together, thus advancing all the primary nodal variables of the problem, displacements and temperatures, simultaneously. This invariably leads to large and unsymmetrical system of equations, usually prohibitively expensive to solve. Furthermore, the use of different standard time-stepping algorithms developed for the single uncoupled problems is not straightforward, and it is not possible to take advantage of the different time-scales possibly involved in the problem for the mechanical and thermal parts. On the other hand, it is relatively simple to devise unconditionally stable schemes using this approach.

A variant of this approach is to attempt the solution of the resulting equations using a *block-iterative* solution. This leads to smaller and usually symmetric system of equations to be solved, but then the study of stability of the algorithms is complicated, as it depends on the tolerances used to assess convergence. The problem of stability in time is then linked to that of convergence within the time step [Cervera & Codina-96].

Staggered time-stepping algorithms are based on the use of an operator split, applied to the coupled system of non-linear ordinary differential equations, and a *product formula* algorithm, which leads to a scheme in which one of the subproblems defined by the partition is solved sequentially, within the framework of classical *fractional step methods.* This lead to the partition of the original problem into smaller and typically symmetric (physical) subproblems. Furthermore, the use of different standard time-stepping algorithms developed for the uncoupled subproblems is now straightforward, and it is possible to take advantage of the different time-scales involved. Additionally, it is now possible to obtain unconditionally stable schemes using this approach, providing that the operator split preserves the underlying dissipative structure of the original problem [Armero & Simo-92], [Armero & Simo-93], [Armero-Thesis-93].

4.1.1 Simultaneous algorithm

The discretization of the continuous problems to be considered will lead to a non-linear algebraic system of equations of the form:

$$\begin{bmatrix} \mathbf{K}_{uu} & \mathbf{K}_{u\theta} \\ \mathbf{K}_{\theta u} & \mathbf{K}_{\theta\theta} \end{bmatrix} \begin{bmatrix} \mathbf{U} \\ \boldsymbol{\Theta} \end{bmatrix} = \begin{bmatrix} \mathbf{F}_u \\ \mathbf{F}_\theta \end{bmatrix} \tag{4.1}$$

where $\mathbf{U}$ and $\boldsymbol{\Theta}$ are the vectors of nodal unknowns at a certain time step of the two fields under consideration, $\mathbf{F}_u$ and $\mathbf{F}_\theta$ are the vectors of forces, and $\mathbf{K}_{i,j}$ $i,j = 1,2$ are matrices generally depending on the unknown fields. The algorithm for the direct solution of problem (4.1) with a simultaneous strategy can be chosen from among the variety of linearization schemes available for the solution of non-linear problems. Here, we can mention the well-known Newton-Raphson method or the somehow more sophisticated Quasi-Newton or Secant-Newton methods. The steps involved in the solution process would follow exactly those necessary to solve an uncoupled non-linear problem of similar characteristics. One disadvantage of this strategy is that the structure of the global matrices $\mathbf{K}_{i,j}$ is such that entries come from different domains or they represent physically different magnitudes. Another disadvantage is the larger size of the global matrix as compared with the ones arising from the different fields. On the other hand, the advantage is that the final algorithm is easily and clearly defined and its analysis, regarding for instance convergence, is feasible.

4.1.2 Block-iterative algorithm

Let us consider now the use of block-iterative algorithms to solve problem (4.1). This will reduce the size of the resulting subproblems at the expense of iterating. Assuming that the first block of equations in (4.1) is solved first, there are two possible block-iterative schemes, namely

$$\mathbf{K}_{uu}^{(i)}\mathbf{U}^{(i)} = \mathbf{F}_u - \mathbf{K}_{u\theta}^{(i-1)}\boldsymbol{\Theta}^{(i-1)} \tag{4.2}$$

and

$$\mathbf{K}_{\theta\theta}^{(i)}\boldsymbol{\Theta}^{(i)} = \mathbf{F}_\theta - \mathbf{K}_{\theta u}^{(k)}\mathbf{U}^{(k)}, \quad k = i-1 \text{ or } i \tag{4.3}$$

Here, superscripts in parenthesis refer to iteration counters. For $k = i-1$ this is the *block-Jacobi* (or *block-total-step*) method, whereas for $k = i$ it is

the *block-Gauss-Seidel* (or *block-single-step*) method. From elementary numerical analysis it is known that, under certain conditions, both the Jacobi and the Guass-Seidel methods converge linearly when applied to linear system, the convergence rate of the latter being twice higher than that of the former. In their counterparts these properties are inherited, the convergence rate depending now on the spectral radius of the matrices involved.

On the other hand, problem (4.1) is non-linear, so that an iterative procedure must be used to deal with this non-linearity. Newton-Raphson method is defined by approximating the generic term $\mathbf{K}_{xx}^{(i)}\mathbf{X}^{(i)}$ as

$$\mathbf{K}_{xx}^{(i)}\mathbf{X}^{(i)} \simeq \mathbf{K}_{xx}^{(i-1)}\mathbf{X}^{(i)} + d_x\mathbf{K}_{xx}^{(i-1)}\left[\mathbf{X}^{(i)} - \mathbf{X}^{(i-1)}\right] \tag{4.4}$$

where $d_x\mathbf{K}_{xx}^{(i-1)}$ arises from the derivation of $\mathbf{K}_{xx}^{(i-1)}$ with respect to $\mathbf{X}$. Using this kind of linearization it is possible to transform non-linear problems (4.2) and (4.3) into their linearized versions: so that either the non-linearity or the coupling could be solved using a nested iterative loop. However, there is the strong temptation to use a single iterative loop to deal both with the non-linearity and the coupling [Cervera & Codina-96].

The staggered solution presented has some advantages: the structure of matrices in the left-hand-side is such that entries come only from the fields currently considered, so that the integrals have to be evaluated only in that domain, and they represent physically homogeneous magnitudes. Moreover, for many practical applications these matrices are symmetrical. Finally, note that the two systems of equations to be solved are smaller in size and with reduced band-width, as well as better conditioned, as compared to that yielding from simultaneous problem (4.1). On the other hand the disadvantage of a block-iterative solution of problems (4.2) and (4.3) is that iterations will be needed even if the problem is linear. This is not especially inconvenient if the problem is non-linear, as equilibrium iterations would be required anyway, or if the coupling effect is not too strong.

It needs to be said that coupled problems are usually time-dependent and their governing equations include time-derivatives. In this case an appropriate step-by-step procedure has to be introduced to obtain the solution of the problem in time. If the time dimension is involved the analysis of any proposed solution strategy must consider the time integration stability of the approach. If direct (simultaneous) solution of the couples problem is considered the stability analysis is analogous to that of a standard uncoupled transient problem [Hughes-87], [Zienkiewicz-91]. Regarding the analysis of the

block-iterative solution it is certainly complicated and very problem/scheme dependent. It may happen that, even if an unconditionally stable algorithm has been used for every one of the fields, the overall block iterative algorithm may still be conditionally stable [Felippa-80], [Zienkiewicz-91]. Finally, an important point regarding the stability of the block-iterative techniques is that time integration stability will also depend on the tolerance demanded to achieve overall convergence. As a limit case, if solution of problems (4.2) and (4.3) is iterated until full overall convergence is achieved, then the stability characteristics of the approach are identical to those of the direct solution problem (4.1).

4.2 Fractional step methods

Here, attention will be placed to the *staggered* time-stepping algorithms based on *product formula* of the governing equations [Armero & Simo-92], [Armero & Simo-93], [Armero-Thesis-93].

4.2.1 Time-stepping algorithms

Let $\mathbb{k}_{\Delta t}[\mathbf{Z}] : \boldsymbol{\nu} \times \Re \rightarrow \boldsymbol{\nu}$ be a one-parameter family of maps, which depends continuously on a *time-step* $\Delta t \geq 0$, referred to as the *time-stepping algorithm*, such that given the approximate solution vector $\mathbf{Z}_n$ at time t_n the solution vector $\mathbf{Z}_{n+1}$ at time t_{n+1} will be given by

$$\mathbf{Z}_{n+1} = \mathbb{k}_{\Delta t}[\mathbf{Z}_n] \tag{4.5}$$

for $\Delta t = t_{n+1} - t_n$ and $\mathbf{Z}_n, \mathbf{Z}_{n+1} \in \boldsymbol{\nu}$.

A time-stepping algorithm is said to be *consistent* with the *semi-flow* generated by the non-linear operator $\mathbf{A}(\cdot)$ if the following conditions hold

$$\lim_{\Delta t \to 0} \mathbb{k}_{\Delta t}[\mathbf{Z}] = \mathbf{Z} \tag{4.6}$$

$$\lim_{\Delta t \to 0} \frac{1}{\Delta t}[\mathbb{k}_{\Delta t}[\mathbf{Z}] - \mathbf{Z}] = \mathbf{A}(\mathbf{Z}) \tag{4.7}$$

A time-stepping algorithm is said to be *convergent* if the following condition holds

$$\lim_{k \to \infty} \mathbb{k}^k_{\Delta t}[\mathbf{Z}_n] = F[\mathbf{Z}_n] \tag{4.8}$$

for $\Delta t = (t - t_n)/k$ and $t \in [t_{n+1}, t_n]$, where the iterated algorithm $\mathbb{k}^k_{\Delta t}$ is defined as

$$\mathbb{k}^k_{\Delta t} = \mathbb{k}_{\Delta t} \circ \cdots \circ \mathbb{k}_{\Delta t} \tag{4.9}$$

An algorithm $\mathbb{k}_{\Delta t}$, consistent with the semi-flow generated by the non-linear operator $\mathbf{A}(\cdot)$ is said to be *B-stable* if it inherits the *contractivity* property relative to the natural norm $\|\cdot\|_{\mathbf{Z}}$, i.e.,

$$\left\| \mathbb{k}_{\Delta t}[\mathbf{Z}_n] - \mathbb{k}_{\Delta t}\left[\tilde{\mathbf{Z}}_n\right] \right\|_{\nu} \leq \left\| \mathbf{Z}_n - \tilde{\mathbf{Z}}_n \right\|_{\nu} \tag{4.10}$$

for $\Delta t \geq 0$ and any two initial conditions $\mathbf{Z}_n, \tilde{\mathbf{Z}}_n \in \boldsymbol{\nu}$.

An algorithm $\mathbb{k}_{\Delta t}$, consistent with the semi-flow generated by the non-linear operator $\mathbf{A}(\cdot)$ is said to be *dissipative-stable* if it inherits the *a-priori estimate* on the dynamics, that is

$$L(\mathbb{k}_{\Delta t}[\mathbf{Z}]) - L(\mathbf{Z}) \leq 0 \tag{4.11}$$

for some $\Delta t < \Delta t_{crit}$ and any $\mathbf{Z} \in \boldsymbol{\nu}$ where $L(\cdot)$ is a *non-negative Lyapunov*-like functional.

The dissipative stability is the appropriate notion of stability for *dissipative dynamical systems*. Observe that if $\Delta t_{crit} = \infty$ the algorithm is said to be *unconditionally stable*. Otherwise the algorithm is said to be only conditionally stable [Armero-Thesis-93].

4.2.2 Local evolution problem

Consider the following (homogeneous first order constrained dissipative local problem of evolution

$$\begin{array}{rcl} \dot{\mathbf{Z}} = \mathbf{A}(\mathbf{Z}, \boldsymbol{\Gamma}) & \text{in} & \Omega \times [0, T] \\ \mathbf{Z}(t_o) = \mathbf{Z}_o & \text{in} & \Omega \end{array} \tag{4.12}$$

along with

$$\begin{array}{rcl} \dot{\boldsymbol{\Gamma}} = \boldsymbol{\gamma}\mathbf{G}(\mathbf{Z}, \boldsymbol{\Gamma}) & \text{in} & \Omega \times [0, T] \\ \boldsymbol{\Gamma}(t_o) = \boldsymbol{\Gamma}_o & \text{in} & \Omega \end{array} \tag{4.13}$$

where $\mathbf{Z}$ is a set of primary independent variables, $\boldsymbol{\Gamma}$ is a set of internal variables, $\mathbf{A}(\mathbf{Z}, \boldsymbol{\Gamma})$ and $\mathbf{G}(\mathbf{Z}, \boldsymbol{\Gamma})$ are non-linear operators and $\boldsymbol{\gamma} = \begin{bmatrix} \gamma^v \cdot \mathbf{I} & \mathbf{0} \\ \mathbf{0} & \gamma^{vp} \cdot \mathbf{I} \end{bmatrix}$ is the tensor of visco-elastic and viscoplastic multipliers. In the formulation

of the fractional step method described below, it is essential to regard the set of internal variables $\mathbf{\Gamma}$ as implicitly defined in terms of the variables $\mathbf{Z}$ via the evolution equations (4.13). Therefore $\mathbf{Z}$ are the only independent variables and their choice becomes a crucial aspect in the formulation of the fractional step method.

Consider the set of independent variables

$$\mathbf{Z} = \left[\mathbf{u}, \mathbf{v}, S^E, S^I, S^{pc}\right] \tag{4.14}$$

and the set of internal variables

$$\mathbf{\Gamma} = \left[\boldsymbol{\varepsilon}^v, \mathbf{E}^{vp}\right] \tag{4.15}$$

where $\mathbf{E}^{vp} = [\boldsymbol{\varepsilon}^{vp}, \boldsymbol{\zeta}, \xi]$ is the set of viscoplastic variables. All the remaining variables can be defined in terms of $\mathbf{Z}$ and $\mathbf{\Gamma}$ by the kinematic and constitutive equations [Alaska-97], [Cancun-99].

With these definitions in hand, the governing equations of the thermoplastic model can be written in the format (4.12) and (4.13), that is

$$\mathbf{A}\left(\mathbf{Z}, \mathbf{\Gamma}\right) = \begin{Bmatrix} \mathbf{v} \\ \dfrac{1}{\rho_o}\left[\nabla \cdot \boldsymbol{\sigma} + \mathbf{b}\right] \\ \dfrac{1}{\Theta}\left[R - \nabla \cdot \mathbf{Q} + D_{mcch} - \dot{L}\right] \\ \dfrac{1}{\Theta} D_{ther} \\ \dfrac{1}{\Theta}\dot{L} \end{Bmatrix} \tag{4.16}$$

and

$$\mathbf{G}\left(\mathbf{Z}, \mathbf{\Gamma}\right) = \begin{Bmatrix} \dfrac{\partial \Lambda\left(\mathbf{s}, \Theta\right)}{\partial \mathbf{s}} \\ \dfrac{\partial \Phi\left(\mathbf{\Sigma}, \Theta\right)}{\partial \mathbf{\Sigma}} \end{Bmatrix} \tag{4.17}$$

where $\mathbf{\Sigma} = [\mathbf{s}, \mathbf{q}, q]$ is the generalized stress tensor.

4.2.3 Product formula algorithm

In this section a product formula algorithm emanating from an operator split of the evolution equations is presented [Chorin-78]. The goal is to examine in detail different classes of fractional step methods arising in the context of the

coupled thermomechanical problem from possible splits of the differential operator $\mathbf{A}$. It is important to point out that these splits are formulated for the continuum operator $\mathbf{A}$ and not for the discrete operator, say $\mathbf{A}^h$, arising from a spatial discretization of the initial-boundary value problem. Consistency of a time-stepping algorithm with $\mathbf{A}^h$ does not imply necessarily consistency with $\mathbf{A}$ as $h \to 0$. Therefore, issues related to conditional consistency do not arise in this approach. However, the final implementation of these algorithms is discussed in the context of the finite element method.

The design of fractional step methods for the solution of problems of the type (4.12, 4.13) exploit additive splits of the differential operator $\mathbf{A}$ of the form

$$\mathbf{A}(\cdot) = \mathbf{A}^{(1)} + \mathbf{A}^{(2)} \tag{4.18}$$

or, more generally, of the sum of a finite number of operators $\mathbf{A}^{(k)}$ defining a well-posed problem by itself. Then, a time-stepping algorithm for the global problem is obtained formally as the product of two algorithms $\mathbb{k}^{(k)}_{\Delta t}[\cdot]$ consistent with each $\mathbf{A}^{(k)}$ respectively, e.g.,

$$\mathbb{k}_{\Delta t}[\cdot] = \left(\mathbb{k}^{(2)}_{\Delta t} \circ \mathbb{k}^{(1)}_{\Delta t}\right)[\cdot] \tag{4.19}$$

That is, the final solution $\mathbf{Z}_{n+1}$ at time t_{n+1} is obtained by solving the sub-problem defined by $\mathbf{A}^{(1)}$ from the known solution $\mathbf{Z}_n$, giving $\bar{\mathbf{Z}}_{n+1}$, followed by the solution of the sub-problem $\mathbf{A}^{(2)}$ form the known *intermediate* value $\bar{\mathbf{Z}}_{n+1}$

Problem-1

$$\mathbf{Z}_n \;\rightarrow\; \dot{\mathbf{Z}} = \mathbf{A}^{(1)}[\mathbf{Z}] \;\rightarrow\; \bar{\mathbf{Z}}_{n+1} \tag{4.20a}$$

Problem-2

$$\bar{\mathbf{Z}}_{n+1} \;\rightarrow\; \dot{\mathbf{Z}} = \mathbf{A}^{(2)}[\mathbf{Z}] \;\rightarrow\; \mathbf{Z}_{n+1} \tag{4.20b}$$

The algorithm presented is only *first order* accurate. A *second order* accurate product formula algorithm can be defined through a *double pass technique* given by,

$$\mathbb{k}_{\Delta t}[\cdot] = \left(\mathbb{k}^{(1)}_{\Delta t/2} \circ \mathbb{k}^{(2)}_{\Delta t} \circ \mathbb{k}^{(1)}_{\Delta t/2}\right)[\cdot] \tag{4.21}$$

with individual second order schemes $\mathbb{k}^{(k)}_{\Delta t}, (k = 1, 2)$. This product algorithms was first proposed by Strang [Strang-69].

As an example, consider the following *linear* initial value problem governing the evolution of $\mathbf{x}(t) \in \Re^n$

$$\begin{cases} \dot{\mathbf{x}}(t) = \mathbf{A}[\mathbf{x}(t)] \equiv \left(\mathbf{A}^{(1)}+\mathbf{A}^{(2)}\right)[\mathbf{x}(t)] \\ \mathbf{x}(t_n) = \mathbf{x}_n \end{cases} \tag{4.22}$$

where the linear operator $\mathbf{A}:\Re^n \to \Re^n$ admits the additive decomposition $\mathbf{A} \equiv \mathbf{A}^{(1)}+\mathbf{A}^{(2)}$. The exact solution of problem (4.22) at time $t_{n+1} = t_n + h$ with $h > 0$ is given by

$$\mathbf{x}(t_{n+1}) = \exp[\mathbf{A}h]\ \mathbf{x}_n = \exp\left[\left(\mathbf{A}^{(1)}+\mathbf{A}^{(2)}\right)h\right]\ \mathbf{x}_n \tag{4.23}$$

In order to approximate this solution, consider the following split problems

$$\begin{array}{ccc} \textit{Problem-1} & \to & \textit{Problem-2} \\ \begin{cases} \dot{\overline{\mathbf{x}}}(t) = \mathbf{A}^{(1)}\overline{\mathbf{x}}(t) \\ \overline{\mathbf{x}}(t_n) = \mathbf{x}_n \end{cases} & & \begin{cases} \dot{\mathbf{x}}(t) = \mathbf{A}^{(2)}\mathbf{x}(t) \\ \mathbf{x}(t_n) = \overline{\mathbf{x}}(t_{n+1}) \end{cases} \end{array} \tag{4.24}$$

Note that the solution of problem-1 is taken as initial condition for problem 2, and that both problems do indeed add up to the original problem (4.22). This sequential solution scheme defines a *product formula algorithm* of the form

$$\mathbf{x}(t_{n+1}) = \exp\left[\mathbf{A}^{(1)}h\right]\exp\left[\mathbf{A}^{(2)}h\right]\mathbf{x}_n \tag{4.25}$$

where $\exp\left[\mathbf{A}^{(k)}h\right]$, $(k = 1, 2)$, are the exact solutions of problems, 1 and 2, respectively. Of course, product formula algorithm (4.24) do not furnish the exact solution to the initial problem (4.22), but can be easily shown that (4.25) defines a first order accurate algorithm and repeated application of formula (4.25) with decreasing time step yields the exact solution; i.e.,

$$\lim_{n\to\infty}\left(\exp\left[\mathbf{A}^{(1)}h/n\right]\exp\left[\mathbf{A}^{(2)}h/n\right]\right)^n = \exp\left[\left(\mathbf{A}^{(1)}+\mathbf{A}^{(2)}\right)h\right] = \exp[\mathbf{A}h] \tag{4.26}$$

This is the so-called *Lie's formula*, see [Abraham-83]. One can show that above results essentially carry over for the case in which $\mathbf{A}$ is a *non-linear* operator and the exact algorithm that solve problem 1 and 2 are replaced by *first order accurate consistent algorithms.*

4.2.4 Operator splits: a-priory stability estimate

Consider the dissipative evolution problem given by (4.12) – (4.13) with the associated non-increasing Lyapunov-like function $L(\cdot)$ given by (2.24). Consider an additive operator split of the vector field $\mathbf{A} = \mathbf{A}^{(1)} + \mathbf{A}^{(2)}$ leading to the following two sub-problems

$$\begin{array}{ll} \textit{Problem-1} & \textit{Problem-2} \\ \dot{\mathbf{Z}} = \mathbf{A}^{(1)}(\mathbf{Z}, \boldsymbol{\Gamma}) & \dot{\mathbf{Z}} = \mathbf{A}^{(2)}(\mathbf{Z}, \boldsymbol{\Gamma}) \\ \dot{\boldsymbol{\Gamma}} = \gamma \mathbf{G}(\mathbf{Z}, \boldsymbol{\Gamma}) & \dot{\boldsymbol{\Gamma}} = \gamma \mathbf{G}(\mathbf{Z}, \boldsymbol{\Gamma}) \end{array} \tag{4.27}$$

The critical restriction on the design of the operator split is that each one of the sub-problems must preserve the underlying dissipative structure of the original problem, that is

$$\frac{d}{dt} L\left(\mathbf{Z}^{(\alpha)}, \boldsymbol{\Gamma}^{(\alpha)}\right) \leq 0 \; ; \; (\alpha = 1, 2) \tag{4.28}$$

where $\mathbf{Z}^{(\alpha)}$ and $\boldsymbol{\Gamma}^{(\alpha)}$ denote the flow generated by the vector fields $\mathbf{A}^{(\alpha)}$, $\alpha = 1, 2$.

Two different operator splits will be considered here. First an *isentropic* operator split, which satisfies the critical design restriction mentioned above, is considered, extending the results of Armero & Simo [Armero & Simo- 91], [Armero & Simo-92], [Armero & Simo-93] to the more general case presented here. This split is compared next with an *isothermal* operator split, which does not satisfy the design restriction.

Isentropic operator split

Consider the following additive isentropic-based operator split of the vector field $\mathbf{A}(\mathbf{Z}, \boldsymbol{\Gamma})$ as follows

$$\mathbf{A}(\mathbf{Z}, \boldsymbol{\Gamma}) = \mathbf{A}^{(1)}_{ise}(\mathbf{Z}, \boldsymbol{\Gamma}) + \mathbf{A}^{(2)}_{ise}(\mathbf{Z}, \boldsymbol{\Gamma}) \tag{4.29}$$

where the vector fields $\mathbf{A}^{(1)}_{ise}(\mathbf{Z}, \boldsymbol{\Gamma})$ and $\mathbf{A}^{(2)}_{ise}(\mathbf{Z}, \boldsymbol{\Gamma})$ are defined as

$$\mathbf{A}^{(1)}_{ise}(\mathbf{Z}, \boldsymbol{\Gamma}) = \left\{ \begin{array}{c} \mathbf{v} \\ \frac{1}{\rho_o}[\nabla \cdot \boldsymbol{\sigma} + \mathbf{b}] \\ 0 \\ 0 \\ 0 \end{array} \right. \tag{4.30}$$

$$\mathbf{A}_{ise}^{(2)}(\mathbf{Z},\boldsymbol{\Gamma}) = \begin{cases} \mathbf{0} \\ \mathbf{0} \\ \frac{1}{\Theta}\left[R - \nabla\cdot\mathbf{Q} + D_{mech} - \dot{L}\right] \\ \frac{1}{\Theta} D_{ther} \\ \frac{1}{\Theta}\dot{L} \end{cases} \tag{4.31}$$

and consider the following two problem of evolution

$$\begin{array}{cc} \textit{Problem-1} & \textit{Problem-2} \\ \dot{\mathbf{Z}} = \mathbf{A}_{ise}^{(1)}(\mathbf{Z},\boldsymbol{\Gamma}) & \dot{\mathbf{Z}} = \mathbf{A}_{ise}^{(2)}(\mathbf{Z},\boldsymbol{\Gamma}) \\ \dot{\boldsymbol{\Gamma}} = \boldsymbol{\gamma}\mathbf{G}(\mathbf{Z},\boldsymbol{\Gamma}) & \dot{\boldsymbol{\Gamma}} = \boldsymbol{\gamma}\mathbf{G}(\mathbf{Z},\boldsymbol{\Gamma}) \end{array} \tag{4.32}$$

Within this operator split, *Problem-1* defines a mechanical phase at fixed total entropy $\dot{S} = 0$ and *Problem-2* defines a thermal phase at fixed configuration. Note that a stronger condition has been placed in the Problem-1 by the additional requirement that all the components of the entropy function are held fixed

$$\dot{S} = \dot{S}^E + \dot{S}^I + \dot{S}^{pc} = 0 \Longleftarrow \begin{cases} \dot{S}^E = 0 \\ \dot{S}^I = 0 \\ \dot{S}^{pc} = 0 \end{cases} \tag{4.33}$$

Note also that the evolution of the internal variables $\boldsymbol{\Gamma}(\mathbf{Z},\boldsymbol{\Gamma})$ is imposed in both sub-problems. Additionally, the temperature field is regarded as the independent variable in two sub-problems defined rather that the entropy.

Denoting by $\mathbf{Z}^{(\alpha)}$ and $\boldsymbol{\Gamma}^{(\alpha)}$ the flow generated by the vector fields $\mathbf{A}_{ise}^{(\alpha)}$, $\alpha = 1, 2$, a straightforward computation shows that the following estimates holds

$$\frac{d}{dt}L\left(\mathbf{Z}^{(1)},\boldsymbol{\Gamma}^{(1)}\right) = -\int_\Omega D_{mech}^{(1)}\, dV \leq 0 \tag{4.34a}$$

$$\frac{d}{dt}L\left(\mathbf{Z}^{(2)},\boldsymbol{\Gamma}^{(2)}\right) = -\int_\Omega \frac{\Theta_o}{\Theta^{(2)}}\left(D_{mech}^{(2)} + D_{cond}^{(2)}\right) dV \leq 0 \tag{4.34b}$$

where $D_{mech}^{(\alpha)}$, $D_{cond}^{(\alpha)}$, and $\Theta^{(\alpha)}$ are the mechanical dissipation, the thermal heat conduction dissipation and the absolute temperature, respectively, in *Problem-α*, $\alpha = 1, 2$.

Thus, the isentropic split preserves the underlying dissipative structure of the original problem. Therefore, in sharp contrast with schemes based on the conventional isothermal split, unconditionally stable algorithms consistent with the full coupled problem can be obtained merely as the product of two unconditionally stable algorithms consistent with each phase. For dissipative dynamical systems if each of the algorithms is *unconditionally dissipative stable* then the product formula algorithm is also *unconditionally dissipative stable*. Note that unconditional stability in the context of non-linear problems is to be understood as the algorithmic solution satisfying the a-priory stability estimate [Armero-Thesis-93].

Isothermal operator split

Consider the following additive isothermal based operator split of the vector field $\mathbf{A}(\mathbf{Z},\boldsymbol{\Gamma})$ as follows

$$\mathbf{A}(\mathbf{Z},\boldsymbol{\Gamma}) = \mathbf{A}^{(1)}_{iso}(\mathbf{Z},\boldsymbol{\Gamma}) + \mathbf{A}^{(2)}_{iso}(\mathbf{Z},\boldsymbol{\Gamma}) \tag{4.35}$$

where the vector fields $\mathbf{A}^{(1)}_{iso}(\mathbf{Z},\boldsymbol{\Gamma})$ and $\mathbf{A}^{(2)}_{iso}(\mathbf{Z},\boldsymbol{\Gamma})$ are defined as

$$\mathbf{A}^{(1)}_{iso}(\mathbf{Z},\boldsymbol{\Gamma}) = \begin{Bmatrix} \mathbf{v} \\ \frac{1}{\rho_o}[\nabla\cdot\boldsymbol{\sigma}+\mathbf{b}] \\ \frac{1}{\Theta}H^{ep} \\ 0 \\ 0 \end{Bmatrix} \tag{4.36}$$

$$\mathbf{A}^{(2)}_{iso}(\mathbf{Z},\boldsymbol{\Gamma}) = \begin{Bmatrix} \mathbf{0} \\ \mathbf{0} \\ \frac{1}{\Theta}\left[R-\nabla\cdot\mathbf{Q}+D_{mech}-\dot{L}-H^{ep}\right] \\ \frac{1}{\Theta}D_{ther} \\ \frac{1}{\Theta}\dot{L} \end{Bmatrix} \tag{4.37}$$

and consider the following two problem of evolution

$$\begin{array}{ll} \textit{Problem: 1} & \textit{Problem: 2} \\ \dot{\mathbf{Z}} = \mathbf{A}^{(1)}_{iso}(\mathbf{Z},\boldsymbol{\Gamma}) & \dot{\mathbf{Z}} = \mathbf{A}^{(2)}_{iso}(\mathbf{Z},\boldsymbol{\Gamma}) \\ \dot{\boldsymbol{\Gamma}} = \boldsymbol{\gamma}\mathbf{G}(\mathbf{Z},\boldsymbol{\Gamma}) & \dot{\boldsymbol{\Gamma}} = \boldsymbol{\gamma}\mathbf{G}(\mathbf{Z},\boldsymbol{\Gamma}) \end{array} \tag{4.38}$$

Within this operator split, *Problem-1* defines a mechanical phase at fixed temperature $\dot{\Theta} = 0$ and *Problem-2* defines a thermal phase at fixed configuration. Note also that the evolution of the internal variables $\mathbf{\Gamma}(\mathbf{Z}, \mathbf{\Gamma})$ is imposed in both sub-problems.

Denoting by $\mathbf{Z}^{(\alpha)}$ and $\mathbf{\Gamma}^{(\alpha)}$ the flow generated by the vector fields $\mathbf{A}_{iso}^{(\alpha)}$, $\alpha = 1, 2$, a straightforward computation shows that the following estimates holds

$$\frac{d}{dt} L\left(\mathbf{Z}^{(1)}, \mathbf{\Gamma}^{(1)}\right) = -\int_\Omega D_{mech}^{(1)}\, dV + \int_\Omega \left(1 - \frac{\Theta_o}{\Theta^{(1)}}\right) H^{ep(1)}\, dV \not\leq 0 \tag{4.39a}$$

$$\frac{d}{dt} L\left(\mathbf{Z}^{(2)}, \mathbf{\Gamma}^{(2)}\right) = -\int_\Omega \frac{\Theta_o}{\Theta^{(2)}} \left(D_{mech}^{(2)} + D_{cond}^{(2)}\right) dV - \int_\Omega \left(1 - \frac{\Theta_o}{\Theta^{(2)}}\right) H^{ep(2)}\, dV \not\leq 0 \tag{4.39b}$$

where $D_{mech}^{(\alpha)}$, $D_{cond}^{(\alpha)}$, $H^{ep(\alpha)}$ and $\Theta^{(\alpha)}$ are the mechanical dissipation, the thermal heat conduction dissipation, the structural elasto-plastic heating and the absolute temperature, respectively, in *Problem-*α, $\alpha = 1, 2$.

The contribution of the structural elasto-plastic heating to the evolution equations of each one of the sub-problem arising from the isothermal split, breaks the underlying dissipative structure of the original problem.

Note that this product formula is *first order accurate* and according to (4.34*a*),(4.34*b*),(4.39*a*) and (4.39*b*) algorithms based on the isothermal operator split will result in staggered schemes at best only *conditionally stables*, and only an isentropic operator split leads to *unconditionally stable* product formula algorithms.

4.3 Time-discrete variational formulation

In this section the time-discrete variational formulation of both isentropic and isothermal formulations is presented.

Consider at typical time increment $[t_n, t_{n+1}]$ with $\Delta t = t_{n+1} - t_n$ and let $\{\mathbf{u}_n, \mathbf{v}_n, \Theta_n\} \in \boldsymbol{\nu}$ be the given initial data at time t_n . The goal is to update these values and compute $\{\mathbf{u}_{n+1}, \mathbf{v}_{n+1}, \Theta_{n+1}\} \in \boldsymbol{\nu}$ at time t_{n+1}. To gain further insight into the implications of the two different splits presented, consider a specific time discretization via a standard backward-Euler method. Let us start from the unconditionally stable algorithms given by the isentropic split, to be compared with the standard isothermal split.

4.3.1 Isentropic split

Let consider the time-discrete variational formulation of the two phases generated by the additive operator split in case of an isentropic formulation. The physical idea behind this method is to partition the problem into a mechanical phase in which the entropy is held constant, followed by a thermal phase in which the configuration (but not the internal variables) are held constant. The strategy proposed below is motivated by the following design conditions:

- The operator split must inherit the stability estimate for the fractional step method to retain unconditional stability.
- The two sub-problem defined by the operator split should have a symmetric structure in the sense that a subsequent spatial discretization yields symmetric stiffness matrices.
- Time-stepping integration algorithm leading to a fractional step method should exhibit good numerical accuracy, comparable to schemes obtained via analogous time-discretization of the full coupled problem.
- The cost involved in the final implementation of the resulting method must be comparable to that involved in the implementation of the conventional isothermal split.

These requirements are necessary if the final class of algorithms must represent a significant improvement over the existing methods. In particular the first condition provides vastly superior stability characteristics while the remaining conditions ensure that this enhanced performance is not obtained at the expense of either accuracy or computational convenience [Armero & Simo- 91], [Armero-Thesis-93].

Mechanical phase (isentropic split)

The problem in this phase is to find solution $\left\{\mathbf{u}_{n+1}, \mathbf{v}_{n+1}, \bar{\Theta}_{n+1}\right\} \in \boldsymbol{\nu}$ using the following time-discrete system of equations

$$\begin{aligned}
\langle dev\left(\nabla^s \boldsymbol{\eta}\right), dev\left(\overline{\boldsymbol{\sigma}}_{n+1}\right)\rangle + \langle div\left(\boldsymbol{\eta}\right), \bar{p}_{n+1}\rangle &= G|_{n+1} && \text{(4.40a)}\\
\left\langle q, \left[div\left(\mathbf{u}\right)|_{n+1} - \bar{\theta}_{n+1}\right]\right\rangle &= 0 && \text{(4.40b)}\\
\left\langle \gamma, \left[-\bar{p}_{n+1} + \frac{1}{3} tr\left(\overline{\boldsymbol{\sigma}}_{n+1}\right)\right]\right\rangle &= 0 && \text{(4.40c)}
\end{aligned}$$

$$\bar{S}^E_{n+1} = S^E_n \qquad (4.40d)$$
$$\bar{S}^I_{n+1} = S^I_n \qquad (4.40e)$$
$$\bar{S}^{pc}_{n+1} = S^{pc}_n \qquad (4.40f)$$

where $\{\boldsymbol{\eta}, q, \gamma\} \in \boldsymbol{\nu}_o$ denotes arbitrary admissible variations, and $G|_{n+1}$ is the work due to the external forces, given by

$$G|_{n+1} = \langle \delta\boldsymbol{\eta}, \mathbf{b}_{n+1} \rangle + \langle \delta\boldsymbol{\eta}, \bar{\mathbf{t}}_{n+1} \rangle_{\partial\Omega} \qquad (4.41)$$

The evolution of the internal variables is assumed in the form

$$\bar{\boldsymbol{\Gamma}}_{n+1} = \boldsymbol{\Gamma}_n + \bar{\gamma}_{n+1} \bar{\mathbf{G}}_{n+1} \qquad (4.42)$$

that is an *isentropic return mapping* algorithm detailed in the next section, as a consequence of isentropic solution proposed.

Observe that even if the balance of momentum equation is enforced in weak form, as will be the case in a finite element context, the temperature evolution equation during the mechanical phase is always enforced in *strong form.* In the context of finite element method, this means that equations ($4.40d, 4.40e$ and $4.40f$) are evaluated at each quadrature points. This is the crucial observation for an efficient numerical implementation [Armero & Simo- 91], [Armero & Simo-92]. It must be also pointed out that the restriction on the entropy is taken into account keeping fixed the different components obtained by the additive split of the total entropy function presented in the continuum formulation (see eq. $2.71a$). This stronger algorithm design requirement is crucial for the symmetry of the final formulation (at least in case of constant material properties). In fact, the consequence of equation ($4.40d$) is the change of the temperature from value Θ_n at the beginning of the time step to the intermediate temperature $\bar{\Theta}_{n+1}$ at the end of the mechanical phase. In view of the evolution equation of the inelastic entropy is proportional to the change of the yield criterion with temperature then condition ($4.40e$) implies that *no thermal softening* is permitted in the mechanical phase. Therefore, the flow stress is frozen at the initial temperature Θ_n. It is this feature that renders the final formulation symmetric in a consistent linearization of the governing equations [Armero & Simo-93], [Armero-Thesis-93].

Finally, taking into account that the rate of entropy due to the phase change is proportional to the latent heat function according to the evolution equation (2.72) then equation ($4.40f$) limits its evolution [Alaska-97],

[Cancun-99]. Therefore, agree with the definition of the latent heat function (2.64), in the mechanical phase both solid and liquid fraction must be frozen at the initial temperature Θ_n.

Remark 5 *Design condition* (4.40*d*) *implies the evolution of the temperature field in terms of the configuration and (possibly) the hardening variables. This equation can be solved numerically, if necessary. The key implication in a finite element context is that* only *the mechanical degrees of freedom* $\{\mathbf{u}, \mathbf{v}\}$ *are involved in the global solution of the first phase, since* $\bar{\Theta}_{n+1}$ *is defined* locally. *This properties renders the numerical implementation essentially identical to that of algorithms based on the traditional isothermal split [Armero & Simo-93].*

Thermal phase (isentropic split)

Application of a backward-Euler to the thermal phase of the isentropic formulation yields the following equations

$$\left\langle \delta\vartheta, \Theta_{n+1}\left(\frac{S^E_{n+1}-S^E_n}{\Delta t}\right)+\frac{L_{n+1}-L_n}{\Delta t}\right\rangle + \left\langle \nabla\left(\delta\vartheta\right), k_{n+1}\nabla\Theta_{n+1}\right\rangle$$
$$= G^{\vartheta}\,|_{n+1} \tag{4.43a}$$

$$S^I_{n+1} = S^I_n + \frac{\Delta t}{\Theta_{n+1}} D_{ther,n+1} \tag{4.43b}$$

$$S^{pc}_{n+1} = \frac{L_{n+1}-L_n}{\Theta_{n+1}} \tag{4.43c}$$

where

$$G^{\vartheta}\,|_{n+1} = \langle \delta\vartheta, R_{n+1}\rangle + \langle \delta\vartheta, D_{mech\,m+1}\rangle - \langle \delta\vartheta, \bar{q}_{n+1}\rangle_{\partial\Omega} \tag{4.44}$$

with the associated evolution equations for the internal variables

$$\boldsymbol{\Gamma}_{n+1} = \boldsymbol{\Gamma}_n + \gamma_{n+1}\mathbf{G}_{n+1} \tag{4.45}$$

given by an isothermal return mapping for the plastic variables and a backward Euler for the viscous strain tensor, detailed in the next section.

Observe that taking advantage from the equality $\bar{S}^E_{n+1} = S^E_n$ satisfied in the mechanical phase the time-discretization of equation (4.43*a*) uses the entropy form of the energy equation. Although the intermediate temperature

$\bar{\Theta}_{n+1}$ in the initial condition for the thermal phase, this special treatment of the energy equation makes the final numerical implementation independent of $\bar{\Theta}_{n+1}$. Thus, this phase reduces to a heat conduction problem at the known fixed configuration $\left\{\mathbf{u}_{n+1} = \bar{\mathbf{u}}_{n+1}, \mathbf{v}_{n+1} = \bar{\mathbf{v}}_{n+1}\right\}$ with the only remaining independent variable Θ_{n+1}.

4.3.2 Isothermal split

Standard staggered time-stepping algorithms for coupled thermomechanical problem consist of a mechanical phase at constant temperature followed by a thermal phase at fixed configuration. Also in this case the evolution equations for the internal variables are enforced in both phases of the operator split. Two different isothermal splits will be compared. In the first one the same set of independent variable $\mathbf{Z} = \left[\mathbf{u}, \mathbf{v}, S^E, S^I, S^{pc}\right]$ and the same format of the energy equation (entropy form) used in the case of isentropic split is considered. A second isothermal operator split is proposed assuming $\mathbf{Z}^* = [\mathbf{u}, \mathbf{v}, \Theta, L]$ as a new set of independent variables and considering the temperature form of the energy equation (2.126).

Mechanical phase (isothermal split)

The following time-discrete system of equations is used to solve the mechanical phase of an isothermal split

$$\begin{aligned}
\langle dev\left(\nabla^s \boldsymbol{\eta}\right), dev\left(\overline{\boldsymbol{\sigma}}_{n+1}\right)\rangle + \langle div\left(\boldsymbol{\eta}\right), \bar{p}_{n+1}\rangle &= G|_{n+1} && \text{(4.46a)}\\
\left\langle q, \left[div\left(\mathbf{u}\right)|_{n+1} - \bar{\theta}_{n+1}\right]\right\rangle &= 0 && \text{(4.46b)}\\
\left\langle \gamma, \left[-\bar{p}_{n+1} + \frac{1}{3} tr\left(\overline{\boldsymbol{\sigma}}_{n+1}\right)\right]\right\rangle &= 0 && \text{(4.46c)}\\
\bar{S}^E_{n+1} &= -\partial\Psi/\partial\Theta && \text{(4.46d)}\\
\bar{S}^I_{n+1} &= S^I_n && \text{(4.46e)}\\
\bar{S}^{pc}_{n+1} &= S^{pc}_n && \text{(4.46f)}
\end{aligned}$$

together with a standard isothermal return mapping for the internal variables

$$\bar{\boldsymbol{\Gamma}}_{n+1} = \boldsymbol{\Gamma}_n + \bar{\gamma}_{n+1} \bar{\mathbf{G}}_{n+1} \tag{4.47}$$

Also in this case the intermediate configuration is the final configuration while the intermediate temperature field is equal to the initial one due to

the restriction on the temperature evolution. As a consequence the value of the elastic entropy must change and it will be used as the initial condition to compute the capacity term of the thermal equation in the thermal phase. It is also possible to observe that keeping constant the temperature field both the inelastic and the phase-change entropy terms are held constant in the mechanical phase so that both the flow stress and the solid fraction are maintained fixed.

Thermal phase (isothermal split)

This phase is characterized by the time-discrete variational form of the energy equation written in the entropy form

$$\left\langle \delta\vartheta, \Theta_{n+1} \left(\frac{S^E_{n+1} - \bar{S}^E_{n+1}}{\Delta t} \right) + \frac{L_{n+1} - L_n}{\Delta t} \right\rangle + \langle \nabla(\delta\vartheta), k_{n+1} \nabla\Theta_{n+1} \rangle = G^\vartheta \big|^{ep}_{n+1} \tag{4.48a}$$

$$S^E_{n+1} = -\partial\Psi / \partial\Theta \tag{4.48b}$$

$$S^I_{n+1} = S^I_n + \frac{\Delta t}{\Theta_{n+1}} D_{ther,\, n+1} \tag{4.48c}$$

$$S^{pc}_{n+1} = \frac{L_{n+1} - L_n}{\Theta_{n+1}} \tag{4.48d}$$

together with the update of the internal variables as a consequence of the update of the temperature field

$$\boldsymbol{\Gamma}_{n+1} = \boldsymbol{\Gamma}_n + \gamma_{n+1} \mathbf{G}_{n+1} \tag{4.49}$$

Observe that in this case the additional term due to the elasto-plastic heating H^{ep}_{n+1} must be taken into account in the definition of the thermal load, so that

$$G^\vartheta \big|^{ep}_{n+1} = G^\vartheta \big|_{n+1} - \langle \delta\vartheta, H^{ep}_{n+1} \rangle \tag{4.50}$$

This contribution come from the constraint on the temperature field assumed in the solution of the mechanical phase of an isothermal spit.

Mechanical phase (temperature form)

It is possible to consider an equivalent isothermal split using as the main variables of the split the temperature field and the latent heat function together with the displacement and velocity fields $\mathbf{Z} \rightarrow \mathbf{Z}^* = [\mathbf{u}, \mathbf{v}, \Theta, L]$.

In this case the time-discrete system of equations governing the mechanical phase is the following

$$\begin{aligned}
\langle dev\left(\nabla^s \boldsymbol{\eta}\right), dev\left(\overline{\boldsymbol{\sigma}}_{n+1}\right)\rangle + \langle div\left(\boldsymbol{\eta}\right), \bar{p}_{n+1}\rangle &= G|_{n+1} && \text{(4.51a)}\\
\left\langle q,\ \left[div\left(\mathbf{u}\right)|_{n+1} - \bar{\theta}_{n+1}\right]\right\rangle &= 0 && \text{(4.51b)}\\
\left\langle \gamma, \left[-\bar{p}_{n+1} + \frac{1}{3} tr\left(\overline{\boldsymbol{\sigma}}_{n+1}\right)\right]\right\rangle &= 0 && \text{(4.51c)}\\
\Theta_{n+1} &= \Theta_n && \text{(4.51d)}\\
L_{n+1} &= L_n && \text{(4.51e)}
\end{aligned}$$

together with the update of the internal variables

$$\bar{\boldsymbol{\Gamma}}_{n+1} = \boldsymbol{\Gamma}_n + \bar{\gamma}_{n+1}\bar{\mathbf{G}}_{n+1} \tag{4.52}$$

It is clear that the solution of the mechanical phase obtained using this operator is identical to the result given by the isothermal operator introduced in the previous section.

Thermal phase (temperature form)

Time discretization of the energy equation is now obtained using the temperature form (2.126).

$$\begin{aligned}
&\left\langle \delta\vartheta, C_{n+1}\left(\frac{\Theta_{n+1}-\Theta_n}{\Delta t}\right) + \frac{L_{n+1}-L_n}{\Delta t}\right\rangle + \left\langle \nabla\left(\delta\vartheta\right), k_{n+1}\nabla\Theta_{n+1}\right\rangle\\
&= G^{\vartheta}\,|_{n+1}^{ep} && \text{(4.53a)}\\
L_{n+1} &= L\left(\Theta_{n+1}\right) && \text{(4.53b)}
\end{aligned}$$

together with the update of the internal variables

$$\boldsymbol{\Gamma}_{n+1} = \boldsymbol{\Gamma}_n + \boldsymbol{\gamma}_{n+1}\mathbf{G}_{n+1} \tag{4.54}$$

The advantage is that in this form it is not necessary the evaluation of the elastic entropy $\bar{S}^E_{n+1}$ at the intermediate configuration.

Remark 6 *It must be pointed out that the entropy form of the energy equation has shown a superior numerical accuracy in a number of numerical tests when compared with the solution of the thermal phase based on the energy*

equation in temperature form. This is essentially due to the fact that the heat capacity term comes from an additional derivative of the free energy function with respect to the term proportional to the rate of elastic entropy (see eq. 2.127a).

Remark 7 *Observe that both formulation are equivalent in a linear context.*

4.4 Time-integration of the constitutive equations

Let $[0,T] \subset \Re$ the time interval of interest, if we use the compact notation, that is, $\mathbf{E} = [\boldsymbol{\varepsilon}, \mathbf{0}, 0]$, $\boldsymbol{\Gamma} = [\boldsymbol{\varepsilon}^v, \mathbf{E}^{vp}]$, $\mathbf{E}^{vp} = [\boldsymbol{\varepsilon}^{vp}, \boldsymbol{\zeta}, \xi]$ and $\boldsymbol{\Sigma} = [\mathbf{s}, \mathbf{q}, q]$, typically at time $t_{n+1} \in [0,T]$ the following steps are involved:

1. The discretized momentum equations generate incremental motions $\mathbf{u}_{n+1}$ which, in turn, are used to calculate the strain history by means of the kinematic relations

$$\mathbf{E}_{n+1} = \left[\nabla^s(\mathbf{u})|_{n+1}, \mathbf{0}, 0\right] \tag{4.55}$$

   where $\nabla^s(\circ)$ denotes the symmetric gradient;

2. for a given strain history, new values of the internal generalized variables $\boldsymbol{\Gamma}_{n+1}$ and generalized stress fields $\boldsymbol{\Sigma}_{n+1}$ are *formally* obtained by integration of the local constitutive equations with given initial conditions

$$\boldsymbol{\Gamma}_{n+1} - \boldsymbol{\Gamma}_n = \gamma_{n+1}\mathbf{G}(\mathbf{Z}, \boldsymbol{\Gamma})_{n+1} \tag{4.56a}$$

$$\boldsymbol{\Gamma}(t_n) = \boldsymbol{\Gamma}_n \tag{4.56b}$$

   and

$$\boldsymbol{\Sigma}_{n+1} = \mathbf{C} \cdot \left(\mathbf{E}_{n+1} - \mathbf{E}^{vp}_{n+1}\right) \tag{4.57}$$

   where $\mathbf{C} = \left[2G\mathbf{I}, \frac{2}{3}K\mathbf{I}, H\right]$ is the generalized moduli tensor;

3. the momentum balance equation is tested for the computed stresses and if violated the iterative process is continued by returning to step 1.

In most of computational architectures currently in use, steps 1 and 3 are carried out at a global level by finite element procedures. In the next sections, we will focus on step 2 as the central problem of computational plasticity as it corresponds to the main role played by constitutive equations.

The developments in this section provide a unified treatment of a number of existing algorithm schemes here extended to accommodate both isentropic and isothermal constraints.

4.4.1 Elasto-plastic operator split

In this section a product formula algorithm emanating from a standard elastic-plastic operator split of the elasto-plastic constitutive equations is presented [Krieg & Krieg-77], [?], [Simo-94]. The basic idea consists of a two-steps-algorithm to be applied to the evolution equations as follows:

1. an *elastic trial predictor*, obtained by freezing the plastic flow during the time step, followed by,
2. a *plastic corrector* that performs the closest-point-projection of the trial state onto the yield surface.

Using the compact notation $\mathbf{\Sigma} = [\mathbf{s}, \mathbf{q}, q]$, $\mathbf{E}^{vp} = [\boldsymbol{\varepsilon}^{vp}, \boldsymbol{\zeta}, \xi]$ and $\mathbf{C} = [2G\,\mathbf{I}, \frac{2}{3}K\,\mathbf{I}, H]$ the additive split results in

$$\begin{array}{ccccc} \text{Total} & = & \text{Elastic predictor} & + & \text{Plastic corrector} \\ \dot{\mathbf{E}}^{p} = \gamma^{p}\,\nabla\Phi\left(\mathbf{\Sigma}\right) & = & \dot{\mathbf{E}}^{vp} = [\mathbf{0}, \mathbf{0}, 0] & + & \dot{\mathbf{E}}^{vp} = \gamma^{vp}\,\nabla\Phi\left(\mathbf{\Sigma}\right) \end{array}$$

Applying an implicit *backward-Euler* difference scheme, it is possible to define a *trial elastic state* given by

$$\mathbf{E}_{n+1}^{vp\,trial} = \mathbf{E}_{n}^{vp} \tag{4.58a}$$

so that the associated trial stress field results in

$$\mathbf{\Sigma}_{n+1}^{trial} = \mathbf{C}\cdot\left(\mathbf{E}_{n+1} - \mathbf{E}_{n+1}^{vp^{trial}}\right) = \mathbf{C}\cdot\left(\mathbf{E}_{n+1} - \mathbf{E}_{n}^{vp}\right) \tag{4.59}$$

At this stage the trial state could be inside or outside the elastic domain E_{σ} , it means that the loading function $\Phi\left(\mathbf{\Sigma}\right)$ must be checked. It is possible to demonstrate that if $\Phi\left(\mathbf{\Sigma}_{n+1}^{trial}\right)$ is convex, then $\Phi\left(\mathbf{\Sigma}_{n+1}^{trial}\right) \geq \Phi\left(\mathbf{\Sigma}_{n+1}\right)$ so that

- if $\Phi\left(\boldsymbol{\Sigma}_{n+1}^{trial}\right) \leq 0 \rightarrow \Phi\left(\boldsymbol{\Sigma}_{n+1}\right) \leq 0$ and $\gamma^p = 0$ so the process is elastic and the trial state is the final state

$$\mathbf{E}_{n+1}^{vp} = \mathbf{E}_{n+1}^{vp^{trial}} = \mathbf{E}_{n}^{vp} \tag{4.60a}$$

and

$$\boldsymbol{\Sigma}_{n+1} = \boldsymbol{\Sigma}_{n+1}^{trial} = \mathbf{C} \cdot \left(\mathbf{E}_{n+1} - \mathbf{E}_{n}^{vp}\right) \tag{4.61}$$

- If, in other hand, $\Phi\left(\boldsymbol{\Sigma}_{n+1}^{trial}\right) > 0 \rightarrow \Phi\left(\boldsymbol{\Sigma}_{n+1}\right) \geq 0$ and $\gamma^p > 0$ the *plastic corrector* must be applied by a *return mapping algorithm*. According to the product formula, the resulting final state becomes in

$$\mathbf{E}_{n+1}^{vp} = \mathbf{E}_{n+1}^{vp^{trial}} + \gamma^{vp} \nabla\Phi\left(\boldsymbol{\Sigma}_{n+1}\right) \tag{4.62a}$$

and according to the *closest-point-projection* algorithm [Wilkins-64],[Krieg & Key-76], the stress fields transform in

$$\boldsymbol{\Sigma}_{n+1} = \mathbf{G} \cdot \left(\mathbf{E}_{n+1} - \mathbf{E}_{n+1}^{vp}\right) = \boldsymbol{\Sigma}_{n+1}^{trial} - \gamma^{vp}\, \mathbf{C} \cdot \nabla\Phi\left(\boldsymbol{\Sigma}_{n+1}\right) \tag{4.63}$$

4.4.2 Linear multi-step methods

A generalization of the classical return mapping algorithm for classical plasticity, described above, uses ideas from linear multi-steps method [Gear-71].

Consider the first order differential equation, subjected to initial condition

$$\left\{ \begin{array}{l} \dot{z} = f\left(z,t\right) \\ z\left(t_0\right) = z_0 \end{array} \right. \tag{4.64}$$

The generic s_{-th} order integration scheme using a linear multi-step method is the following

$$\sum_{k=0}^{s} \alpha_k z_{n+1-k} = \Delta t \sum_{k=0}^{s} \beta_k f\left(z_{n+1-k}, t_{n+1-k}\right) \tag{4.65}$$

In particular, if we consider a *Backward-Difference scheme* then the definition for coefficients α_k and β_k result in

$$\left.\begin{array}{r} \alpha_k = 0 \\ \beta_k = 1 \end{array}\right\} \rightarrow \quad k = 0 \tag{4.66a}$$

$$\left.\begin{array}{r} \alpha_k z_{n+1-k} = \frac{1}{k} D^{(k)} z_{n+1} \\ \beta_k = 0 \end{array}\right\} \rightarrow \quad k \geq 1 \tag{4.66b}$$

where the operator $D^{(k)}z_{n+1}$ is defined as

$$D^{(k+1)}z_{n+1} = D^{(k)}z_{n+1} - D^{(k)}z_n \tag{4.67a}$$

$$D^{(0)}z_{n+1} = z_{n+1} \tag{4.67b}$$

It is possible to show that this method is stable only when $s = 1$ or $s = 2$. In case of $s = 1$ we recover the *Backward-Euler method* so that the integration algorithm for the first order differential equation reduce in

$$z_{n+1} - z_n = \Delta t \; f\left(z_{n+1}, t_{n+1}\right) \tag{4.68}$$

while, if $s = 2$ the resulting algorithm is named *Gear method* and its structure is the following

$$\frac{3}{2}z_{n+1} - 2z_n + \frac{1}{2}z_{n-1} = \Delta t \; f\left(z_{n+1}, t_{n+1}\right) \tag{4.69}$$

These two algorithms could be summarized in the single relation

$$z_{n+1} = z_n + \frac{1}{3}\left(s-1\right)\left(z_n - z_{n-1}\right) + \Delta t \; f\left(z_{n+1}, t_{n+1}\right) \tag{4.70}$$

It is important to observe that Backward-Euler method (B.E.) presents *linear* convergence while in case of Gear method the convergence is *quadratic*.

Taking into account relation (4.70), it is possible to define a more general elasto-plastic operator split in which the *trial state* is given by

$$z_{n+1}^{trial} = z_n + \frac{1}{3}\left(s-1\right)\left(z_n - z_{n-1}\right) \tag{4.71}$$

4.4.3 Isentropic algorithm

At time t_n in a typical time increment $[t_n, t_{n+1}]$, the primary variables $\{\mathbf{u}_n, \Theta_n\}$ and the internal variables $\{\boldsymbol{\varepsilon}_n^v, \boldsymbol{\varepsilon}_n^{vp}, \zeta_n, \xi_n\}$ are given. In this phase of the product formula, one solves for the current configuration $\mathbf{u}_{n+1}$ via an iterative procedure in which the current iterate is assumed given. The computation of the new iterate involves the evaluation of the current stress and temperature fields $\bar{\boldsymbol{\sigma}}_{n+1}$ and $\bar{\Theta}_{n+1}$, and of the updated internal variables $\left\{\bar{\boldsymbol{\varepsilon}}_{n+1}^v, \bar{\boldsymbol{\varepsilon}}_{n+1}^{vp}, \bar{\zeta}_{n+1}, \bar{\xi}_{n+1}\right\}$ [1]. Given a finite element discrctization, this update is performed at each quadrature point and proceeds as follows.

[1] For notational convenience, the *bar* will be dropped in what follows. The values obtained in this mechanical phase have to be understood, however, as intermediate values that will be modified to its final value in the thermal phase.

Trial state (kinematics)

According to the elasto-plastic operator split,

$$\boldsymbol{\varepsilon}^{vp}_{n+1} = \boldsymbol{\varepsilon}^{vp^{trial}}_{n+1} + \gamma^{vp}_{n+1}\mathbf{n}_{n+1} \tag{4.72a}$$

$$\boldsymbol{\zeta}_{n+1} = \boldsymbol{\zeta}^{trial}_{n+1} - \gamma^{vp}_{n+1}\mathbf{n}_{n+1} \tag{4.72b}$$

$$\xi_{n+1} = \xi^{trial}_{n+1} + \gamma^{vp}_{n+1}\sqrt{\frac{2}{3}} \tag{4.72c}$$

where the *elastic trial predictor* for the plastic variables is computed as

$$\boldsymbol{\varepsilon}^{vp^{trial}}_{n+1} = \boldsymbol{\varepsilon}^{vp}_{n} + \frac{1}{3}(s-1)\left(\boldsymbol{\varepsilon}^{vp}_{n} - \boldsymbol{\varepsilon}^{vp}_{n-1}\right) \tag{4.73a}$$

$$\boldsymbol{\zeta}^{trial}_{n+1} = \boldsymbol{\zeta}_{n} + \frac{1}{3}(s-1)\left(\boldsymbol{\zeta}_{n} - \boldsymbol{\zeta}_{n-1}\right) \tag{4.73b}$$

$$\xi^{trial}_{n+1} = \xi_{n} + \frac{1}{3}(s-1)\left(\xi_{n} - \xi_{n-1}\right) \tag{4.73c}$$

The intermediate temperature $\bar{\Theta}_{n+1}$ is computed using the local equation $\dot{S}^E = 0 \rightarrow \bar{S}^E_{n+1} = S^E_n$. Note that due to the fact that the final state is unknown, this temperature is calculated assuming the trial state so that the result is a *trial temperature* filed $\bar{\Theta}^{trial}_{n+1}$. A local Netwon-Raphson is used to get the zero of function $\Delta S^E = 0$, starting from the initial temperature Θ_n, so that:

$$\begin{aligned}
\Delta\Theta^{(o)} &= 0 \\
&\text{loop} \\
d\Theta^{(k)} &= -\frac{\bar{S}^E_{n+1}\left(\Theta_n + \Delta\Theta^{(k)}\right) - S^E_n\left(\Theta_n\right)}{d\bar{S}^E_{n+1}/\,d\Theta} \\
\Delta\Theta^{(k+1)} &= \Delta\Theta^{(k)} + d\Theta^{(k)} \\
&\text{end_loop} \\
\bar{\Theta}^{trial}_{n+1} &= \Theta_n + \Delta\Theta
\end{aligned}$$

The trial viscous strain tensor $\boldsymbol{\varepsilon}^{v^{trial}}_{n+1}$ is computed applying a *backward-Euler scheme* to the evolution law of the viscous strain tensor, so that considering the following system of equations, it results

$$\begin{cases} \boldsymbol{\varepsilon}^{v^{trial}}_{n+1} = \boldsymbol{\varepsilon}^{v}_{n} + \dfrac{\Delta t}{\eta^v\left(\bar{\Theta}^{trial}_{n+1}\right)}\mathbf{s}^{trial}_{n+1} \\ \mathbf{s}^{trial}_{n+1} = 2\bar{G}\left(\bar{\Theta}^{trial}_{n+1}\right)\left[dev\left(\boldsymbol{\varepsilon}_{n+1}\right) - \boldsymbol{\varepsilon}^{vp^{trial}}_{n+1} - \boldsymbol{\varepsilon}^{v^{trial}}_{n+1}\right] \end{cases} \tag{4.74a}$$

where it is possible to observe that the trial viscous strain tensor depends on a trial deviatoric stress tensor considered by assuming the trial values of the internal variables. Let τ^{trial} be the trial relaxation time, given by

$$\tau^{trial} = \frac{\eta^v\left(\bar{\Theta}_{n+1}^{trial}, \Theta_n\right)}{2\bar{G}\left(\bar{\Theta}_{n+1}^{trial}, \Theta_n\right)} = \frac{\eta\left(\bar{\Theta}_{n+1}^{trial}\right)}{2G\left(\bar{\Theta}_{n+1}^{trial}\right)} \frac{f_S\left(\Theta_n\right)}{\lambda\left(\Theta_n\right)} \tag{4.75}$$

where it must be pointed out that the solid fraction f_S (and consequently parameter λ) has been evaluated at time t_n due to the restriction on the evolution law of the phase change entropy term

$$\dot{S}^{pc} = \frac{1}{\Theta} L \dot{f}_S = 0 \rightarrow f_S = const = f_S\left(\Theta_n\right) \tag{4.76a}$$

This given, the trial viscous strain tensor results in

$$\boldsymbol{\varepsilon}_{n+1}^{v^{trial}} = \boldsymbol{\varepsilon}_n^v + \frac{\Delta t}{\tau^{trial} + \Delta t}\left[dev\left(\boldsymbol{\varepsilon}_{n+1}\right) - \boldsymbol{\varepsilon}_{n+1}^{vp^{trial}} - \boldsymbol{\varepsilon}_n^v\right] \tag{4.77}$$

The limit cases are shown in the following table

$$\begin{array}{llllll} \text{If} & \Theta \geq \Theta_L & \text{then} & \tau^{trial} = 0 & \rightarrow & \boldsymbol{\varepsilon}_{n+1}^{v^{trial}} = dev\left(\boldsymbol{\varepsilon}_{n+1}\right) - \boldsymbol{\varepsilon}_{n+1}^{vp^{trial}} \\ \text{If} & \Theta \leq \Theta_S & \text{then} & \tau^{trial} = \infty & \rightarrow & \boldsymbol{\varepsilon}_{n+1}^{v^{trial}} = \boldsymbol{\varepsilon}_n^v \end{array} \tag{4.78}$$

Note that when the material is liquid, that is $\Theta \geq \Theta_L$, all the deformation are viscous, otherwise when it is solid, that is $\Theta \leq \Theta_S$, the viscous strain tensor is 'frozen'.

Trial (generalized) stresses

Using the trial values obtained for the internal variables it is now possible to compute the trial generalized stresses as follows

$$p_{n+1}^{trial} = k\left(\bar{\Theta}_{n+1}^{trial}\right)\left[e_{n+1} - e^{\theta}\left(\bar{\Theta}_{n+1}^{trial}\right)\right] \tag{4.79a}$$

$$\mathbf{s}_{n+1}^{trial} = 2\bar{G}\left(\bar{\Theta}_{n+1}^{trial}\right)\left[dev\left(\boldsymbol{\varepsilon}_{n+1}\right) - \boldsymbol{\varepsilon}_{n+1}^{vp^{trial}} - \boldsymbol{\varepsilon}_{n+1}^{v^{trial}}\right] \tag{4.79b}$$

$$= \frac{\tau^{trial}}{\tau^{trial} + \Delta t} 2\bar{G}\left(\bar{\Theta}_{n+1}^{trial}\right)\left[dev\left(\boldsymbol{\varepsilon}_{n+1}\right) - \boldsymbol{\varepsilon}_{n+1}^{vp^{trial}} - \boldsymbol{\varepsilon}_n^v\right] \tag{4.79c}$$

$$\mathbf{q}_{n+1}^{trial} = -\frac{2}{3} K\left(\bar{\Theta}_{n+1}^{trial}\right) \boldsymbol{\zeta}_{n+1}^{trial} \tag{4.79d}$$

$$q_{n+1}^{trial} = -K_{\xi}\left(\xi_{n+1}^{trial}, \bar{\Theta}_{n+1}^{trial}\right) \tag{4.79e}$$

where K_ξ is given by

$$K_\xi\left(\xi_{n+1}^{trial}, \bar{\Theta}_{n+1}^{trial}\right) = \left[\sigma_\infty\left(\bar{\Theta}_{n+1}^{trial}\right) - \sigma_o\left(\bar{\Theta}_{n+1}^{trial}\right)\right]\left[1 - exp\left(-\delta\, \xi_{n+1}^{trial}\right)\right] + H\left(\bar{\Theta}_{n+1}^{trial}\right)\xi_{n+1}^{trial} \tag{4.80}$$

and finally, the trial thermal deformation is computed as

$$e^\theta\left(\bar{\Theta}_{n+1}^{trial}\right) = 3\left[\alpha\left(\bar{\Theta}_{n+1}^{trial}\right)\left(\bar{\Theta}_{n+1}^{trial} - \Theta_{ref}\right) - \alpha\left(\Theta_o\right)\left(\Theta_o - \Theta_{ref}\right)\right] + \left[e^{pc}\left(\Theta_n\right) - e^{pc}\left(\Theta_o\right)\right] \tag{4.81}$$

where it is possible to observe that the current straining deformation e^{pc} is evaluated at time t_n due to the restriction (4.76*a*).

Observe that due to the change in the temperature field given by the restriction on the elastic entropy, all the material properties must be recovered at current temperature $\bar{\Theta}_{n+1}^{trial}$ and updated following the temperature evolution in the iterative process.

Trial yield function

The trial yield function is computed as

$$\Phi_{n+1}^{trial} = \left\|\boldsymbol{\beta}_{n+1}^{trial}\right\| - \sqrt{\frac{2}{3}}\left[\sigma_o\left(\Theta_n\right) - q_{n+1}^{trial}\right] \tag{4.82}$$

where

$$\boldsymbol{\beta}_{n+1}^{trial} = \mathbf{s}_{n+1}^{trial} - \mathbf{q}_{n+1}^{trial} \tag{4.83}$$

is the so called back-stress tensor. Observe that the initial flow stress σ_o is evaluated at the initial temperaturc Θ_n due to the restriction on the inelastic entropy S^I,

$$\dot{S}^I = \frac{D_{ther}}{\Theta} = -\gamma^{vp}\sqrt{\frac{2}{3}}\frac{d\,\sigma_0\left(\Theta\right)}{d\Theta}\Theta = 0 \tag{4.84}$$

so that

$$\boldsymbol{\sigma}_o = const = \boldsymbol{\sigma}_o\left(\Theta_n\right) \tag{4.85}$$

If $\Phi_{n+1}^{trial} \leq 0$ then the trial state is the final intermediate state,

$$\boldsymbol{\varepsilon}_{n+1}^{v} = \boldsymbol{\varepsilon}_{n+1}^{v^{trial}} \tag{4.86a}$$

$$\boldsymbol{\varepsilon}_{n+1}^{vp} = \boldsymbol{\varepsilon}_{n+1}^{vp^{trial}} \tag{4.86b}$$

$$\boldsymbol{\zeta}_{n+1} = \boldsymbol{\zeta}_{n+1}^{trial} \tag{4.86c}$$

$$\xi_{n+1} = \xi_{n+1}^{trial} \tag{4.86d}$$

otherwise, if $\Phi_{n+1}^{trial} > 0$ the plastic corrector must be applied. In this case it is not possible to use a standard isothermal return mapping, in fact the constrain on the entropy evolution must be assumed during all the process.

Isentropic return mapping

First, let us evaluate the unit normal to the yield surface defined as

$$\mathbf{n}_{n+1} = \frac{\mathbf{s}_{n+1} - \mathbf{q}_{n+1}}{\|\mathbf{s}_{n+1} - \mathbf{q}_{n+1}\|} = \frac{\boldsymbol{\beta}_{n+1}}{\|\boldsymbol{\beta}_{n+1}\|} \tag{4.87}$$

The final back-stress tensor $\boldsymbol{\beta}_{n+1}$ is unknown but it can be expressed in terms of the plastic multiplier γ_{n+1}^{vp} and the final intermediate temperature $\bar{\Theta}_{n+1}$ as

$$\boldsymbol{\beta}_{n+1} = \bar{\boldsymbol{\beta}}_{n+1}^{trial} - \left[\frac{\tau}{\tau + \Delta t} 2\bar{G}\left(\bar{\Theta}_{n+1}\right) + \frac{2}{3} K\left(\bar{\Theta}_{n+1}\right)\right] \gamma_{n+1}^{vp} \frac{\boldsymbol{\beta}_{n+1}}{\|\boldsymbol{\beta}_{n+1}\|} \tag{4.88}$$

where $\bar{\boldsymbol{\beta}}_{n+1}^{trial}$ is a modified version of the trial back-stress tensor, given by

$$\bar{\boldsymbol{\beta}}_{n+1}^{trial} = \frac{\tau\left(\tau^{trial} + \Delta t\right)}{\tau^{trial}\left(\tau + \Delta t\right)} \frac{\bar{G}\left(\bar{\Theta}_{n+1}\right)}{\bar{G}\left(\bar{\Theta}_{n+1}^{trial}\right)} \mathbf{s}_{n+1}^{trial} - \frac{K\left(\bar{\Theta}_{n+1}\right)}{K\left(\bar{\Theta}_{n+1}^{trial}\right)} \mathbf{q}_{n+1}^{trial} \tag{4.89}$$

and is defined as

$$\tau = \frac{\eta^{v}\left(\bar{\Theta}_{n+1}, \Theta_n\right)}{2\bar{G}\left(\bar{\Theta}_{n+1}, \Theta_n\right)} = \frac{\eta\left(\bar{\Theta}_{n+1}\right)}{2G\left(\bar{\Theta}_{n+1}\right)} \frac{f_S\left(\Theta_n\right)}{\lambda\left(\Theta_n\right)} \tag{4.90}$$

Developing expression (4.88) it is possible to obtain

$$\left[1 + \left(\frac{\tau}{\tau + \Delta t} 2\bar{G}\left(\bar{\Theta}_{n+1}\right) + \frac{2}{3} K\left(\bar{\Theta}_{n+1}\right)\right) \frac{\gamma_{n+1}^{vp}}{\|\boldsymbol{\beta}_{n+1}\|}\right] \boldsymbol{\beta}_{n+1} = \bar{\boldsymbol{\beta}}_{n+1}^{trial} \tag{4.91}$$

and if we take the norm of above expression

$$\|\boldsymbol{\beta}_{n+1}\| + \left(\frac{\tau}{\tau + \Delta t} 2\bar{G}\left(\bar{\Theta}_{n+1}\right) + \frac{2}{3} K\left(\bar{\Theta}_{n+1}\right)\right) \gamma_{n+1}^{vp} = \left\|\bar{\boldsymbol{\beta}}_{n+1}^{trial}\right\| \tag{4.92}$$

the result is

$$\mathbf{n}_{n+1} = \frac{\bar{\boldsymbol{\beta}}_{n+1}^{trial}}{\left\|\bar{\boldsymbol{\beta}}_{n+1}^{trial}\right\|} \tag{4.93}$$

Note that in case of either constant material properties or zero kinematic hardening the standard hypothesis used in isothermal J2-plastic algorithm is recovered

$$\mathbf{n}_{n+1} = \mathbf{n}_{n+1}^{trial} = \frac{\boldsymbol{\beta}_{n+1}^{trial}}{\left\|\boldsymbol{\beta}_{n+1}^{trial}\right\|} = \frac{\mathbf{s}_{n+1}^{trial} - \mathbf{q}_{n+1}^{trial}}{\left\|\mathbf{s}_{n+1}^{trial} - \mathbf{q}_{n+1}^{trial}\right\|} \tag{4.94}$$

Next step is the evaluation of the yield function at time t_{n+1} as

$$\Phi_{n+1} = \left\|\boldsymbol{\beta}_{n+1}\right\| - \sqrt{\frac{2}{3}}\left[\sigma_o\left(\Theta_n\right) - q_{n+1}\right] \tag{4.95}$$

where $\left\|\boldsymbol{\beta}_{n+1}\right\|$ is obtained using equation (4.92) as

$$\left\|\boldsymbol{\beta}_{n+1}\right\| = \left\|\bar{\boldsymbol{\beta}}_{n+1}^{trial}\right\| - \left(\frac{\tau}{\tau + \Delta t} 2\bar{G}\left(\bar{\Theta}_{n+1}\right) + \frac{2}{3} K\left(\bar{\Theta}_{n+1}\right)\right) \gamma_{n+1}^{vp} \tag{4.96}$$

To obtain the final values of the plastic multiplier γ_{n+1}^{vp} and of the intermediate temperature $\bar{\Theta}_{n+1}$ the following system of equation must be verified:

$$\begin{cases} \Delta S_{n+1}^{E}\left(\gamma_{n+1}^{vp}, \bar{\Theta}_{n+1}\right) = 0 \\ g_{n+1}\left(\gamma_{n+1}^{vp}, \bar{\Theta}_{n+1}\right) = 0 \end{cases} \tag{4.97}$$

where function $g_{n+1}\left(\gamma_{n+1}^{vp}, \bar{\Theta}_{n+1}\right)$ is given by

$$g_{n+1}\left(\gamma_{n+1}^{vp}, \bar{\Theta}_{n+1}\right) = \Phi_{n+1}\left(\gamma_{n+1}^{vp}, \bar{\Theta}_{n+1}\right) - \left[\eta^{vp}\left(\bar{\Theta}_{n+1}\right)\ \gamma_{n+1}^{vp}\right]^{\frac{1}{n}} \tag{4.98}$$

Observing that both equations are non-linear a local Newton-Raphson algorithm can be used to find the solution. The linearized system of equation results in

$$\begin{cases} \Delta S_{n+1}^{E} + \left.\dfrac{\partial \Delta S^{E}}{\partial \gamma}\right|_{n+1} d\gamma + \left.\dfrac{\partial \Delta S^{E}}{\partial \Theta}\right|_{n+1} d\Theta = 0 \\ g_{n+1} + \left.\dfrac{\partial g}{\partial \gamma}\right|_{n+1} d\gamma + \left.\dfrac{\partial g}{\partial \Theta}\right|_{n+1} d\Theta = 0 \end{cases} \tag{4.99}$$

with initial conditions

$$\bar{\Theta}_{n+1} = \bar{\Theta}_{n+1}^{trial} \tag{4.100}$$

$$\gamma_{n+1} = 0 \tag{4.101}$$

Taking into account that the material properties must be actualized to the current temperature at each iteration, the iterative process is the following:

$$
\begin{aligned}
\Delta\Theta^{(o)} &= 0 \\
\Delta\gamma^{(o)} &= 0 \\
&\quad \text{loop} \\
d\Theta^{(k)} &= -\frac{\Delta S^E_{n+1} + \left.\dfrac{\partial \Delta S^E}{\partial \gamma}\right|_{n+1} d\gamma^{(k-1)}}{\left.\dfrac{\partial \Delta S^E}{\partial \Theta}\right|_{n+1}} \\
d\gamma^{(k)} &= -\frac{\Phi_{n+1} + \left.\dfrac{\partial \Phi}{\partial \Theta}\right|_{n+1} d\Theta^{(k-1)}}{\left.\dfrac{\partial \Phi}{\partial \gamma}\right|_{n+1}} \\
\Delta\Theta^{(k+1)} &= \Delta\Theta^{(k)} + d\Theta^{(k)} \\
\Delta\gamma^{(k+1)} &= \Delta\gamma^{(k)} + d\gamma^{(k)} \\
&\quad \text{end\_loop} \\
\bar{\Theta}_{n+1} &= \bar{\Theta}^{trial}_{n+1} + \Delta\Theta \\
\gamma_{n+1} &= \Delta\gamma
\end{aligned}
$$

Update database

Let's first update the plastic variables as

$$\boldsymbol{\varepsilon}^p_{n+1} = \boldsymbol{\varepsilon}^{p^{trial}}_{n+1} + \gamma_{n+1}\mathbf{n}_{n+1} \tag{4.103a}$$

$$\boldsymbol{\zeta}_{n+1} = \boldsymbol{\zeta}^{trial}_{n+1} - \gamma_{n+1}\mathbf{n}_{n+1} \tag{4.103b}$$

$$\xi_{n+1} = \xi^{trial}_{n+1} + \gamma_{n+1}\sqrt{\frac{2}{3}} \tag{4.103c}$$

then it is possible to evaluate the viscous strain tensor as

$$\boldsymbol{\varepsilon}^v_{n+1} = \boldsymbol{\varepsilon}^v_n + \frac{\Delta t}{\tau + \Delta t}\left[dev\left(\boldsymbol{\varepsilon}_{n+1}\right) - \boldsymbol{\varepsilon}^{vp}_{n+1} - \boldsymbol{\varepsilon}^v_n\right] \tag{4.104}$$

Finally, using the intermediate temperature $\bar{\Theta}_{n+1}$ compute the volumetric thermal deformation $e^\theta_{n+1}\left(\bar{\Theta}_{n+1}\right)$ as

$$e^\theta_{n+1} = 3\left[\alpha\left(\bar{\Theta}_{n+1}\right)\left(\bar{\Theta}_{n+1} - \Theta_{ref}\right) - \alpha\left(\Theta_o\right)\left(\Theta_o - \Theta_{ref}\right)\right]$$

$$+\left[e^{pc}\left(\Theta_n\right)-e^{pc}\left(\Theta_o\right)\right] \tag{4.105}$$

Compute stresses

The deviatoric stress fields and the hardening stress tensors are computed as follows

$$\begin{aligned}
\mathbf{s}_{n+1} &= \frac{\tau\left(\tau^{trial}+\Delta t\right)}{\tau^{trial}\left(\tau+\Delta t\right)}\frac{\bar{G}\left(\bar{\Theta}_{n+1}\right)}{\bar{G}\left(\bar{\Theta}_{n+1}^{trial}\right)}\mathbf{s}_{n+1}^{trial} \\
&\quad -\frac{\tau}{\tau+\Delta t}2\bar{G}\left(\bar{\Theta}_{n+1}\right)\,\gamma_{n+1}\mathbf{n}_{n+1} && (4.106a)\\
\mathbf{q}_{n+1} &= -\frac{2}{3}K\left(\bar{\Theta}_{n+1}\right)\boldsymbol{\zeta}_{n+1} \\
&= \frac{K\left(\bar{\Theta}_{n+1}\right)}{K\left(\bar{\Theta}_{n+1}^{trial}\right)}\mathbf{q}_{n+1}^{trial}+\frac{2}{3}K\left(\bar{\Theta}_{n+1}\right)\,\gamma_{n+1}\mathbf{n}_{n+1} && (4.106b)\\
q_{n+1} &= q\left(\xi_{n+1},\bar{\Theta}_{n+1}\right) && (4.106c)
\end{aligned}$$

so that the total stress tensor can be evaluated as

$$\boldsymbol{\sigma}_{n+1}=p_{n+1}\mathbf{1}+\mathbf{s}_{n+1} \tag{4.107}$$

where the pressure is given by

$$p_{n+1}=k\left(\bar{\Theta}_{n+1}\right)\left(e_{n+1}-e_{n+1}^{\theta}\right) \tag{4.108}$$

Limit cases

It is interesting to show in this section the simplifications that take part in the model when the limit cases are considered.

1. *Liquid behavior.* In this case the condition is $f_S=0$. As a consequence parameters λ and μ are given by

$$\lambda_{n+1}=1 \tag{4.109a}$$
$$\mu_{n+1}=0 \tag{4.109b}$$

so that the viscous parameters transform in

$$\eta^{v}=\eta \tag{4.110a}$$
$$\eta^{vp}=\infty \tag{4.110b}$$

and the viscous and visco-plastic multipliers follow as

$$\gamma^{v}_{n+1} = \frac{1}{\eta}\left\|\mathbf{s}_{n+1}\right\| \tag{4.111a}$$

$$\gamma^{vp}_{n+1} = 0 \tag{4.111b}$$

The result is that no plastic increment can occur

$$\boldsymbol{\varepsilon}^{vp}_{n+1} = \boldsymbol{\varepsilon}^{vp}_{n} \tag{4.112a}$$

$$\boldsymbol{\zeta}_{n+1} = \boldsymbol{\zeta}_{n} \tag{4.112b}$$

$$\xi_{n+1} = \xi_{n} \tag{4.112c}$$

and the final viscous strain tensor is given by

$$\boldsymbol{\varepsilon}^{v\,trial}_{n+1} = dev\left(\boldsymbol{\varepsilon}_{n+1}\right) - \boldsymbol{\varepsilon}^{vp}_{n+1} = dev\left(\boldsymbol{\varepsilon}_{n+1}\right) - \boldsymbol{\varepsilon}^{vp}_{n} \tag{4.113}$$

The stress field results in *purely viscous deviatoric model* so that

$$\boldsymbol{\sigma}_{n+1} = p_{n+1}\mathbf{1} + \mathbf{s}_{n+1} \tag{4.114a}$$

$$p_{n+1} = k\left(\bar{\Theta}_{n+1}\right)\left(e_{n+1} - e^{\theta}_{n+1}\right) \tag{4.114b}$$

$$\mathbf{s}_{n+1} = \frac{\eta\left(\bar{\Theta}_{n+1}\right)}{\Delta t}\left[dev\left(\boldsymbol{\varepsilon}_{n+1}\right) - \boldsymbol{\varepsilon}^{vp}_{n} - \boldsymbol{\varepsilon}^{v}_{n}\right] \tag{4.114c}$$

where the thermal deformation e^{θ}_{n+1} is given by

$$e^{\theta}_{n+1} = 3\left[\alpha\left(\bar{\Theta}_{n+1}\right)\left(\bar{\Theta}_{n+1} - \Theta_{ref}\right) - \alpha\left(\Theta_{o}\right)\left(\Theta_{o} - \Theta_{ref}\right)\right] + \left[e^{pc}\left(\Theta_{n+1}\right) - e^{pc}\left(\Theta_{o}\right)\right] \tag{4.115}$$

and the intermediate temperature $\bar{\Theta}_{n+1}$ is evaluated assuming the restriction on the evolution of the elastic entropy.

2. *Mushy zone* and *no plasticity.* Consider a temperature field that verifies the condition $\Theta_S < \Theta < \Theta_L$ and suppose that no plastic effects will occur, that is $\Phi_{n+1} < 0$. This is the case of a visco-elastic model in which the viscosity and the shear modulus are respectively given by

$$\eta^{v} = \eta \tag{4.116a}$$

$$\bar{G} = \frac{G}{f_s} \tag{4.116b}$$

The viscous strain tensor is computed as

$$\boldsymbol{\varepsilon}^{v}_{n+1} = \boldsymbol{\varepsilon}^{v}_{n} + \frac{\Delta t}{\tau + \Delta t}\left[dev\left(\boldsymbol{\varepsilon}_{n+1}\right) - \boldsymbol{\varepsilon}^{vp}_{n} - \boldsymbol{\varepsilon}^{v}_{n}\right] \tag{4.117}$$

where parameter τ is given by

$$\tau = \frac{\eta\left(\bar{\Theta}_{n+1}\right)}{2G\left(\bar{\Theta}_{n+1}\right)} f_S\left(\Theta_n\right) \tag{4.118}$$

The stress field results in

$$\boldsymbol{\sigma}_{n+1} = p_{n+1}\mathbf{1} + \mathbf{s}_{n+1} \tag{4.119}$$

$$p_{n+1} = k\left(\bar{\Theta}_{n+1}\right)\left(e_{n+1} - e^{\theta}_{n+1}\right) \tag{4.120}$$

$$\mathbf{s}_{n+1} = \frac{\tau}{\tau + \Delta t} 2\bar{G}\left(\bar{\Theta}_{n+1}\right)\left[dev\left(\boldsymbol{\varepsilon}_{n+1}\right) - \boldsymbol{\varepsilon}^{vp}_{n} - \boldsymbol{\varepsilon}^{v}_{n}\right] \tag{4.121}$$

and the thermal deformation e^{θ}_{n+1} is given by

$$\begin{aligned} e^{\theta}_{n+1} = 3\left[\alpha\left(\bar{\Theta}_{n+1}\right)\left(\bar{\Theta}_{n+1} - \Theta_{ref}\right) - \alpha\left(\Theta_o\right)\left(\Theta_o - \Theta_{ref}\right)\right] \\ + \left[e^{pc}\left(\Theta_n\right) - e^{pc}\left(\Theta_o\right)\right] \end{aligned} \tag{4.122}$$

and the intermediate temperature $\bar{\Theta}_{n+1}$ is evaluated assuming the restriction on the evolution of the elastic entropy.

3. *Solid behavior.* In this case $f_L = 0$ and an elasto-viscoplastic model is recovered. The consequence is that the purely viscous strain tensor must remain fixed

$$\boldsymbol{\varepsilon}^{v}_{n+1} = \boldsymbol{\varepsilon}^{v}_{n} \tag{4.123}$$

and the deviatoric stress tensor is computed as

$$\mathbf{s}_{n+1} = 2G\left(\bar{\Theta}_{n+1}\right)\left[dev\left(\boldsymbol{\varepsilon}_{n+1}\right) - \boldsymbol{\varepsilon}^{vp}_{n+1} - \boldsymbol{\varepsilon}^{v}_{n}\right] \tag{4.124}$$

where the isentropic return mapping algorithm is used to evaluate the viscoplastic strain $\boldsymbol{\varepsilon}^{vp}_{n+1}$.

4.4.4 Isothermal algorithm

Let's consider now the isothermal algorithm used either to compute stresses in the mechanical phase of an isothermal operator split or to update the internal variable in the thermal phase of both splits proposed.

Trial state (kinematics)

According to the elasto-plastic operator split,

$$\begin{aligned} \boldsymbol{\varepsilon}_{n+1}^{vp} &= \boldsymbol{\varepsilon}_{n+1}^{vp^{trial}} + \gamma_{n+1}^{vp}\mathbf{n}_{n+1} && (4.125a)\\ \boldsymbol{\zeta}_{n+1} &- \boldsymbol{\zeta}_{n+1}^{trial} - \gamma_{n+1}^{vp}\mathbf{n}_{n+1} && (4.125b)\\ \xi_{n+1} &= \xi_{n+1}^{trial} + \gamma_{n+1}^{vp}\sqrt{\frac{2}{3}} && (4.125c) \end{aligned}$$

the *elastic trial predictor* for the plastic variables is computed as

$$\begin{aligned} \boldsymbol{\varepsilon}_{n+1}^{vp^{trial}} &= \boldsymbol{\varepsilon}_{n}^{vp} + \frac{1}{3}(s-1)\left(\boldsymbol{\varepsilon}_{n}^{vp} - \boldsymbol{\varepsilon}_{n-1}^{vp}\right) && (4.126a)\\ \boldsymbol{\zeta}_{n+1}^{trial} &= \boldsymbol{\zeta}_{n} + \frac{1}{3}(s-1)\left(\boldsymbol{\zeta}_{n} - \boldsymbol{\zeta}_{n-1}\right) && (4.126b)\\ \xi_{n+1}^{trial} &= \xi_{n} + \frac{1}{3}(s-1)\left(\xi_{n} - \xi_{n-1}\right) && (4.126c) \end{aligned}$$

The intermediate temperature is the temperature at the beginning of the time step due to the restriction on the temperature evolution, so that

$$\bar{\Theta}_{n+1} = \Theta_n \tag{4.127}$$

The trial viscous strain tensor $\boldsymbol{\varepsilon}_{n+1}^{v^{trial}}$ is computed considering the following system of equations

$$\begin{cases} \boldsymbol{\varepsilon}_{n+1}^{v^{trial}} = \boldsymbol{\varepsilon}_{n}^{v} + \dfrac{\Delta t}{\eta^{v}(\Theta_n)}\mathbf{s}_{n+1}^{trial} \\ \mathbf{s}_{n+1}^{trial} = 2\bar{G}(\Theta_n)\left[dev\left(\boldsymbol{\varepsilon}_{n+1}\right) - \boldsymbol{\varepsilon}_{n+1}^{vp^{trial}} - \boldsymbol{\varepsilon}_{n+1}^{v^{trial}}\right] \end{cases} \tag{4.128a}$$

and the result is

$$\boldsymbol{\varepsilon}_{n+1}^{v^{trial}} = \boldsymbol{\varepsilon}_{n}^{v} + \frac{\Delta t}{\tau + \Delta t}\left[dev\left(\boldsymbol{\varepsilon}_{n+1}\right) - \boldsymbol{\varepsilon}_{n+1}^{vp^{trial}} - \boldsymbol{\varepsilon}_{n}^{v}\right] \tag{4.129}$$

where the relaxation time τ is given by

$$\tau = \frac{\eta^{v}(\Theta_n)}{2\bar{G}(\Theta_n)} = \frac{\eta(\Theta_n)}{2G(\Theta_n)}\frac{f_S(\Theta_n)}{\lambda(\Theta_n)} \tag{4.130}$$

Trial (generalized) stresses

Using the trial values obtained for the internal variables it is now possible to compute the trial generalized stresses as follows

$$
\begin{aligned}
p_{n+1}^{trial} &= k\left(\Theta_n\right)\left[e_{n+1} - e^{\theta}\left(\Theta_n\right)\right] && \text{(4.131a)}\\
\mathbf{s}_{n+1}^{trial} &= 2\bar{G}\left(\Theta_n\right)\left[dev\left(\boldsymbol{\varepsilon}_{n+1}\right) - \boldsymbol{\varepsilon}_{n+1}^{vp^{trial}} - \boldsymbol{\varepsilon}_{n+1}^{v^{trial}}\right] && \text{(4.131b)}\\
&= \frac{\tau}{\tau+\Delta t} 2\bar{G}\left(\Theta_n\right)\left[dev\left(\boldsymbol{\varepsilon}_{n+1}\right) - \boldsymbol{\varepsilon}_{n+1}^{vp^{trial}} - \boldsymbol{\varepsilon}_{n}^{v}\right] && \text{(4.131c)}\\
\mathbf{q}_{n+1}^{trial} &= -\frac{2}{3} K\left(\Theta_n\right)\boldsymbol{\zeta}_{n+1}^{trial} && \text{(4.131d)}\\
q_{n+1}^{trial} &= -K_{\xi}\left(\xi_{n+1}^{trial}\right) && \text{(4.131e)}
\end{aligned}
$$

where K_{ξ} is given by

$$
\begin{aligned}
K_{\xi}\left(\xi_{n+1}^{trial}\right) &= \left[\sigma_{\infty}\left(\Theta_n\right) - \sigma_o\left(\Theta_n\right)\right]\left[1 - exp\left(-\delta\xi_{n+1}^{trial}\right)\right]\\
&\quad + H\left(\Theta_n\right)\xi_{n+1}^{trial} && \text{(4.132)}
\end{aligned}
$$

and finally, the thermal deformation is computed as

$$
\begin{aligned}
e^{\theta}\left(\Theta_n\right) &= 3\left[\alpha\left(\Theta_n\right)\left(\Theta_n - \Theta_{ref}\right) - \alpha\left(\Theta_o\right)\left(\Theta_o - \Theta_{ref}\right)\right]\\
&\quad + \left[e^{pc}\left(\Theta_n\right) - e^{pc}\left(\Theta_o\right)\right] && \text{(4.133)}
\end{aligned}
$$

that in this case it is also its final value.

Trial yield function

The trial yield function is computed as

$$
\Phi_{n+1}^{trial} = \left\|\boldsymbol{\beta}_{n+1}^{trial}\right\| - \sqrt{\frac{2}{3}}\left[\sigma_o\left(\Theta_n\right) - q_{n+1}^{trial}\right] \qquad \text{(4.134)}
$$

where the trial back-stress tensor is given by

$$
\boldsymbol{\beta}_{n+1}^{trial} = \mathbf{s}_{n+1}^{trial} - \mathbf{q}_{n+1}^{trial} \qquad \text{(4.135)}
$$

If $\Phi_{n+1}^{trial} \leq 0$ then the trial state is the final intermediate state,

$$\varepsilon^{v}_{n+1} = \varepsilon^{v^{trial}}_{n+1} \tag{4.136a}$$
$$\varepsilon^{vp}_{n+1} = \varepsilon^{vp^{trial}}_{n+1} \tag{4.136b}$$
$$\zeta_{n+1} = \zeta^{trial}_{n+1} \tag{4.136c}$$
$$\xi_{n+1} = \xi^{trial}_{n+1} \tag{4.136d}$$

otherwise, if $\Phi^{trial}_{n+1} > 0$ the plastic corrector must be applied. A standard isothermal return mapping can be used due to the constrain on the temperature field.

Isothermal return mapping

In this case the unit normal to the yield surface is given by

$$\mathbf{n}_{n+1} = \mathbf{n}^{trial}_{n+1} = \frac{\boldsymbol{\beta}^{trial}_{n+1}}{\left\|\boldsymbol{\beta}^{trial}_{n+1}\right\|} = \frac{\mathbf{s}^{trial}_{n+1} - \mathbf{q}^{trial}_{n+1}}{\left\|\mathbf{s}^{trial}_{n+1} - \mathbf{q}^{trial}_{n+1}\right\|} \tag{4.137}$$

in fact, it results

$$\left[1 + \left(\frac{\tau}{\tau + \Delta t} 2\bar{G}\left(\Theta_n\right) + \frac{2}{3} K\left(\Theta_n\right)\right) \frac{\gamma^{vp}_{n+1}}{\left\|\boldsymbol{\beta}_{n+1}\right\|}\right] \boldsymbol{\beta}_{n+1} = \boldsymbol{\beta}^{trial}_{n+1} \tag{4.138}$$

where it is possible to see that vectors $\boldsymbol{\beta}_{n+1}$ and $\boldsymbol{\beta}^{trial}_{n+1}$ have the same direction and the difference is in the value of the norm

$$\left\|\boldsymbol{\beta}_{n+1}\right\| = \left\|\boldsymbol{\beta}^{trial}_{n+1}\right\| - \left(\frac{\tau}{\tau + \Delta t} 2\bar{G}\left(\Theta_n\right) + \frac{2}{3} K\left(\Theta_n\right)\right) \gamma^{vp}_{n+1} \tag{4.139}$$

Using the above expression the yield function at time t_{n+1} can be evaluated as

$$\begin{aligned} \Phi_{n+1} &= \Phi^{trial}_{n+1} - \left(\frac{\tau}{\tau + \Delta t} 2\bar{G}\left(\Theta_n\right) + \frac{2}{3} K\left(\Theta_n\right)\right) \gamma^{vp}_{n+1} \\ &\quad + \sqrt{\frac{2}{3}} \left[q_{n+1} - q_n\right] \end{aligned} \tag{4.140}$$

The plastic multiplier γ^{vp}_{n+1} is obtained by solving the non-linear equation

$$g_{n+1}\left(\gamma^{vp}_{n+1}\right) = 0 \tag{4.141}$$

where function $g_{n+1}\left(\gamma_{n+1}^{vp}\right)$ is given by

$$g_{n+1}\left(\gamma_{n+1}^{vp}\right) = \Phi_{n+1}\left(\gamma_{n+1}^{vp}\right) - \left[\eta^{vp}\left(\Theta_n\right)\ \gamma_{n+1}^{vp}\right]^{\frac{1}{n}} \tag{4.142}$$

Using a local Newton-Raphson the plastic multiplier γ_{n+1}^{vp} is obtained as

$$\begin{aligned}
\Delta\gamma^{(o)} &= 0 \\
&\quad \text{loop} \\
d\gamma^{(k)} &= -\frac{\Phi_{n+1}}{\left.\dfrac{\partial\Phi}{\partial\gamma}\right|_{n+1}} \\
\Delta\gamma^{(k+1)} &= \Delta\gamma^{(k)} + d\gamma^{(k)} \\
&\quad \text{end_loop} \\
\gamma_{n+1} &= \Delta\gamma
\end{aligned}$$

Update database

The plastic variables are updated first, as

$$\varepsilon_{n+1}^{p} = \varepsilon_{n+1}^{p^{trial}} + \gamma_{n+1}\mathbf{n}_{n+1} \tag{4.144a}$$

$$\boldsymbol{\zeta}_{n+1} = \boldsymbol{\zeta}_{n+1}^{trial} - \gamma_{n+1}\mathbf{n}_{n+1} \tag{4.144b}$$

$$\xi_{n+1} = \xi_{n+1}^{trial} + \gamma_{n+1}\sqrt{\frac{2}{3}} \tag{4.144c}$$

so that it is possible to evaluate the viscous strain tensor as

$$\varepsilon_{n+1}^{v} = \varepsilon_{n}^{v} + \frac{\Delta t}{\tau + \Delta t}\left[dev\left(\boldsymbol{\varepsilon}_{n+1}\right) - \varepsilon_{n+1}^{vp} - \varepsilon_{n}^{v}\right] \tag{4.145}$$

Compute stresses

The deviatoric stress fields and the hardening-like stress tensors are computed as follows

$$\mathbf{s}_{n+1} = \mathbf{s}_{n+1}^{trial} - \frac{\tau}{\tau + \Delta t} 2\bar{G}\left(\Theta_n\right)\ \gamma_{n+1}\mathbf{n}_{n+1} \tag{4.146a}$$

$$\mathbf{q}_{n+1} = -\frac{2}{3}K\left(\Theta_n\right)\boldsymbol{\zeta}_{n+1} = \mathbf{q}_{n+1}^{trial} + \frac{2}{3}K\left(\Theta_n\right)\ \gamma_{n+1}\mathbf{n}_{n+1} \tag{4.146b}$$

$$q_{n+1} = q\left(\xi_{n+1}\right) \tag{4.146c}$$

so that the total stress tensor can be evaluated as

$$\boldsymbol{\sigma}_{n+1}=p_{n+1}\mathbf{1}+\mathbf{s}_{n+1} \tag{4.147}$$

where the pressure is given by

$$p_{n+1}=k\left(\Theta_n\right)\left(e_{n+1}-e_{n+1}^{\theta}\right) \tag{4.148}$$

4.5 Phase-change integration

In the literature there are many approaches to integrate the phase change contribution: among others the so called *entalpy methods* [Comini-74], the methods based on the *apparent capacity* [Salcudea-86], [Salcudean-88] and finally the *source methods* [Dusimberre-45], [Roph-82].

In this work the rate of latent heat $\dot{L}_{n+1}$ at time t_{n+1} is computed as the rate of change of the latent heat function $L\left(\Theta\right)$ as

$$\dot{L}_{n+1}=\frac{L\left(\Theta_{n+1}\right)-L\left(\Theta_n\right)}{\Delta t} \tag{4.149}$$

This proposal is attractive because the rate of released (or absorbed) latent heat $\dot{L}_{n+1}$ is consistently computed:

- for any time step size Δt used ;
- for any number of phase changes NPC considered;
- for any solid-fraction functions $f^{(k)}\left(\Theta\right)$ chosen.

A possible alternative is the following

$$\dot{L}_{n+1}=\left.\frac{dL}{d\Theta}\right|_{n+1}\dot{\Theta}_{n+1} \tag{4.150}$$

Due to fact that the latent heat function is a stepwise function then it results

$$\left.\frac{dL}{d\Theta}\right|_{n+1}=L\left.\frac{df_S}{d\Theta}\right|_{n+1}=\begin{cases}0 & \text{if} \quad \Theta\geq\Theta_L\\ L\left.\dfrac{df_S}{d\Theta}\right|_{n+1} & \text{if} \quad \Theta_S<\Theta<\Theta_L\\ 0 & \text{if} \quad \Theta\leq\Theta_S\end{cases} \tag{4.151}$$

so that $\frac{dL}{d\Theta}\big|_{n+1} \neq 0$ only if the temperature Θ_{n+1} is included in the intervals (Θ_S, Θ_L) in which the phase change occurs, eventually only at the phase change temperature $\Theta_{SL} = \Theta_L = \Theta_S$ for an isothermal process [Celentano-94]. This is a strong restriction because a very small time increment must be used to capture the phase change and the total amount of latent heat released $L = \int \dot{L}\, dt$ is not ensured.

It must be observed that this alternative becomes useless when the phase change process tents to be isothermal, in fact, $\frac{dL}{d\Theta} \to \infty$ and $\dot{\Theta} \to 0$. It is not the case when $\dot{L}_{n+1}$ is computed as $\frac{L(\Theta_{n+1}) - L(\Theta_n)}{\Delta t}$ in fact its value it is always included in the range $[0,\, L/\,\Delta t]$.

Finally, the expression for the consistent tangent operator C^{pc} due to the phase change is computed as

$$C^{pc} = \begin{cases} \left.\dfrac{dL}{d\Theta}\right|_{n+1} & \text{if} \quad \left.\dfrac{dL}{d\Theta}\right|_{n+1} \neq 0 \\ \dfrac{L_{n+1} - L_n}{\Delta\Theta} & \text{if} \quad \left.\dfrac{dL}{d\Theta}\right|_{n+1} - 0 \end{cases} \tag{4.152}$$

It is possible to observe, that even if it exists a latent heat contribution in the evaluation of the residual forces its consistent linearization is often useless so that it is impossible the convergence procedure. To avoid that case a secant value is proposed and it is used only when the tangent value is useless.

Chapter 5

Time Integration of the Contact Problem

This chapter deals with the time integration of the coupled thermo-mechanical contact problem. Discussion will be focussed on the contact evolution occurring on $\Gamma^{(1)}$, and on the numerical integration scheme to be applied on that surface [Laursen-98], [Cancun-99]. Conceptually the idea behind the numerical algorithm follows the procedure introduced for the bulk continua so that a product formula strategy is used leading to an isentropic and isothermal operator splits of the governing equations [Armero & Simo- 91], [Armero & Simo-92].

5.1 Local evolution problem

Consider the following homogeneous, first order constrained, dissipative, local problem of evolution defined at the contact interface $\Gamma^{(1)}$,

$$\begin{array}{rcl} \dot{\mathbf{Z}}_c = \mathbf{A}_c\left(\mathbf{Z}, \mathbf{Z}_c, \boldsymbol{\Gamma}_c\right) & \text{on} & \Gamma^{(1)} \times [0,T] \\ \mathbf{Z}_c\left(t_o\right) = \mathbf{Z}_{c,o} & \text{on} & \Gamma^{(1)} \end{array} \tag{5.1}$$

along with

$$\begin{array}{rcl} \dot{\boldsymbol{\Gamma}}_c = \gamma_c \mathbf{G}_c\left(\mathbf{Z}_c, \boldsymbol{\Gamma}_c\right) & \text{on} & \Gamma^{(1)} \times [0,T] \\ \boldsymbol{\Gamma}_c\left(t_o\right) = \boldsymbol{\Gamma}_{c,o} & \text{on} & \Gamma^{(1)} \end{array} \tag{5.2}$$

where the set of primary independent variables $\mathbf{Z}_c$ and the set of internal variables $\boldsymbol{\Gamma}_c$ are defined as

$$\mathbf{Z}_c \;=\; [\mathcal{S}_c^e, \mathcal{S}_c^p] \tag{5.3a}$$

$$\mathbf{\Gamma}_c = [g^p_{T\alpha}, \zeta_c] \tag{5.3b}$$

With these definitions in hand, the operators that specify the governing equations of the frictional thermo-mechanical model can be defined as

$$\mathbf{A}_c(\mathbf{Z}, \mathbf{Z}_c, \mathbf{\Gamma}_c) = \begin{cases} \dfrac{1}{\Theta_c}\left[\left(Q_c^{(1)} + Q_c^{(2)}\right) + D_{c,\,mech}\right] \\ \dfrac{1}{\Theta_c} D_{c,\,ther} \end{cases} \tag{5.4}$$

and

$$\mathbf{G}_c(\mathbf{Z}_c, \mathbf{\Gamma}_c) = \begin{cases} \dfrac{\partial \Phi_c(t_{T\alpha}, q_c, \Theta_c)}{\partial^b \mathbf{t}_T^{ref}} \\ \dfrac{\partial \Phi_c(t_{T\alpha}, q_c, \Theta_c)}{\partial \Theta_c} \end{cases} \tag{5.5}$$

5.2 Operator splits

In analogy with the formulation introduced for the solution of the bulk continua, an additive operator split of the vector field $\mathbf{A}_c = \mathbf{A}_c^{(1)} + \mathbf{A}_c^{(2)}$ is considered. Both the *isentropic* and the *isothermal* operator splits will be compared. It will be shown that also in this case the critical restriction defined via the a-priori stability estimate is not satisfied when the standard isothermal operator split is used braking the underlying dissipative structure of the original problem [Laursen-98].

5.2.1 Isentropic operator split

Consider the following additive isentropic-based operator split of the vector field $\mathbf{A}_c$ as follows

$$\mathbf{A}_c = \mathbf{A}_{c,\,ise}^{(1)} + \mathbf{A}_{c,\,ise}^{(2)} \tag{5.6}$$

where the vector fields $\mathbf{A}_{c,\,ise}^{(1)}$ and $\mathbf{A}_{c,\,ise}^{(2)}$ are defined as

$$\mathbf{A}_{c,\,ise}^{(1)}(\mathbf{Z}, \mathbf{Z}_c, \mathbf{\Gamma}_c) = \begin{cases} 0 \\ 0 \end{cases} \tag{5.7a}$$

$$\mathbf{A}_{c,\,ise}^{(2)}(\mathbf{Z}, \mathbf{Z}_c, \mathbf{\Gamma}_c) = \begin{cases} \dfrac{1}{\Theta_c}\left[\left(Q_c^{(1)} + Q_c^{(2)}\right) + D_{c,\,mech}\right] \\ \dfrac{1}{\Theta_c} D_{c,\,ther} \end{cases} \tag{5.7b}$$

and consider the following two problem of evolution

$$\begin{array}{cc} \textit{Problem-1} & \textit{Problem-2} \\ \dot{\mathbf{Z}}_c = \mathbf{A}^{(1)}_{c,ise}(\mathbf{Z}, \mathbf{Z}_c, \boldsymbol{\Gamma}_c) & \dot{\mathbf{Z}}_c = \mathbf{A}^{(2)}_{c,ise}(\mathbf{Z}, \mathbf{Z}_c, \boldsymbol{\Gamma}_c) \\ \dot{\boldsymbol{\Gamma}}_c = \gamma_c \mathbf{G}_c(\mathbf{Z}, \mathbf{Z}_c, \boldsymbol{\Gamma}_c) & \dot{\boldsymbol{\Gamma}}_c = \gamma_c \mathbf{G}_c(\mathbf{Z}, \mathbf{Z}_c, \boldsymbol{\Gamma}_c) \end{array} \tag{5.8}$$

Taking into account that the operator split proposed must be applied together with the isentropic split on the bulk continua, then it is possible to observe that *Problem-1* defines a mechanical phase at fixed entropy $\dot{S}_c = \dot{S}^e + \dot{S}^p = 0$ and *Problem-2* defines a thermal phase at fixed configuration.

Denoting by $\mathbf{Z}_c^{(\alpha)}$ and $\boldsymbol{\Gamma}_c^{(\alpha)}$ the flow generated by the vector fields $\mathbf{A}^{(\alpha)}_{c,ise}$, $\alpha = 1, 2$, a straightforward computation shows that the following estimates holds

$$\frac{d}{dt}L^{(1)} = -\int_\Omega D^{(1)}_{mech}\, dV - \int_{\Gamma^{(1)}} D^{(1)}_{c,mech}\, dS \leq 0 \tag{5.9a}$$

$$\begin{aligned} \frac{d}{dt}L^{(2)} = &-\int_\Omega \frac{\Theta_o}{\Theta^{(2)}}\left(D^{(2)}_{mech} + D^{(2)}_{cond}\right) dV \\ &-\int_{\Gamma^{(1)}} \frac{\Theta_o}{\Theta^{(2)}_c}\left(D^{(2)}_{c,mech} + D^{(2)}_{c,cond}\right) dS \leq 0 \end{aligned} \tag{5.9b}$$

Thus, the isentropic operator split, including the interaction at the contact interface, preserves the underlying dissipative structure of the original problem. Therefore, unconditionally stable algorithms consistent with the full coupled problem can be obtained merely as the product of two unconditionally stable algorithms consistent with each phase.

5.2.2 Isothermal operator split

The usual isothermal operator split can be obtained considering the following additive split

$$\mathbf{A}_c = \mathbf{A}^{(1)}_{c,iso} + \mathbf{A}^{(2)}_{c,iso} \tag{5.10}$$

where the vector fields $\mathbf{A}^{(1)}_{c,iso}$ and $\mathbf{A}^{(2)}_{c,iso}$ are defined as

$$\mathbf{A}^{(1)}_{c,iso}(\mathbf{Z}, \mathbf{Z}_c, \boldsymbol{\Gamma}_c) = \begin{Bmatrix} \dfrac{1}{\Theta_c} H^{fp} \\ 0 \end{Bmatrix} \tag{5.11a}$$

$$\mathbf{A}^{(2)}_{c,iso}(\mathbf{Z}, \mathbf{Z}_c, \boldsymbol{\Gamma}_c) = \begin{Bmatrix} \dfrac{1}{\Theta_c}\left[\left(Q^{(1)}_c + Q^{(2)}_c\right) + D_{c,mech} - H^{fc}\right] \\ \dfrac{1}{\Theta_c} D_{c,ther} \end{Bmatrix} \tag{5.11b}$$

Within this operator split, two problems of evolution follows

$$\begin{array}{cc} \textit{Problem-1} & \textit{Problem-2} \\ \dot{\mathbf{Z}}_c = \mathbf{A}^{(1)}_{c,iso}(\mathbf{Z}, \mathbf{Z}_c, \boldsymbol{\Gamma}_c) & \dot{\mathbf{Z}}_c = \mathbf{A}^{(2)}_{c,iso}(\mathbf{Z}, \mathbf{Z}_c, \boldsymbol{\Gamma}_c) \\ \dot{\boldsymbol{\Gamma}}_c = \gamma_c \mathbf{G}_c(\mathbf{Z}, \mathbf{Z}_c, \boldsymbol{\Gamma}_c) & \dot{\boldsymbol{\Gamma}}_c = \gamma_c \mathbf{G}_c(\mathbf{Z}, \mathbf{Z}_c, \boldsymbol{\Gamma}_c) \end{array} \tag{5.12}$$

Problem-1 defines a mechanical phase at fixed temperature for both the bulk continua and the contact interface while *Problem-2* defines a thermal phase at fixed configuration.

Denoting by $\mathbf{Z}_c^{(\alpha)}$ and $\boldsymbol{\Gamma}_c^{(\alpha)}$ the flow generated by the vector fields $\mathbf{A}^{(\alpha)}_{c,iso}$, $\alpha = 1, 2$, a straightforward computation shows that the following estimates holds

$$\begin{aligned} \frac{d}{dt}L^{(1)} &= -\int_\Omega D^{(1)}_{mech}\, dV + \int_\Omega \left(1 - \frac{\Theta_o}{\Theta^{(1)}}\right) H^{ep(1)}\, dV \\ &\quad - \int_{\Gamma^{(1)}} D^{(1)}_{c,mech}\, dS + \int_{\Gamma^{(1)}} \left(1 - \frac{\Theta_o}{\Theta^{(1)}_c}\right) H^{fc(1)}\, dS \not\leq 0 \qquad (5.13a) \\ \frac{d}{dt}L^{(2)} &= -\int_\Omega \frac{\Theta_o}{\Theta^{(2)}} \left(D^{(2)}_{mech} + D^{(2)}_{cond}\right) dV \\ &\quad - \int_\Omega \left(1 - \frac{\Theta_o}{\Theta^{(2)}}\right) H^{ep(2)}\, dV \\ &\quad - \int_{\Gamma^{(1)}} \frac{\Theta_o}{\Theta^{(2)}_c} \left(D^{(2)}_{c,mech} + D^{(2)}_{c,cond}\right) dS \\ &\quad - \int_{\Gamma^{(1)}} \left(1 - \frac{\Theta_o}{\Theta^{(2)}_c}\right) H^{fc(2)}\, dS \not\leq 0 \qquad (5.13b) \end{aligned}$$

The contribution of both the structural elasto-plastic heating and the frictional contact heating to the evolution equations of each one of the sub-problems arising from the isothermal split, breaks the underlying dissipative structure of the original problem [Cancun-99].

It must be pointed out that the frictional contact heating term only exists if a *temperature dependent* hardening-like behavior is taken into account (see eq. 3.67b). Therefore, if a *constant* frictional coefficient is assumed in the analysis of the frictional contact problem both the isentropic and the isothermal split proposed satisfy the a-priori stability estimate [Laursen-98]. Moreover, the isothermal split is in any case unstable due to the elasto-plastic heating term obtained in the bulk continua formulation [Armero & Simo- 91], [Armero & Simo-92].

5.3 Time-discrete Contribution to the Weak form

The frictional contact contribution to the weak form of the momentum balance equation can be conveniently expressed as

$$G_c|_{n+1} = \langle \delta g_{N\,n+1}, t_{N\,n+1} \rangle_{\Gamma^{(1)}} + \left\langle \delta \bar{\xi}^{\alpha}_{n+1}, t_{T\alpha\,n+1} \right\rangle_{\Gamma^{(1)}} \tag{5.14}$$

where the time-discrete expressions for $\delta g_{N\,n+1}$ and $\delta \bar{\xi}_{n+1}\alpha$ can be found in [Laursen & Simo-91] and therefore will not be given here.

The contribution to the energy balance equation results in

$$G^{\vartheta}_{c}\,|_{n+1} = -\left\langle \delta\vartheta^{(1)}_{n+1}, Q^{(1)}_{c\,n+1} \right\rangle_{\Gamma^{(1)}} - \left\langle \delta\vartheta^{(2)}_{n+1}, Q^{(2)}_{c\,n+1} \right\rangle_{\Gamma^{(1)}} \tag{5.15}$$

In what follows, the expressions for normal pressure $t_{N\,n+1}$, the tangential traction $t_{T\alpha\,n+1}$and the heat fluxes $Q^{(k)\,trial}_{c\,n+1}$, $k = 1, 2$ are evaluated for both the isentropic and the isothermal algorithms.

5.4 Isentropic Algorithm

This algorithm consists of a mechanical and a thermal phase. In the mechanical phase the normal pressure $t_{N\,n+1}$ and the tangential traction $t_{T\alpha\,n+1}$ are computed to be used in the evaluation of the contact contribution to the weak form of the balance of momentum equation.

The thermal phase is necessary to compute the heat fluxes $Q^{(k)\,trial}_{c\,n+1}$, $k = 1, 2$ and the frictional dissipation $D_{c,\,mech\,n+1}$, and to update the internal variable of the contact problem.

5.4.1 Mechanical phase (isentropic split)

The evolution equations of the frictional contact problem are solved using the same strategy introduced for the solution of the thermo-plastic problem in the bulk continua. In fact, it is possible to observe that the regularization of the frictional constraints produces a constrained system of equations very similar to that obtained for the plastic case. The solution is so achieved through the introduction of a *trial* state (freezing the irreversible slip and hardening response) followed by a *frictional return mapping* to enforce the contact constraints [Laursen-98], [Cancun-99].

Trial state (kinematics)

According to the elasto-plastic operator split introduced for the solution of the plastic problem, consider the trial state

$$g^{p\,\alpha\,trial}_{T\,n+1} = g^{p\,\alpha}_{T\,n} \tag{5.16a}$$

$$\zeta^{trial}_{c\,n+1} = \zeta_{c\,n} \tag{5.16b}$$

The trial temperature at the contact interface is obtained solving the following equation

$$\bar{S}^{e}_{c\,n+1}\left(\Theta^{trial}_{c\,n+1}, \zeta^{trial}_{c\,n+1}\right) - S^{e}_{c\,n} = 0 \tag{5.17}$$

Observe that if a *linear thermal softening* is assumed, it results

$$\Theta^{trial}_{c\,n+1} = \Theta_{c\,n} \tag{5.18}$$

Trial (generalized) tractions

The normal contact pressure is obtained as

$$t_{N\,n+1} = \begin{cases} \dfrac{1}{2}\,\epsilon_N\,\dfrac{\langle g_{N\,n+1}\rangle^2 - \langle g_{N\,n}\rangle^2}{g_{N\,n+1} - g_{N\,n}} & \text{if} \quad g_{N\,n+1} \neq g_{N\,n} \\ \epsilon_N\,\langle g_{N\,n+1}\rangle & \text{if} \quad g_{N\,n+1} = g_{N\,n} \end{cases} \tag{5.19}$$

while the tangential contact traction and the hardening variable are evaluated according to the trial state as

$$t^{trial}_{T\,\alpha\,n+1} = \epsilon_T\,M_{\alpha\beta}\left(g^{\beta}_{T\,n+1} - g^{p\,\beta\,trial}_{T\,n+1}\right) \tag{5.20a}$$

$$q^{trial}_{c\,n+1} = -\sum_{p=1}^{m}\mu_p\left(\Theta^{trial}_{c\,n+1}\right)\left(\zeta^{trial}_{c\,n+1}\right)^p \tag{5.20b}$$

Trial slip function

The trial slip function is computed as

$$\Phi^{trial}_{c\,n+1} = \Phi_c\left(t_{N\,n+1}, t^{trial}_{T\,\alpha\,n+1}, q^{trial}_{c\,n+1}, \Theta_{c\,n}\right) \tag{5.21a}$$

$$= \left\|{}^{b}\mathbf{t}^{trial}_{T\,n+1}\right\|_{ref} - \left[\mu_o\left(\Theta_{c\,n}\right) - q^{trial}_{c\,n+1}\right]\,t_{N\,n+1} \tag{5.21b}$$

where it must be pointed out that the frictional coefficient μ_o is computed at time t_n according to the constraint on the plastic entropy evolution

$$\bar{S}^p_{c\,n+1} = S^p_{c\,n} \rightarrow \mu_o = const = \mu_o\,(\Theta_{c\,n}) \tag{5.22}$$

If $\Phi^{trial}_{c\,n+1} \leq 0$ then the trial state is the final intermediate state,

$$g^{p\,\alpha}_{T\,n+1} = g^{p\,\alpha\,trial}_{T\,n+1} \tag{5.23a}$$
$$\zeta_{c\,n+1} = \zeta^{trial}_{c\,n+1} \tag{5.23b}$$
$$\Theta_{c\,n+1} = \Theta^{trial}_{c\,n+1} \tag{5.23c}$$

otherwise, if $\Phi^{trial}_{c\,n+1} > 0$ the plastic corrector must be applied.

Mechanical isentropic contact return mapping

To obtain the final values of the plastic multiplier $\gamma_{c\,n+1}$ and of the intermediate contact temperature $\Theta_{c\,n+1}$ the following system of equations must be verified:

$$\begin{cases} \Phi_c\,(\gamma_{c\,n+1}, \Theta_{c\,n+1}) = 0 \\ \Delta S^e_{c\,n+1}\,(\Theta_{c\,n+1}, \gamma_{c\,n+1}) = 0 \end{cases} \tag{5.24}$$

where $\Delta S^e_{c\,n+1}$ is given by

$$\Delta S^e_{c\,n+1}\,(\Theta_{c\,n+1}, \gamma_{c\,n+1}) = \bar{S}^e_{c\,n+1} - S^e_{c\,n} \tag{5.25}$$

and the slip function at time t_{n+1} is obtained as

$$\begin{aligned} \Phi_{c\,n+1}\,(\gamma_{c\,n+1}, \Theta_{c\,n+1}) &= \Phi^{trial}_{c\,n+1} - \in_T \gamma_{c\,n+1} \\ &\quad + \left[q_{c\,n+1} - q^{trial}_{c\,n+1}\right]\, t_{N\,n+1} \end{aligned} \tag{5.26}$$

A local Newton-Raphson algorithm is used to find the solution of the non-linear system of equations. The linearized system results in

$$\begin{cases} \Delta S^e_{c\,n+1} + \left.\dfrac{\partial \Delta S^e_c}{\partial \gamma_c}\right|_{n+1} d\gamma_c + \left.\dfrac{\partial \Delta S^e_c}{\partial \Theta_c}\right|_{n+1} d\Theta_c = 0 \\ \Phi_{c\,n+1} + \left.\dfrac{\partial \Phi_c}{\partial \gamma_c}\right|_{n+1} d\gamma_c + \left.\dfrac{\partial \Phi_c}{\partial \Theta_c}\right|_{n+1} d\Theta_c = 0 \end{cases} \tag{5.27}$$

and the iterative process is the following:

$$
\begin{aligned}
\Delta\Theta_c^{(o)} &= 0 \\
\Delta\gamma_c^{(o)} &= 0 \\
&\quad \text{loop} \\
d\Theta_c^{(k)} &= -\frac{\Delta S^e_{c\,n+1} + \left.\dfrac{\partial \Delta S^e_c}{\partial \gamma_c}\right|_{n+1} d\gamma_c^{(k-1)}}{\left.\dfrac{\partial \Delta S^e_c}{\partial \Theta_c}\right|_{n+1}} \\
d\gamma_c^{(k)} &= -\frac{\Phi_{c\,n+1} + \left.\dfrac{\partial \Phi_c}{\partial \Theta_c}\right|_{n+1} d\Theta_c^{(k-1)}}{\left.\dfrac{\partial \Phi_c}{\partial \gamma_c}\right|_{n+1}} \\
\Delta\Theta_c^{(k+1)} &= \Delta\Theta_c^{(k)} + d\Theta_c^{(k)} \\
\Delta\gamma_c^{(k+1)} &= \Delta\gamma_c^{(k)} + d\gamma_c^{(k)} \\
&\quad \text{end\_loop} \\
\Theta_{c\,n+1} &= \Theta^{trial}_{c\,n+1} + \Delta\Theta_c \\
\gamma_{c\,n+1} &= \Delta\gamma_c
\end{aligned}
$$

starting from the initial conditions

$$\Theta_{c\,n+1} = \Theta^{trial}_{c\,n+1} \tag{5.28a}$$

$$\gamma_{c\,n+1} = 0 \tag{5.28b}$$

Update database and compute contact traction

The internal variable are updated as usual as

$$g^{p\,\alpha}_{T\,n+1} = g^{p\,\alpha\,trial}_{T\,n+1} + \gamma_{c\,n+1} n^{\alpha}_{c\,n+1} \tag{5.29a}$$

$$\zeta_{c\,n+1} = \zeta^{trial}_{c\,n+1} + \gamma_{c\,n+1}\, t_{N\,n+1} \tag{5.29b}$$

where the normal to the slip function $n_{c\,n+1}$ is computed as

$$n^{\alpha}_{c\,n+1} = n^{\alpha\,trial}_{c\,n+1} = \frac{M^{\alpha\beta}_{n+1}\, t^{trial}_{T\beta\,n+1}}{\sqrt{t^{trial}_{T\alpha\,n+1}\, M^{\alpha\beta}_{n+1}\, t^{trial}_{T\beta\,n+1}}} \tag{5.30}$$

Finally the generalized contact tractions are evaluated as

$$t_{T\,\alpha\,n+1} = \in_T M_{\alpha\beta}\left(g^{\beta}_{T\,n+1} - g^{p\,\beta}_{T\,n+1}\right) \tag{5.31a}$$

$$q_{c\,n+1} = -\sum_{p=1}^{m} \mu_p\left(\Theta_{c\,n+1}\right)\left(\zeta_{c\,n+1}\right)^p \tag{5.31b}$$

5.4.2 Thermal phase (isentropic split)

In this phase the internal variables are updated to the final value at time t_{n+1} starting again from the initial step value at time t_n. The goal is to obtain the heat fluxes $Q^{(k)}_{c\,n+1}$, $k = 1, 2$ and the frictional dissipation $D_{c,\,mech\,n+1}$ to evaluate the contribution to the weak form of the balance of energy equation.

Trial state (kinematics)

Both the plastic slip and the hardening variable are initialized at the initial values

$$g^{p\,\alpha\,trial}_{T\,n+1} = g^{p\,\alpha}_{T\,n} \tag{5.32a}$$

$$\zeta^{trial}_{c\,n+1} = \zeta_{c\,n} \tag{5.32b}$$

The trial temperature is evaluated according to the isentropic operator split as

$$\Theta^{trial}_{c\,n+1}\left[\frac{S^e_{c\,n+1}\left(\Theta^{trial}_{c\,n+1}, \zeta^{trial}_{c\,n+1}\right) - S^e_{c\,n}}{\Delta t}\right] = Q^{(1)\,trial}_{c\,n+1} + Q^{(2)\,trial}_{c\,n+1} \tag{5.33}$$

where a trial value of the heat fluxes $Q^{(k)\,trial}_{c\,n+1}$, $k = 1, 2$ at the contact interface, either for the conduction or for the convection case, is given by

$$Q^{(k)\,trial}_{c\,n+1} = \begin{cases} h^{(k)}_{cond}\left(t_{N\,n+1}, \Theta^{trial}_{g\,n+1}\right)\left(\Theta^{(k)}_{n+1} - \Theta^{trial}_{c\,n+1}\right) \\ \text{or} \\ h^{(k)}_{conv}\left(\Theta^{(k)}_{n+1} - \Theta^{trial}_{g\,n+1}\right) \end{cases} \tag{5.34}$$

Trial (generalized) contact tractions

The normal contact pressure $t_{N\,n+1}$ and the trial contact traction $t^{trial}_{T\,\alpha\,n+1}$ are respectively computed as

$$t_{N\,n+1} = \begin{cases} \dfrac{1}{2} \in_N \dfrac{\langle g_{N\,n+1}\rangle^2 - \langle g_{N\,n}\rangle^2}{g_{N\,n+1} - g_{N\,n}} & \text{if} \quad g_{N\,n+1} \neq g_{N\,n} \\ \in_N \langle g_{N\,n+1}\rangle & \text{if} \quad g_{N\,n+1} = g_{N\,n} \end{cases} \tag{5.35}$$

and

$$t^{trial}_{T\,\alpha\,n+1} = \in_T M_{\alpha\beta} \left(g^{\beta}_{T\,n+1} - g^{p\,\beta\,trial}_{T\,n+1} \right) \tag{5.36}$$

Finally, $q^{trial}_{c\,n+1}$ is given by

$$q^{trial}_{c\,n+1} = -\sum_{p=1}^{m} \mu_p \left(\Theta^{trial}_{c\,n+1} \right) \left(\zeta^{trial}_{c\,n+1} \right)^p \tag{5.37}$$

Trial slip function

The trial slip function is computed as

$$\begin{aligned} \Phi^{trial}_{c\,n+1} &= \Phi_c \left(t_{N\,n+1}, t^{trial}_{T\,\alpha\,n+1}, q^{trial}_{c\,n+1}, \Theta^{trial}_{c\,n+1} \right) && \text{(5.38a)} \\ &= \left\| {}^{b}\mathbf{t}^{trial}_{T\,n+1} \right\|_{ref} - \left[\mu_o \left(\Theta^{trial}_{c\,n+1} \right) - q^{trial}_{c\,n+1} \right] t_{N\,n+1} \leq 0 && \text{(5.38b)} \end{aligned}$$

where in this case the frictional coefficient μ_o is computed at time t_{n+1} according to the trial temperature $\Theta^{trial}_{c\,n+1}$.

If $\Phi^{trial}_{c\,n+1} \leq 0$ the trial state is the final state, that is

$$\begin{aligned} g^{p\,\alpha}_{T\,n+1} &= g^{p\,\alpha\,trial}_{T\,n+1} && \text{(5.39a)} \\ \zeta_{c\,n+1} &= \zeta^{trial}_{c\,n+1} && \text{(5.39b)} \\ \Theta_{c\,n+1} &= \Theta^{trial}_{c\,n+1} && \text{(5.39c)} \end{aligned}$$

otherwise, if $\Phi^{trial}_{c\,n+1} > 0$ the plastic corrector must be applied.

Thermal contact return mapping

The frictional return mapping results in the solution of the following non-linear system of equations

$$\begin{cases} \Phi_c\left(\gamma_{c\,n+1}, \Theta_{c\,n+1}\right) = 0 \\ g_{c\,n+1}\left(\gamma_{c\,n+1}, \Theta_{c\,n+1}\right) = 0 \end{cases} \tag{5.40}$$

where the slip function at time t_{n+1} is computed as

$$\begin{aligned} \Phi_{c\,n+1}\left(\gamma_{c\,n+1}, \Theta_{c\,n+1}\right) &= \Phi^{trial}_{c\,n+1} - \in_T \gamma_{c\,n+1} \\ &\quad + \left[q_{c\,n+1} - q^{trial}_{c\,n+1}\right] t_{N\,n+1} \end{aligned} \tag{5.41}$$

while function $g_{c\,n+1}\left(\gamma_{c\,n+1}, \Theta_{c\,n+1}\right)$ is obtained as

$$\begin{aligned} g_{c\,n+1}\left(\gamma_{c\,n+1}, \Theta_{c\,n+1}\right) &= \Theta_{c\,n+1}\left[\frac{S^e_{c\,n+1}\left(\Theta_{c\,n+1}, \gamma_{c\,n+1}\right) - S^e_{c\,n}}{\Delta t}\right] \\ &\quad - \left[Q^{(1)}_{c\,n+1}\left(\Theta_{c\,n+1}\right) + Q^{(2)}_{c\,n+1}\left(\Theta_{c\,n+1}\right)\right] \\ &\quad - D_{c,\,mech\,n+1}\left(\Theta_{c\,n+1}, \gamma_{c\,n+1}\right) \end{aligned} \tag{5.42}$$

where in this case it appears the frictional dissipation term given by

$$D_{c,\,mech\,n+1} = \frac{\gamma_{c\,n+1}}{\Delta t}\mu_o\left(\Theta_{c\,n+1}\right) t_{N\,n+1} \tag{5.43}$$

The linearized system of equations results in

$$\begin{cases} g_{c\,n+1} + \left.\dfrac{\partial g_c}{\partial \gamma_c}\right|_{n+1} d\gamma_c + \left.\dfrac{\partial g_c}{\partial \Theta_c}\right|_{n+1} d\Theta_c = 0 \\ \Phi_{c\,n+1} + \left.\dfrac{\partial \Phi_c}{\partial \gamma_c}\right|_{n+1} d\gamma_c + \left.\dfrac{\partial \Phi_c}{\partial \Theta_c}\right|_{n+1} d\Theta_c = 0 \end{cases} \tag{5.44}$$

and the initial conditions

$$\Theta_{c\,n+1} = \Theta^{trial}_{c\,n+1} \tag{5.45a}$$

$$\gamma_{c\,n+1} = 0 \tag{5.45b}$$

The iterative process is the usual:

$$\Delta\Theta^{(o)}_c = 0$$

$$
\begin{aligned}
\Delta\gamma_c^{(o)} &= 0 \\
&\quad \text{loop} \\
d\Theta_c^{(k)} &= -\frac{g_{c\,n+1} + \left.\dfrac{\partial g_c}{\partial \gamma_c}\right|_{n+1} d\gamma_c^{(k-1)}}{\left.\dfrac{\partial g_c}{\partial \Theta_c}\right|_{n+1}} \\
d\gamma_c^{(k)} &= -\frac{\Phi_{c\,n+1} + \left.\dfrac{\partial \Phi_c}{\partial \Theta_c}\right|_{n+1} d\Theta_c^{(k-1)}}{\left.\dfrac{\partial \Phi_c}{\partial \gamma_c}\right|_{n+1}} \\
\Delta\Theta_c^{(k+1)} &= \Delta\Theta_c^{(k)} + d\Theta_c^{(k)} \\
\Delta\gamma_c^{(k+1)} &= \Delta\gamma_c^{(k)} + d\gamma_c^{(k)} \\
&\quad \text{end\_loop} \\
\Theta_{c\,n+1} &= \Theta_{c\,n+1}^{trial} + \Delta\Theta_c \\
\gamma_{c\,n+1} &= \Delta\gamma_c
\end{aligned}
$$

Update database and compute (generalized) contact tractions

The internal variables are updated first, as

$$g_{T\,n+1}^{p\,\alpha} = g_{T\,n+1}^{p\,\alpha\,trial} + \gamma_{c\,n+1}\, n_{c\,n+1}^{\alpha} \tag{5.46a}$$

$$\zeta_{c\,n+1} = \zeta_{c\,n+1}^{trial} + \gamma_{c\,n+1}\, t_{N\,n+1} \tag{5.46b}$$

being

$$n_{c\,n+1}^{\alpha} = n_{c\,n+1}^{\alpha\,trial} = \frac{M_{n+1}^{\alpha\beta}\, t_{T\beta\,n+1}^{trial}}{\sqrt{t_{T\alpha\,n+1}^{trial}\, M_{n+1}^{\alpha\beta}\, t_{T\beta\,n+1}^{trial}}} \tag{5.47}$$

so the tangential contact traction and the hardening conjugate variable result in

$$t_{T\,\alpha\,n+1} = \in_T M_{\alpha\beta} \left(g_{T\,n+1}^{\beta} - g_{T\,n+1}^{p\,\beta} \right) \tag{5.48}$$

$$q_{c\,n+1} = -\sum_{p=1}^{m} \mu_p \left(\Theta_{c\,n+1}\right) \left(\zeta_{c\,n+1}\right)^p \tag{5.49}$$

Heat flux and frictional dissipation

According to the values of the contact pressure and temperature obtained, the heat fluxes $Q^{(k)}_{c\,n+1}$, $k = 1, 2$ at the contact interface results in

$$Q^{(k)}_{c\,n+1} = \begin{cases} h^{(k)}_{cond}\left(t_{N\,n+1}, \Theta_{g\,n+1}\right)\left(\Theta^{(k)}_{n+1} - \Theta_{c\,n+1}\right) \\ \text{or} \\ h^{(k)}_{conv}\left(\Theta^{(k)}_{n+1} - \Theta_{g\,n+1}\right) \end{cases} \tag{5.50}$$

and the frictional dissipation is given by

$$D_{c,\,mech\,n+1} = \frac{\gamma_{c\,n+1}}{\Delta t}\mu_o\left(\Theta_{c\,n+1}\right) t_{N\,n+1} \tag{5.51}$$

5.5 Isothermal Algorithm

The isothermal algorithm follows the same steps indicated for the isentropic algorithm but in this case the constraint will be on the evolution of the temperature field at the contact interface.

5.5.1 Mechanical phase (isothermal split)

The following steps will solve the mechanical phase in the hypothesis of an isothermal split.

Trial state (kinematics)

Let us start assuming a trial state for the inelastic slip and the hardening variable

$$g^{p\,\alpha\,trial}_{T\,n+1} = g^{p\,\alpha}_{T\,n} \tag{5.52a}$$

$$\zeta^{trial}_{c\,n+1} = \zeta_{c\,n} \tag{5.52b}$$

In the other hand let us fix the contact temperature to its initial value

$$\Theta_{c\,n+1} = \Theta_{c\,n} \tag{5.53}$$

due to the restriction enforced by the isothermal algorithm

Trial (generalized) traction

As usual compute the normal pressure as

$$t_{N\,n+1} = \begin{cases} \dfrac{1}{2}\,\epsilon_N\,\dfrac{\langle g_{N\,n+1}\rangle^2 - \langle g_{N\,n}\rangle^2}{g_{N\,n+1} - g_{N\,n}} & \text{if} \quad g_{N\,n+1} \neq g_{N\,n} \\ \epsilon_N\,\langle g_{N\,n+1}\rangle & \text{if} \quad g_{N\,n+1} = g_{N\,n} \end{cases} \tag{5.54}$$

then evaluate the frictional tangential traction using the trial value chosen for the plastic slip

$$t^{trial}_{T\,\alpha\,n+1} = \epsilon_T\, M_{\alpha\beta}\left(g^{\beta}_{T\,n+1} - g^{p\,\beta\ trial}_{T\,n+1}\right) \tag{5.55}$$

and in the same way for $q^{trial}_{c\,n+1}$, as

$$q^{trial}_{c\,n+1} = -\sum_{p=1}^{m} \mu_p\left(\Theta_{c\,n}\right)\left(\zeta^{trial}_{c\,n+1}\right)^p \tag{5.56}$$

Trial slip function

Compute the trial slip function $\Phi^{trial}_{c\,n+1}$ using the trials above defined

$$\Phi^{trial}_{c\,n+1} = \Phi_c\left(t_{N\,n+1}, t^{trial}_{T\,\alpha\,n+1}, q^{trial}_{c\,n+1}, \Theta_{c\,n}\right) \tag{5.57a}$$

$$= \left\|{}^{b}\mathbf{t}^{trial}_{T\,n+1}\right\|_{ref} - \left[\mu_o\left(\Theta_{c\,n}\right) - q^{trial}_{c\,n+1}\right]\, t_{N\,n+1} \leq 0 \tag{5.57b}$$

As usual if $\Phi^{trial}_{c\,n+1} \leq 0$ then the trial solution is the final intermediate solution, that is

$$g^{p\,\alpha}_{T\,n+1} = g^{p\,\alpha\ trial}_{T\,n+1} \tag{5.58a}$$

$$\zeta_{c\,n+1} = \zeta^{trial}_{c\,n+1} \tag{5.58b}$$

$$\Theta_{c\,n+1} = \Theta_{c\,n} \tag{5.58c}$$

otherwise, if $\Phi^{trial}_{c\,n+1} > 0$ the plastic corrector must be applied.

Mechanical isothermal contact return mapping

The frictional return mapping results in the solution of equation

$$\Phi_c\left(\gamma_{c\,n+1}\right) = 0 \tag{5.59}$$

where the slip function at time t_{n+1}results in

$$\begin{aligned}\Phi_{c\,n+1}\left(\gamma_{c\,n+1}\right) &= \Phi^{trial}_{c\,n+1} - \in_T \gamma_{c\,n+1} \\ &\quad + \left[q_{c\,n+1} - q^{trial}_{c\,n+1}\right]\, t_{N\,n+1}\end{aligned} \tag{5.60}$$

A local Newton-Raphson algorithm can be used to find the solution starting from the initial conditions $\gamma_{c\,n+1} = 0$ as follows

$$\begin{aligned}\Delta\gamma_c^{(o)} &= 0 \\ &\quad \text{loop} \\ d\gamma_c^{(k)} &= -\frac{\Phi_{c\,n+1}}{\left.\dfrac{\partial\Phi_c}{\partial\gamma_c}\right|_{n+1}} \\ \Delta\gamma_c^{(k+1)} &= \Delta\gamma_c^{(k)} + d\gamma_c^{(k)} \\ &\quad \text{end\_loop} \\ \gamma_{c\,n+1} &= \Delta\gamma_c\end{aligned}$$

Update database and compute generalized traction

First, let us update the internal variables as

$$g^{p\,\alpha}_{T\,n+1} = g^{p\,\alpha\,trial}_{T\,n+1} + \gamma_{c\,n+1} n^{\alpha}_{c\,n+1} \tag{5.61a}$$

$$\zeta_{c\,n+1} = \zeta^{trial}_{c\,n+1} + \gamma_{c\,n+1}\, t_{N\,n+1} \tag{5.61b}$$

where also in this case it results

$$n^{\alpha}_{c\,n+1} = n^{\alpha\,trial}_{c\,n+1} = \frac{M^{\alpha\beta}_{n+1}\, t^{trial}_{T\,\beta\,n+1}}{\sqrt{t^{trial}_{T\,\alpha\,n+1}\, M^{\alpha\beta}_{n+1}\, t^{trial}_{T\,\beta\,n+1}}} \tag{5.62}$$

Then, compute the tangential traction with the final values of the internal variables

$$t_{T\,\alpha\,n+1} = \in_T M_{\alpha\beta}\left(g^{\beta}_{T\,n+1} - g^{p\,\beta}_{T\,n+1}\right) \tag{5.63a}$$

$$q_{c\,n+1} = -\sum_{p=1}^{m} \mu_p\left(\Theta_{c\,n}\right)\left(\zeta_{c\,n+1}\right)^p \tag{5.63b}$$

5.5.2 Thermal phase (isothermal split)

This phase is exactly the same as in the isentropic case with only a small difference in the evaluation of the function $g_{c\,n+1}(\gamma_{c\,n+1}, \Theta_{c\,n+1})$, in fact in this case it must be taken into account the frictional contact heating H^{fc}_{n+1}, so that

$$\begin{aligned} g_{c\,n+1}(\gamma_{c\,n+1}, \Theta_{c\,n+1}) \;=\; & \Theta_{c\,n+1}\left[\frac{S^{e}_{c\,n+1}(\Theta_{c\,n+1}, \gamma_{c\,n+1}) - \bar{S}^{e}_{c\,n+1}}{\Delta t}\right] \\ & - \left[Q^{(1)}_{c\,n+1}(\Theta_{c\,n+1}) + Q^{(2)}_{c\,n+1}(\Theta_{c\,n+1})\right] \\ & - D_{c,int\,n+1}(\Theta_{c\,n+1}, \gamma_{c\,n+1}) \\ & + H^{fc}_{n+1}(\Theta_{c\,n+1}, \gamma_{c\,n+1}) \end{aligned} \tag{5.64}$$

Finally, note that the initial value of the elastic entropy is the final value of the mechanical phase. To avoid this fact it is also possible to solve the isothermal phase using the equivalent form of the energy equation defined at the contact interface in which the main variable is the contact temperature field.

Chapter 6

Space Discretization

In this chapter the *Galerkin projection* of the weak form of both the balance of momentum and the balance of energy equations given in the continuum case is presented.

Moreover, in the context of the general mixed approximation based on the three-filed Hu-Washizu variational principle, the projection procedure referred to as *B-bar method* is presented.

6.1 The Galerkin projection

In the context of the *finite element method*, the discrete problem can be obtained through the Galerkin projection of the continuum case in the finite dimension sub-spaces $\nu_u^h \subset \nu_u$ and $\nu_\Theta^h \subset \nu_\Theta$.

Let consider the standard spatial discretization $\Omega^h = \bigcup_{e=1}^{NEL} \Omega_e^h$ and let $\mathbf{N}_u \in \nu_u^h \subset H^1(\Omega)$ and $\mathbf{N}_\Theta \in \nu_\Theta^h \subset H^1(\Omega)$ be the general interpolations of the displacement and temperature field on a typical element Ω_e, so that

$$\mathbf{u}^h\big|_{\Omega_e} = \mathbf{N}_u \mathbf{U} \tag{6.1a}$$

$$\nabla^s \mathbf{u}^h\big|_{\Omega_e} = \mathbf{B}_u \mathbf{U} \tag{6.1b}$$

and

$$\Theta^h\big|_{\Omega_e} = \mathbf{N}_\Theta \boldsymbol{\Theta} \tag{6.2a}$$

$$\nabla \Theta^h\big|_{\Omega_e} = \mathbf{B}_\Theta \boldsymbol{\Theta} \tag{6.2b}$$

where $\mathbf{B}_u$ and $\mathbf{B}_\Theta$ are spatial derivatives vectors.

If Galerkin method is applied then the test functions $\boldsymbol{\eta}$ and ϑ associated to the displacement and temperature field, $\mathbf{u}^h|_{\Omega_e}$ and $\Theta^h|_{\Omega_e}$, respectively, are given by

$$\boldsymbol{\eta} = \mathbf{N}_u \mathbf{U} \tag{6.3a}$$
$$\delta\boldsymbol{\eta} = \mathbf{N}_u \delta\mathbf{U} \tag{6.3b}$$
$$\nabla^s \boldsymbol{\eta} = \mathbf{B}_u \mathbf{U} \tag{6.3c}$$

and

$$\vartheta = \mathbf{N}_\Theta \boldsymbol{\Theta} \tag{6.4a}$$
$$\delta\vartheta = \mathbf{N}_\Theta \delta\boldsymbol{\Theta} \tag{6.4b}$$
$$\nabla\vartheta = \mathbf{B}_\Theta \boldsymbol{\Theta} \tag{6.4c}$$

The space and time discretized form of the balance of momentum equation results in

$$\langle \mathbf{B}_u \delta\mathbf{U}, \boldsymbol{\sigma}^h_{n+1} \rangle = G|^h_{n+1} \tag{6.5a}$$

where the full discrete term associated to both the external load and the contact interaction [Laursen & Simo-91] is given by

$$\begin{aligned} G|^h_{n+1} &= \langle \mathbf{N}_u \delta\mathbf{U}, \mathbf{b}^h_{n+1} \rangle + \left\langle \mathbf{N}_u \delta\mathbf{U}, \bar{\mathbf{t}}^h_{n+1} \right\rangle_{\partial\Omega_e} \\ &\quad + \left\langle \delta g^h_{N\,n+1}, t^h_{N\,n+1} \right\rangle_{\Gamma^{(1)}_e} + \left\langle \delta\bar{\xi}^{\alpha\,h}_{n+1}, t^h_{T\,\alpha\,n+1} \right\rangle_{\Gamma^{(1)}_e} \end{aligned} \tag{6.6}$$

where the space and time discrete expressions for $\delta g^h_{N\,n+1}$ and $\delta\bar{\xi}^{\alpha\,h}_{n+1}$ can be found in [Laursen & Simo-91] and therefore will not be given here.

The full discretized form of the energy equation results in

$$\begin{aligned} &\left\langle \mathbf{N}_\Theta \delta\boldsymbol{\Theta}, \Theta^h_{n+1} \left(\frac{S^E_{n+1} - \bar{S}^E_{n+1}}{\Delta t} \right) + \frac{L_{n+1} - L_n}{\Delta t} \right\rangle + \langle \mathbf{B}_\Theta \delta\boldsymbol{\Theta}, k_{n+1} \nabla\Theta^h_{n+1} \rangle \\ &= \begin{cases} G^\vartheta|^h_{n+1} & \text{if } \textit{isentropic} \\ G^\vartheta|^{ep\,h}_{n+1} & \text{if } \textit{isothermal} \end{cases} \end{aligned} \tag{6.7}$$

where the full discretized thermal load for an isentropic split is given by

$$\begin{aligned} G^\vartheta|^h_{n+1} &= \langle \mathbf{N}_\Theta \delta\boldsymbol{\Theta}, R_{n+1} \rangle + \langle \mathbf{N}_\Theta \delta\boldsymbol{\Theta}, D_{mech,n+1} \rangle - \left\langle \mathbf{N}_\Theta \delta\boldsymbol{\Theta}, \bar{q}_{n+1} \right\rangle_{\partial\Omega_e} \\ &\quad - \left\langle \delta\vartheta^{(1)\,h}_{n+1}, Q^{(1)}_{c\,n+1} \right\rangle_{\Gamma^{(1)}_e} - \left\langle \delta\vartheta^{(2)\,h}_{n+1}, Q^{(2)}_{c\,n+1} \right\rangle_{\Gamma^{(1)}_e} \end{aligned} \tag{6.8}$$

or

$$G^{\vartheta}\,|_{n+1}^{ep\,h} = G^{\vartheta}\,|_{n+1}^{h} - \left\langle \mathbf{N}_{\Theta}\,\delta\boldsymbol{\Theta}, H_{n+1}^{ep} \right\rangle \tag{6.9}$$

for an isothermal split.

6.2 Mixed approximation: *B-bar* projection method

In what follows we consider a general mixed approximation based on the three-filed Hu-Washizu variational principle. It is possible to show that this formulation is equivalent to the projection procedure referred to as *B-bar method* [Simo-85]. The present approach provides a variational framework for B-bar type projection methods in the general non-linear situation in which pressure may depend on the strain deviator an non-constant elasticities are permitted.

Let consider the standard discretization $\Omega = \bigcup_{e=1}^{NEL} \Omega_e$ in the subspace $H^h \subset H^1(\Omega)$ so that over a typical element Ω_e one has the general interpolations

$$\mathbf{u}^h\big|_{\Omega_e} = \sum_{I=1}^{N} N_I \mathbf{u}_I \tag{6.10a}$$

$$\nabla^s \mathbf{u}^h\big|_{\Omega_e} = \sum_{I=1}^{N} \mathbf{B}_I \mathbf{u}_I \tag{6.10b}$$

where $N_I = N_I(\mathbf{x})$ are the standard shape functions. It is also possible to consider the interpolations for the spherical and deviatoric parts of the symmetric gradient operator

$$tr\left(\nabla^s \mathbf{u}^h\big|_{\Omega_e}\right) = div\left(\mathbf{u}^h\big|_{\Omega_e}\right) = \sum_{I=1}^{N} \mathbf{b}_I^{vol} \mathbf{u}_I \tag{6.11a}$$

$$dev\left(\nabla^s \mathbf{u}^h\big|_{\Omega_e}\right) = \sum_{I=1}^{N} \mathbf{B}_I^{dev} \mathbf{u}_I \tag{6.11b}$$

since $\mathbf{b}_I^{vol}$ and $\mathbf{B}_I^{dev}$ are given in term of the projection operators $\mathbf{I}^{vol}$ and $\mathbf{I}^{dev}$, see (2.136*a*), (2.136*b*),according to the expressions

$$\mathbf{b}_I^{vol} = \mathbf{1} \cdot \mathbf{B}_I \tag{6.12a}$$

$$\mathbf{B}_I^{vol} = \mathbf{I}^{vol} : \mathbf{B}_I = \frac{1}{3}\mathbf{1} \otimes \mathbf{b}_I^{vol} \tag{6.12b}$$

$$\mathbf{B}_I^{dev} = \mathbf{I}^{dev} : \mathbf{B}_I = \mathbf{B}_I \ominus \mathbf{B}_I^{vol} \tag{6.12c}$$

$$\mathbf{B}_I = \mathbf{B}_I^{vol} \oplus \mathbf{B}_I^{dev} \tag{6.12d}$$

so that it is possible to express $\nabla^s \mathbf{u}^h\big|_{\Omega_e}$ as

$$\begin{aligned} \nabla^s \mathbf{u}^h\big|_{\Omega_e} &= \mathbf{1} \otimes \frac{1}{3} div\left(\mathbf{u}^h\big|_{\Omega_e}\right) + dev\left(\nabla^s \mathbf{u}^h\big|_{\Omega_e}\right) \\ &= \frac{1}{3}\sum_{I=1}^{N} \mathbf{1} \otimes \mathbf{b}_I^{vol}\mathbf{u}_I + \sum_{I=1}^{N} \mathbf{B}_I^{dev}\mathbf{u}_I \\ &= \sum_{I=1}^{N} \left(\mathbf{B}_I^{vol} \oplus \mathbf{B}_I^{dev}\right)\mathbf{u}_I = \sum_{I=1}^{N} \mathbf{B}_I\mathbf{u}_I \end{aligned} \tag{6.13}$$

Next step is to consider the volume and pressure approximations $\theta^h$and p^h, respectively, in the subspace $K^h \subset L^2(\Omega)$ so that over the typical element Ω_e one has the general interpolations

$$\theta^h\big|_{\Omega_e} = \sum_{k=1}^{\overline{N}} \Psi_k \theta_k = \mathbf{\Psi} \cdot \boldsymbol{\theta} \tag{6.14a}$$

$$p^h\big|_{\Omega_e} = \sum_{k=1}^{\overline{N}} \Psi_k p_k = \mathbf{\Psi} \cdot \mathbf{p} \tag{6.14b}$$

where $\mathbf{\Psi} = \mathbf{\Psi}(\mathbf{x}) = [\Psi_1 \Psi_2 \cdots \Psi_{\overline{N}}]^T$, $\boldsymbol{\theta} = \boldsymbol{\theta}(\mathbf{x}) = [\theta_1 \theta_2 \cdots \theta_{\overline{N}}]^T$and $\mathbf{p} = \mathbf{p}(\mathbf{x}) = [p_1 p_2 \cdots p_{\overline{N}}]^T$.

Note that *no inter-element continuity* is enforced on θ^h and p^h and as a result of this discontinuous approximation, the discrete versions of variational equations (2.146*c*), (2.146*b*) is

$$\int_{\Omega_e} q^h \left[div\left(\mathbf{u}^h\right) - \theta^h\right] dV = 0 \rightarrow \forall q^h \in K^h \tag{6.15a}$$

$$\int_{\Omega_e} \gamma^h \left[-p^h + \frac{1}{3} tr\left(\overline{\boldsymbol{\sigma}}^h\right)\right] dV = 0 \rightarrow \forall p^h \in K^h \tag{6.15b}$$

so that it is possible to eliminate the fields θ^h and p^h at element level. In fact, substituting θ^h from equation (6.14*a*) into equation (6.15*a*) the result is

$$\mathbf{q} \cdot \int_{\Omega_e} \boldsymbol{\Psi}(\mathbf{x}) \left[div\left(\mathbf{u}^h\right) - \boldsymbol{\Psi}(\mathbf{x}) \right] \cdot \boldsymbol{\theta}\, dV = 0 \tag{6.16}$$

that is

$$\int_{\Omega_e} \boldsymbol{\Psi}(\mathbf{x})\, div\left(\mathbf{u}^h\right)\, dV = \int_{\Omega_e} \left[\boldsymbol{\Psi}(\mathbf{x}) \otimes \boldsymbol{\Psi}(\mathbf{x})\right] \cdot \boldsymbol{\theta}\, dV \tag{6.17}$$

and if we define

$$\mathbf{H}^e(\mathbf{x}) = \int_{\Omega_e} \boldsymbol{\Psi}(\mathbf{x}) \otimes \boldsymbol{\Psi}(\mathbf{x})\, dV \tag{6.18}$$

then it is possible to obtain $\boldsymbol{\theta}(\mathbf{x})$ as

$$\boldsymbol{\theta} = \frac{1}{\mathbf{H}^e(\mathbf{x})} \int_{\Omega_e} \boldsymbol{\Psi}(\mathbf{x})\, div\left(\mathbf{u}^h\right)\, dV \tag{6.19}$$

and taking into account that $\theta^h\big|_{\Omega_e} = \boldsymbol{\Psi}(\mathbf{x}) \cdot \boldsymbol{\theta}$ then the fields θ^h at element level result in

$$\theta^h\big|_{\Omega_e} = \frac{\boldsymbol{\Psi}(\mathbf{x})}{\mathbf{H}^e(\mathbf{x})} \int_{\Omega_e} \boldsymbol{\Psi}(\mathbf{x})\, div\left(\mathbf{u}^h\right)\, dV \tag{6.20}$$

Following the same procedure in the case of the pressure field p^h we obtain

$$p^h\big|_{\Omega_e} = \frac{\boldsymbol{\Psi}(\mathbf{x})}{\mathbf{H}^e(\mathbf{x})} \int_{\Omega_e} \boldsymbol{\Psi}(\mathbf{x})\, \frac{1}{3} tr\left(\overline{\boldsymbol{\sigma}}^h\right)\, dV \tag{6.21}$$

It is now interesting the definition of a new divergence operator $\overline{div}(\cdot)$ as follows

$$\overline{div}(\cdot) = \frac{\boldsymbol{\Psi}(\mathbf{x})}{\mathbf{H}^e(\mathbf{x})} \int_{\Omega_e} \boldsymbol{\Psi}(\mathbf{x})\, div(\cdot)\, dV \tag{6.22a}$$

and taking into account that $div(\cdot) = \sum_{I=1}^{N} \mathbf{b}_I^{vol}(\cdot)$, see (6.11*a*), it leads to the definition of $\overline{\mathbf{b}}_I^{vol}$ as

$$\overline{\mathbf{b}}_I^{vol} = \frac{\boldsymbol{\Psi}(\mathbf{x})}{\mathbf{H}^e(\mathbf{x})} \int_{\Omega_e} \boldsymbol{\Psi}(\mathbf{x}) \otimes \mathbf{b}_I^{vol}\, dV \tag{6.23}$$

so that in mixed formulation, operators (6.12*b*), (6.12*c*) and (6.12*d*) are specified as

$$\overline{\mathbf{B}}_I^{vol} = \frac{1}{3}\mathbf{1}\otimes\overline{\mathbf{b}}_I^{vol} \tag{6.24a}$$

$$\mathbf{B}_I^{dev} = \mathbf{B}_I \ominus \mathbf{B}_I^{vol} \tag{6.24b}$$

$$\overline{\mathbf{B}}_I = \overline{\mathbf{B}}_I^{vol} \oplus \mathbf{B}_I^{dev} \tag{6.24c}$$

Elimination of the field variables θ^h and p^h at element level yields a reduced residual involving the modified discrete gradient operator $\overline{\mathbf{B}}_I$. Remarkably, pressure field drops out from the formulation. Substituting (6.21)into the discrete version of the variational equation (2.146a) the residual at element level $R^h\big|_{\Omega_e}$ can be computed as follow

$$\begin{aligned}
R^h\big|_{\Omega_e} &= \int_{\Omega_e} dev\left(\overline{\boldsymbol{\sigma}}^h\right) : dev\left(\nabla^s \boldsymbol{\eta}^h\right) dV + \int_{\Omega_e} p^h div\left(\boldsymbol{\eta}^h\right) dV - G|_{\Omega_e} \\
&= \int_{\Omega_e} \left[dev\left(\overline{\boldsymbol{\sigma}}^h\right) : dev\left(\nabla^s \boldsymbol{\eta}^h\right) + \frac{1}{3} tr\left(\overline{\boldsymbol{\sigma}}^h\right) \cdot \overline{div}\left(\boldsymbol{\eta}^h\right) \right] dV - G|_{\Omega_e} \\
&= \sum_{I=1}^{N} \boldsymbol{\eta}_I \cdot \int_{\Omega_e} \left[\left(\mathbf{B}_I^{dev}\right)^T dev\left(\overline{\boldsymbol{\sigma}}^h\right) + \left(\overline{\mathbf{B}}_I^{vol}\right)^T \frac{1}{3} tr\left(\overline{\boldsymbol{\sigma}}^h\right) \cdot \mathbf{1} \right] dV - G|_{\Omega_e} \\
&= \sum_{I=1}^{N} \boldsymbol{\eta}_I \cdot \int_{\Omega_e} \left(\mathbf{B}_I^{dev} \oplus \overline{\mathbf{B}}_I^{vol}\right)^T \left[dev\left(\overline{\boldsymbol{\sigma}}^h\right) + \frac{1}{3} tr\left(\overline{\boldsymbol{\sigma}}^h\right) \cdot \mathbf{1} \right] dV - G|_{\Omega_e} \\
&= \sum_{I=1}^{N} \boldsymbol{\eta}_I \cdot \int_{\Omega_e} \left(\overline{\mathbf{B}}_I\right)^T \overline{\boldsymbol{\sigma}}^h \, dV - G|_{\Omega_e}
\end{aligned} \tag{6.25a}$$

where the stress field $\overline{\boldsymbol{\sigma}}^h$ is given by

$$\overline{\boldsymbol{\sigma}}^h = \left. \frac{\partial \overline{W}\left(\bar{\boldsymbol{\varepsilon}}\right)}{\partial \bar{\boldsymbol{\varepsilon}}} \right|^h \tag{6.26}$$

Observe that to compute the symmetric gradient $\overline{\nabla}^s \mathbf{u}$ we can make use of the operator $\overline{\mathbf{B}}_I$, in fact taking into account the discrete divergence operator (6.22a)the approximation for the volumetric strain θ^h can be expressed as

$$\theta^h\big|_{\Omega_e} = \overline{div}\left(\mathbf{u}^h\right) = \sum_{I=1}^{N} \overline{\mathbf{b}}_I^{vol} \mathbf{u}_I \tag{6.27}$$

so that the strain field $\overline{\boldsymbol{\varepsilon}}^h$ results in

$$\begin{aligned}
\overline{\boldsymbol{\varepsilon}}^h &= \mathbf{e}^h + \frac{1}{3}\theta^h \mathbf{1} && (6.28)\\
&= \overline{\nabla}^s \mathbf{u}^h && (6.29)\\
&= dev\left(\nabla^s \mathbf{u}^h\right) + \mathbf{1} \otimes \frac{1}{3}\overline{div}\left(\mathbf{u}^h\right) && (6.30)\\
&= \left(\mathbf{B}_I^{dev} \oplus \overline{\mathbf{B}}_I^{vol}\right) \mathbf{u}^h = \overline{\mathbf{B}}_I\, \mathbf{u}^h && (6.31)
\end{aligned}$$

Finally, the expression for the consistent tangent operator easily follows from (6.25*a*)

$$\begin{aligned}
D\, R^h\big|_{\Omega_e} &= \int_{\Omega_e} \left[\overline{\nabla}^s \boldsymbol{\eta}^h : \left(\frac{\partial^2 \overline{W}\left(\overline{\boldsymbol{\varepsilon}}\right)}{\partial\, \overline{\boldsymbol{\varepsilon}}\, \partial\, \overline{\boldsymbol{\varepsilon}}}\bigg|^h\right) : \overline{\nabla}^s \mathbf{u}^h\right] dV\\
&= \int_{\Omega_e} \left[\overline{\nabla}^s \boldsymbol{\eta}^h : \overline{\mathbf{C}}^h : \overline{\nabla}^s \mathbf{u}^h\right] dV\\
&= \sum_{I=1}^{N}\sum_{J=1}^{N} \boldsymbol{\eta}_I \cdot \overline{\mathbf{K}}_{IJ} \cdot \mathbf{u}_J \qquad (6.32a)
\end{aligned}$$

where

$$\overline{\mathbf{K}}_{IJ} = \int_{\Omega_e} \left[\left(\overline{\mathbf{B}}_I\right)^T : \overline{\mathbf{C}}^h : \overline{\mathbf{B}}_J\right] dV \qquad (6.33)$$

Looking at the final result it is possible to observe that the only differences between a mixed formulation and the standard one are that gradient operator $\mathbf{B}_I$ must be replaced by $\overline{\mathbf{B}}_I$ and the stress field must be computed taking into account the definition of the strain field above defined.

Example 1 *A possible application is the Q1/P0 mixed element. In this case a constant pressure field is assumed*

$$\boldsymbol{\Psi}\left(\mathbf{x}\right) = \mathbf{1} \rightarrow \mathbf{H}^e\left(\mathbf{x}\right) = Vol^e$$

so that the volumetric strain field θ^h *is given by the relation*

$$\theta^h\big|_{\Omega_e} = \frac{1}{Vol^e}\int_{\Omega_e} \overline{div}\left(\mathbf{u}^h\right)\, dV = \sum_{I=1}^{N} \overline{\mathbf{b}}_I^{vol} \mathbf{u}_I$$

where the resulting B-bar *volumetric operator is*

$$\overline{\mathbf{b}}_I^{vol} = \frac{1}{Vol^e} \int_{\Omega_e} \mathbf{b}_I^{vol} dV$$

and consequentially

$$\overline{\mathbf{B}}_I^{vol} = \frac{1}{3} \mathbf{1} \otimes \overline{\mathbf{b}}_I^{vol}$$
$$\mathbf{B}_I^{dev} = \mathbf{B}_I \ominus \mathbf{B}_I^{vol}$$
$$\overline{\mathbf{B}}_I = \overline{\mathbf{B}}_I^{vol} \oplus \mathbf{B}_I^{dev}$$

Finally the pressure field p^h *is given by*

$$\begin{aligned} p^h|_{\Omega_e} &= \frac{1}{Vol^e} \int_{\Omega_e} \frac{1}{3} tr\left(\overline{\boldsymbol{\sigma}}^h\right) dV \\ &= \frac{1}{Vol^e} \int_{\Omega_e} k\theta^h \, dV \\ &= k\, \theta^h|_{\Omega_e} \end{aligned}$$

6.3 Integration Rules

In the context of the finite element method it is possible to say that the Gauss integration rule is the most popular numerical integration technique [Bathe-81], [Hughes-87] and [Zienkiewicz-91]. For this reason most of the numerical integrals that appear in the formulation of the coupled problem presented can be solved using the Gauss integration rule. However in the solidification processes, two are the situation in which this procedure could fail:

- in case of very high temperature gradient, typically at the beginning of the cooling process at the contact interface between the part and the mould;
- when the movement of phase change front is to slow to be captured by the sample points selected for the Gauss integration rule.

In the following the strategies adopted in this work to solve the mentioned problems are introduced.

6.3.1 Integration of the thermal problem

To introduce this phenomenon let us assume the following test: consider the cooling process defined by a cylindrical cast-iron specimen in a sand mould. The initial temperatures are 1000 ^oC and 20 ^oC degrees for the part and for the mould, respectively. Typical material properties have been assumed for the specified materials. The finite element mesh is composed by 30 2-node linear elements.

If a standard Gauss integration rule is used a number of oscillation can be observed in the temperature distribution along the cylinder radius: typically an overshoot or an undershoot effects could appear, see figure (6.1*a*). On the other hand, using a Lobatto close integration rule the temperature oscillations disappear and the solution is much closer to the real one: see figure (6.1*b*).

Mathematically, the difference between the use of an open or close integration rule is due to the evaluation of the matrix $\mathbf{A}$ that define the system of equation $\mathbf{A} \cdot \mathbf{x} = \mathbf{b}$ that solves the problem. It can be demonstrate ([Ciarlet & Raviart-73], [Kikuchi-77]) that if matrix $\mathbf{A}$ is of *non-negative type* then the solution of the transient problem does not present any oscillation. Matrix $\mathbf{A}_{N,N} = [a_{ik}]$ is of non-negative type if the following conditions hold:

$$\begin{aligned} &\sum_{k=1}^{N} a_{ik} \geq 0 \qquad \forall i = 1, ..., N \\ &a_{ik} \leq 0 \quad \text{if} \quad i \neq k \end{aligned} \tag{6.34}$$

It is possible to show that for a 2-node linear element the elemental mass matrix M^e that contribute to form the assembled system matrix $\mathbf{A}$ assumes the forms:

1. $M^e_{open} = \dfrac{h^e}{6} \begin{bmatrix} 2 & 1 \\ 1 & 2 \end{bmatrix}$ in case of an open (Gauss) integration rule or

2. $M^e_{close} = \dfrac{h^e}{2} \begin{bmatrix} 1 & 0 \\ 0 & 1 \end{bmatrix}$ in case of an close (Lobatto) integration rule,

where h^e is the element length. Therefore, only the close rule forms a non-negative type matrix that avoids the oscillation in the final solution. The result can be easily extended to a $2D$ or $3D$ finite element mesh. Figure (6.1) clearly shows the advantages of the close integration rule compared with the open rule.

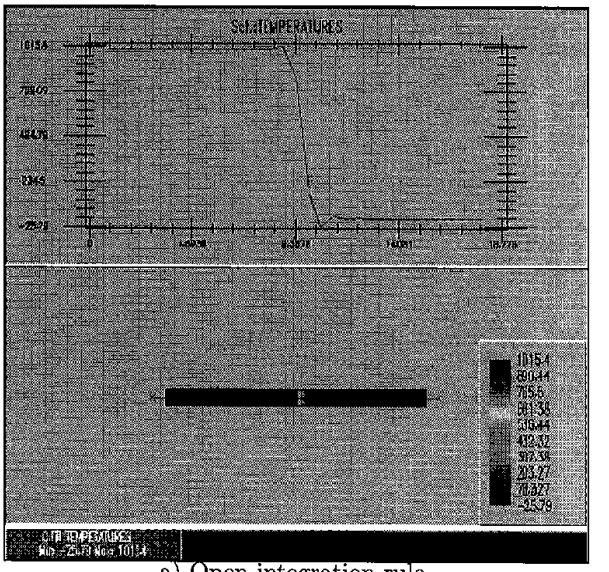

a) Open integration rule

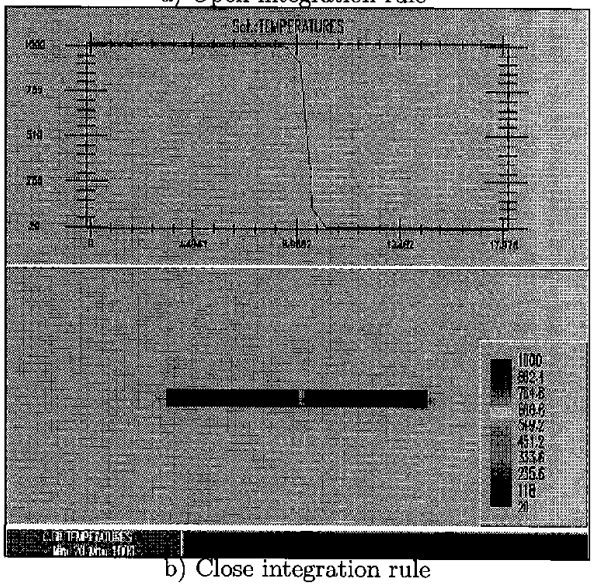

b) Close integration rule

Figure 6.1: Cooling of an indefinite cylinder. (a) Open integration rule (b) Close integration rule.

Remark 8 *A possible alternative to the close rule is the use of a* lumped mass matrix *to force the conditions of non-negative type matrix.*

6.3.2 Phase change integration

Another possible situation in which the standard Gauss integration rule can fail results in the integration of the phase change contribution. In fact, this contribution presents a discontinuity, situated along the phase change front, due to the proper definition of the latent heat function. This problem becomes much more complicate to be solved if an isothermal phase change is assumed. In the literature it is possible to find different procedures and element technologies to deal with this kind problems (see: [Crivelli & Idelsohn-86], [Steven-82] and [Storti *et al. 87*]).

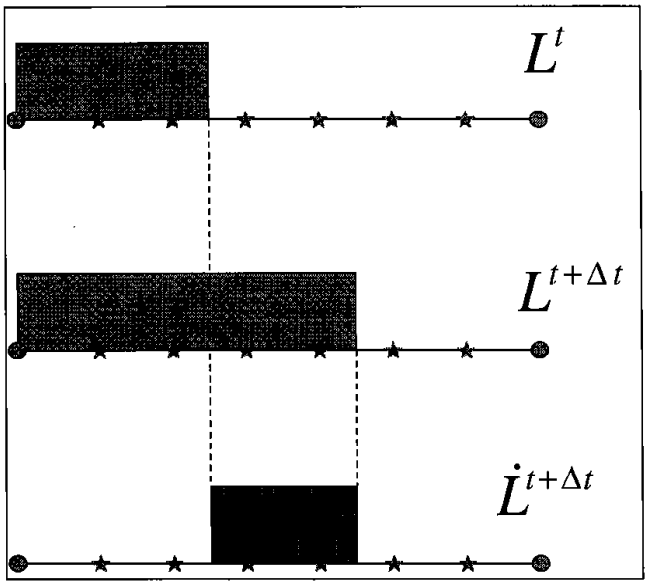

Figure 6.2: Space integration of the latent heat function.

Keeping in mind the final goal of this work that is the numerical simulation of industrial processes, it can be observed that typically the liquid and

the solid temperatures are not so close. Hence the phase change process for an industrial casting material is generally not isothermal so that the transition is slower that is easier to be integrated. For this reason in this work a standard open/close integration rule is adopted: the only peculiarity consists in the number of sample points assumed. Figure (6.2) clearly shows the advantages of this choice to capture the position of the phase change front.

Chapter 7

Numerical Simulations

The formulation presented in the previous chapters is illustrated here in a number of representative numerical simulations. The goal is to demonstrate the unconditionally stability and good accuracy properties of the proposed staggered algorithms in the framework of infinitesimal strain thermoplasticity. First a numerical assessment of accuracy and stability behavior of both the isothermal and the isentropic operator splits is presented in the context of quasi-static and fully dynamic cooling analysis of a thermo-elastic and thermo-plastic pressurized thick-walled cylinder. Next, an interesting test to show the evolution of the frictional coefficient is presented. Finally, the goals are either to provide a practical accuracy assessment of the thermomechanical model or to demonstrate the robustness of the overall coupled formulation in a number of solidification examples, including industrial processes.

The computations are performed with the finite element code COMET developed by the author together with Prof. Carlos Agelet de Saracibar and Prof. Miguel Cervera, project supported by the International Center for Numerical Method in Engineering (C.I.M.N.E.). Newton-Raphson method, combined with a line-search optimization procedure, is used to solve the nonlinear system of equations arising from the spatial and temporal discretization of the weak form of the governing equations. Convergence of the incremental iterative solution procedure was monitored by requiring a tolerance of 0.1% in the residual based error norm.

7.1 Cooling of a Pressurized Thick-walled Cylinder

This problem corresponds to the cooling of a pressurized thick-walled cylinder. This example has been used by several authors as a test to compare the performance of different time-stepping algorithms [Argyris & Doltsinis-81], [Simo & Miehe-92]. The goals are to provide a numerical assessment of accuracy and stability behavior showed by the isothermal and the isentropic operator splits. Different analyses have been carried out using either a thermoelastic or a thermoplastic constitutive model in the context of quasi-static and fully dynamic analysis. It has also been considered the case of strongly coupled problem multiplying the thermal expansion coefficient α by a factor of 6 in the quasi-static cases and by a factor of 3 in the fully dynamic cases. Plane strain conditions are assumed in the axial direction, so that a unit band of standard bi-linear isoparametric axisymmetric finite elements has been considered.

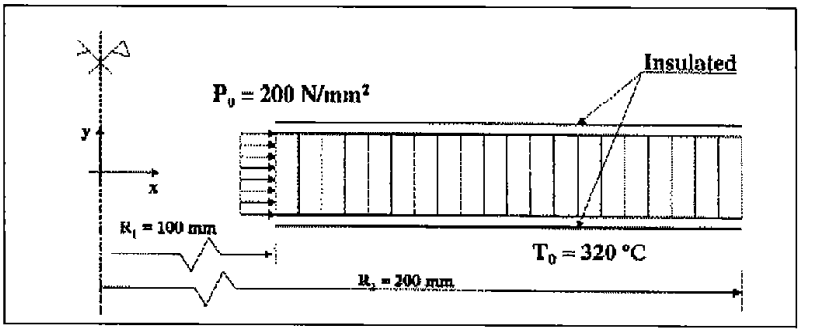

Figure 7.1: Cooling of a pressurized thick-walled cylinder. Initial geometry and boundary conditios.

Figure (7.1) depicts the initial geometry, as well as the prescribed boundary conditions. The inner and outer radii are $R_1 = 100$ $[mm]$ and $R_2 = 200$ $[mm]$, respectively. The initial temperature of the cylinder is 593 $[K]$, while the environment temperature is 293 $[K]$. The values of the material properties used in the numerical simulations are summarized in tables [7.1] and [7.2].

Density	DENSI
7.8E-9	$N\ s^2/mm^4$
Poisson ratio	POISS
0.3	–
Flow stress	YEINI
320.0	N/mm^2

Table 7.1: Cooling of a pressurized thick-walled cylinder: constant material properties

	Young modulus	YOUNG
273 K	221.9E+3	N/mm^2
673 K	183.9E+3	N/mm^2
	Thermal expansion coeff.	ALPHA
273 K	1.19E-5	K^{-1}
673 K	1.39E-5	K^{-1}
	Specific capacity	SHEAT
273 K	0.34E+9	mm^2/s^2K
673 K	0.39E+9	mm^2/s^2K
	Conductivity	CONDU
273 K	45.29	N/sK
673 K	39.42	N/sK

Table 7.2: Cooling of a pressurized thick-walled cylinder: temperature dependent material properties

Different (constant) convection coefficients are considered for the inner and outer surfaces, respectively given by $h_1 = 1.16\ [N/mm\ s\ K]$ and $h_2 = 0.01\ [N/mm\ s\ K]$. The simulations are performed applying a pressure $P_o = 200\ [Pa]$ at the inner surface of the cylinder.

The results obtained in case of quasi-static analyses are collected in figures $(7.2 - 7.3)$ and $(7.4 - 7.5)$ for the thermo-elastic and thermo-plastic constitutive response, respectively. Figures $(7.6 - 7.7)$ and $(7.8 - 7.9)$ show the results for the fully dynamic case assuming both the thermo-elastic and the thermo-plastic constitutive behavior. In each of these figures, it is presented the radial displacement and temperature evolution at the inner and outer surfaces obtained using the isothermal and the isentropic operator split for both the weakly and strongly coupled cases.

As expected, the results show that for strongly coupled problems the isothermal split leads to a completely unstable behavior ending with a blow-up of the solution, while the isentropic split provides always the right solution. Despite this fact, for weakly coupled problems the two splits provide practically the same solution. This behavior has been shown for both quasi-static and dynamic analyses, as well as for both thermo-elastic and thermo-plastic responses.

These results demonstrate the limitations of the isothermal split in the analysis of strongly coupled problems. The isentropic split, on the other hand, circumvents entirely this limitation while retaining good accuracy and leads to an efficient implementation, improving considerably over the cost of the monolithic scheme.

7.2 Flat Sheet Sliding Test

This example is taken from [De Souza Neto *et al. 95*] and is concerned with the numerical simulation of flat sheet sliding tests. The experimental tests are as follows. A steel flat sheet is clamped to the sliding table. A prescribed normal force is then applied to the tip of the tool material (SKD-11). The tip is kept fixed during the experiment to avoid rotation and ensure high precision in the measurement of the friction coefficient. Once the normal force has been applied, the table slides 300 mm driven by a hydraulic cylinder. After sliding, the normal force is released and the table returns to its initial position. The normal force is then reapplied and the cycle is repeated a number of times.

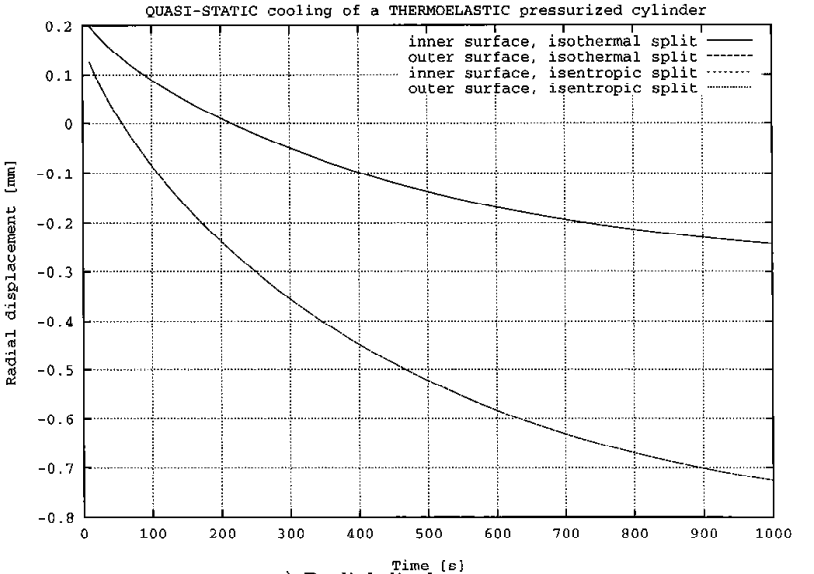

a) Radial displacement

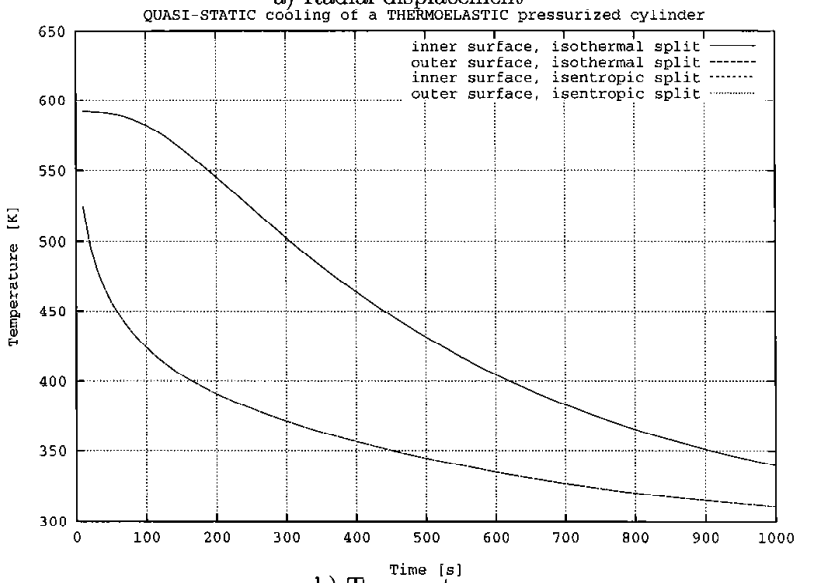

b) Temperature

Figure 7.2: Quasi-static cooling of a thermo-elastic pressurized cylinder. Radial displacement (a) and temperature evolution (b) at the inner and outer surfaces, using both the isothermal and the isentropic operator splits, for the weakly coupled case.

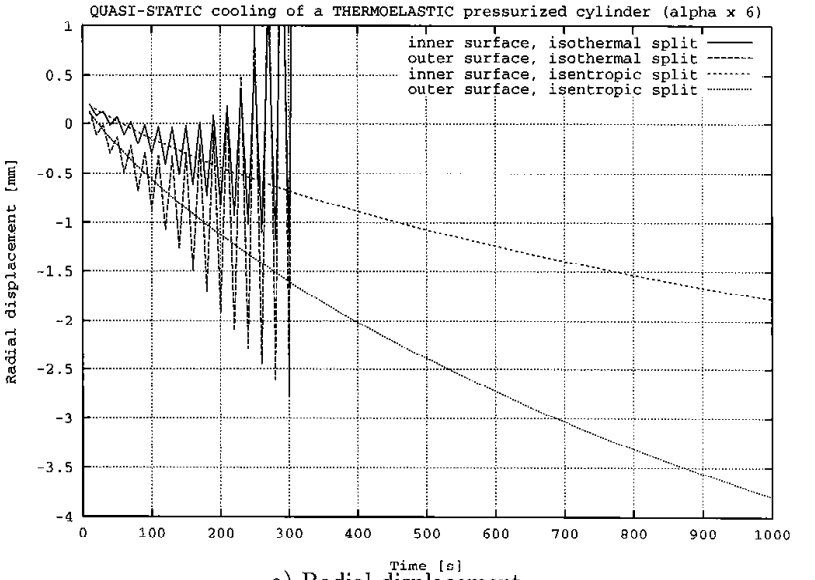

a) Radial displacement

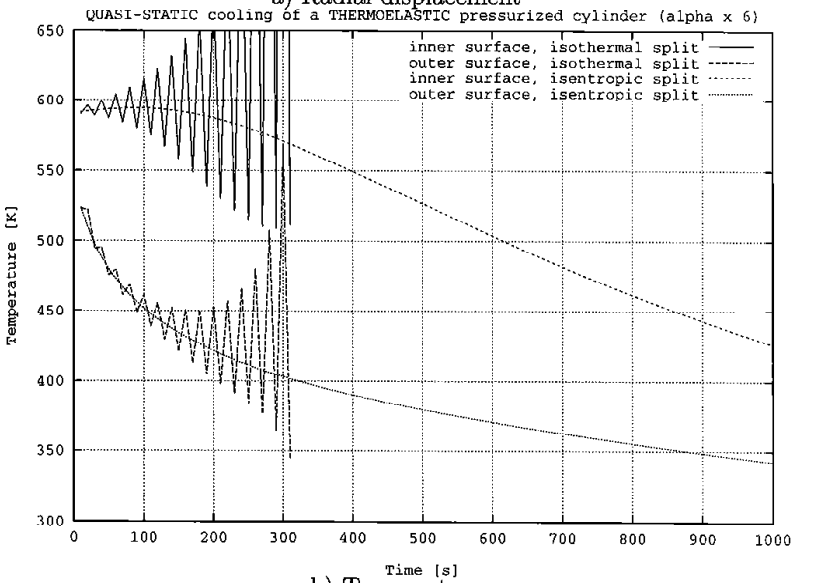

b) Temperature

Figure 7.3: Quasi-static cooling of a thermo-elastic pressurized cylinder. Radial displacement (a) and temperature evolution (b) at the inner and outer surfaces, using both the isothermal and the isentropic operator splits, for the strongly coupled case.

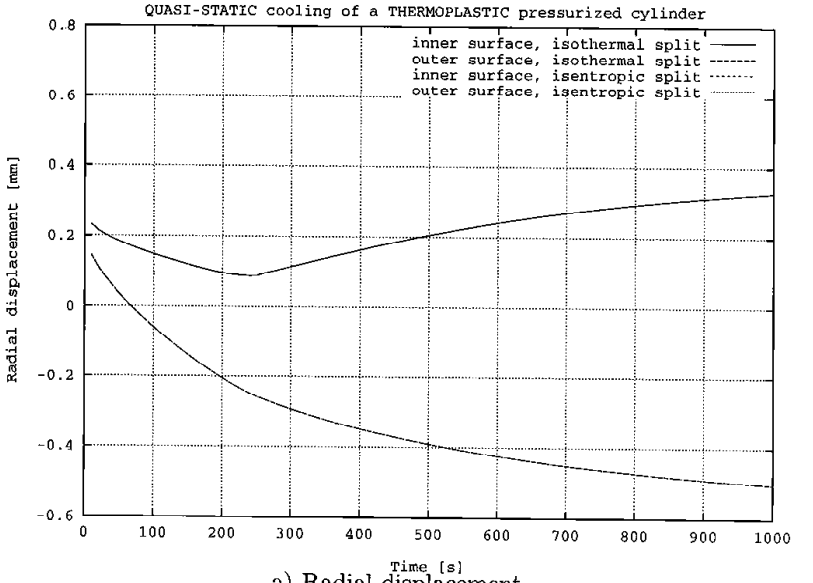

a) Radial displacement

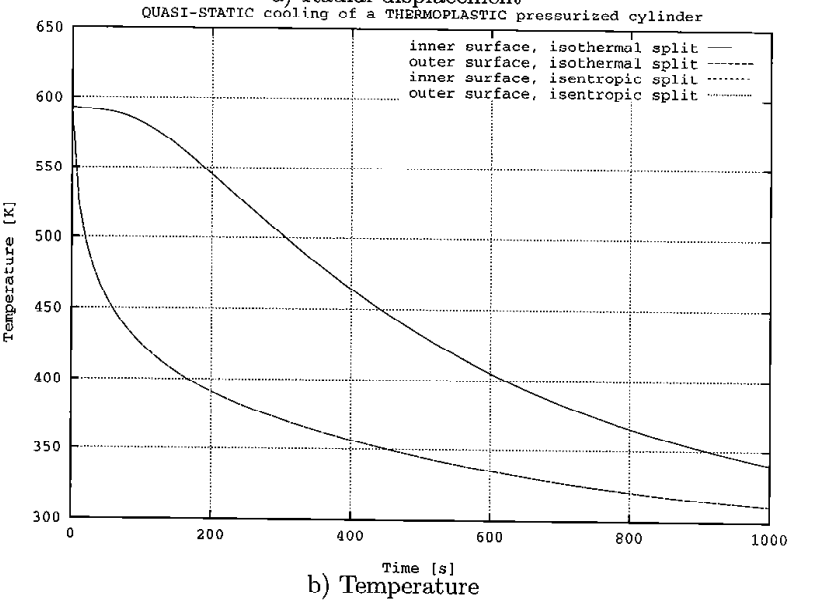

b) Temperature

Figure 7.4: Quasi-static cooling of a thermo-plastic pressurized cylinder. Radial displacement (a) and temperature evolution (b) at the inner and outer surfaces, using both the isothermal and the isentropic operator splits, for the weakly coupled case.

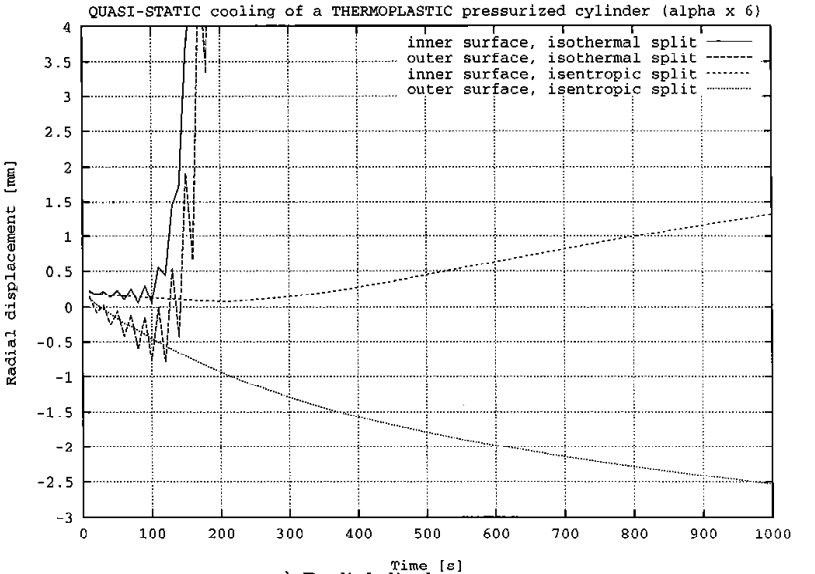

a) Radial displacement

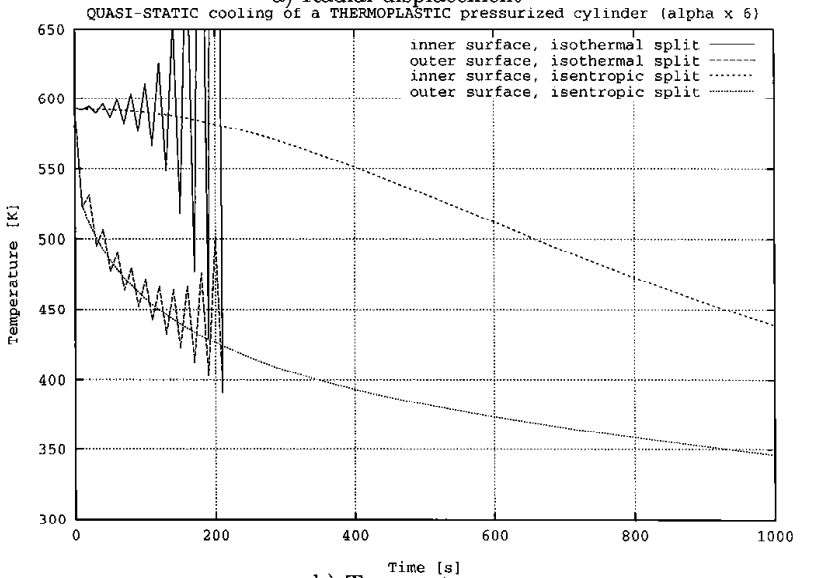

b) Temperature

Figure 7.5: Quasi-static cooling of a thermo-plastic pressurized cylinder. Radial displacement (a) and temperature evolution (b) at the inner and outer surfaces, using both the isothermal and the isentropic operator splits, for the strongly coupled case.

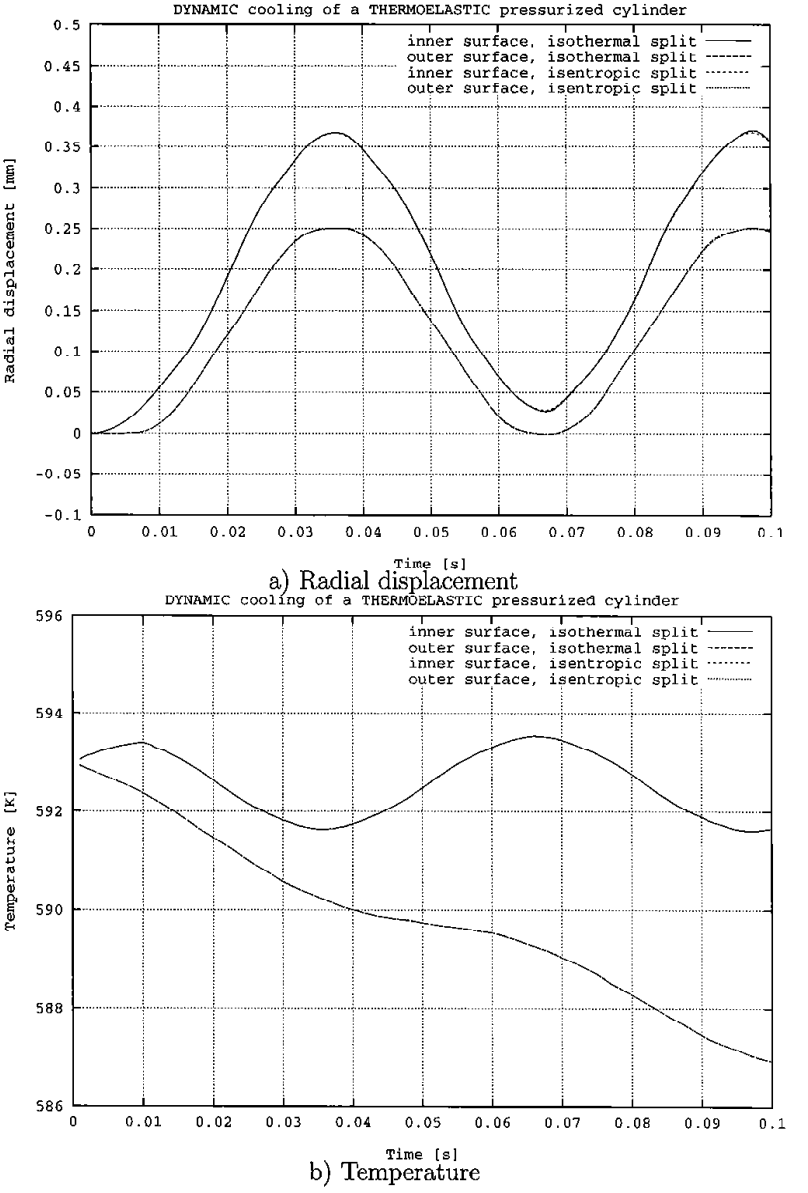

Figure 7.6: Dynamicic cooling of a thermo-elastic pressurized cylinder. Radial displacement (a) and temperature evolution (b) at the inner and outer surfaces, using both the isothermal and the isentropic operator splits, for the weakly coupled case.

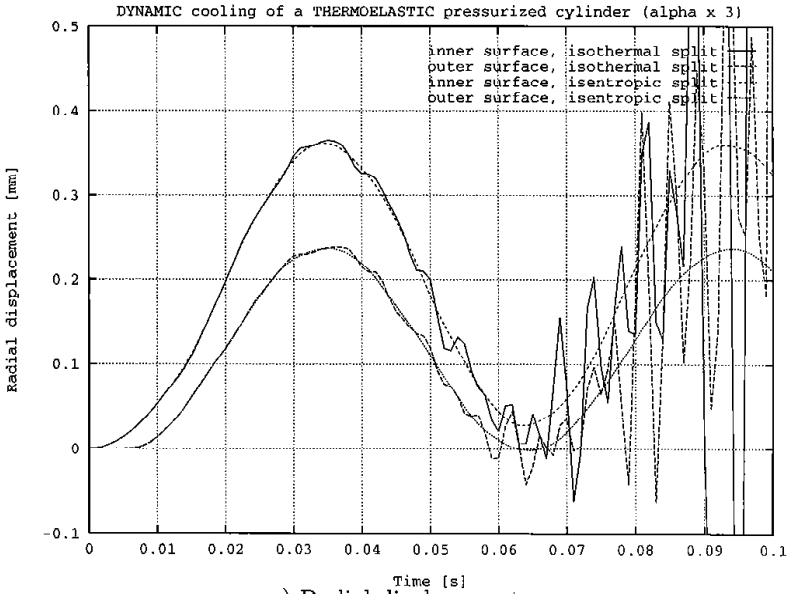

a) Radial displacement

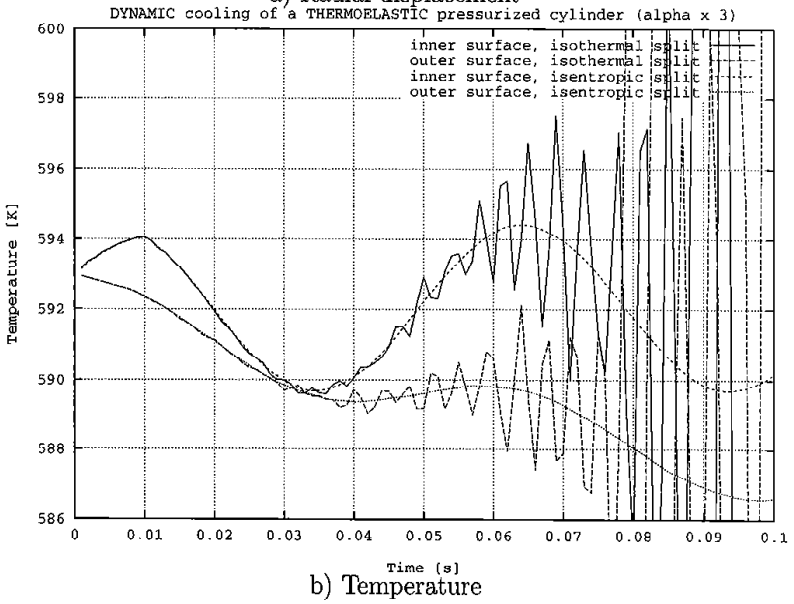

b) Temperature

Figure 7.7: Dynamic cooling of a thermo-elastic pressurized cylinder. Radial displacement (a) and temperature evolution (b) at the inner and outer surfaces, using both the isothermal and the isentropic operator splits, for the strongly coupled case.

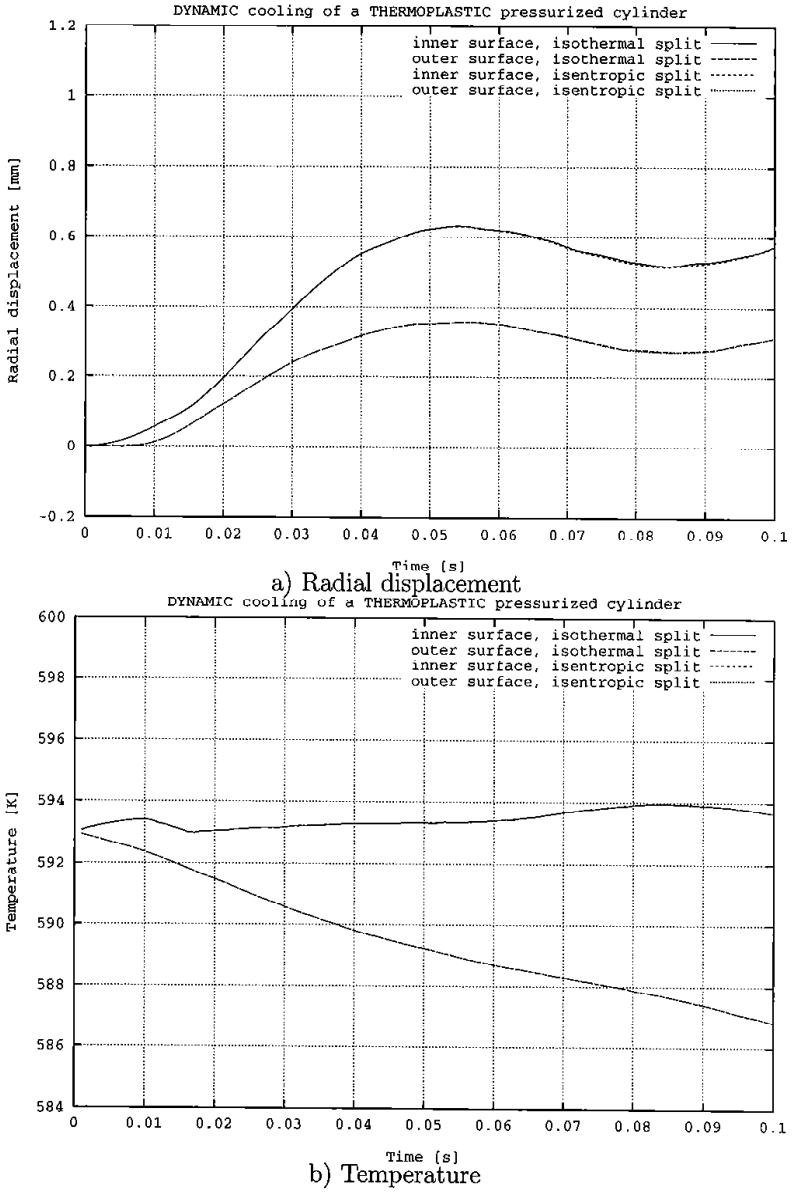

Figure 7.8: Dynamic cooling of a thermo-plastic pressurized cylinder. Radial displacement (a) and temperature evolution (b) at the inner and outer surfaces, using both the isothermal and the isentropic operator splits, for the weakly coupled case.

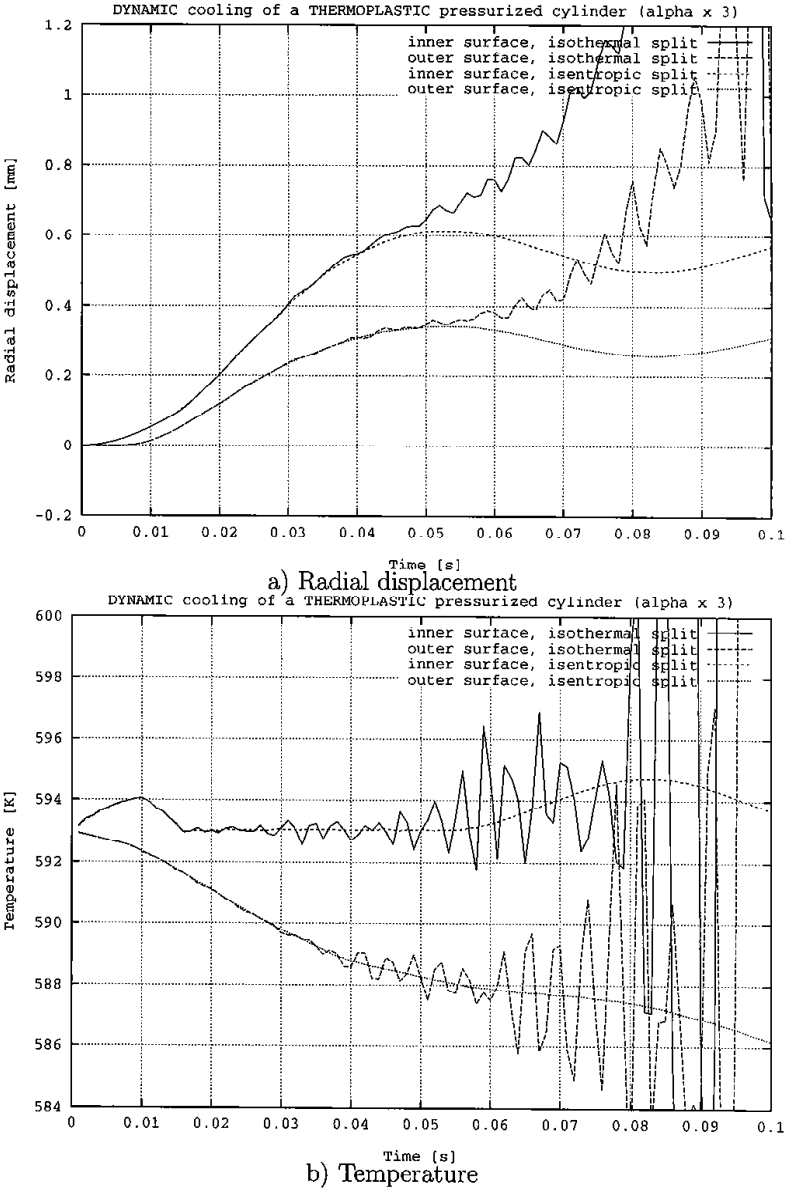

Figure 7.9: Dynamic cooling of a thermo-plastic pressurized cylinder. Radial displacement (a) and temperature evolution (b) at the inner and outer surfaces, using both the isothermal and the isentropic operator splits, for the strongly coupled case.

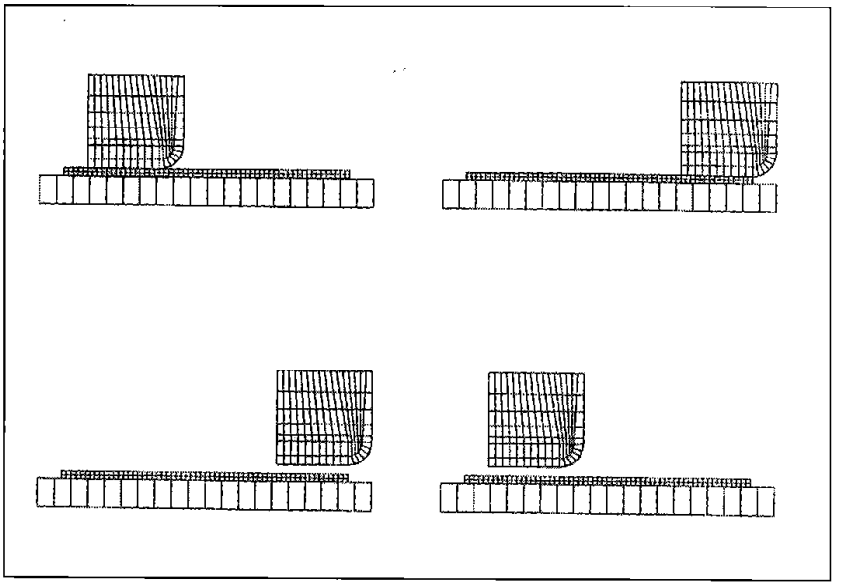

Figure 7.10: Flat sheet sliding test. Finite element mesh and sliding cycle. (a) Initial configuration and application of the normal force; (b) Sliding process; (c) Release of the normal force and (d) return to the initial position.

Young modulus	YOUNG
158.40E+3	N/mm^2
Poisson ratio	POISS
0.3	–
Initial yield stress	YEINI
199.1E+3	N/mm^2
MAximum tensile strength	YEFIN
319.3E+3	N/mm^2

Table 7.3: Material properties assumed for the GA steel

Young modulus	YOUNG
158.40E+3	N/mm^2
Poisson ratio	POISS
0.3	–
Initial yield stress	YEINI
169.2E+3	N/mm^2
MAximum tensile strength	YEFIN
310.0E+3	N/mm^2

Table 7.4: Material properties assumed for the EG steel

Two zinc coated sheet metals, typically employed in the manufacture of automotive body shells, have been considered: Galvannealed (GA) and Electrogalvanised (EG) steel sheets. The mechanical properties for the GA and EG steel sheets are shown in tables [7.3] and [7.4]. Figure (7.11a) shows the hardening plasticity law of the GA and EG steel materials.

Frictional behavior was modeled as a polynomial function of the frictional hardening ζ_c

$$\mu\left(\zeta_c\right) = \mu_o + \sum_{p=1}^{m} \mu_p \, \zeta_c^p \tag{7.1}$$

The presence of a hard surface coating, difficult to remove, in the GA steel sheet leads to a progressive softening of the frictional behavior. In contrast with this behavior, the EG steel sheet experiences an initial softening, due to flattening of microasperities, followed by a substantial increase of the friction coefficient, due to the removal of its relatively soft zinc coat. The coefficients of the frictional hardening law, for a frictional dissipation ζ_c mea-

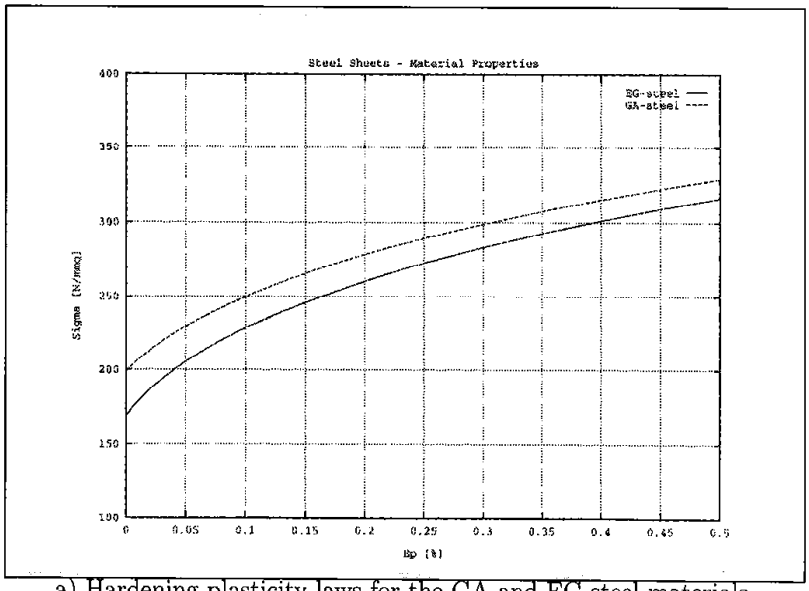

a) Hardening plasticity laws for the GA and EG steel materials.

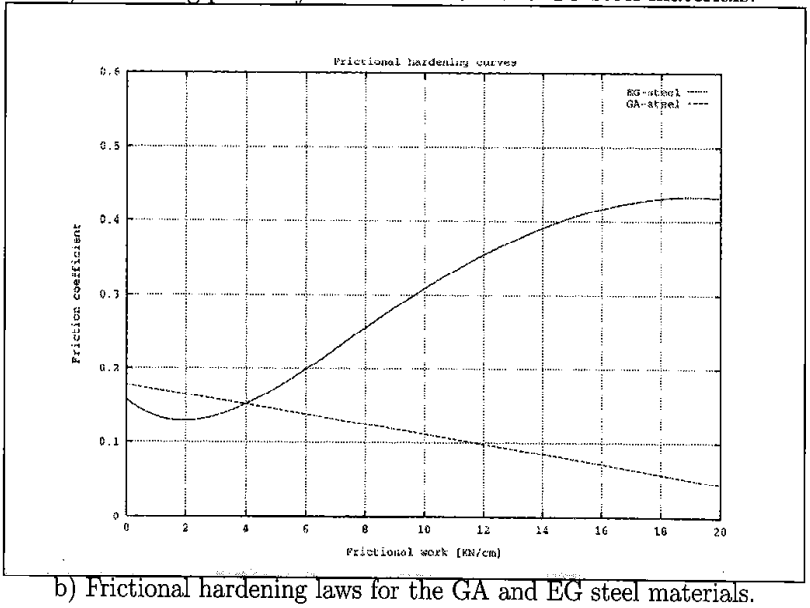

b) Frictional hardening laws for the GA and EG steel materials.

Figure 7.11: Flat sheet sliding test. (a) Hardening plasticity and (b) frictional hardening laws for the GA and EG steel materials.

	μ_o	μ_1	μ_2	μ_3	μ_4	μ_5
GA	0.178	-0.666E-2	-	-	-	-
EG	0.157	-0.315E-1	0.104E-1	-0.821E-3	0.289E-4	-0.410E-6

Table 7.5: Frictional hardening law for GA and EG steel sheets. Coefficients of the polynomial function for frictional dissipation measured in KN/cm

sured in $[KN/mm]$, for the GA and EG steel sheets are shown in table [7.5]. Frictional hardening behavior for the GA and EG steel sheets is shown in figure (7.11*b*).

The sheet initially measured 400 mm long, 100 mm wide and 0.8 mm thick. The tip of the tool measured 10 mm long and 10 mm wide, with an inner radius of 2.5 mm at the bottom corner of the right edge. Then the tested surface at the experiment measured 300 mm long and 10 mm wide.

For simplicity, only 30 mm of the sheet length has been considered in the numerical simulation and a plane strain state has been assumed. The sliding cycle has been repeated 20 times for different compressive constant normal forces of 3.92, 2.94, 1.96 and 0.98 KN applied to the tip of the tool.

A mesh of 111 four noded quadrilateral elements has been used for the discretization of the tool. The sheet has been discretized by two layers of 60 continuum elements and the nodes of its left edge have been considered as constrained. A mixed Q1/P0 finite element formulation has been used. The table has been considered as rigid.

At the beginning of a sliding cycle, the tip lies at 2.5 mm from the left edge of the sheet. Starting from this initial configuration and after the normal force has been applied, a relative sliding of 20 mm between the table and the tip is incrementally imposed. This ensures an approximately 10 mm long evenly worn region on the sheet surface (between 12.5 mm and 22.5 mm from the left edge). Then the normal force is released, the tip is lifted up and returned to its initial position, thereby closing a cycle. Note that a steady state frictional force will occur when the entire surface of the tip contacts the evenly worn region of the sheet. The finite element mesh as well as the description of a sliding cycle is shown in figure (7.10).

Frictional contact constraints were regularized by means of penalty method and the normal and tangential penalty parameters were taken as $\in_N = 5.0E+11\ [N/m^3]$ and $\in_T = 1.0E+11\ [N/m^3]$, respectively. A typical loading cycle was achieved in 30 time steps: 5 steps to applied the normal force, 20

steps for sliding and 5 steps to remove the normal force.

Figures (7.12 – 7.13) and (7.14 – 7.15) show the tangential forces obtained in the numerical analysis of the sliding tests, using GA steel and EG steel sheets, respectively, at different constant normal forces. In order to compare the results obtained in this work with the (average) experimental and numerical results given by [De Souza Neto *et al. 95*], it is important to observe that one must consider only an average value within the central part of the sheet for each pass, in the evenly worn region, disregarding the values at the beginning and at the end of each pass, where the distribution of the friction coefficient is not uniform. A detail of the wear profile in the sheet is depicted in figure (7.16), for the GA steel and for a normal force of 0.98 KN. The figure clearly shows an evenly worn region in the central part of the sheet, between 12.5 and 22.5 mm from the left edge, while the wear at the edges is not uniform.

In (7.12 – 7.13) and (7.14 – 7.15), it is clearly evident the different wear evolution experimented by the GA and EG steel sheets. For the GA steel, due to the softening of the friction coefficient law, the tangential force presents a local minimum within a pass at the central part of the sheet, in the evenly worn region. In contrast, for the EG steel, particularly for high normal pressures, the tangential force at the central part of the sheet moves from a local minimum towards a local maximum within a pass, according to the frictional softening/hardening behavior. Remarkably, a significant hardening is observed for the EG steel at high normal pressures, while a slight softening appears at low normal pressures. These results clearly show that a classical frictional Coulomb law, using a constant friction coefficient, would not be able to capture this behavior, leading to useless inaccurate predictions.

The tangential forces predicted by the numerical analyses, for both GA and EG steel sheets and for all levels of constant normal force, agree well with the experimental and numerical (average) results given by [De Souza Neto *et al. 95*].

7.3 Cylindrical Aluminium Solidification Test

This example, taken from [Celentano-94], is concerned with the solidification process of a cylindrical aluminium specimen in a steel mould. In this case, the main goal is to show the accuracy of the full coupled model proposed in this work for a solidification analysis. In fact in this case the numerical results will be compared with the experimental values obtained by [Nishida-86].

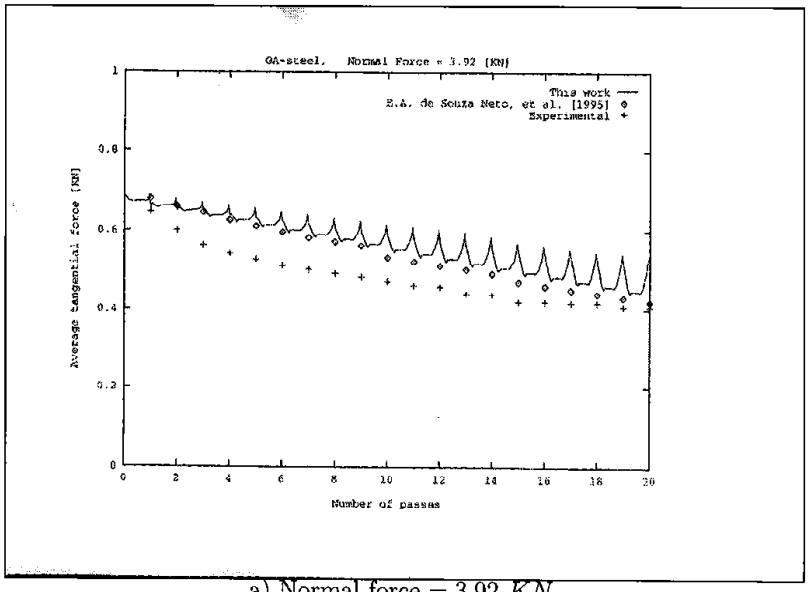

a) Normal force = 3.92 KN.

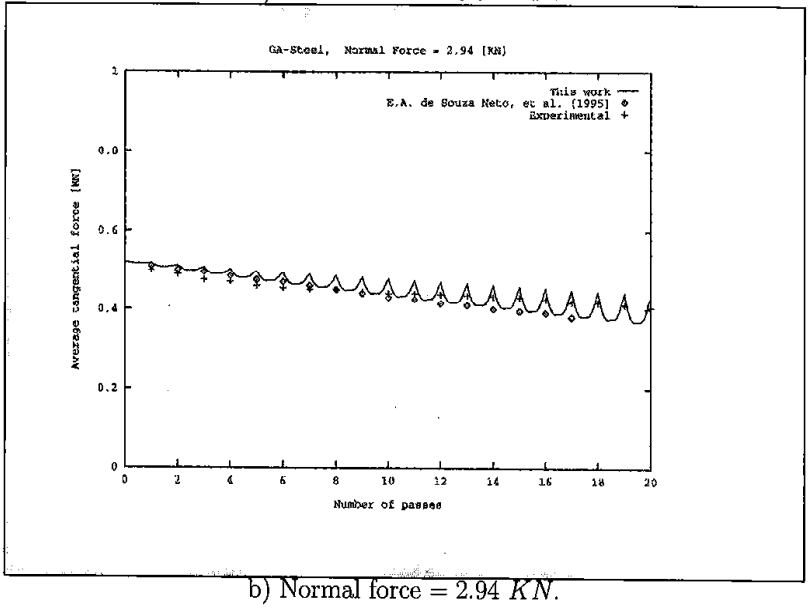

b) Normal force = 2.94 KN.

Figure 7.12: Flat sheet sliding test. Tangential force versus number of passes during the sliding tests using a GA steel sheet at different constant normal forces.

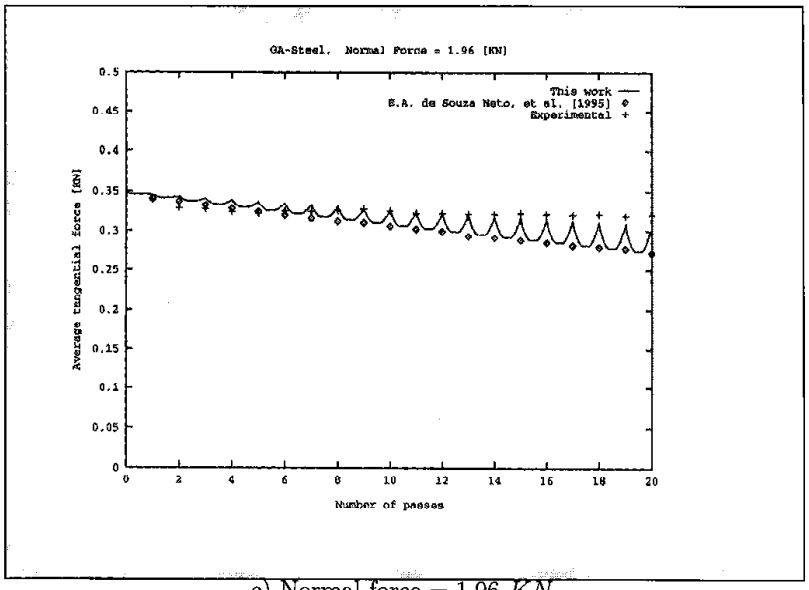

c) Normal force = 1.96 KN.

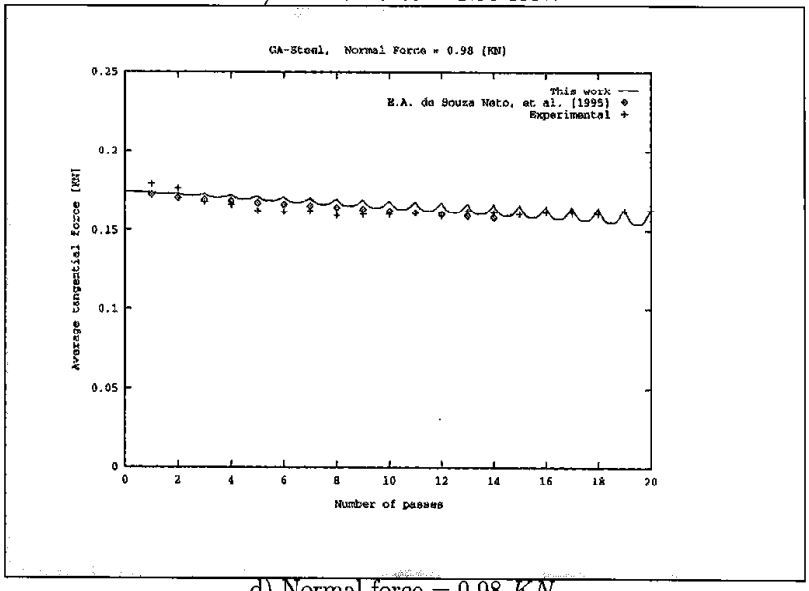

d) Normal force = 0.98 KN.

Figure 7.13: Flat sheet sliding test. Tangential force versus number of passes during the sliding tests using a GA steel sheet at different constant normal forces.

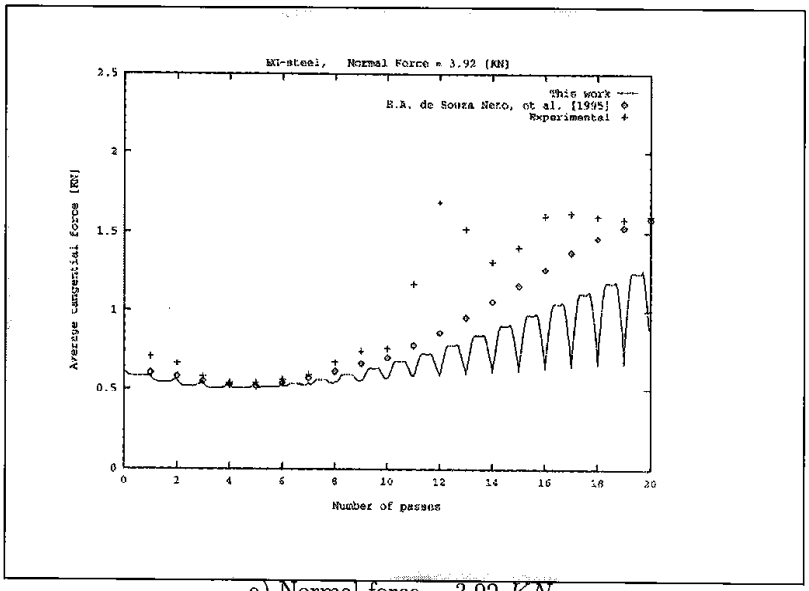

a) Normal force = 3.92 KN.

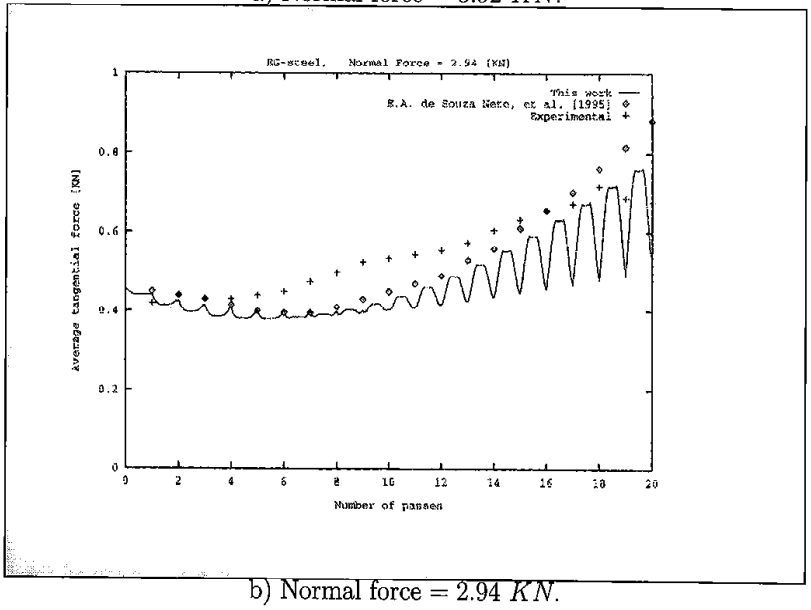

b) Normal force = 2.94 KN.

Figure 7.14: Flat sheet sliding test. Tangential force versus number of passes during the sliding tests using a GA steel sheet at different constant normal forces.

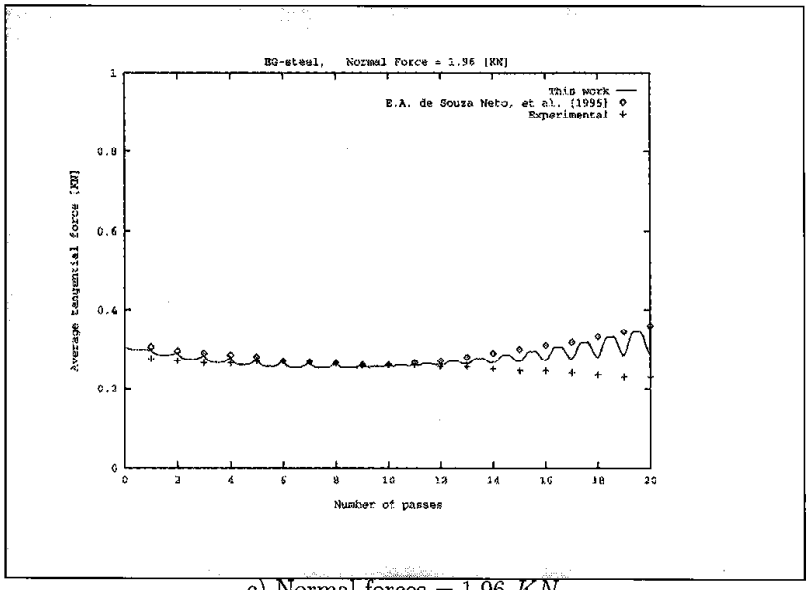

c) Normal forces = 1.96 KN.

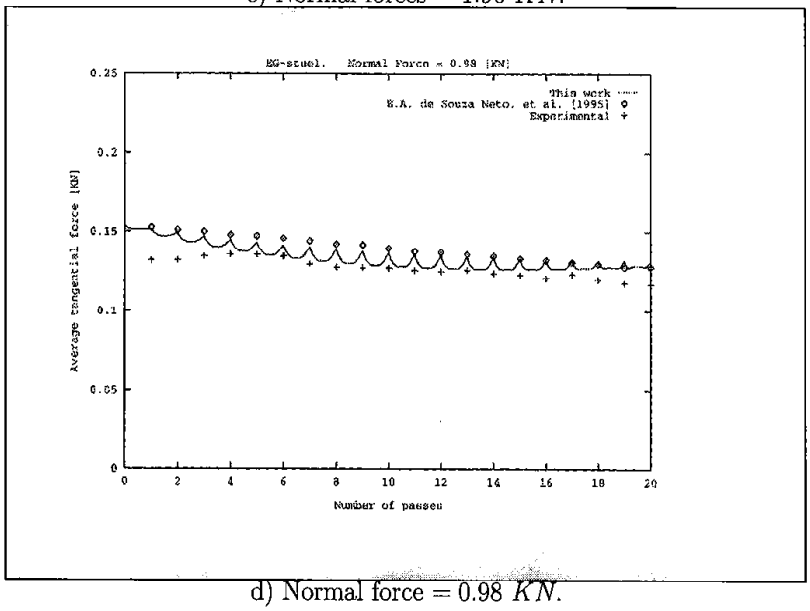

d) Normal force = 0.98 KN.

Figure 7.15: Flat sheet sliding test. Tangential force versus number of passes during the sliding tests using a GA steel sheet at different constant normal forces.

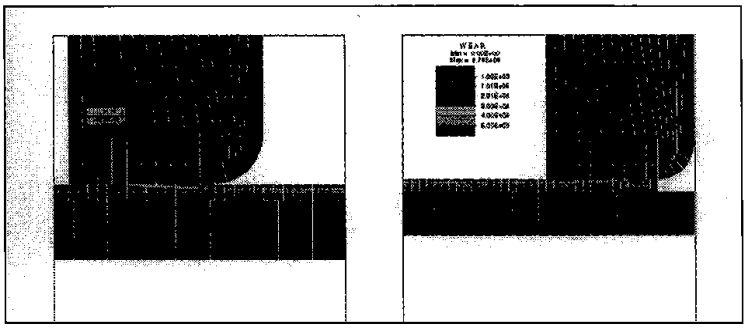

Figure 7.16: Flat sheet sliding test. Wear profile.

The experimental apparatus is shown in figure (7.17). The experiment consisted of casting commercial purity aluminium into an instrumented mould. Thermocouples were placed in the mould wall and in the mould cavity. The thermocouple locations are shown in figure (7.17). Two quarz rod were inserted into the mould to measure both the displacement of the solidifying cylinder and the mould deflection.

The geometry of the problem is shown in figure (7.18). Assumed starting conditions in the numerical simulation are given by a completely filled mould with aluminium in liquid state at uniform temperature of 670^oC. The initial temperature of the mould is 200^oC. A thermo-viscoelastic constitutive model has been used to simulate the material behavior of both the aluminium casting and the steel mould. Most of the material properties for the aluminium have been assumed to be temperature dependent, while constant material properties have been considered for the steel mould: see tables [7.6] , [7.7] and [7.8].

The external surfaces of the mould as well as the upper surface of the casting metal have been assumed perfectly insulated. A constant conduction heat transfer coefficient $h_{co} = 2.30\ N/mm\,s\ ^oC$ and a gap dependent convection-radiation coefficient between the aluminium part and the steel mould is given in table [7.9].

Only gravitational forces have been assumed. Spatial discretization of the casting cylinder and the mould has been done using a finite element mesh of axisymmetric 3-node triangles. Numerical simulation was done up to 90 secs. of the solidification test using a time increment of 1 sec. A close integration

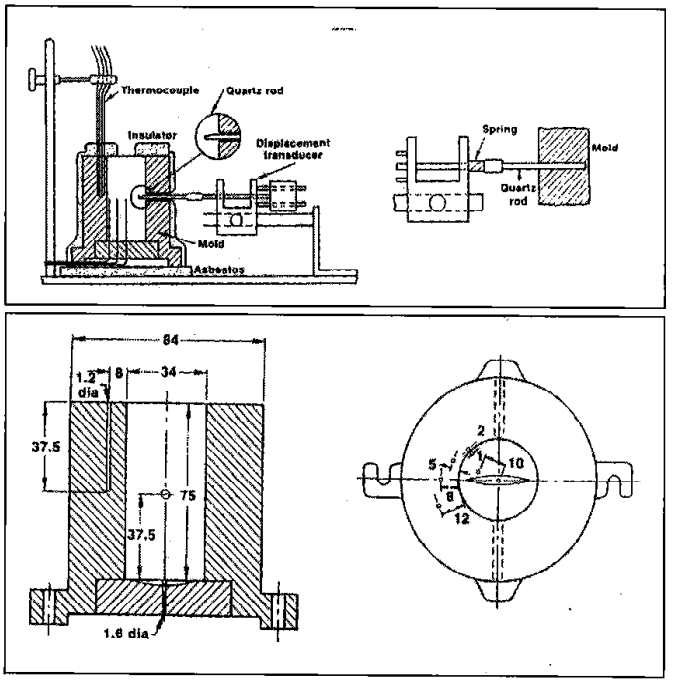

Figure 7.17: Cylindrical aluminiun solidification test. Thermocouple locations in the mould and casting.

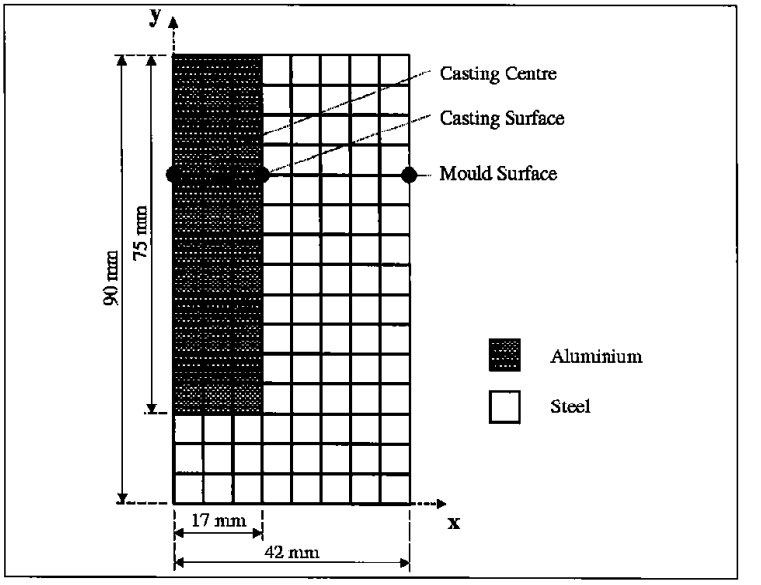

Figure 7.18: Cylindrical aluminium solidification test. Geometry.

Density	DENSI
2.65E-9	$N\ s^2/mm^4$
Poisson ratio	POISS
0.37	–
Viscosity	ELVIS
1.0E+7	$N\ s/mm^2$
Latent heat	LATEN
3.95E+11	mm^2/s^2
Liqiud temperature	TLIQU
659	^oC
Solid temperature	TSOLI
660	^oC

Table 7.6: Constant material properties assumed for the aluminium speciment

	Young modulus	YOUNG
0.0 ^oC	69.3E+3	N/mm^2
659 ^oC	25.6E+3	N/mm^2
	Thermal expansion coeff.	ALPHA
200 ^oC	1.47E-5	$^oC^{-1}$
659 ^oC	1.47E-5	$^oC^{-1}$
700 ^oC	1.38E-5	$^oC^{-1}$
	Specific capacity	SHEAT
350 ^oC	1.40E+9	$mm^2/s^2\ ^oC$
659 ^oC	1.50E+9	$mm^2/s^2\ ^oC$
	Conductivity	CONDU
100 ^oC	234.46	$N/s\ ^oC$
200 ^oC	226.08	$N/s\ ^oC$
400 ^oC	221.90	$N/s\ ^oC$
600 ^oC	217.77	$N/s\ ^oC$
659 ^oC	209.34	$N/s\ ^oC$

Table 7.7: Temperature dependent material properties assumed for the aluminium speciment

Density	DENSI
7.8E-9	$N\ s^2/mm^4$
Young modulus	YOUNG
196.0E+3	N/mm^2
Poisson ratio	POISS
0.3	–
Thermal expansion coeff.	ALPHA
1.2E-5	$^oC^{-1}$
Conductivity	CONDU
45.64	$N/s\ ^oC$
Specific capacity	SHEAT
0.5E+9	$mm^2/s^2\ ^oC$

Table 7.8: Constant material properties assumed for the steel mould

Gap $[mm]$	Convection-radiation coefficient $[N/mm\,s\,^{o}C]$
0.0	2.30
1.0E-2	2.20
2.0E-2	1.40
6.0E-2	0.35
1.0E-1	0.30

Table 7.9: Convection-radiation coefficient between the aluminium part and the steel mould

rule has been used to deal with the overshoot problems in the solution of the thermal partition.

Figure (7.20*a*) shows the temperature evolution at the casting center, casting surface and mould surface for a intermediate section. A typical temperature plateau due to the release of latent heat during solidification can be seen in the casting center point of this section up to 15 secs. approximately. Figure (7.20*b*) shows the evolution of the radial displacements at the casting and mould surfaces for the chosen section. The difference between the two curves gives the gap distance evolution. Temperature and air gap evolution predicted by the model compare very well with the experimental results. A data sensitivity analysis has shown a strong influence of the heat convection coefficient between the casting part and the mould in the temperature evolution.

Figure (7.21) compare the results obtained applying both the isothermal and the isentropic splits for the solution of the coupled problem considered. It is possible to note that the curves obtained are superposed verifying the accuracy of the isentropic solution in case of phase change phenomena.

7.4 Solidification of a RENAULT Clio Crankshaft

The goal of this analysis is the validation of a real industrial solidification problem, that is a RENAULT Clio crankshaft (see figure (7.23*a*)). In this case the analysis is concerned with the solidification process of a cast-iron specimen in a green-sand mould. Geometrical and material data, as well as experimental results, were provided by RENAULT. Figure (7.23*b*) shows a view of the finite element mesh used for the part, consisting in 13151 4-noded

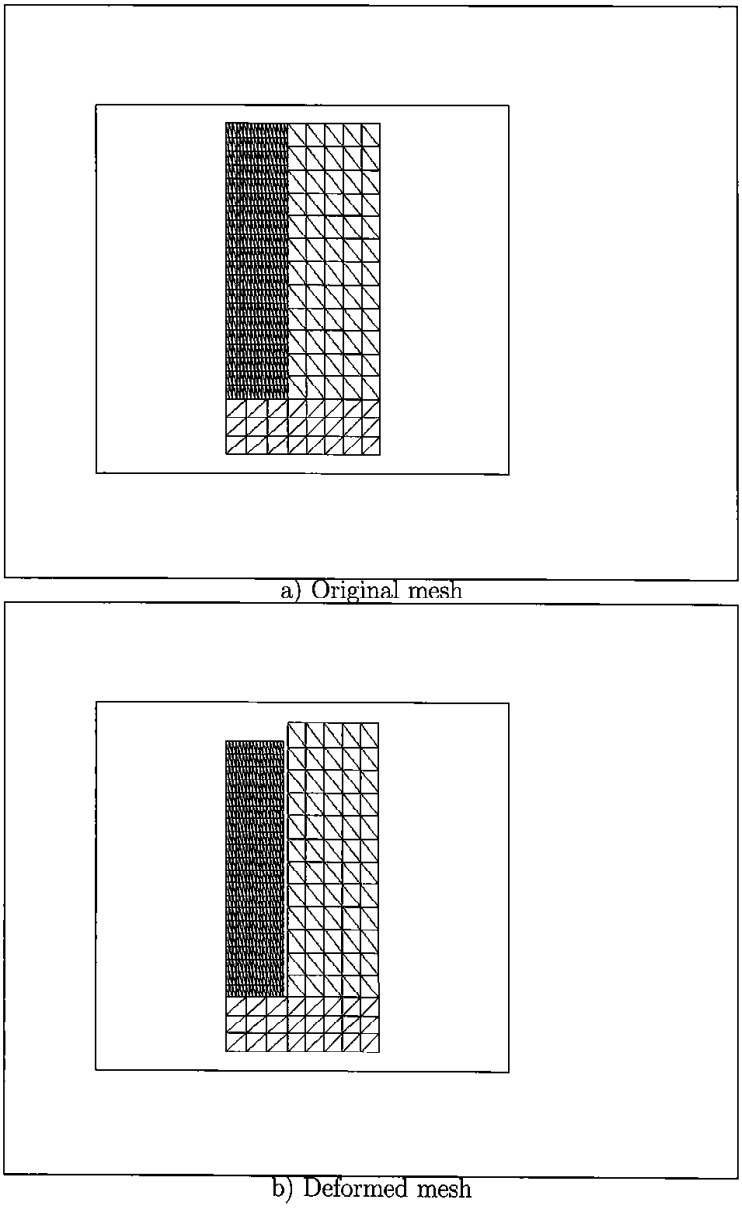

Figure 7.19: Cylindrical aluminiun solidification test. (a) Original and (b) deformed mesh.

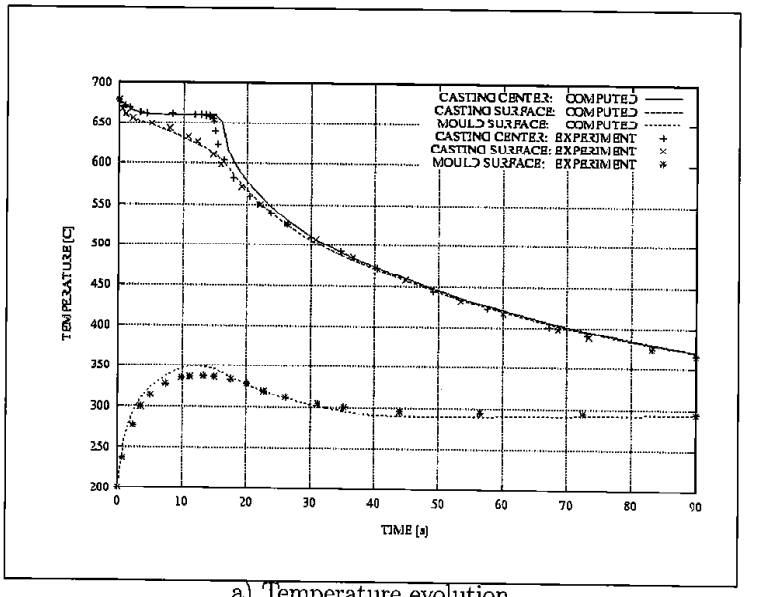

a) Temperature evolution

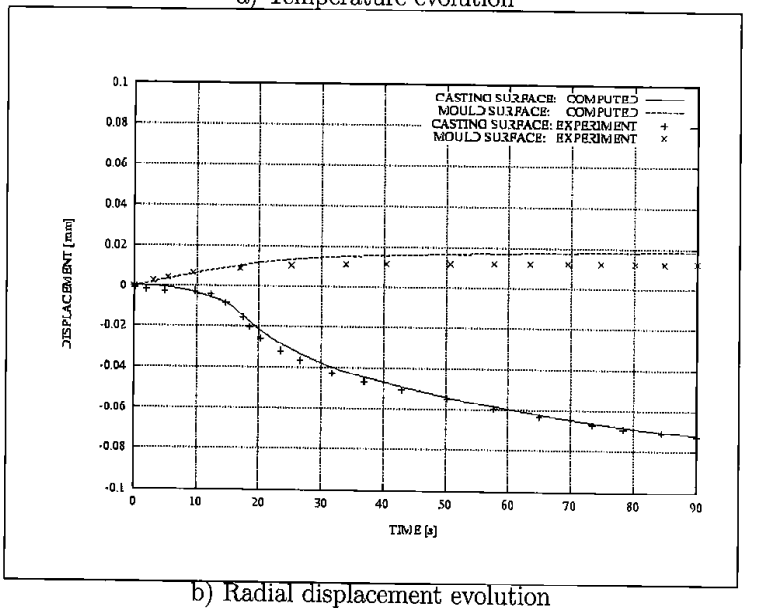

b) Radial displacement evolution

Figure 7.20: Cylindrical aluminiun solidification test. Comparison between computed and experimental results. (a) Temperature evolution at the casting center, casting surface and mould surface. (b) Radial displacement at the casting and mould surfaces.

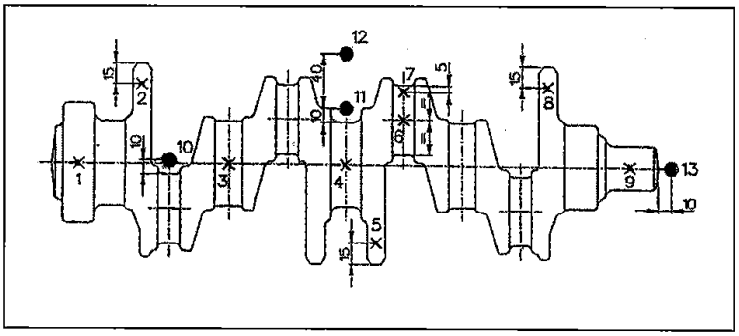

Figure 7.24: Solidification of a RENAULT Clio Crankshaft. Thermocouples positions.

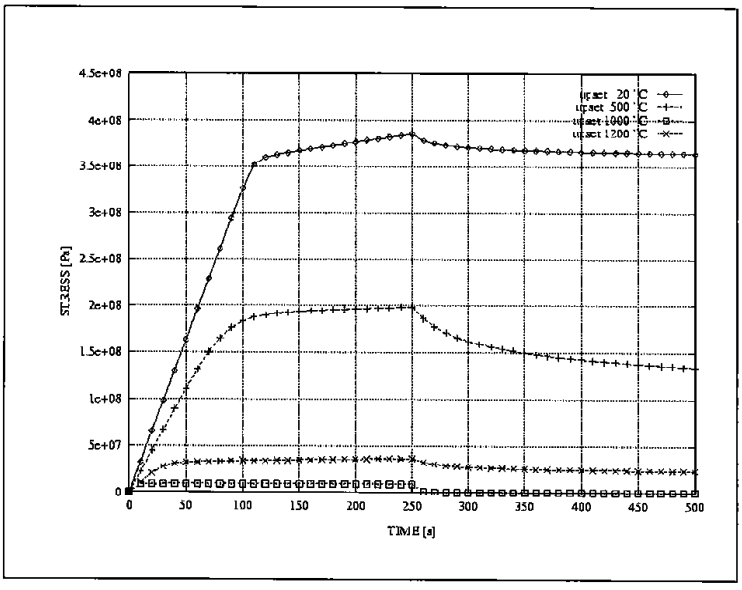

Figure 7.25: Solidification of a RENAULT Clio Crankshaft. Material upsetting.

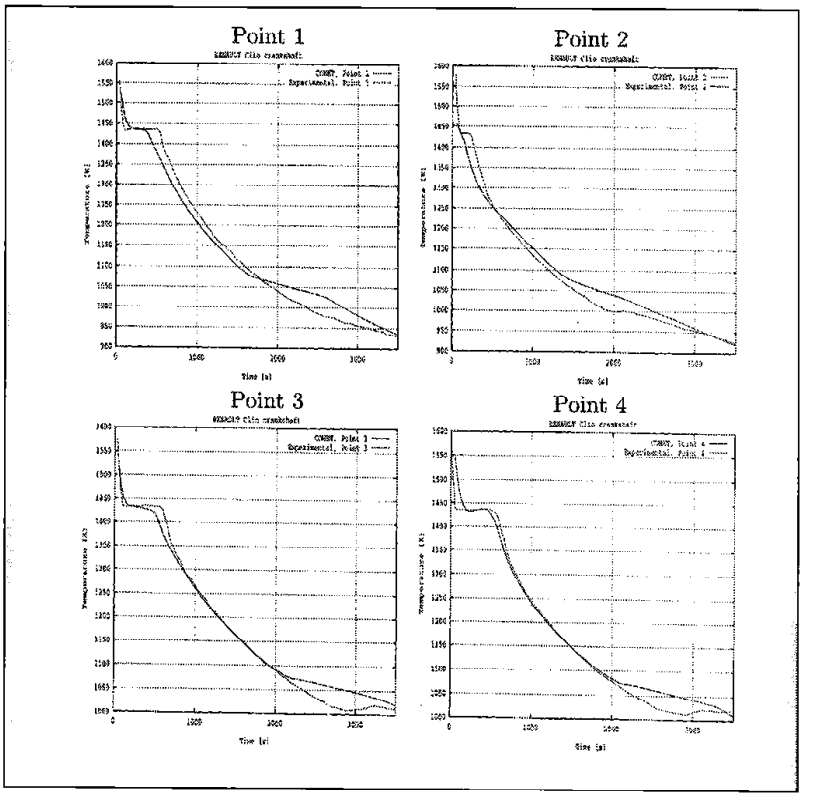

Figure 7.26: Solidification of a RENAULT Clio Crankshaft. Temperature evolution at different points.

Bibliography

[Abraham-83] Abraham, R., J.E. Marsden and T. Ratiu [1983] *Manifolds, Tensor Analysis and Applications.* Addison-Wesley, Mass.

[Complas-97] Agelet de Saracibar, C., M. Cervera and M. Chiumenti [1997] *Vulcan-2000: A Finite Element System for the Simulation of Casting Processes.* Proceedings of V International Conference on Computational Plasticity, COMPLAS-97, Barcelona, Spain, 1997.

[Costa-Rica-97] Agelet de Saracibar, C., M. Cervera and M. Chiumenti [1997] *Current Issues in the Numerical Simulation of Casting Processes.* Proceedings of International Conference on Computational Engineering Science, ICES-97, San Jose', Costa Rica, 1997.

[Agelet & Chiumenti-95] Agelet de Saracibar, C. and M. Chiumenti [1995] *Numerical Analysis of Frictional Wear Contact problems. Computational Model and Applications.* Publication CIMNE #70, September 1995.

[Agelet-97] Agelet de Saracibar, C., M. Cervera and M. Chiumenti [1997] *On the Formulation of Thermoplastic Problems with Phase-Change.* Publication C.I.M.N.E. #123, October 1997.

[Agelet-97a] Agelet de Saracibar, C. [1997] *A New Frictional Time Integration Algorithm for Multi-Body Large Slip Frictional Contact Problems.* Computer

Methods in Applied Mechanics and Engineering, Vol. 142, pp. 303-334.

[Agelet-97b] Agelet de Saracibar, C. [1997] *Numerical Analysis of Coupled Thermomechanical Problems. Computational Model and Applications.* Arch. of Comp. Meth. in Engin., to be published.

[Agelet & Chiumenti-98] Agelet de Saracibar, C. and M. Chiumenti [1998] *On the Numerical Modeling of Frictional Wear Phenomena.* Computer Methods in Applied Mechanics and Engineering, to be published.

[Alaska-97] Agelet de Saracibar, C., M. Cervera and M. Chiumenti [1997] *Current Issues in the Numerical Simulation of Casting Processes.* Proceedings of VI Symposium on plasticity and its Current Applications, Juneau, Alaska, U.S.A., 1997.

[Cancun-99] Agelet de Saracibar, C., M. Cervera and M. Chiumenti [1999] *On the Constitutive Modeling of Thermoplastic Phase-change Problems.* 7th International Symposium on Plasticity and its Current Applications, Cancun, Mexico, January 5-13, 1999.

[Archard-53] Archard, J.F. [1953] *Contact and Rubbing of Flat Surfaces.* Journal of Applied Physics, Vol. 24, pp. 981-988.

[Argyris & Doltsinis-79] Argyris, J.H. and J.St. Doltsinis [1979] *On the Large Strain Inelastic Analysis in Natural Formulation. Part I: Quasi-static Problems.* Computer Methods in Applied Mechanics and Engineering. Vol. 20, pp. 214-252.

[Argyris & Doltsinis-81] Argyris, J.H. and J.St. Doltsinis [1981] *On the Natural Formulation and Analysis of Large deformation Coupled Thermomechanical Problems.*

Computer Methods in Applied Mechanics and Engineering. Vol. 25, pp. 195-253.

[Armero & Petocz-98] Armero, F. and E. Petocz [1998] *Formulation and Analysis of Conserving Algorithms for Dynamic Contact-Impact Problems.* Computer Methods in Applied Mechanics and Engineering, in press. (1998)

[Armero & Simo- 91] Armero, F and J.C. Simo [1992] *A New Unconditionally Stable Fractional Step Method for Nonlinear Coupled Thermomechanical Problems.* Int. Journal for Num. Meth. in Engin., Vol. 35, pp. 737-766.

[Armero & Simo-92] Armero, F and J.C. Simo [1992] *Product Formula Algorithms for Nonlinear Coupled Thermoplasticity: Formulation and Nonolinear Stability Analysis.* Sudam Report #92-4, Department of Mechanical Engineering, Stanford University, Stanford, California, 1992.

[Armero & Simo-93] Armero, F and J.C. Simo [1993] *A Priori Stability Estimate and Unconditionally Stable Product Formula Algorithms for Nonlinear Coupled Thermoplasticity.* Inter. Jour. of Plasticity, Vol. 9, pp. 749-782.

[Armero-Thesis-93] Armero F. [1993] *Numerical Analysis of Dissipative Dynamical Systems in Solid and Fluid Mechanics, with Special Emphasis on Coupled Problems.* Ph.D. Thesis, Department of Mechanical Engineering, Stanford University, Stanford, California, # 94305.

[Bathe-81] Bathe, K. [1981] *Finite Element Procedures in Engineering Analysis.* Prentice Hall, 1981.

[Bellet-93] Bellet, M. et al. [1993] *Finite Element Modelling of Cooling Phase in casting Processes.* Proceedings of VI International Conference on Modelling

of Casting, Welding and Advanced Solidification processes, pp. 561-568, 1993.

[Celentano-94] Celentano, D.J. [1994] *Un Modelo Termomecanico para Problemas de Solidificacion de Metales.* Ph.D. Thesis, Universidad Politecnica de Cataluña U.P.C., Barcelona, Spain, May 14, 1994.

[SanDiego-98] Cervera, M., C. Agelet de Saracibar and M. Chiumenti [1998] *Coupled Thermo-mechanical Simulation of Industrial processes.* Proceedings of VIII International Conference on Modelling of Casting, Welding and Advanced Solidification processes, San Diego, California, U.S.A., 1998.

[Buenos-Aires-98] Cervera, M., C. Agelet de Saracibar and M. Chiumenti [1998] *Thermo-mechanical Analysis of Industrial processes.* Proceedings of IV World Congress on Computational Mechanics, WCCM IV, Buenos Aires, Argentina, 1998.

[Cervera & Codina-96] Cervera, M., R. Codina and M. Galindo [1996] *On the Computational Efficiency and Implementation of Block-iterative Algorithms for Nonlinear Coupled Problems.* Inter. Jour. for Computer-Aided Engin. and Soft., Vol. 13, pp. 4-30.

[Carey & Oden-83] Carey, J. and J.T. Oden [1983] *Finite Element, Vol. II.* Texas Series in Computational Mechanics, Prentice-Hall, Englewood Cliff, New Jersey.

[Cheng & Kikuchi-85] Cheng, J.-H. and N. Kikuchi [1985] *An Analysis of Metal Forming Processes Using Large Deformation Elastic-Plastic Formulations.* Computer Methods in Applied Mechanics and Engineering, Vol. 49, pp. 71-108.

[Chiumenti & Agelet-95] Chiumenti, M. and C. Agelet de Saracibar [1995] *Numerical Simulation of Wear Phenomena.* Publication CIMNE #68, July 1995.

[Chorin-78] Chorin, A., T.J.R. Hughes, M.F. McCracken and J.E. Marsden [1978] *Product Formulas and Numerical Algorithms.* Communications in Pure Applied Mathematics. Vol. 31, pp. 205-256.

[Ciarlet & Raviart-73] Ciarlet, P.G. and P.A. Raviart [1973] *Maximum Principle and Uniform Convergence for the Finite Element Method.* Computer Methods in Applied Mechanics and Engineering, Vol. 2, pp. 17-31.

[Coleman-64] Coleman, B.D. [1964] *Thermodynamics of Material with Memory.* Arch. Rat. Mech. Anal., Vol. 17 p. 1.

[Coleman-67] Coleman, B.D. and M. Gurtin [1967] *Thermodynamics with Internal Variables.* Journ. of Chemistry and Physics, Vol. 47, pp. 597-613

[Coleman & Dill-73] Coleman, B.D. and E.H. Dill [1973] *On Thermodynamics and Stability of Motions of Materials with Memory.* Archives for Rational Mechanics, Vol. 17, pp. 1-46.

[Comini-74] Comini, G., S. Del Giudice, R. Lewis and O. Zienkiewicz [1974] *Finite Element Solution of Non-linear Heat Conduction Problem with Special Reference to Phase-Change.* Inter. Jour. Num. Method Engineer., Vol. 8, pp. 613-624.

[Crivelli & Idelsohn-86] Crivelli, G. and S. Idelsohn [1986] *Temperature-Based Finite Element Solution for Phase Change Problems.* International Journal for Numerical Methods in Engineering, Vol. 23, pp. 99-119.

[De Souza Neto *et al. 95*] De Souza Neto, K. Hashimoto, D. Peric and D.R.J. Owen [1995] *A Phenomenological Model for Frictional Contact of Coated Steel Sheets Accounting for Wear Effects: Theory, Experiments and Numerical Simulation.* International Journal for Numerical Methods in Engineering, to appear.

[Dusimberre-45] Dusinberre, G. [1945] *Numerical Method for Transient Heat Flow.* ASME, 67, 703.

[Duvaut & Lions-72] Duvaut, G. and J.L. Lions [1972] *Les Inequations en Mecanique et en Physique.* Dunod, Paris.

[Felippa-80] Felippa, C.A. and K.C. Park [1980] *Staggered Transient Analysis Procedures for Coupled Mechanical Systems: Formulation.* Computer Methods in Applied Mechanics and Engineering. Vol. 24, pp. 61-111.

[Fortin-82] Fortin, M. and R. Glowinsky [1982] *Resolution Numerique de Problemes aux Limites par des Methodes de Lagrangient Augmente.* Methodes Mathematiques de l'Informatique, Dunod-Bordas, Paris.

[Fortin-85] Fortin, M. and A. Fortin [1985] *Experiments with Several Elements for Viscous Incompressible Flow.* Int. Jur. Num. Meth. Fluids Vol. 5, pp. 911-928.

[Gear-71] Gear, C.W. [1971] *Numerical Initial Boundary Problems in Ordinary Differential Equations.* Prentice-Hall Englewood Cliffs, New Jersey.

[Giannakopoulos-89] Giannakopoulos, A.E. [1989] *The Return Mapping Method for the Integration of Friction Constitutive Relations.* Computers and Structures, Vol. 32, pp. 157-167.

[Hestenes-69] Hestenes, M. [1969] *Multipliers and Gradient Method.* Journ. of Optim. Theory and Applicat. Vol. 4, pp. 303-320.

[Hughes-79] Hughes, T.J.R., W.K. Liu and A. Brooks [1979] *Review of Finite Element Analysis of Incompressible Viscous Flows by the Penalty Function formulation.* Journ. Comput. Physics, Vol. 30 pp. 1-60.

[Hughes-87] Hughes, T.J.R. [1987] *The Finite Element Method: Linear Static and Dynamic Finite Element Analysis.* Prentice-Hall International, Hernel Hempstead, 1987.

[Kikuchi-77] Kikuchi, F. [1977] *Discrete Maximum Principle and Artificial Viscosity in Finite Element Approximations of Convective Diffusion Equations.* ISAS Report no. 550, Vol. 42, no. 5, Tokyo, 1977.

[Kikuchi-88] Kikuchi, N. and J.T. Oden [1988] *Contact Problems in Elasticity: A Study of Variational Inequalities and Finite Element Methods.* SIAM, Philadelphia.

[Khan & Huang-95] Khan, A.S. and S. Huang [1995] *Continuum Theory of Plasticity.* John Wiley & Sons, Inc.

[Krieg & Key-76] Krieg, R.D. and S.W. Key [1976] *Implementation of a Time Dependent Plasticity Theory into Structural Computer programs.* Constitutive Equations in Viscoplasticity: Computational and Engineering aspects. Editors: J.A. Stricklin and K.J. Saczlski, AMD-20, AMSE, New York.

[Krieg & Krieg-77] Krieg, R.D. and D.B. Krieg [1977] *Accuracies of Numerical Solution Method for the Elastic-Perfectly Plastic Model.* Journal of Pressure Vessel Technology. ASME-99.

[Lassen-93] Lassen, S. [1993] *Formulation of Wear Models for Forming Dies.* Internal Report, IPU, Technical University of Denmark.

[Lassen & Bay-93] Lassen, S. and N. Bay [1993] *Evaluation of Tribology tests for sheet Metal Forming.* Internal Report, IPU, Technical University of Denmark.

[Laursen-92] Laursen, T.A. [1992] *Formulation and Treatment of Frictional Contact Problems Using Finite El-*

ements. Ph.D. Dissertation, Stanford University, Division of Applied Mechanics, Report no. 92-6.

[Laursen-98] Laursen, T.A. [1998] *On the Development of Thermodynamically Consistent Algorithms for Thermomechanical Frictional Contact.* Comp. Meth. in Appl. Mech. Engineer., Preprint.

[Laursen & Chawla-97] Laursen, T.A. and V. Chawla [1998] *Design of Energy Coserving Algorithms for Frictionless Dynamic Contact Problems.* Int. Journal for Num. Meth. in Engin., Vol. 40, pp. 863-886.

[Laursen & Simo-91] Laursen, T.A. and J.C. Simo [1991] *On the Formulation and Numerical Treatment of Finite Deformation Frictional Contact Problems.* Nonlinear Computational Mechanics–State of the Art., P. Wriggers & W. Wagner, eds., Springer-Verlag, Berlin, pp. 716-736.

[Laursen & Simo-92] Laursen, T.A. and J.C. Simo [1992] *Formulation and Regularization of Frictional Contact Problems for Lagrangian Finite Element Computations.* Proc. of The Third International Conference on Computational Plasticity: Fundamentals and Applications, COMPLAS III, D.R.J. Owen, E. Onate & E. Hinton, eds., Pineridge Press, Swansea, pp. 395-407.

[Laursen & Simo-93] Laursen, T.A. and J.C. Simo [1993] *A Continuum-Based Finite Element Formulation for the Implicit Solution of Multi-Body, Large Deformation Frictional Contact Problems.* International Journal for Numerical Methods in Engineering, Vol. 36, pp. 3451-3485.

[Laursen & Simo-93b] Laursen, T.A. and J.C. Simo [1993] *Algorithmic Symmetrization of Coulomb Frictional Problems*

Using Augmented Lagrangians. Computer Methods in Applied Mechanics and Engineering. Vol. 108, pp. 133-146.

[Malvern-69] Malvern, L.E. [1969] *Introduction to the Mechanics of a Continuous Medium.* Prentice Hall.

[Mandel-72] Mandel, J. [1972] *Plasticité Classique et Viscoplasticité.* CISM Udine, Springer-Verlag, Vienna 1972.

[Nagtegaal-74] Nagtegaal, J.C., D.M. Parks and J.R. Rice [1974] *On Numerical Accurate Finite Element Solutions in the Fully Plastic Range.* Comp. Meth. in Appl. Mech. Engineer. Vol. 4, pp.153-177.

[Nickell & Sackman-68] Nickell, R.E. and J.L. Sackman [1968] *Approximate Solutions in Linear Coupled Thermoelasticity.* Jour. of Applied Mech., pp. 255-266.

[Oden-69] Oden, J.T. [1969] *Finite Element Analysis of Nonlinear Problems in the Dynamical Theory of Thermoelasticity.* Nuclear Engin. and Design, vol- 10, pp. 465-475.

[Oden & Pires-84] Oden, J.T. and E.B. Pires [1984] *Algorithms and Numerical Results for Finite Element Approximations of Contact Problems with Non-Classical Friction Laws.* Computer and Structures. Vol. 19, pp. 137-147.

[Ortega-70] Ortega, J.M. and W.C. Rheinboldt [1970] *Iterative Solutions of Nonlinear Equations in Several Variables.* Academic Press, New York.

[Owen & Peric-95] Owen, D.R.J., D. Peric, A.J.L. Crook, E.A. de Souza Neto, J. Yu and M. Dutko [1995] *Advanced Computational Strategies for 3D Large Scale Metal Forming Simulations.* Proceedings of the Fifth International Conference on Numerical

Methods in Industrial Forming Processes, to appear.

[Nishida-86] Nishida, Y., W. Droste and S. Engler [1986] *The Air-gap Formation Process at the Casting-Mould Interface and the Heat Transfer Mechanism through the Gap.* Metallurgical Transaction B, 17B, pp. 833-844.

[Parish-89] Parisch, H. [1989] *A Consistent Tangent Stiffness Matrix for Three-Dimensional Non-Linear Contact Analysis.* International Journal for Numerical Methods in Engineering, Vol. 28, pp. 1803-1812.

[Park-83] Park, K.C. [1983] *Stabilization of Partitioned Solution Procedure for Fluid-Soil Interaction Analysis.* Inter. Jour. Num. Method Engineer., Vol. 19, pp. 1669-1673.

[Ransing-98] Ransing, R.S. and R.W. Lewis [1998] *A Thermo-Elasto-Visco-Plastic Analysis for Determining Air Gap and Interfacial Heat Transfer Coupled with the Lewis-Ransing Correlation for Optimal Feeding Design.* Proceedings of VIII International Conference on Modelling of Casting, Welding and Advanced Solidification processes, San Diego, California, U.S.A., 1998.

[Roph-82] Rolph, W. and K. Bathe [1982] *An Efficient Algorithm for Analysis of Nonlinear Heat Transfer with Phase Change.* Inter. Jour. Num. Method Engineer., Vol. 18, pp. 119-134.

[Salcudea-86] Salcudean M., Z. Abdullah and K. Davis [1986] *Modelling of Solidification of Cast-iron in Permanent Moulds.* Inter. Jour. Num. Method Engineer., Vol. 25, pp. 445-473.

[Salcudean-88] Salcudean M. and Z. Abdullah [1988] *On the Numerical Modeling of Heat Transfer During Solid-*

ification. Symp. on Computer Modelling of Fabrication Processes and Const. behavior of Metals, Ottawa, Canada, May 15-16, 1988.

[Simo-85] Simo, J.C., R.L. Taylor and K.S. Pister [1985] *Variational and Projection methods for the Volume Constraint in Finite Deformation Elasto-plasticity.* Computer method in Applied Mech. and Engineer. Vol. 51, pp. 177-208.

[Simo-94] Simo, J.C. [1994] *Numerical Analysis Aspects of Plasticity. Handbook of Numerical Analysis.* Volume IV, P.G. Ciarlet and J.J. Lions, eds., Nort-Holland.

[Simo & Laursen-92] Simo, J.C. and T.A. Laursen [1992] *An Augmented Lagrangian Treatment of Contact Problems Involving Friction.* Computers and Structures, Vol. 42, pp. 97-116.

[Simo & Miehe-92] Simo, J.C. and C. Miehe [1992] *Associative Coupled Thermoplasticity at Finite Strains: Formulation, Numerical Analysis and Implementation.* Comp. Meth. Appl. Mech. and Egineer., Vol. 98, pp. 41-104.

[Song-87] Song, S. and M.M. Yovanovich [1987] *Explicit relative contact pressure expression: dependence upon surface roughness parameters and Vickers microhardness coefficients.* AIAA, Paper 87-0152.

[Steven-82] Steven, J. [1982] *Internally Discontinuous Finite Element for Moving Interface Problems.* Inter. Jour. Num. Method Engineer., Vol. 18, pp. 569-582.

[Storti *et al. 87*] Storti, M., G. Crivelli and S. Idelsohn [1987] *An Efficient Tangent Scheme for Solving Phase Change Problems.* Comp. Meth. Appl. Mech. and Egineer., Vol. 88, pp. 65-86.

[Strang-69] Strang, G. [1969] *Approximating Semigroups and the Consistency of Difference Schemes.* Proc. American Mathematical Society, Vol. 20, pp. 1-7.

[Stromberg-96] Stromberg, N., L. Johansson and A. Klarbring [1996] *Derivation and analysis of a generalized standard model for contact, friction and wear.* International Journal of Solids and Structures, Vol. 33, pp. 1817-1836.

[Truesdell-65] Truesdell, C. and W. Noll [1965] *The Nonlinear Field Theories of Mechanics.* Encyclopedia of Physics, Vol. 3, S. Flugge. Berlin: Springer-Verlag.

[Wilkins-64] Wilkins, M.L. [1964] *Calculation on Elastic-Plastic Flow.* Methods of Computational Physics. Editor: B. Alder et al., Accademic Press, New York.

[Wriggers-87] Wriggers, P. [1987] *On Consistent Tangent Matrices for Frictional Contact Problems.* Proceedings of the Intern. Conf. NUMETA'87, J. Middleton and G.N. Pande, eds., Nijhoff, Dordrecht.

[Wriggers & Miehe-92] Wriggers, P. and C. Miehe [1992] *Recent Advances in the Simulation of Thermomechanical Contact Processes.* Proc. of The Third International Conference on Computational Plasticity: Fundamentals and Applications, COMPLAS III, D.R.J. Owen, E. Oñate and E. Hinton, eds., Pineridge Press, Swansea, pp. 325-347.

[Wriggers & Simo-85] Wriggers, P. and J.C. Simo [1985] *A Note on Tangent Stiffness for Fully Nonlinear Contact Problems.* Communications in Applied Numerical Methods, Vol. 1, pp. 199-203.

[Wriggers & Vu Van-90] Wriggers, P., T. Vu Van and E. Stein [1990] *Finite Element Formulation of Large Deformation*

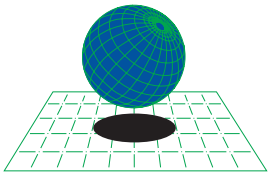

INTERNATIONAL
CENTER
FOR
NUMERICAL METHODS
IN ENGINEERING

Edificio C-1 Campus Norte - UPC, Gran Capitán, s/n.
08034 Barcelona - Spain - Phone 34-93 205 70 16 - Fax 34-93 401 65 17